THE UNIVERSITY
of EDINBURGH

THE EFFECTS OF FGF-2 ON E11-MEDIATED OSTEOCYTOGENESIS IN SKELETAL HEALTH AND DISEASE

Ekele Ikpegbu

This thesis is presented for the degree of Doctor of Philosophy at The University of Edinburgh

2018

Declaration

I declare that this thesis has been composed entirely by the candidate, Ekele Ikpegbu. This work has not previously been submitted for a Doctor of Philosophy, a degree or any professional qualification. I have done all the work, unless acknowledged otherwise. All sources of information have been acknowledged.

Ekele Ikpegbu

Acknowledgements

I sincerely acknowledge the support from my supervisors Colin Farquharson, Katherine Staines, and Dylan Clements. Colin has re-defined postgraduate supervision in my wonderful experience here. He simply took me from nowhere to somewhere, that now I can appreciate asking research question and do my best to answer it. He was just there for me throughout this life transforming experience especially his close attention to details that I greatly appreciate. Katherine was very helpful to me from day one. She never knew how scared I was on my first day in the lab. Her encouragement like my other supervisors reassured me it is possible to appreciate molecular biology. Dylan was always there to remind me of my veterinary background, and he readily brought that skill into the team. I will always remain grateful to you all for the invaluable support and kindness, which made life fun and memorable even when I thought I have reached my wits end. Also the kind support from other members of the lab - Elaine Seawright, Dean Houston, Lucy Cui Lin, Tsang Hiu, Scott Dillon, James Ozanne, Erika Abbondati, Fiona Roberts, Alisia Sim, Seungmee Lee, Lewis Hsu, and our summer students – Erin Unger and Lena Basta. Lena's contribution to some of the data in Chapter 4 is specifically acknowledged. I specially appreciate Elaine whose job was to navigate me though the Roslin Institutes' lab- that was for me an Alice in a wonderland experience.

To members of my thesis committee David Collie and Vicky Macrae, I do appreciate your painstaking discussion during these meetings. I learnt a lot from my chat with

you as it made me see how UK universities especially, the University of Edinburgh FastTrack postgraduate programme for excellence and timely delivery of set objectives. I would also say a big thank you to our collaborators Tonia L. Vincent for the *Fgf-2* knockout (KO) mice and DMM material; David J. Buttle and Andrew A. Pitsillides for all their support during the course of my PhD. In addition, I would like to thank Gordon Melville and the BSU staff for their asistance with the animal studies. The bio-imaging team of Bob Fleming and Graeme Robertson were nice; actually, they never got tired of me. Will not fail to say how much help I received from the Roslin community too numerous to mention but will list a few like Greg Markby, William Ho, Marco Esposito. Also appreciated is the encouragements from Abejide Oluyinka and Idoko-Akoh Alewo for his help in protein sequencing in Chapter 5. I am also very grateful to TETFUND Nigeria and Roslin Institute for their funding.

I will specially thank my loving wife Peace and our funny daughters Ifunanyachukwu and Chiamaka (Princes), for their understanding and affection despite my absence during this period. I will also thank my parents, siblings and numerous friends for all your kind words and prayers.

Abstract

Fibroblast growth factor 2 (FGF-2) is known to be released from cartilage upon injury and is able to influence chondrocyte gene expression in *vitro*. In cartilage, FGF-2 regulates E11/podoplanin expression in murine joints following surgical destabilisation (DMM model of osteoarthritis (OA)), and in cartilage explant injury models. In bone, E11 is critical for the early stages of osteocytogenesis and is responsible for the acquisition of the osteocyte dendritic phenotype. This dendritic phenotype is dysregulated in OA and given the known role of the osteocyte in controlling bone remodelling, this may contribute to the subchondral bone thickening observed in OA. Hence, the aim of this study was to elucidate the nature of FGF-2-mediated E11 expression and osteocytogenesis in skeletal health and disease.

This thesis has shown that FGF-2 dose-dependently increased *E11* mRNA expression in MC3T3 cells, primary osteoblasts and in primary calvaria organ cultures, which was confirmed by E11 protein western blotting data. The FGF-2 induced changes in E11 expression were accompanied by significant increases in the mRNA expression of the osteocyte markers *Phex* and *Dmp1*, and significant decreases in the mRNA expression of the osteoblast markers *Col1a1*, *Postn*, *Bglap* and *Alpl* expression. This thus supports the hypothesis that FGF-2 drives osteocytogenesis.

The acquisition of osteocyte phenotype involves the re-organisation of the cytoskeleton, such as F-actin. This step is important for the transition of cuboidal-shaped osteoblasts to the stellate-shaped osteocyte phenotype. FGF-2 stimulation of MC3T3 cells and primary osteoblasts revealed more numerous and longer dendrites,

as visualised by phalloidin staining for F-actin and indicative of the acquisition of the osteocyte phenotype. In contrast, control cells had a typical rounded morphology with fewer and shorter dendrites. Furthermore, immunofluorescence labelling for E11 in control cells revealed uniform distribution throughout the cytoplasm, especially in the perinuclear region. In contrast, FGF-2 treated cells showed a modified distribution where E11 was negligible in the cytoplasm, but concentrated in the dendrites. The use of siRNA knockdown of E11 achieved a 70% reduction of basal *E11* mRNA expression. This knockdown also effectively abrogated FGF-2-related changes in *E11* expression and dendrite formation as disclosed by mRNA and protein expression, immunofluorescence and F-actin staining with phalloidin. Despite these FGF-2 driven increases in E11 and osteocyte dendrite formation *in vitro*, immunohistochemical labelling revealed no differences in E11 expression in subchondral, trabecular and cortical osteocytes from naïve *Fgf-2* deficient mice in comparison to wild-type mice. Similar results were observed upon sclerostin immunolabelling.

FGF-2 stimulation of MC3T3 cells elicited activation of ERK1/2, Akt and p38 MAPK. However, inhibition of the aforementioned pathways failed to reduce FGF-2-mediated E11 expression and as such, the specific signalling pathway responsible remains unclear. Upstream, the expression of *Fgfr1* was increased (>10-fold) over 24 h time point, while a reduction was seen in *Fgfr2/3* expression over same time point especially in the FGF-2 treated cultures. This suggests that increased E11 expression and the acquisition of the osteocyte phenotype may be speculatively though upregulation of *Fgfr1.*

The expression of E11 and sclerostin in OA pathology in mice, human and dogs were investigated. Initially sequence homology using the Clustal Omega alignment program showed both proteins to be homologous in the domestic animals under study. A comparative study using canine subchondral bone osteocytes revealed increased E11 expression in the OA samples relative to the control. This feature may be related to newly embedded osteocytes during sclerosis. However, E11 and sclerostin were unchanged in both murine (DMM) and human OA subchondral bone osteocytes in comparison to controls. In mice, this may be due to limited OA development; whilst in humans the sample size, age, stage of the disease and sourcing from same diseased joint may be important in the interpretation of the results.

The expression of E11 and sclerostin during OA pathology was also investigated in *Fgf-2* deficient mice in which OA was induced using the DMM model. There was no difference in E11 expression between the OA and control (sham-operated) samples, suggesting that compensation of E11 expression may be mediated by growth factors from the FGF family. Surprisingly, increased E11 expression was observed in the control *Fgf-2* deficient mice, in comparison to the wild-type control mice. This suggests a potential adjustment to loading by the contralateral knee, as this was not observed in naïve mice from both groups.

Together, these data show that FGF-2 promotes the osteocyte phenotype, and that this is mediated by increased E11 expression. These results may help explain (1) the altered osteocyte phenotype and (2) increased subchondral bone thickening observed in OA. This knowledge will be of interest in the search for disease modifying therapeutics for skeletal health, including OA and osteoporosis.

Lay Abstract

The mammalian skeleton, which supports body weight, aids locomotion and protects important organs like the heart and lungs, is a dynamic organ. Inside the skeleton are three types of cells that are regularly changing form and function, enabling the skeleton to adapt to changes in body weight, recover from fracture, or even help the kidney in mineral balance control. One of these cell types are called osteoblasts. Osteoblasts have a rounded shape and make new bone. Eventually, the osteoblast surrounds itself with new bone and then undergoes a transition into a smaller star-like cell, called an osteocyte.

The osteocyte is the most abundant bone cell and makes up about 95% of the total number of bone cells. The osteocyte is now regarded as the master regulator cell, regulating how bone adapts to changes in shape and size. The formation of the osteocyte's star-like projections, called dendrites is controlled by a molecule called E11. E11 helps the osteocyte to communicate with other osteocytes, and other bone cell to regulate bone health and diseases. These dendrites are reportedly malformed in some bone related diseases like osteoarthritis. However, how E11 helps in the transition from osteoblast to osteocyte in healthy bone is largely unknown and similarly what factors might increase or reduce E11 expression are also unknown.

One growth factor that plays an important role in skeletal growth and development is called FGF-2. In this thesis, it was shown that FGF-2 is able to increase E11 expression. Furthermore, FGF-2 was able to promote the formation of osteocyte

dendrites, though these increases in E11 expression. The findings of this thesis help to expand the knowledge surrounding the process of osteocyte formation in healthy bone. Importantly, this knowledge will contribute towards our understanding of osteoarthritis and other bone diseases with malformed osteocyte dendrites.

Publications

Original peer reviewed papers

1. **Ikpegbu E.,** Basta L., Clements D.N., Vincent T.L., Buttle D.J., Pitsillides A.A., Staines K.A., Farquharson C. 2017 FGF-2 promotes osteocyte differentiation though increased E11/podoplanin expression *in vitro. Journal of Cellular Physiology.* In pres.

2. Staines K.A., Javaheri B., Hohenstein P., Fleming R., **Ikpegbu E.,** Unger E., Hopkinson M., Buttle D.J., Pitsillides A.A., Farquharson C. 2017 Hypomorphic conditional deletion of E11/Podoplanin reveals a pivotal role in osteocyte dendrite elongation. *Journal of Cellular Physiology*. 232(11):3006-3019

Presented Abstracts

1. **Ikpegbu E.,** Basta L., Clements D.N., Buttle D.J., Pitsillides A.A., Staines K.A., Farquharson C. Deciphering the signalling mechanisms underpinning FGF-2 mediated osteocytogenesis. Bone Research Society, Bristol (2017)

2. **Ikpegbu E.,** Clements D.N., Basta L., Vincent T.L., Buttle D.J., Pitsillides A.A., Staines K.A., Farquharson C. FGF-2 promotes osteocyte differentiation though increased E11/podoplanin expression . OARSI World Congres on Osteoarthritis, Las Vegas (2017). Osteoarthritis and Cartilage , Volume 25 , S141 - S142

3. **Ikpegbu E.,** Clements D.N., Basta L., Buttle D.J., Pitsillides A.A., Staines K.A., Farquharson C. FGF-2 promotes osteocyte differentiation though increased E11 expression in vitro. Bone Research Society, Liverpool (2016)

4. **Ikpegbu E.,** Clements D.N., Buttle D.J., Pitsillides A.A., Staines K.A., Farquharson C. FGF2 promotes osteocyte differentiation though increased E11 expression in vitro. 3rd Joint Bone Research Society/British Society of Matrix Biology Meeting, Edinburgh (2015) *Frontiers in Bone Research doi: 10.3389/978-2-88919-659-3*

Abbreviations

AC	Articular cartilage
ALP	Alkaline phosphatase
ATP	Adenosine tri-Phosphate
α-MEM	α-modified essential medium
ANOVA	Analysis of variance
AP-1	Activator protein 1
Akt	Protein kinase B
ATFs	Activating transcription factors
Bglap	Osteocalcin
BMPs	Bone morphogenic proteins
BSA	Bovine serum albumin
Ca^{2+}	Calcium ions
Cas9	CRISPR-associated protein-9 nuclease (Cas9)
CC	Calcified cartilage
cAMP	Adenosine mono-Phosphate
cDNA	Complimentary DNA
cKO	conditional knock out
CLEC-2	C-type lectin-like receptor -2
Col1a1	Collagen type 1 alpha 1
CO_2	Carbon dioxide
CREB	cAMP response element binding protein
CRISPR	Clustered Regularly Interspersed Short Palindromic Repeats
CT	Cytoplasmic tail
DAPI	4', 6-diamidino-2-phenylindole
DAB	Diaminobenzidine
DC	Detergent compatible
DMA	Disease modifying agent

DMM	Destabilisation of the medial meniscus
DMP1	Dentin matrix protein 1
DMSO	Dimethyl sulfoxide
DNA	Deoxyribonucleic acid
dNTP	Deoxyribonucleotide triphosphate
DKK1	Dickkopf-related protein 1
DTT	Dithiotheitol
E11	Podoplanin
EC	Extracellular domain
ECL	Enhanced chemiluminescence
ECM	Extracellular matrix
EDTA	Ethylenediaminetetraacetic acid
EGF	Epidermal growth factor
EGFR	Epidermal growth factor receptor
EMT	Epithelial-mesenchymal transition
ERK1/2	Extracellular signal-regulated kinases 1/2
ERM	Ezrin, Radixin and Moesin
Ets	E26 transformation-specific
FAK	Focal adhesion kinase
FBS	Foetal bovine serum
FGF-2	basic Fibroblast growth factor
FGF-23	Fibroblast growth factor-23
FGFR	Fibroblast growth factor receptor
FRS2	Fibroblast Growth Factor Receptor Substrate 2
GAPDH	Glyceraldehyde-3-phosphate dehydrogenase
GABI	GRB2 Associated Binding Protein 1
GRB2	Growth factor receptor-bound protein 2
H_2O	Water
dH_2O	distilled H_2O

HA	Hydroxyapaptite
HBS	Hank's balanced salt solution
H&E	Haemotoxylin and eosin
HP	Horseradish peroxidase
IgG	Immunoglobulin G
IGF-1	Insulin growth factor 1
JNK	c-Jun N-terminal kinase
KDa	Kilodalton
KO	Knock out
LRP5/6	Low-density lipoprotein receptor-related protein 5/6
MAPKs	Mitogen activated protein kinases
M-CSF	Macrophage colony stimulating factor
MEK	Mitogen activated protein kinase kinase
Micro-CT	Micro–computed tomography
MOPS	3-(N-morpholino) propanesulfonic acid
MMP	Matrix metalloproteinase
mRNA	Mesenger RNA
MSCs	Mesenchymal stem cells
MV	Matrix vesicles
NBF	Neutral buffered formalin
NC	Nitrocellulosse
NCP	non-collagenous proteins
NF-kB	Nuclear factor kappa B
NFW	Nuclease free water
NGF	Nerve growth factor
NO	Nitric oxide
OA	Osteoarthritis
OCT	Optimal cutting temperature
OPG	Osteoprotegerin

PBS	Phosphate buffered solution
PCR	Polymerase chain reaction
PFA	Paraformaldehyde
PGE_2	Prostaglandin E_2
PHEX	Phosphate regulating gene with homologies to endopeptidases on the X chomosome
Pi	Inorganic phosphate
PI3K	Phosphatidylinositol 3-kinase
PKC	Protein kinase C
PLC-ɣ	Phospholipase C-ɣ
Postn	Periostin
qPCR	Quantitative polymerase chain reaction
Rac1	Ras-related C3 botulinum toxin substrate 1
RANK	Receptor for activation of nuclear factor kappa B
RANKL	Receptor for activation of nuclear factor kappa B ligand
RhoA	Ras homolog gene family, member A
RIPA	Radio-immunoprecipitation assay
RNA	Ribonucleic acid
RT	Room temperature
RTK	Receptor Tyrosine Kinase
RT-qPCR	Reverse transcription quantitative polymerase chain reaction
Runx2	Runt-related transcription factor 2
SAPK	Stress-activated protein kinase
SCB	Subchondral bone
SEM	Standard error of the mean
sFRP1	secreted frizzled-related protein 1
SH2	Src homology region 2
SHP-2	SH2-containing protein tyrosine phosphatase-2
siRNA	small interfering RNA
Sox	SRY-box

SOST	Sclerostin
SRY	Sex-determining region Y protein
TBS	Tris-buffered saline
TBS/T	Tris-buffered saline/Tween-20
TGF-β	Transforming growth factor – beta
TIMPs	Tissue inhibitors of metalloproteinases
TM	Transmembrane Section
TNAP	Tissue non-specific ALP
TNF	Tumour necrosis factor
TRAF	TNF receptor-associated factor
TRAP	Tartrate-resistant acid phosphatase
Tris	Tris(hydroxymethyl)aminomethane
VEGFR	Vascular endothelial growth factor receptor
WNT	Wingless integration
WT	Wild type

Table of Contents

Chapter 1

Introduction

Preface

The skeleton has been considered by some to be a dull and lifeles tissue however it is actually a dynamic organ constantly adapting to demands placed upon it. The skeleton is essential for locomotion and soft tissue protection, and is involved in other body homeostasis responses such as the regulation of mineral and energy metabolism. It is accepted that the bone is constantly modelling itself in response to changes in weight bearing activities during locomotion. The adaptation to loading is regulated by osteocyte expressed signals that influence the activities of osteoblasts and osteoclasts. Osteocytes are terminally differentiated osteoblasts, formed though a process termed osteocytogenesis. This process is under the influence of various late osteoblast/osteocyte-expressed molecules such as E11 (podoplanin). E11, is essential for osteocyte dendrite formation and its expression is known to be regulated by growth factors such as fibroblast growth factor (FGF)-2 in cartilage. Despite this, the regulation of E11 expression in bone is completely unknown. This work reported in this thesis investigates the role of FGF-2 during osteoblast to osteocyte transition, and test the hypothesis that FGF-2 regulates E11 mediated osteocytogenesis. The importance of understanding this is highlighted by the central role that dendrites play in osteocyte communication in health, and their dysfunction in some skeletal disorders like osteoarthritis (OA). Understanding the role of E11 during osteocyte formation in subchondral bone (SCB) of healthy and OA joints will contribute immensely to the search for therapeutic targets in OA.

1.1 Bone structure and function

The skeleton is a highly complex but organised organ structurally specialised for locomotion, protecting critical internal organs, mineral homeostasis and energy metabolism regulation (Weiner et al., 1999, Feng, 2009, Oldknow et al., 2015). Bone is a composite structure made up of organic and inorganic material and together the hydroxyapatite (HA) mineral (stiff and brittle) and the organic collagen (tough and soft) provide a structure that is tough, stiff, and resistant to fracture (Staines et al. 2012). The resident cells that are responsible for maintaining this structure are the osteoblasts, osteocytes and osteoclasts. Whilst collagen type 1 is the major organic component of the extracellular matrix (ECM), there are many other osteoblast secreted non-collagenous proteins (NCPs) such as glycosaminoglycans, osteopontin, and dentine matrix protein 1 (DMP1) (Sommerfeldt and Rubin, 2001).

The skeleton is comprised of compact or cortical (compact) and trabecular (cancellous) bone. The trabecular bone located within the marrow compartment has an open lattice network making it light but strong (Fig. 1.1A). It has a higher bone turnover rate than cortical bone and its lamellar organisation does not contain osteons (Sommerfeldt and Rubin, 2001). It can adapt to loading in various directions and its surrounding marrow is the site for haematopoiesis.

The cortical bone, which makes up ~ 80% of the bone mass, is found on the external aspect of bone shaft. Cortical bone is relatively hard and dense; but well organised into osteon building units of the Harversian system (Sommerfeldt and Rubin, 2001, Brandi, 2009). The mineralised osteonal rings have resident osteocytes (encased

within a lacuna) which are characterised by dendritic cytoplasmic projections radiating from the cell membrane. They run though a canaliculi network, which connects neighbouring osteocytes and osteocytes with bone surface osteoblasts and osteoclasts. The central Harversian canal has blood vessels, lymphatics and nerve traversing though (Fig. 1.1B). Cortical bone is specialised for weight bearing especially along the vertical axis of the body.

1.2 Bone formation

Bone development and formation involves two distinct mechanisms - intramembranous and endochondral ossification (Shapiro, 2008, Yang, 2009). While intramembranous ossification involves the differentiation of mesenchymal cells into osteoprogenitor cells on collagen surfaces, endochondral ossification is the replacement of hyaline cartilage anlagen by osteoprogenitor cells and bone (Henrikson et al., 1997, Percival and Richtsmeier, 2013). The fate of osteoprogenitor cells during bone formation is under tight signalling regulation. Upregulation of Wingless integration (Wnt)/β-catenin signalling in the region of mesenchymal condensations drive osteoblast differentiation, hence intramembranous ossification. Conversely, the initial decrease in Wnt/β-catenin signalling in mesenchymal condensations promotes the formation of the chondrocyte anlagen for endochondral ossification. In advanced stages of endochondral ossification, upregulated Wnt/β-catenin signalling drives subsequent osteoblast differentiation in the cartilage

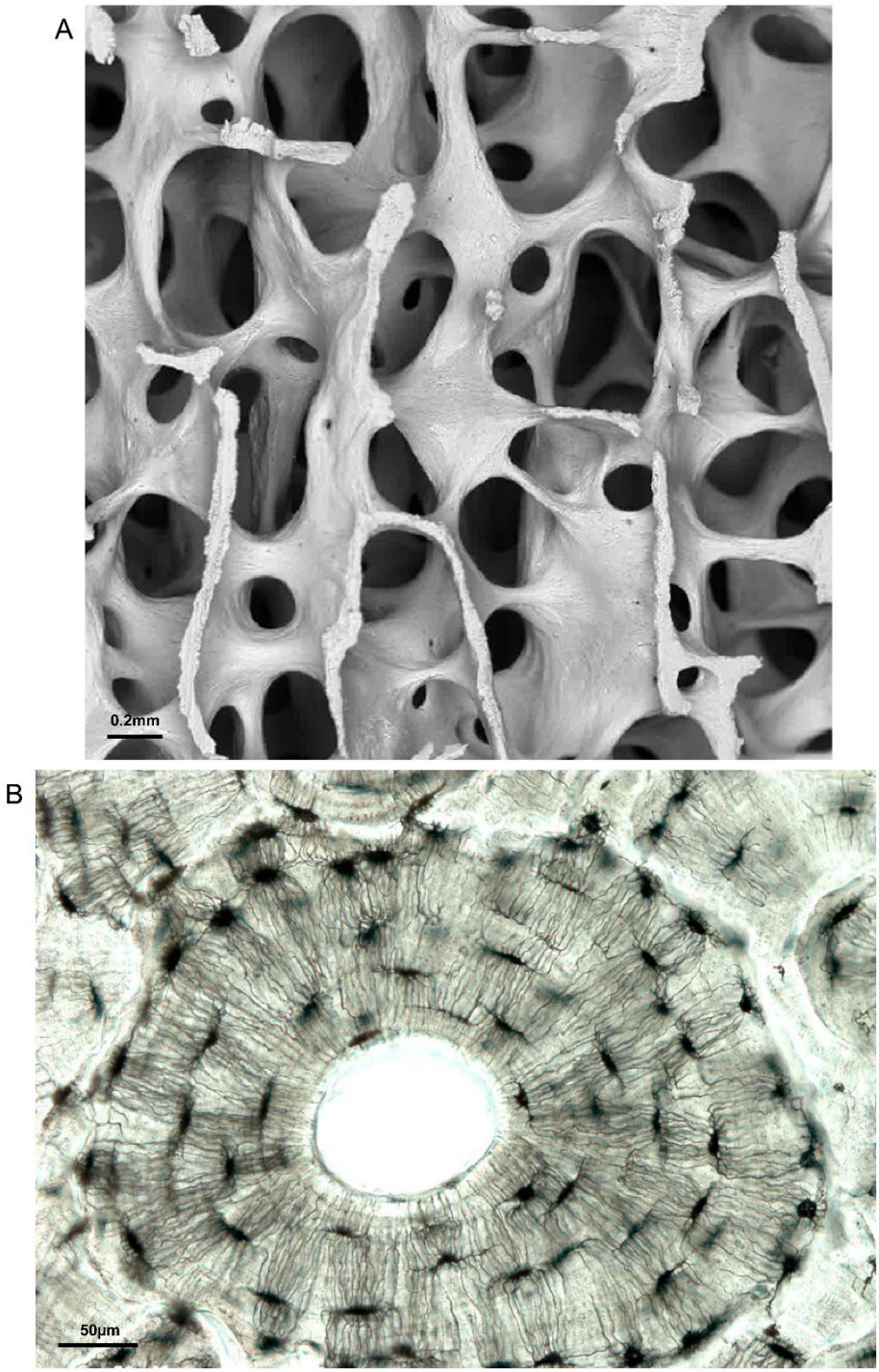

Figure 1.1 The structure of cancellous and cortical bone

Low power scanning electron microscopy of normal cancellous bone design (**A**), showing bone trabecular and open lattice shape, which contains bone marrow. Cortical bone architecture found in the diaphysis of long bone (**B**). The centrally located Haversian canal provides passage for nerves and blood vessels. Note the concentric layers of bone matrix and osteocytes surrounding it. Images sourced from the Bone Research Society, by kind permission of (A) Alan Boyde (B) Tim Arnett.

periphery (Yang, 2013). The role of transcription factors SRY-box 9 (Sox9) and Runt-related transcription factor 2 (Runx2), which are master regulators of chondrocyte and osteoblast differentiation from mesenchymal cells respectively, have also been documented (Ducy et al., 1997, Bi et al., 1999). Fibroblast growth factor receptor 2c, is expressed by early mesenchymal cells where it is activated by FGF-18 during both endochondral and intramembranous bone formation (Eswarakumar et al., 2002).

1.2.1 Intramembranous Ossification

Intramembranous ossification is responsible for the development and formation of flat bones like the maxilla and palate in the skull (Netter, 1987, Mackie et al., 2011, Jiang et al., 2014). It also occurs during natural fracture healing of flat bones (Brighton and Robert, 1991). Intramembranous ossification involves four distinct but continuous stages: (i) formation of ossification centres and differentiation of mesenchymal cells into osteoblasts (ii) matrix formation and vascular invasion of the bone anlagen (iii) periosteum and trabeculae formation (iv) lamellar bone formation around trabeculae (Thompson et al., 1989).

1.2.2 Endochondral ossification

Endochondral ossification is responsible for the formation of the long bones of the body and in the natural fracture healing process (Brighton and Robert, 1986, Jiang et al., 2014). In this process, a hyaline cartilage model is established from mesenchymal cell condensation, and later replaced by osteoblasts from the vascular system (Horton, 1990, Yang, 2009). This process is critically regulated by factors such as growth hormone, insulin like growth factor 1, thyroid hormone, bone morphogenic proteins

(BMPs), vascular endothelial growth factor, Indian hedgehog, FGFs and Wnts (Mackie et al., 2011, Yang et al., 2012). In short, the process involves condensation of the mesenchymal cells and their differentiation to chondrocytes under the influence of Sox 5,6 & 9 to form the cartilage anlagen (Bi et al., 1999). This is quickly followed by hypertrophy of the chondrocytes and their subsequent vascular invasion and matrix mineralisation leading to the establishment of primary centres of ossification. The establishment of the secondary ossification centre within the epiphyses results in the formation of the epiphyseal growth plates at the proximal and distal ends of the newly formed bone (Fig. 1.2) (Kanczler and Oreffo, 2008, Mackie et al., 2011). The growth plate regulates the pace on bone growth until it closes in humans at puberty.

1.2.3 Bone mineralisation

The hardness of bone can be attributed to the product of HA crystal deposition on collagen fibrils. The mineralisation process which is initiated by the precipitation of calcium ions (Ca^{2+}), and inorganic phosphate (Pi), at discrete sites of the skeleton is regulated by several factors which include NCPs, sibling proteins, nucleotide pyrophosphate phosphodiesterase 1, ankylossis protein and phosphatases such as PHOSPHO1 and alkaline phosphatase (ALP) (Anderson, 2003, Yadav et al., 2011). The mineralisation of the ECM is initiated with membrane limited bound matrix vesicles (MV), formed by hypertrophic chondrocytes and osteoblasts. The MV provide a protected microenvironment for the concentration of Ca^{2+} and Pi (Anderson, 2003). On reaching appropriate concentrations within MV, the two minerals precipitate HA crystals. These HA crystals increase in size, and perforate the

MV membrane when they are subsequently deposited onto the collagen fibrils of the ECM. Matrix mineralisation is a key step during osteoblast differentiation into osteocyte (Clarke, 2008, Staines et al., 2012, Prideaux et al., 2012).

1.3 Bone modelling and remodelling

Bone modelling results in changes to the shape and size of bone due to uncoupled bone formation and resorption. This is required for bone to adapt to changes in the mechanical load it senses *i.e.* the tennis players serving arm. In contrast, bone remodelling involves coupled bone formation, resorption, and no change in bone mass *i.e.* the same amount of bone removed is replaced by new bone (Seeman, 2009). Bone turnover is an active remodelling process spanning the entire life of mammals where the human adult skeleton is replaced every 10 years (Palumbo et al., 2003). The process is precisely regulated by autocrine, paracrine and endocrine factors to prevent osteoporosis and osteopetrosis (Manolagas, 2000). While bone formation is principally a function of the osteoblast, osteoclasts mediate bone resorption. Bone remodelling is also under active regulation by osteocyte synthesised proteins such as sclerostin, secreted frizzled-related protein 1 (sFRP1); and the Dickkopf-related protein 1 (DKK1) which negatively regulate the differentiation of osteoblasts from osteoprogenitor cells (Fig. 1.3). In contrast, prostaglandin E_2 (PGE_2), nitric oxide (NO) and adenosine triphosphate (ATP) promote osteoblast differentiation (Bakker et al., 2001, Watanuki et al., 2002, Li et al., 2005a, Wang et al., 2013). Osteocyte derived factors also regulate osteoclast formation. Examples of this are receptor activator of nuclear factor kappa-B ligand (RANKL) and macrophage colony stimulating factor

(M-CSF) which both activate osteoclast differentiation (Fig. 1.3). Other factors such as osteoprotegerin (OPG), a RANKL decoy receptor and NO inhibit osteoclast formation (Nakashima et al., 2011a, Xiong et al., 2011, Dallas et al., 2013).

1.3.1 Osteoclasts

Osteoclasts are multinucleated cells that poses the capacity for bone resorption (Hotokezaka et al., 2002). Bone resorption, as stated earlier, is an integral part of bone modelling and remodelling, that is closely regulated to prevent bone disorders like periodontal diseases, osteoporosis and osteopetrosis (Hotokezaka et al., 2002). Osteoclasts differentiate from the monocyte/macrophage cell lineage within the bone marrow under the influence of MCSF and RANKL (Nakagawa et al., 1998, Kong et al., 1999). RANKL is expressed mostly by osteocytes and to leser degree by osteoblasts (Nakashima et al., 2011b, Xiong et al., 2011). The receptor activator of nuclear factor kappa-B (RANK) is expressed on osteoclast precursor cell surfaces and has an intracellular domain called tumour necrosis factor (TNF) receptor-associated factor (TRAF). RANK, when phosphorylated by the attachment of RANKL, mediates the activation of downstream molecules via TRAF to initiate the osteoclast differentiation program. This cascade of events involves nuclear factor kappa B (NF-kB), mitogen activated protein kinases (MAPKs), and phosphatidylinositol 3-kinase/ protein kinase B (PI3K/Akt) (Wong et al., 1998, Lee et al., 2002). These downstream signals are involved in activating the expression of tartrate-resistant acid phosphatase (TRAP) - which is a hallmark marker of osteoclast differentiation (Ishida et al., 2009).

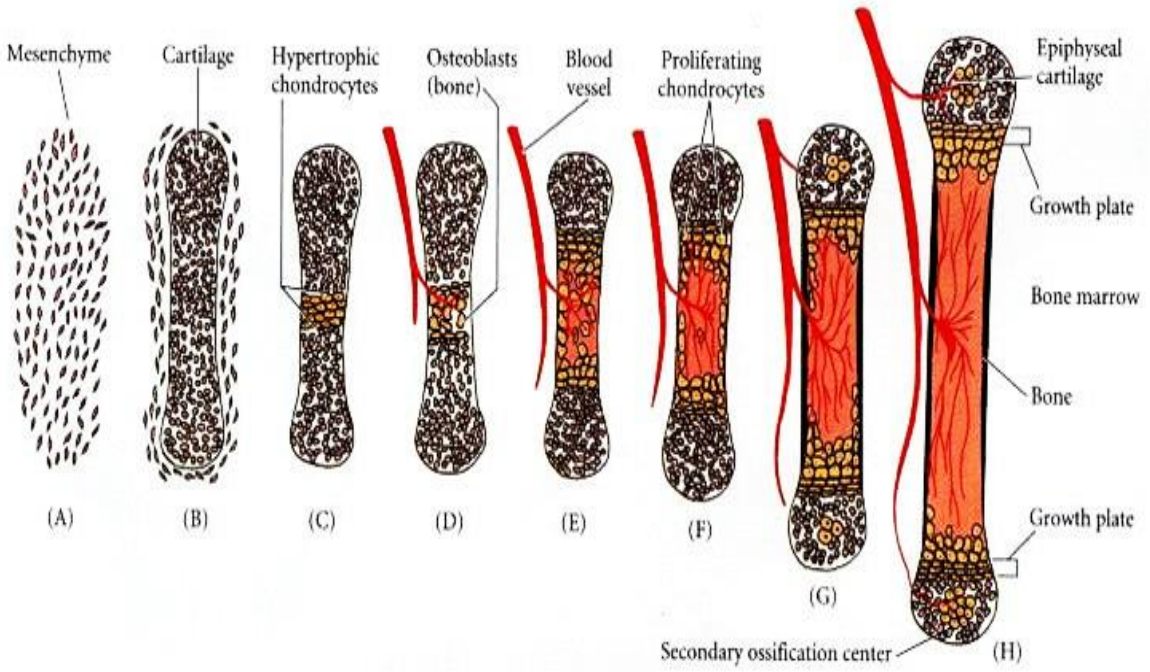

Figure 1.2. The process of endochondral ossification.
(A) Mesenchymal condensation to form the hyaline cartilage model or anlagen (B). (C) Chondroprogenitor cells differentiate into chondrocytes that proliferate and secret extracellular matrix (ECM). (D) Stage of chondrocyte enlargement, vascular invasion, and matrix mineralisation. (E) Primary ossification centre formation. (F) Elongation of diaphysis and bone marrow. (G) Establishment of epiphyseal plate and, (H) secondary centre of ossification in the epiphysis (Gilbert, 2006).

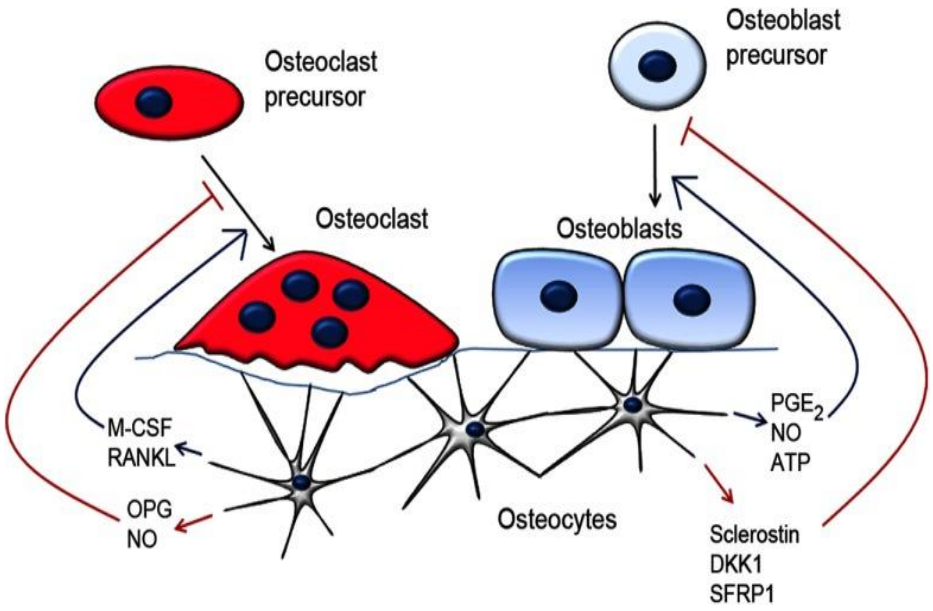

Figure 1.3. Diagrammatic model of osteocyte regulation of bone remodelling.

Note the central role of signalling molecules expressed by osteocytes to promote or inhibit differentiation of osteoblast and osteoclasts from their respective precursor cells (Dallas et al., 2013). While PGE_2, NO, and ATP activate osteoblast differentiation and bone formation, expression of sclerostin, DKK1 and SFRP1 inhibit this process and less bone is formed. Osteocyte factors like RANKL, M-CSF activate osteoclast formation, subsequently increasing bone resorption. However, OPG and NO antagonise this pathway leading to less bone loss. These factors have established the osteocyte as the master regulator of bone remodelling.

Osteoclasts have a specialised plasma membrane modified to increase its surface area to aid the breakdown of both organic and inorganic material. To do this, its membrane assembles into folds and invaginations at the bone interface and this is known as the osteoclast-ruffled border. During bone resorption upon activation by RANKL, osteoclastic proteolytic enzymes such as TRAP and cathepsin K are released at the ruffled border where they degrade collagen and other bone matrix proteins; a process that is favoured by an acidic micro resorption environment (de Vernejoul, 1998). This acidic micro-compartment is made possible by the release of protons by carbonic anhydrase-II at the ruffled border (Schlesinger et al., 1997). The large acid production by osteoclasts dissolves bone mineral in the Howship lacunae (Vaananen et al., 2000).

1.3.2 Osteoblasts

Osteoblasts are differentiated from multipotent mesenchymal bone marrow stromal cells, which are also the progenitors for chondrocytes and adipocytes (Manolagas, 2000, Xiao et al., 2010b). Osteoblasts secrete osteoid - the bone matrix - which when mineralised offers rigidity and strength to the skeleton. At the cellular level, the osteoblast is characterised by well-developed and abundant mitochondria, Golgi body, ribosomes and smooth endoplasmic reticulum, reflecting the high need for bone matrix synthesis (Dudley and Spiro, 1961).

Mesenchymal cell differentiation into the osteoblast is a complex process and is tightly regulated. Osteoblast differentiation requires the actions of the transcription factors Runx2, Osterix and Twist-1 and -2 and also other growth factors and signalling

molecules such as transforming growth factor beta (TGFβ), Sonic hedgehog, Indian hedgehog, Bone morphogenic proteins (BMPs) and FGF-2 (Yamaguchi et al., 2000, Ducy, 2000, Behr et al., 2010, Marie, 2012). The two major Wnt signalling pathways are also recognised to be critical role for osteoblast form and function. The Wnt –β-catenin pathway also called the canonical Wnt signalling pathway, whilst the non-canonical pathway involves Wnt–planar cell polarity and the Wnt-calcium pathways (MacDonald et al., 2009, Baron and Kneissel, 2013). The canonical Wnt signalling pathway is critical for osteoblastogenesis and bone mass; and is regulated by FGF-2 (Xiao et al., 2009). This pathway is activated by the Wnt ligand binding to the Frizzled receptor (Frz), in the presence of a co-receptor; low-density lipoprotein related protein (LRP) 5/6 complex. This prevents the axin-complex induced ubiquitination of β-catenin and the avoidance of proteasomal degradation (MacDonald et al., 2009). The stabilised β-catenin then relocates to the nucleus, and activates T-cell factor/lymphoid enhancer factor (TCF/LEF) transcription factor for upregulation of Wnt target genes, which drives recruitment of osteoblasts for bone formation (MacDonald et al., 2009, Baron and Kneissel, 2013). This canonical Wnt pathway can be inhibited by secreted frizzled-related protein 1 (sFRP1); the dickkopf (DKK1) proteins; and the master negative regulator of bone formation – sclerostin (Kawano and Kypta, 2003, Bodine et al., 2004, Semenov et al., 2005). The marker genes of the osteoblast phenotype include the *Col1a1*, *Bglap*, *Alpl*, and *Postn* (Fakhry et al., 2005).

After deposition of bone matrix by mature osteoblast and its subsequent mineralisation, the fate of the osteoblast includes cell death (apoptosis), reversion to

surface lining cells or terminal differentiation into osteocyte by a process known as osteocytogenesis (Dallas and Bonewald, 2010).

1.3.2.1 Alkaline phosphatase

ALP is the family name for a group of enzymes found in various tissues. Each have different properties and functions and the ALP expressed in bone is also expressed in liver and kidney. Traditionally this ALP isoform was called bone/liver/kidney ALP but today it is more commonly referred to as Tissue non-specific ALP (TNAP) and in mice is encoded by the *Alpl* gene. TNAP is a prominent osteoblast marker that is critical for matrix mineralisation as it degrades extracellular inorganic pyrophosphate (PPi), an effective inhibitor of mineralisation. TNAP hydrolyses PPi to generate optimum Pi/PPi ratio that enhances HA formation (Meyer, 1984, Anderson, 2003). The loss of the *Alpl* gene in experimental KO mice or with humans with hypophoshatasia showed decreased ECM mineralisation which was not unexpected but surprisingly mineral was still found within the MVs of long bones (Anderson et al., 1997, Anderson et al., 2004). This implied that another phosphatase was present to provide Pi for the initiation of mineralisation within the MVs. One such enzyme is PHOSPHO1, a bone specific phosphatase essential for the initiation of matrix mineralisation (Houston et al., 2002) The double knockout of both *Alpl* and *Phospho1* genes led to complete absence of bone mineralisation in embryonic mice (Houston et al., 2002, Yadav et al., 2011).

1.3.2.2 Osteocalcin

Osteocalcin, encoded by the gene *Bglap* in mice is an abundant osteoblast protein expressed later on in the differentiation process. It downregulates bone formation, and it is now regarded as having an endocrine function where it has been shown to regulate energy metabolism (Zanatta et al., 2014). Erroneously thought to be involved in bone mineralisation, as osteocalcin null mice phenotype presented increased bone mass with adequate mineralisation, and excessive visceral adipose tissue deposition (Ducy et al., 1996, Wei and Karsenty, 2015).

1.3.2.3 Collagen type 1 alpha 1

Collagen type 1 protein (encoded by *Col1a1 in mice)*, secreted by mature osteoblasts, is the principal organic component of the bone ECM (Mizuno et al., 2000, Uchihashi et al., 2013, Florencio-Silva et al., 2015). It provides the scaffold for the deposition of HA crystals during bone mineralisation and also regulates this process (Nudelman et al., 2010). Its sub chains Col1a1 and Col1a2 are expressed in the ratio 2:1. The Col1a1 mutation phenotype has been extensively studied in the brittle-bone disorder osteogenesis impecta (Eimar et al., 2016). This mutation is characterised by reduced collagen type 1 synthesis, high bone turnover, increased bone material density, poor mineralisation and a high incidence of fractures (Willing et al., 1994, Chen et al., 2014, Roschger et al., 2014).

1.3.2.4 Periostin

The *Postn* gene is expressed in osteoblasts and in foetal periosteum, cardiac valves, and periodontal ligament of the mouse. Its loss of function mutation results in les than 20% peri-natal mortality, but in adult life, mice show reduced growth with scant trabecular bone and periodontal disorders (Rios et al., 2005).

1.3.3 Osteocytes

Osteocytes are long-lived (>25 years) bone cells and constitute about 90-95% of all bone cells (Franz-Odendaal et al., 2006). Osteocytes are flat cells with dendritic cellular processes located deep in the lacunae/canaliculi of the mineralised bone ECM (Holmbeck et al., 2005). These dendrites enable the osteocyte to communicate with other osteocytes, osteoblasts, osteoclasts and the vasculature by means of their interconnecting dendritic gap junctions of the lacunae/canaliculi system (Fig. 1.4). Osteocytes are characterised by a reduction in biosynthesis of osteoblast marker proteins such as *Col1a1*, *Alpl*, *Bglap* (Sasano et al., 2000, Knothe Tate et al., 2004); but upregulation of osteocyte gene markers such as *E11, Dmp1, Phex* and *Sost* (Fig. 1.5). Osteocytes are involved in mechano-reception and transduction, calcium homeostasis, osteoid development and calcification and bone remodelling regulation (Zhang et al., 2011, Dallas et al., 2013). The mechano-reception and transduction role of osteocytes is a response to form more bone during skeletal loading (walking, running) or stimulate bone loss when the body is immobilized for an extended period (Bonewald and Johnson, 2008). This function has been validated by dendrite and gap junction hemichannels' response to fluid flow shear stress loading models using

MLO-A4 osteocyte-like cells (Burra et al., 2010). In addition, osteocyte deletion studies have revealed reduced formation of bone, more bone resorption and lack of response to loading (Bonewald, 2006, Tatsumi et al., 2007). While the precise mechanism for this function is still largely unknown, some authors believe the dendrites are the mechano-sensing structures of the osteocyte (Han et al., 2004, Adachi et al., 2009), whereas others propose that both dendrites and the cell body are required (Nicolella et al., 2008). Furthermore, others have contended that the mechano-sensing role is the responsibility of the primary cilia (Xiao et al., 2006, Malone et al., 2007).

Some authors have also concluded that osteocytes should be categorised as endocrine cells because of their production of factors such as FGF-23, RANKL, OPG and sclerostin into the vascular system (Quarles, 2008, Dallas et al., 2013, Florencio-Silva et al., 2015).

1.3.3.1 Osteocytogenesis

Osteocytogenesis, once regarded as a passive process of osteoblast differentiation, is now believed to be an active, well-regulated mechanism involving both osteoblast and osteocytes in its molecular regulation (Dallas et al., 2013). As the osteoblast lays down osteoid, that is subsequently mineralised, it changes shape from cuboidal to the characteristic spindle shaped osteocyte with cytoplasmic processes (dendrites) containing fewer organelles and increased nucleus-to-cytoplasm ratio (Palumbo, 1986). Recruitment of new osteoblasts committed to this pathway has been reported to be influenced by osteocyte secreted molecules like PGE_2, insulin growth factor 1 (IGF-1), NO, and sclerostin which antagonises the pathway (Schaffler et al., 2014).

Also the products of the osteocyte genes such as *Sost*, *Dmp1*, and *Phex* have been reported to be actively involved in bone mineralisation (Fig. 1.5), phosphate homeostasis and cytoskeletal organisation (Guo et al., 2010, Dallas et al., 2013).

1.3.3.2 Dentin matrix protein 1 (Dmp1)

Dmp1 is a member of the small, integrin-binging ligand, N-linked glycoprotein (SIBLING), located in bones and dentin regulating matrix mineralisation amongst other functions (Staines et al., 2012). Dmp1 is expressed in embryonic chondroblasts and osteoblasts but limited in osteocytes during adult life (Toyosawa et al., 2001). It regulates phosphate homeostasis and bone mineralisation as disclosed in the study of *Dmp1*-null mice which have low blood phosphate levels and poor mineralisation (Feng et al., 2006). Similarly in humans *DMP1* loss of function mutation has been diagnosed in hypophosphatemia rickets (Feng et al., 2006). *Dmp1* gain of function studies in mice have reported conflicting results; some studies have shown the absence of any effect on bone whereas others have reported elevated bone mineral density. The mechanism of Dmp1 regulation of bone mineralisation and osteocyte differentiation is sequel to its action in maintaining body phosphate homeostasis (Lu et al., 2011, Zhang et al., 2011, Bhatia et al., 2012).

1.3.3.3 Phosphate-regulating gene with homologies to endopeptidases on the X chomosome (Phex).

Phex is expressed by maturing osteocytes and is involved in bone matrix phosphate and mineralisation regulation in a similar manner to Dmp1 (Liu et al., 2007). *Phex* loss of function is seen in X-linked hypophosphatemic rickets, a disease characterised by

poor growth, deficient bone mineralisation, and hypophosphatemia caused by poor phosphate retention in the kidneys (Sabbagh et al., 2003). The effects of Phex on phosphate regulation is though moderation of FGF-23, another osteocyte signalling factor, that acts like an endocrine factor on the kidneys' sodium/phosphate cotransporters that are crucial for renal phosphate uptake (Larsson et al., 2004, Gattineni et al., 2009). Hence, in *Phex* loss of function mutations, FGF-23 levels increase by an unclear mechanism leading to hypophosphatemia (Larsson et al., 2004).

1.3.3.4 Sclerostin

The *Sost* gene that encodes the protein sclerostin was first identified as a mutation manifesting in Sclerostosis and Van Buchem diseases in humans, both of which are characterised by high bone mass (Bezooijen et al., 2005). The gene is expressed only in mature osteocytes (Brunkow et al., 2001, Winkler et al., 2003). Sclerostin is a negative regulator of bone formation and acts via the Wnt/β-catenin pathway (Li et al., 2005b). *Sost* loss of function mutations in mice are characterised by increased bone mass and strength, while reduced bone mass is seen in *Sost* gain of function mutations (Winkler et al., 2003, Li et al., 2008b). One function ascribed to osteocytes is their ability to regulate bone turnover in response to load bearing. This property is, mediated in part by sclerostin expression, which is consistent with the observation that loading down-regulates sclerostin expression and thereby promoting bone formation. Recently anti-sclerostin monoclonal antibodies (Romosozumab (AMG

785)) have undergone clinical trials for the management of bone disorders associated with low bone mass such as osteoporosis (Ominsky et al., 2011, Padhi et al., 2011).

1.4 Podoplanin/E11

The protein podoplanin/E11 is a mucin type transmembrane glycoprotein of about 38-42 KDa , encoded by the *Pdpn* gene (Fig. 1.6; written in this thesis as 'E11'). The name E11 was first used to describe its expression in rat osteocytes (Wetterwald et al., 1996). Moderately conserved homologues exists in other species which include humans, mice, rats, dogs and hamsters (Astarita et al., 2012). It has several regulatory functions that include cell development and differentiation, epithelial-mesenchymal transition (EMT), oncogenesis and invasiveness (Thiery, 2002, Wicki and Christofori, 2007, Martín-Villar et al., 2009, Astarita et al., 2012).

1.4.1 The structure and expression of E11

The protein E11 has an extracellular domain (EC), transmembrane Section (TM) and a cytoplasmic tail (CT) (Fig. 1.6). The CT has the fewest amino acids and is therefore short in relation to the other domains/Sections (Martin-Villar et al., 2005, Kaneko et al., 2006). While the EC domain is involved in stimulating platelet aggregation (Kaneko et al., 2006) the TM domain has been reported to be a key factor in initiating EMT (Fernández-Muñoz et al., 2011) whereas the CT is associated with intercellular adhesion stability and is a binding site for ezrin, radixin and moesin (ERM) proteins (Astarita et al., 2012).

In platelets and immune cells, a C-type lectin-like receptor CLEC-2 has been described for E11 , where it facilitates platelet clumping on oncogenic cells despite the

absence of blood clotting factors (Sawa, 2010). This interaction of E11 with CLEC-2 is associated with lymphatic vessel integrity and invasive cancer regulation (Kato et al., 2005, Bertozzi et al., 2010). Owing to its expression in several body tissues (Fig. 1.7), E11 has several names, which include podoplanin in kidney podocytes; T1α in alveolar type 1 epithelial cells; and OTS-8 in osteoblasts following phobol ester treatment. It is also called PA2.26 in skin keratinocytes, gp38 in lymphoid organs and E11 in lymphatic endothelial cells and bone cells (Farr et al., 1992, Wetterwald et al., 1996, Breiteneder-Geleff et al., 1997, Scholl et al., 1999, Ramirez et al., 2003). It is highly expressed by various cell types in many tissues and in bone; it is expressed highly by embedding osteocytes but not osteoblasts. Specifically, it is highly expressed by the both the osteocyte body and its dendritic processes which connect neighbouring osteocytes but also surface osteoblasts (Fig. 1.6). The essential expression of E11 in lung cells and lymphatics results in E11 global KO mice are non-viable immediately after birth due to respiratory failure and generalised lymphoedema (Ramirez et al., 2003, Ekwall et al., 2011).

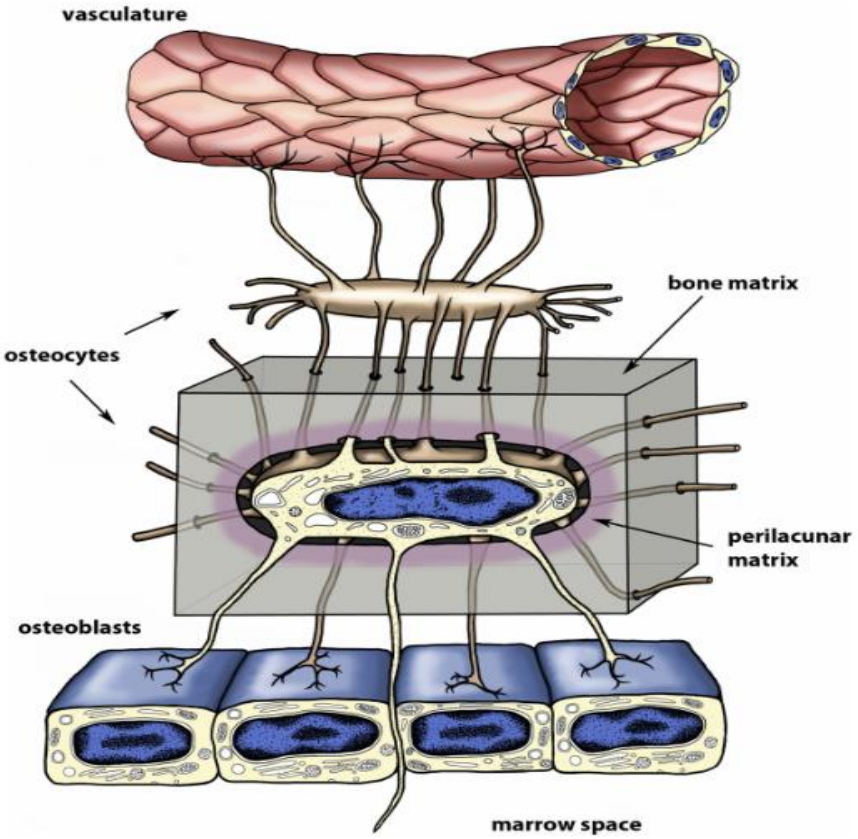

Figure 1.4. Graphic representation of an osteocyte embedded in mineralised matrix.

Note the extending dendrites connected to other osteocytes, osteoblasts and vasculature (Dallas et al., 2013).

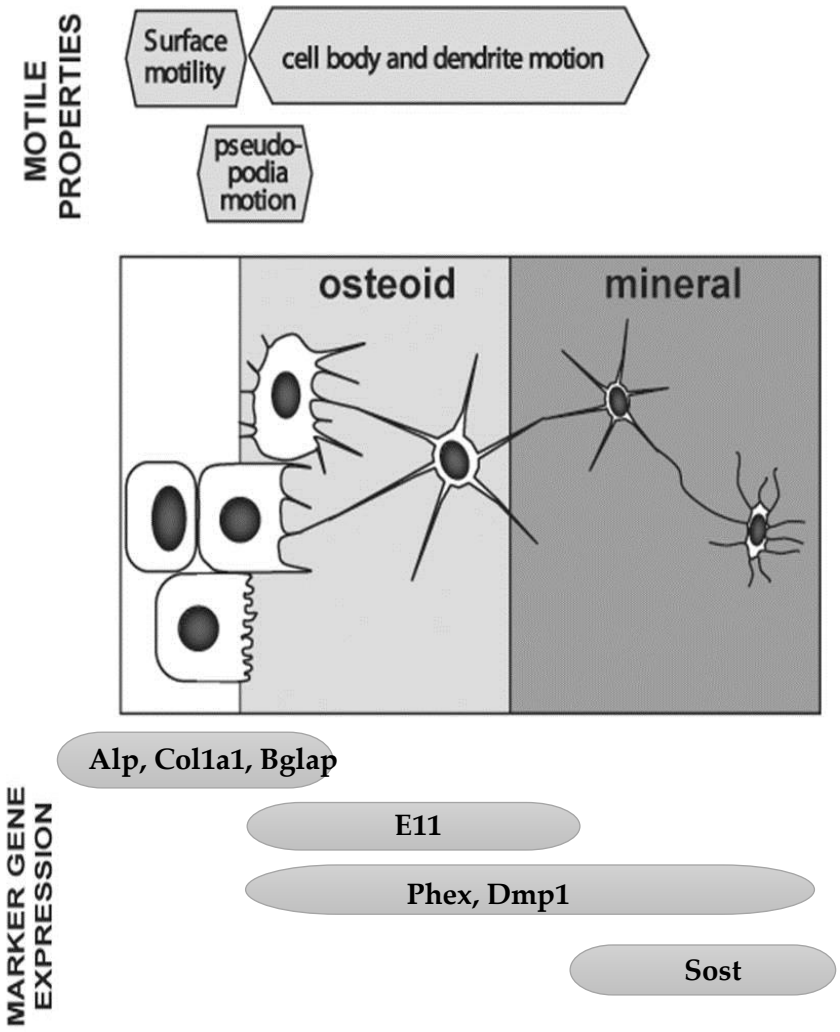

Figure 1.5 Gene markers expressed as osteocytogenesis progresses from osteoblast to mature osteocyte.

E11 early osteocyte marker is expressed as dendrites form while sclerostin expression indicates attainment of mature osteocyte. Adapted from (Dallas and Bonewald, 2010)

1.4.2 The function of E11 in osteocytogenesis

Plasma membrane shape, stability and re-organisation is the function of the cells cytoskeleton. The elements involved in this cytoskeletal/plasma membrane interaction include actin and keratin filaments, CD44, ERM proteins, small GTPase RhoA, and E11 (Fig. 1.6) (Hirao et al., 1996, Astarita et al., 2012). The ERM family of related proteins are associated with having a cross-linker function in their relationship with the plasma membrane protein CD44, forming the CD44/ERM complex that is enhanced by phosphatidylinositol 4,5-bisphosphate (Hirao et al., 1996), and RhoA is believed to act as a molecular regulator of this complex (Hirao et al., 1996). E11 is a recognised early osteocyte marker associated with the acquisition of the dendritic morphology, as enhanced post translational stability of E11 through the prevention of its proteosomal degradation extended osteocyte dendrite length and promoted osteocytogenesis (Zhang et al., 2006, Gupta et al., 2010, Staines et al., 2016). This osteocyte dendritic phenotype which reflects a re-arranged actin cytoskeleton, can be linked to the ability of E11 to regulate RhoA as is the case during EMT (Sawa, 2010). E11 expression has been reported to be increased by mechanical loading and during differentiation and mineralisation of some osteoblast cell lines such as 2T3 and OCT1 (Zhang et al., 2006).

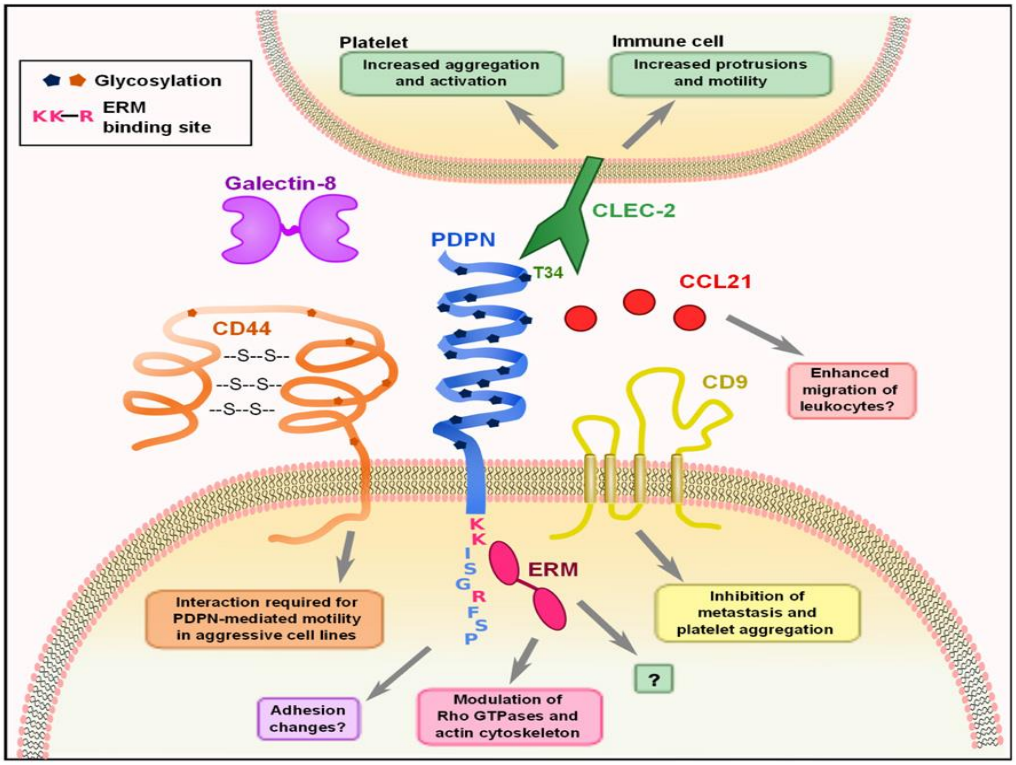

Figure 1.6 Schematic representation of E11 (PDPN) showing interaction with other molecules especially as it regards cytoskeletal reorganisation.

Note its receptor CLEC-2; relationship with cytoskeletal apparatus molecules like CD44, ERM and RhoA (Astarita et al., 2012).

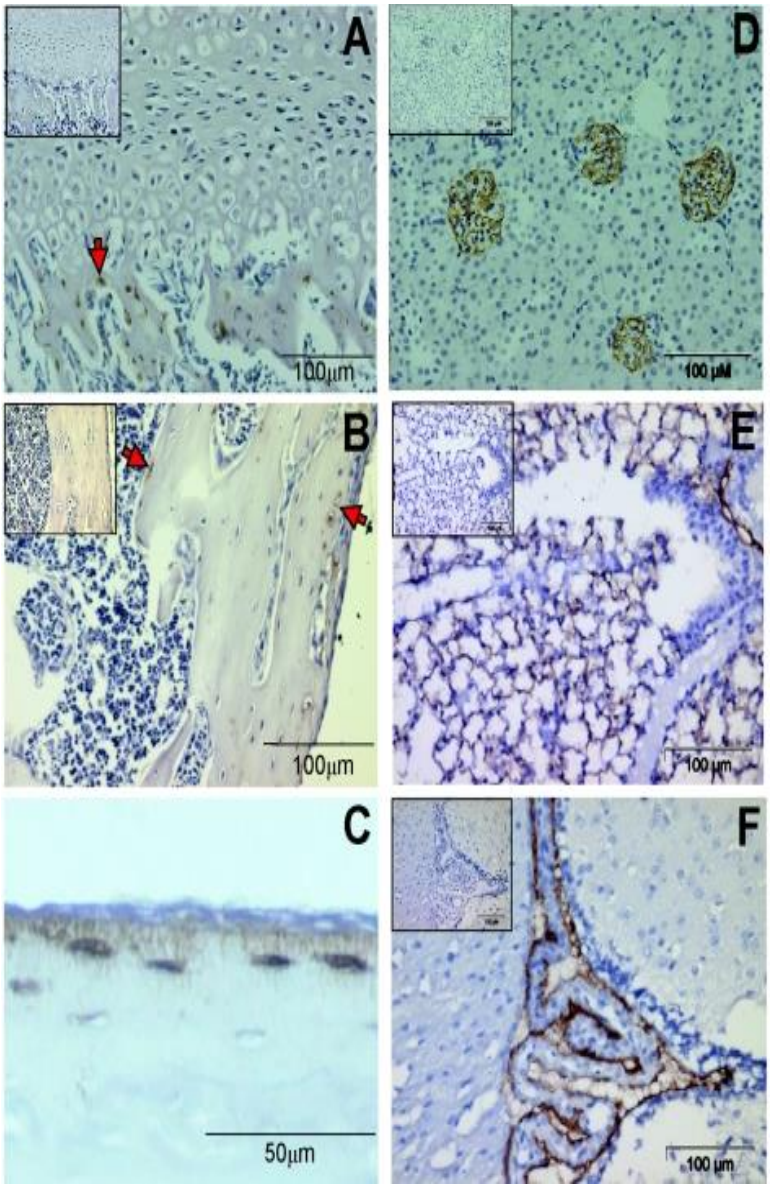

Figure 1.7 Immunostaining of E11 in various body tissues

Immunostaining for E11 in various tissues showed positive staining in trabecular bone osteocyte (A), cortical bone osteocytes (B), cortical bone osteocyte cell body and dendrites are positive, and not the surface osteoblasts (C), podocytes of the kidney glomeruli (D), lung type 1 alveolar cells (E), and (F) the brain choroid plexus. Insets show negative controls (Zhang et al., 2006).

1.5 Fibroblast growth factor (FGF) biology

The FGF family of signalling molecules interact with receptors, co-receptors and mediating molecules to play critical roles in vertebrate growth, development, body homeostasis, and disease pathogenesis (Powers et al., 2000, Bottcher and Niehrs, 2005). Members of the family include the ligands, which are the growth factors (FGFs); their transmembrane receptors called fibroblast growth factor receptors (FGFRs) that are cell surface receptor tyrosine kinases (RTKs). The FGFs are transcribed from 10 genes in zebrafish and 22 genes in mice and humans (Table 1.1) (Thisse and Thisse, 2005). FGF1-10, FGF16-18, FGF-20 and FGF-22 are secreted ligands with paracrine signalling properties and bind to FGFRs in close association with heparan sulphate proteoglycan (HSPG) co-factors. In contrast, FGF19, FGF-21 and FGF-23 are endocrine molecules that require Klotho proteins to activate FGFRs (Yang et al., 2015, Katoh, 2016, Sarabipour and Hristova, 2016) .

1.5.1 Fibroblast growth factor receptors (FGFRs)

Central to the activating property of the FGFs are the single-pas transmembrane proteins referred to as the FGFRs (Dailey et al., 2005, Sarabipour and Hristova, 2016). In mammals, FGFRs are encoded by four specific genes (*Fgfr1-4*), with 55-72% amino acid homology (Givol and Yayon, 1992, Powers et al., 2000, Bottcher and Niehrs, 2005). Also documented are the generation though splicing of other isoforms like FGFR5/FGFRL1 (Rieckmann et al., 2008).

The importance of FGFR activation or downregulation is not limited to physiological growth and development, FGFR mutations and over-expression have been

demonstrated in several developmental and post-natal disorders including Crouzon, Apert, and Pfeiffer syndromes (Burke et al., 1998, Sarabipour and Hristova, 2016). Also these FGFR have been implicated in cancer aetiology *e.g.* 1) FGFR4 expression is increased in terminal stages of mouse pancreatic β-cells cancer but not in the early stages of the disease (Olson et al., 1998), 2) FGFR3 is detected in human multiple myeloma (Richelda et al., 1997), 3) FGFR2 has been implicated in T-lymphocyte metastasis (Hattori et al., 1992) 4) FGFR1 has been reported in human breast cancer (Yoshimura et al., 1998), and 5) some myeloproliferative diseases (Popovici et al., 1998, Reiter et al., 1998).

Structural analysis of the FGFRs reveals an extracellular (EC) ligand binding immunoglobulin-like domain (IgD), a short transmembrane (TM) connecting domain, and two intracellular tyrosine kinase (TK) domains. The latter contains a juxtamembrane domain and a kinase domain containing an ATP-binding site and a cytoplasmic tail (CT) (Thisse and Thisse, 2005, Gotink and Verheul, 2010). FGFR5/FGFRL1 unlike other FGFRs lacks a TK (Ornitz and Itoh, 2015). The FGFR extracellular domain has several IgDs but IgD1, -2, and -3 have been most widely studied. While IgD1 is not associated with any specific function, IgD2 has a heparin binding site, and the region between IgD2 and IgD3 is the active FGF binding site (Thisse and Thisse, 2005). The IgD3 of FGFR1-3 has two main splice variants IgD3b and IgD3c.

Receptor dimerisation occurs with FGF binding and this initiates the cascade of events that accumulates in FGFR phosphorylation at its CT. This activates

downstream signalling pathway including MAPKs, PI3K/Akt, protein kinase C (PKC) and signal transducer and activator of transcription (STAT) (Turner and Grose, 2010, Su et al., 2014).

There is evidence that while the biological effects of FGFs can be dose-dependent, they can also be stage-dependent following activation of a specific receptor, even though redundancy has been reported amongst the FGFRs in the mature skeleton (Jackson et al., 2006, Soltanoff et al., 2009). In cartilage, FGFR1 is mostly upregulated by mitogens, whereas FGFR3 is upregulated during differentiation and morphogenic response (Weksler et al., 1999, Wang et al., 2001, Li et al., 2008a). In osteoblasts, FGFR1 is expressed principally during differentiation whereas FGFR2 expression is predominantly observed during osteoblast proliferation. Interestingly FGFR3 expression is observed in during both differentiation and proliferation (Marie, 2003, Fakhry et al., 2005, Jackson et al., 2006, Marie, 2012).

1.5.2 FGF-2 and its downstream signalling molecules

FGF-2 initially was characterised as a 15kDa molecule isolated from bovine pituitary and brain, with mitogenic capacity on mouse 3T3 fibroblasts (Armelin, 1973, Gospodarowicz et al., 1974). It was then named basic FGF (bFGF) to buttres its high isoelectric point (Gospodarowicz, 1975, Gospodarowicz et al., 1978). FGF-2 is described as the most studied member of the FGFs family (Mundhenke et al., 2002, Behr et al., 2010). This almost ubiquitously expressed FGF-2 (Dailey et al., 2005), has three isoforms: one low molecular weight isoform of 18kDa that is cytoplasmic located. Its secretion is associated with typical FGF-2 effects on bone formation. The

other isoforms are two high molecular weight isoforms of 21 and 22kDa located in the nucleus and mostly related to phosphate homeostasis (Xiao et al., 2010a, Su et al., 2014).

Basic fibroblast growth factor or FGF-2 is expressed by osteoblasts and stored in the ECM (Hurley et al., 2002, Fei et al., 2011). It is a member of the FGF large family of polypeptide growth factors involved in several developmental mechanisms including skeletal development in several multicellular organisms (Itoh and Ornitz, 2004, Thisse and Thisse, 2005). At optimal expression, it is involved in normal bone formation, where as its absence in genetically altered knockout mice is associated with poor bone formation and mass (Coffin et al., 1995, Montero et al., 2000). *In vitro*, FGF-2 down regulates osteoblast markers such as collagen type 1 and regulates genes controlling mineralisation during osteoblast differentiation (Fang et al., 2001, Kyono et al., 2012). FGF-2 is also involved in the regulation of bone matrix protection by inducing the expression of tissue inhibitors of metalloproteinases – TIMPs (Varghese et al., 1995). It is involved in the catabolic pathways of the bovine intervertebral disc (Li et al., 2008a). While redundancy amongst the FGFs is known, the attachment of HSPG to the EC domain of the FGFR confers some specificity to the FGF ligand including FGF-2 (Ornitz and Marie, 2002, Mundhenke et al., 2002, Debiais et al., 2004). The regulatory effects of FGF-2 ligand after attachment to FGFR1-4 is mediated though cell signalling pathways such as MAPKs, PI3K/Akt and phospholipase C (PLC) ɣ pathways. The MAPKs family (Fig 1.8) include the extracellular signal-related kinases (ERK1/2), stress-activated protein kinase/c-Jun N-terminal kinase

(SAPK/JKN) and p38 MAPK pathways (Kim et al., 2003, Jackson et al., 2006, Li et al., 2008a, Eda et al., 2008, Kyono et al., 2012, Fei and Hurley, 2012). MAPK signalling is controlled by three-level kinase cascades consisting of MAPK, MAPK kinase (MEK, MKK, and MAPKK), and MAPKK kinase or MEK kinase (MAPKKK or MEKK) (English et al., 1999, Chang and Karin, 2001, Chaudhary and Hruska, 2001).

1.5.2.1 Extracellular signal-related kinases (ERK1/2)

ERK1/2 has been described as the major pathway mediating FGF effects in skeletal cells (Murakami et al., 2004, Matsushita et al., 2009b), especially osteoblast and chondroblast differentiation (Matsushita et al., 2009a). Studies using the MEK (upstream to ERK1/2 in the Ras-MAPK pathway) inhibitor U0126, revealed the downregulation of the skeletal cell mineralisation gene *Dmp1*, and lack of the osteocyte dendritic phenotype in MLO-Y4 cells (Kyono et al., 2012). This report supports the increasing data on the central role of ERK1/2 molecules in FGF signalling during osteocyte differentiation (Murakami et al., 2004). ERK1/2 activation is associated with cell proliferation, differentiation, survival, and protection against apoptosis (Allan et al., 2003, Arrington et al., 2012).

Species	Number of FGFs	FGF ligands (Subfamilies)	Receptor	Co-receptor	Signalling property
Zebrafish	10	FGF2–4, 6, 8, 10, 17a, 17b, 18, 24	FGFR	HSPG	paracrine
Xenopus	6	FGF2–4, 8–10	FGFR	HSPG	paracrine
Chickens	13	FGF1–4, 8–10, 12, 13, 16, 18,20	FGFR	HSPG	paracrine
		FGF19	FGFR	Klotho	endocrine
Mice	22	FGF1–18,20	FGFR	HSPG	paracrine
		21, 23	FGFR	Klotho	endocrine
Human	22	FGF1–14, 16–18, 20, 22	FGFR	HSPG	paracrine
		FGF19, 21, 23	FGFR	Klotho	endocrine

Table 1.1 Summary of FGFs biology
Note the ligand number per species, specific co-receptors and the different signalling property (Yun et al., 2010).

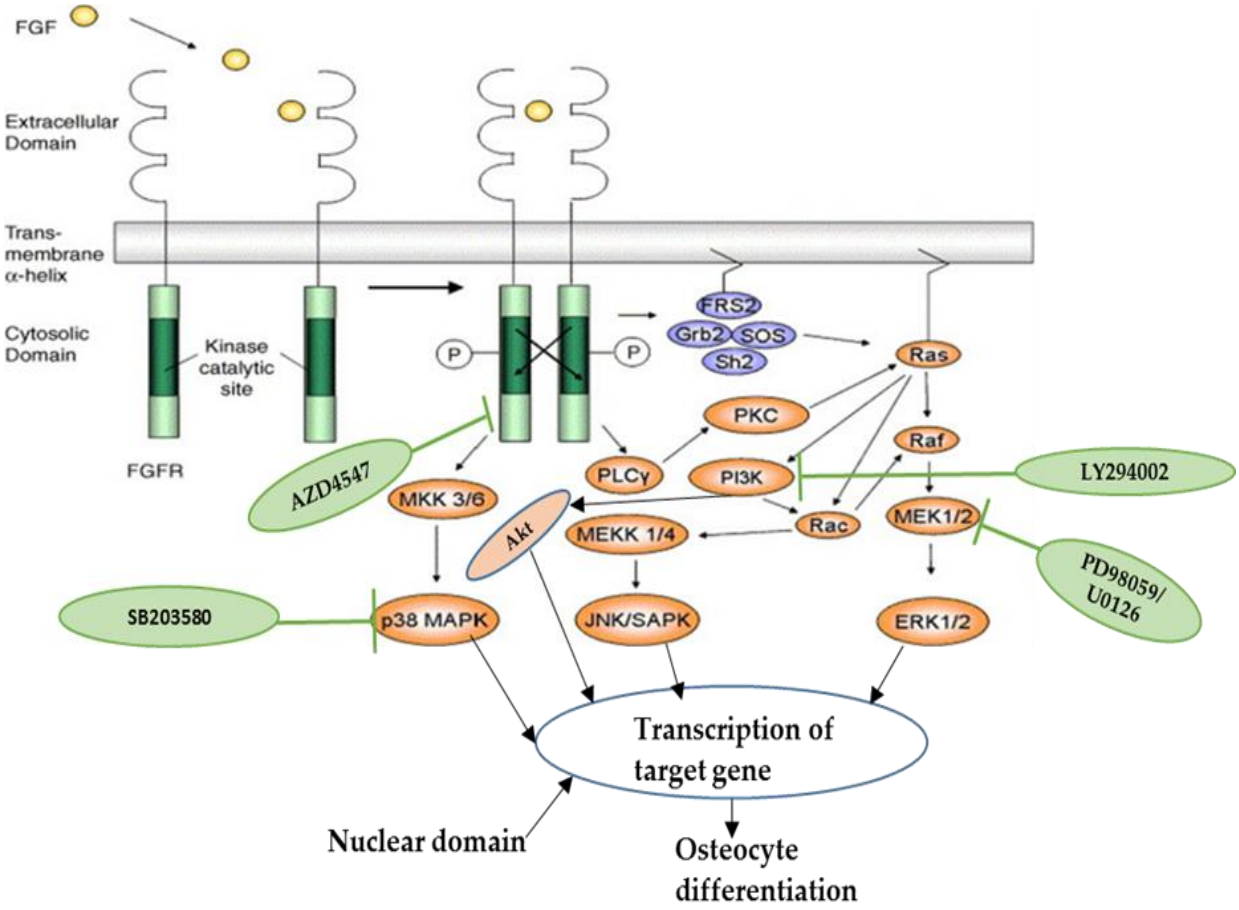

Figure 1.8 Schematic of FGF signalling.

Binding of the FGF to its receptor (FGFR) activates downstream signalling pathways including MAPK-mediated pathways. The inhibitors to these pathways are highlighted in green oval shapes (MEK inhibitors, PD98059 and U0126; PI3K inhibitor, LY294002; p38 MAPK inhibitor, SB203580; and FGFR1/2/3 inhibitor, AZD4547. Adapted from (Jackson et al., 2006).

1.5.2.2. Phosphatidylinositol 3 kinase/Akt (PI3K/Akt)

Protein kinase B (PKB), also known as Akt, in mammals. It has three isoforms expressed by three genes namely: *PKBα*/*Akt1*, *PKBβ*/*Akt2*, and *PKBɣ*/*Akt3* (Song et al., 2005). Generally, Akt phosphorylation is involved in the regulation of tissue size, metabolite homeostasis like glucose, new blood vessel formation, cell cycle progression, apoptosis, and cell survival (Chaudhary and Hruska, 2001, Suhara et al., 2002). In osteoblasts, the activation of the PI3K/Akt pathway after FGF-2 stimulation, mediates cell survival including protection from apoptosis signalling (Debiais et al., 2004). This role of phosphorylated Akt in the inhibition of apoptosis signalling involves caspase-3 cleavage, activation of B-cell lymphoma 2 (Bcl-2), Bcl-2 associated death promoter (Bad) and blocking of mitochondrial cytochrome C release (Suhara et al., 2002, Song et al., 2005). During neuronal differentiation of pheochomocytoma cell line (PC12) under the stimulation of nerve growth factor (NGF), Akt is involved in cytoskeletal re-organisation leading to neurite formation (Jeon et al., 2010).

1.5.2.3 p38 MAPK

This p38 MAPK molecule has four isoforms including p38α, p38β, p38ɣ, and p38δ MAPKs, which are all activated by MEK3/6 of the MAPK pathway (Chang and Karin, 2001). The isoforms p38α and p38β MAPKs are expressed universally in most tissues; p38ɣ MAPK has been localised in the muscle; while p38δ MAPK is limited to kidney and lungs (Hu et al., 2003, Cuenda and Rousseau, 2007). Even though p38 MAPK is associated with apoptosis, there is a growing body of evidence that it has a critical role in embryogenesis, as deletion of one of its isoforms p38α, leads to embryonic

death due to inadequate synthesis of erythopoietin (Chang and Karin, 2001). Functionally in a number of cells including the osteoblast, it regulates cell growth and differentiation, stress and inflammatory response that enhances cell survival (Hu et al., 2003, Hong et al., 2015).

1.5.2.4 Stress-activated protein kinase/c-Jun N-terminal kinase (SAPK/JNK)

JNK consists of 3 isoforms and was originally characterised by its specific capacity to phosphorylate the transcription factor c-Jun at its N-terminal transactivation domain (Hibi et al., 1993). These isoforms are JNK1, 2 and 3, which are expressed by individual genes, have been localised in most body tissues, with the exception of JNK3 that is principally isolated to the brain, testis and heart (Kyriakis and Avruch, 2001). The molecular weight of these isoforms varies, as JNK1 is 46kDa, whereas JNK2 and JNK3 are predominantly 56kDa (Matsuguchi et al., 2009). Functional and structural similarities, as well as specific differences exist amongst these isoforms. JNK1 up-regulates c-Jun-dependent fibroblast proliferation (Sabapathy et al., 2004), and TNF-α stimulated apoptosis (Liu et al., 2004). There is a report of JNK signalling being involved in apoptosis regulation in vascular smooth muscle cells (Villunger et al., 2000). These isoforms are activated by MEK4/7 in the MAPK cascade signalling (Chang and Karin, 2001).

1.5.2.5 Cell signalling and the use of inhibitors

Signalling pathways are integrated protein to protein interactions mediating cell activities and relationships with other cells (Martin, 2003). Even though they are complex networks, they are strictly conserved, with some reports of redundancy (McCormick, 2000). Various models have been utilised in exploring the nature and

mechanism of action of these signalling pathways. These include the use of monoclonal antibodies, siRNA gene silencing, dominant negative mutants and chemical inhibitors (Alessi et al., 1995, McCormick, 2000, Gotink and Verheul, 2010). Chemical inhibitors are small sized hydrophobic molecules with the ability to pas though the cell membrane. This property readily distinguishes them from monoclonal antibodies (Imai and Takaoka, 2006). Inside the cell, some of these hydrophobic molecules quickly associate with cytoplasmic domain of receptors and their downstream signalling molecules especially at their Adenosine Tri-Phosphate (ATP) binding site. This association is marked by their competition with ATP, denying the receptors or downstream molecules the critical ability to be phosphorylated (Fig. 1.9). This prevents the cascade of such signalling pathways (Gotink and Verheul, 2010). This mechanism is observed with type I inhibitors such as epidermal growth factor receptor (EGFR) inhibitors PD15870 and ZD1839, FGFR inhibitors BGJ398 and AZD4547, PI3K/Akt inhibitor LY294002, and p38 MAPK inhibitor SB203580 (Rewcastle et al., 1996, Wakeling et al., 1996, McCormick, 2000, Tan et al., 2014, Fisk et al., 2014).

Another mechanism of action of some kinase inhibitors, which are not direct ATP-competition dependent, involves the binding to the hydrophobic pocket situated adjacent to the ATP-binding site (Fig. 1.9). This induces a conformational change in the kinase. This indirectly prevents kinase activity as the allosteric change stops ATP binding. Examples of these are type II inhibitors such as MEK inhibitors PD98059 and

U0126 and the VEGFR inhibitor, sorafenib (Alessi et al., 1995, Favata et al., 1998, Wan et al., 2004, Fisk et al., 2014).

Some kinase inhibitors have been classified into type III inhibitors based on their ability to form covalent bonds with cysteines at designated locations of the kinase (Gotink and Verheul, 2010). They are thus referred to as *covalent* inhibitors and most of their effects are irreversible like the FGFR inhibitors FIIN-2 and FIIN-3 (Tan et al., 2014).

On a general note, the ability of these three classes of kinase inhibitors described above to prevent the specific action of any target pathway without hindering the activation of other pathways in cells have been exploited in their deployment as therapeutic agents in some diseases such as cancer (McCormick, 2000, Gotink and Verheul, 2010).

1.6. Osteoarthritis (OA)

OA is a painful joint disorder and a major world-wide health concern. It has significant implications for health budgets and is associated with the loss of productive working hours due to attendant morbidity (Funck-Brentano and Cohen-Solal, 2011, Bouaziz et al., 2015). OA is characterised by articular cartilage (AC) loss, subchondral bone (SCB) sclerosis, joint space narrowing, synovitis, thickened fibrous capsule, osteophyte formation, cysts and loss of joint function (Funck-Brentano and Cohen-Solal, 2011, Blom et al., 2009, Quasnichka et al., 2006).

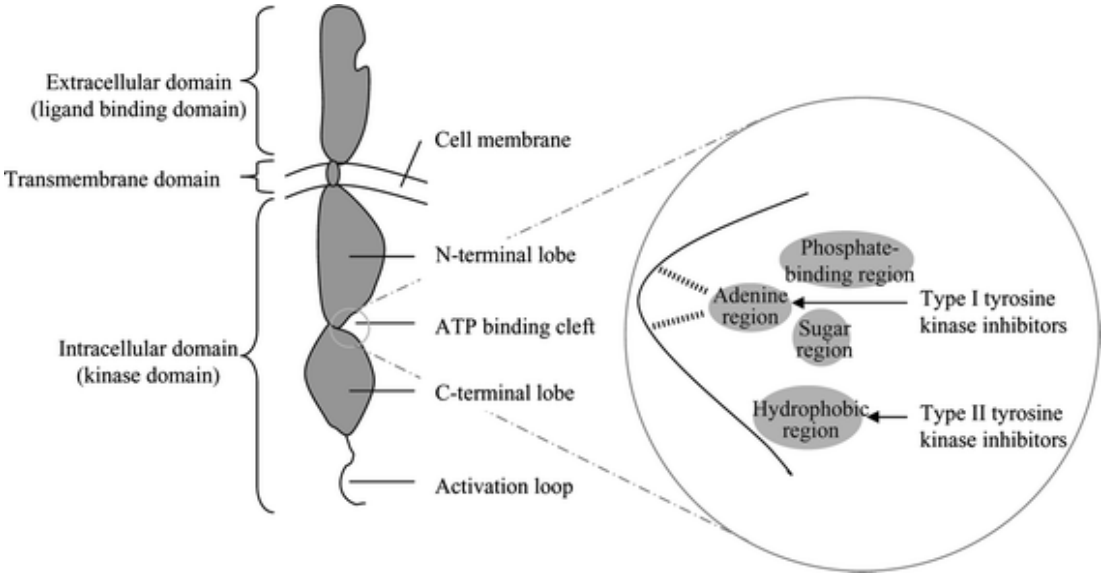

Figure 1.9 Structure of receptor tyrosine kinase.

Note the sites of action of its inhibitors (Gotink and Verheul, 2010).

While OA can develop in any synovial joint, knee, hip, hands and vertebrae remain the most prevalent predilection sites.

OA affects mostly middle aged and older people with older women affected more severely due to reduced oestrogen levels in post-menopausal life (Buckwalter and Martin, 2006, Roman-Blas et al., 2009). Oestrogen, as a sex steroid, is generally protective to both bone and cartilage via activation of an anti-apoptotic pathways in osteocytes and upregulates chondrocyte glycosaminoglycan's expression (Chen et al., 2005, Maneix et al., 2008). Although the fundamental cause(s) of OA are unknown, it is recognised to be a multifactorial disorder (Lorenzo et al., 2004, Lajeunesse, 2002, Jaiprakash et al., 2012). OA has been broadly divided into primary and secondary types based on some predisposing factors such as ageing which is associated with primary OA, whereas secondary OA is correlated with sporting injury, joint malalignment, hereditary, sedentary life and obesity (Blom et al., 2009).

The initiation and progression of OA remains an issue of controversy to both clinicians and researchers alike (Kawcak et al., 2001). Owing to the observable cartilage destruction and loss at late stages of OA, it has traditionally been designated an AC disorder (Quasnichka et al., 2006). However, changes in the SCB thickness is one of the earliest detectable radiographic signs in OA (Jaiprakash et al., 2012). This sclerosis physically negatively impacts on AC during repetitive loading or stress leading to AC damage, thereby suggesting that the SCB should be targeted to relieve the pathogenesis of OA (Radin and Rose, 1986, McIlwraith et al., 2010). Regardless, it is clear that OA is a disorder of the entire joint including the AC, SCB, synovium,

capsular tissues, and ligaments (Kannus and Rvinen, 1989, Lajeunesse, 2002, Quasnichka et al., 2006, Goldring and Goldring, 2010, Li et al., 2013).

1.6.1 Normal synovial joint: structure and function

A joint simply described is where bones meet and articulate. Structurally, it is classified based on the binding tissue into fibrous, cartilaginous and synovial joints. Functionally, a joint can also be classified based on the type and gradation of movement allowable and in this classification we have synarthodial, amphiarthodial and diarthodial joints (van Weeren, 2016a). Of these types, the synovial joint is the most abundant in the mammalian body allowing the most movement, hence is also referred to as a diarthodial joint.

Structurally, a typical synovial joint consist of a joint capsule which comprises of an outer fibrous membrane continuous with the articulating bone periosteum, and an inner synovial membrane secreting the synovial fluid (Pacifici et al., 2005). There is a smooth slippery articular cartilage of the hyaline type with no perichondrium (Lorenz and Richter, 2006). This AC covers the underlying SCB in articulating bones (Decker et al., 2014). The AC is separated into a superficial non-calcified cartilage and a deeper calcified cartilage (CC) by a non-fixed borderline referred to as tidemark that appears basophilic in routine light microscopy (Li et al., 2013). The CC component is in direct contact with the SCB at the osteochondral junction. The SCB consist of two anatomical components: the subchondral bone plate and the subchondral trabecular bone (Goldring and Goldring, 2010). Other synovial joint structures include articular discs

or menisci, articular fat pad, tendon, bursa, and accesory ligaments that maybe extracapsular-fibular collateral ligament or intracapsular-cruciate ligament (Pacifici et al., 2005).

Functionally, the synovial joint allows movements such as abduction, adduction, extension, flexion and rotation. The joint components such as synovial fluid are involved in lubrication, shock absorption, nourishment and metabolic waste removal (Lorenz and Richter, 2006). The AC is associated with shock absorption and reduction in friction during movement (Kawcak et al., 2001) whereas the SCB is the major load absorber across the joint and it maintains the joint space and nourishes the CC by diffusion though its vascular network (Milz and Putz, 1994, Li et al., 2013). The bursa develops to reduce mechanical friction between structures like bone and ligaments whereas the supportive role of ligaments help resist strains during movements dangerous to articulation. In general, the joint components are adapted for support, aiding ease of body movements in several directions (Kawcak, 2016).

Deviations from the normal anatomy and physiology of the synovial joints results in painful joint disorders like dislocation, gout, arthritis and sprains. Arthritis is a large family of illnesses within the joint disorders, including OA, rheumatoid arthritis, septic arthritis, and Still's disease (Wright et al., 2014, Bouaziz et al., 2015, van Weeren, 2016b). It may occur as a distinct condition, or appear secondary to other diseases.

1.6.2 Changes in AC in OA

Articular cartilage homeostasis involves the maintenance of the components of the ECM in a dynamic equilibrium in relation to the chondrocytes. The components of the inter-territorial matrix of the ECM include a network of collagen fibres and proteoglycans where aggrecan predominates. The collagen fibres present are mostly type II, type XI and type IX whereas the pericellular matrix is reported to contain mostly type VI collagen fibres (Goldring and Goldring, 2010).

The AC gradually losses colour, form and function during advancing OA. This phenotypic change is driven by increased levels of matrix degrading enzymes such as matrix metalloproteinases (MMPs), and aggrecanases (Lorenz and Richter, 2006); making the AC les viscoelastic, which are features associated with increased production of collagen type I and decreased production of type II collagen (Wenz et al., 2000, Lorenz and Richter, 2006). As OA progresses, the catabolic actions of these degrading enzymes is enhanced by the downregulation of their inhibitors by inflammatory cytokines such as Interleukins (IL) IL-1, IL-17, IL-18 and tumour necrosis factor alpha (TNF-α) (Martel-Pelletier, 1998). To compound this catabolic state, new cartilage ECM is not commensurately synthesised by the chondrocyte anabolic activities. The anabolic activities of healthy articular chondrocytes are induced by growth factors which include IGF-1, TGF-β, BMP, and FGFs (Fortier et al., 2011). This somewhat negative balance in cartilage ECM turnover results in the clasical feature of cartilage degradation and loss observed in most late OA radiographs (Sharma et al., 2013). This cartilage loss makes for the direct contact

between two articulating bones or bones and intact AC aggravating the symptomatic excruciating pain associated with late OA.

There are reports of increased vascularisation of the SCB (Fig. 1.10), which invades the CC during OA pathogenesis (Goldring, 2012, Jaiprakash et al., 2012). This vascular invasion of CC from SCB causes the establishment of new secondary centres of ossification in the CC leading to advancement and duplication of the tidemark towards the non-calcified cartilage, hence, thinning and the formation of microcracks in the AC and consequent loss due to shear stress (Radin et al., 1995, Goldring, 2012). This osteoarthritic CC expresses type X collagen, typical of hypertrophic cartilage in secondary centres of ossification providing supportive evidence for the reactivation of secondary centres of ossification (Hoyland et al., 1991). At this site of vascular invasion and newly established secondary ossification centre, nerve growth factor (NGF) and vascular endothelial growth factor (VEGF), are expressed by sensory nerve fibres and fibro-vascular tissue respectively (Walsh et al., 2007, Walsh et al., 2010, Ashraf et al., 2011).

1.6.3. Changes in the SCB in OA

The SCB of healthy joints is continuously remodelled which results in changes to its shape, architecture, volume, and mechanical properties. Alterations in elasticity are due to changes in ECM mineralisation (Kawcak et al., 2001). This remodelling is suggested to be orchestrated by osteocytes (Section1.3), and it enables the skeleton to actively respond to bone injury repair, and adapt to changing mechanical loading in the body (Burr, 2004, Martin, 2007, Chan et al., 2011).

SCB sclerosis, one of the defining features of OA observed prior to joint space narrowing (Jaiprakash et al., 2012), has been described as a product of bone remodelling in response to microdamage in the CC and SCB (Sokoloff, 1993, Radin et al., 1995). This sclerosis is characterised at the cellular level by dysregulated osteoblasts making more bone as there is a down regulation of sclerostin expression ; morphological and phenotypic changes in osteoclasts showing early increased resorption rate and later reduction; and decreased osteocyte dendrite number (Fig. 1.10) (Logar et al., 2007, Sanchez et al., 2008, Jaiprakash et al., 2012). Structurally, it is associated with stiffness, poor mineralisation, and poor adaptation to loading (Pool and Meagher, 1990). Osteocytes, though their expression of sclerostin, RANKL and OPG, are directly involved in bone remodelling and consequently SCB sclerosis (Li et al., 2005b, Nakashima et al., 2011b, Xiong et al., 2011). The down-regulation of sclerostin expression in OA may also aid AC degradation, as chondrocyte sclerostin expression has been demonstrated to be chondro-protective though its action on antagonising the cartilage catabolic protease, aggrecanase - a disintegrin and metalloproteinase with thombospondin motifs (ADAMSTS) 4/5 (Chan et al., 2011). Also MMP-1, -9, and ADAMTS4/5, which are well known mediators of matrix degradation are upregulated in sclerotic SCB (Jaiprakash et al., 2012).

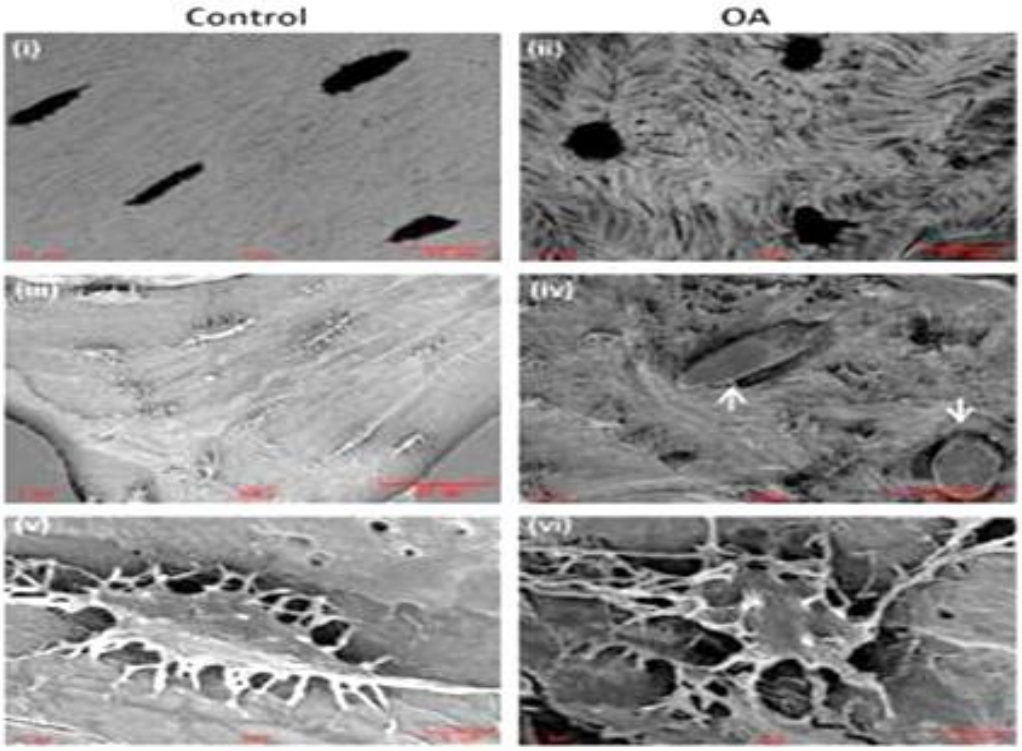

Figure 1.10 Architecture of dysregulated subchondral bone during OA.

Scanning electron microscopy images of osteocytes in OA showing poor osteocyte phenotype, vascular invasion, and dysregulated dendrites are suggestive of active involvement in OA pathogenesis (Jaiprakash et al., 2012).

1.6.4. Osteophyte formation

The development of osteophytes which cause pain and loss of function has been described as one of the hallmarks of OA (van der Kraan and van den Berg, 2007). They are mostly seen near joint margins, arising in the periosteal covering at the osteochondral junction (Menkes and Lane, 2004). Endogenous growth factors such as TGF-β, BMP2, and FGF-2 have been associated with their development and growth (Blaney Davidson et al., 2007, Kwan Tat et al., 2010). Also altered biomechanical forces on the joint have been implicated as drivers of their formation as osteophytes may help in the maintenance of joint stability (Menkes and Lane, 2004, Lorenz and Richter, 2006). This view is not universally accepted however as others have proposed that osteophytes may cause joint malalignment (Felson et al., 2005).

1.6.5. Other features of the OA joint

Bone marrow oedema or cyst formation is a frequent feature of the SCB in most OA patients. First described by Wilson et al., in 1988, it represents localised areas of bone marrow lesions of fat necrosis and fibrosis (Wilson et al., 1988, Taljanovic et al., 2008, Leydet-Quilici et al., 2010). Their formation are now considered part of the healing process for loading induced micro-fractures in SCB. Local ischaemia during SCB remodelling also contributes to cyst development (Bancroft et al., 2004, Carrino et al., 2006, Findlay, 2007). Histological evidence from studies on the role of synovial inflammation in OA pathogenesis is very suggestive that lymphocytic infiltration, cellular hyperplasia and changes in mediators of inflammation like ILs and TNFα are very common in OA (Benito et al., 2005, Wenham and Conaghan, 2010, Johnson et al.,

2016), although they are inconsistent between different studies. In a recent scholarly review a strong argument was made for the huge impact of synovitis in driving OA pathology such as inducing cartilage damage and early SCB thinning (Hügle and Geurts, 2017). However, some earlier reports have indicated absence of correlation between inflammation of the synovium and induced collagen destruction in the dog AC (Pelletier et al., 1985). Nevertheless, synovitis is very common in OA and studies exploring therapies targeting its inflammatory molecules during OA pathophysiology illustrates the importance of synovial health for proper joint function (Wenham and Conaghan, 2010).

1.7. FGF-2 signalling in OA

The role of FGFR in OA development is still unfolding. What is known now from both ligand and receptor knockout/inhibition studies suggest some species and developmental stage variation, and to some degree, ligand specificity (Weng et al., 2012). In human AC stimulated with FGF-2, the most expressed receptor is FGFR1, which has a catabolic effect by upregulating MMP-1 and MMP-13 and down-regulating aggrecan expression (Yan et al., 2012). The catabolic effect of FGFR1 signalling in human AC after FGF-2 stimulation has been corroborated in adult mice showing extensive AC degeneration (Weng et al., 2012). However, contrasting reports in murine OA cartilage shows that FGFR2 and 4 are the most commonly expressed receptors, in addition to the upregulation of FGFR3 may help explain the reported anabolic and chondro-protective effects of FGF-2 in this species (Chia et al., 2009, Li et al., 2012). However, while this possible explanation subsists, some researchers

insist that the specific roles of FGFR2 and 4 remain largely yet to be deciphered (Nummenmaa et al., 2015).

Nevertheless, some researchers have documented evidence associating FGF-2 with chondroprotection and delayed onset of OA in surgically destabilised murine joints (Chia et al., 2009, Li et al., 2012, Chong et al., 2013). This species variation maybe related to the type of FGFR activated by FGF-2 (Li et al., 2012, Nummenmaa et al., 2015).

FGF-2 is known to be released from cartilage upon injury and is able to change chondrocyte gene expression in *vitro*. One gene known to be regulated by FGF-2 is *E11* and this has been found in murine joints following surgical destabilisation (DMM model) and cartilage explant injury models. Specifically, *E11* expression was found to be FGF-2 dependent following injury to cartilage *in vitro* and to joint tissues *in vivo* (Chong et al., 2013). The importance of FGF-2 in driving gene (and protein) changes in the aetiology of OA is further emphasised by the observations that FGF-2 promotes both E11 expression in osteoblasts and the osteocyte phenotype (Gupta et al., 2010). It is therefore conceivable that whilst the role of E11 in osteocyte differentiation remains unclear in OA aetiology, *E11* expression and stability is controlled at various junctures and this may be key in terminal osteoblast differentiation and the acquisition of the osteocyte phenotype.

1.8 Aims and strategy

Cognizant of FGF-2 stimulation of E11 expression in cartilage explants and osteoblast-like cells, it is likely that FGF-2 will influence bone remodelling via increased osteoblast E11 expression and concomitant osteocyte dendrite formation. This in turn would therefore protect against the abnormal osteocyte morphology observed in SCB sclerosis in OA. Therefore, the aim of this project was to test the hypothesis that:

FGF-2 regulates E11 mediated osteocytogenesis and that E11 expression in SCB osteocytes protects against OA pathophysiology.

To undertake this investigation, the following aims were undertaken.

1. Examine the potential regulation of E11 expression and osteocyte formation by FGF-2.

   The osteoblast-like cell line (MC3T3), and primary osteoblasts (murine) in Chapter 3 were studied in culture and the relationship between FGF-2 stimulation and (i) E11 expression (gene and protein) (ii) the attainment of the osteocyte morphology and (iii) the expression of osteocyte markers like *Sost*, *Dmp1*, and *Phex*, was examined. This aim elucidated that FGF-2 upregulates E11 and other osteocyte marker genes in both MC3T3 cells and primary osteoblasts; thus promoting osteocytogensis in these cells.

2. Investigate the signalling pathways and cytoskeletal changes involved in FGF-2 regulation of E11 expression and dendrite formation in MC3T3 cells using chemical

inhibitors. The molecules under investigation were analysed using western blots, RT-qPCR and GLISA cytoskeleton assay kit.

The results of these in Chapter 4 indicated that the promotion of the osteocyte phenotype by FGF-2 is possibly via *Fgfr1* activation and increased E11 expression. The signalling pathway(s) involved however, remains unclear but may involve phosphorylation of signalling molecules such as ERK1/2, Akt and p38 MAPK.

3. Examination of E11 expression during OA pathology in *Fgf*-2 KO mice and canine tissues.

The relative expression of E11 in AC and SCB in normal and OA tissues was specifically examine using immunohistochemistry technique (Chapter 5). In addition, sclerostin was also examined. Optimisation of anti-mouse and anti-human E11 antibodies using various antigen-demasking agents on the SCB samples from the ovine, canine, feline and equine tissues were used for comparative studies. The canine OA samples showed significant increase in E11 immunolabelled SCB osteocytes when compared with the control samples. The SCB from mice and human OA samples showed no difference in osteocyte E11 and sclerostin immunolabeling.

In conclusion, these studies have established that FGF-2 regulates E11 during osteocytogenesis (Fig. 1.11), a mechanism that can help in understanding the biology of osteocyte during OA pathology.

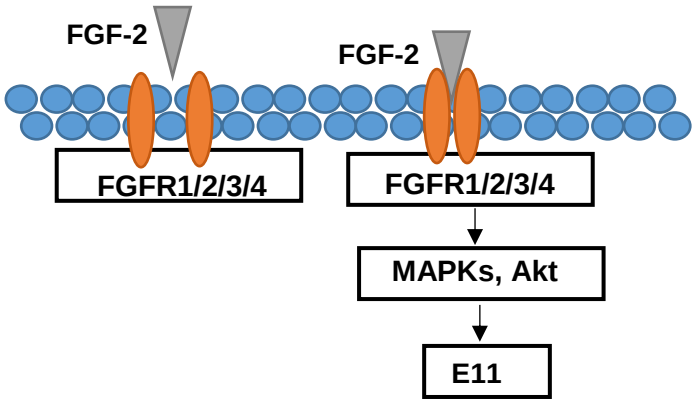

Fig. 1.11 Schematic of my project hypothesis.

This thesis will examine the hypothesis that: FGF-2 drives increased E11 expression during osteocytogenesis in MC3T3 osteoblast-like cells and primary osteoblasts, and this regulation occurs during OA pathophysiology.

Chapter 2

Materials and Methods

2.1. Biochemicals and solutions

Reagents for this work were obtained from Sigma-Aldrich (Dorset, U.K.) and cell/organ culture media and additives were sourced from Thermo Fisher Scientific (Paisley, U.K.) unless otherwise stated.

2.2. Cell and organ culture protocols

2.2.1. Thawing of cell lines

Murine MC3T3 osteoblast-like cells (clone 14; American Type Culture Collection ATCC, USA) were utilised throughout this thesis. Frozen cryovials of cells were thawed quickly from -150°C storage by warming in a beaker of 37°C water (Rosser and Bonewald, 2012). Cells were slowly pipetted into a universal and 5ml of warm (37°C) culture medium (αMEM supplemented with 10% v/v foetal bovine serum (FBS), and 0.05 mg/ml gentamycin) was added drop-wise to prevent osmotic shock and rupture of the cells. Cells were centrifuged at 9300 g for 5 min (Eppendorf Centrifuge 5415R, Eppendorf UK Limited), and the supernatant discarded. Cells were resuspended in 2ml of culture medium, and seeded into a T175 flask containing 23 ml (total volume) of culture medium in a humidified environment maintained at 37^{o}C and 5.0% CO_2 for approximately 3 days. When the cells were semi-confluent, the media was carefully removed from the flask and cells washed in phosphate buffered saline (PBS). Subsequently, 0.25% v/v trypsin-EDTA was added to detach the cells from the plastic surface. The detached cells were transferred to a universal, and 8ml of culture media was used to wash out the remaining cells in the flask and then transferred to the universal to deactivate the trypsin. The universal was centrifuged

at 1100g for 5 min. The supernatant was disposed of and the pellet dispersed with gentle pipetting in 1 ml of culture medium to enable resuspension of the cells. After thorough mixing, a haemocytometer was used to count the cells. The cells were subsequently plated down in 6-well plates at a seeding density of 1.0×10^4 cells/cm^2.

2.2.2. Calvarial osteoblast isolation

Under sterile conditions, the calvaria of 3 days old mice (strain C57BL/6) were dissected out and osteoblasts were isolated according to published literature (Orriss et al., 2012). After a brief wash in a universal containing Hank's balanced salt solution (HBS), they were digested with collagenase type II (1mg/ml) for 10 min at 37^{0}C in an automatic shaker. The supernatant was discarded. The collagenase digestion was repeated and the supernatant retained (fraction 1). The remaining calvaria were washed with PBS and the PBS was added to fraction 1. The calvaria were further incubated with 4 mM ethylenediaminetetraacetic acid (EDTA) for 10 min at 37^{0}C in an automatic shaker and the supernatant retained (fraction 2). The calvaria were washed with HBS and added to fraction 2. Fractions 1 and 2 were combined into one universal, centrifuged at 9300 g for 5 min. Subsequently, the cells were re-suspended in 3 ml of αMEM containing 10% v/v FBS and 0.05% v/v gentamycin before dividing equally into three T75 flasks containing 11 ml of culture media. Meanwhile, the calvaria were subjected to another 30 min collagenase digestion and the resultant supernatant was retained as fraction 3. Fraction 3 was centrifuged to pellet the cells before resuspending in 3 ml of culture media and dividing equally (1 ml each) into each of the three T75 flasks containing combined fractions 1 and 2. After 3 h

incubation in a humidified environment (37^0C and 5.0% CO2), the media was changed and the cells were expanded by maintaining them in culture for 3 days. The cells were then washed in PBS, trypsinised, pelleted and seeded in three T175 flasks containing 15 ml growth media and returned to a humidified incubator maintained at 37^0C and 5.0% CO_2 for approximately 3 days. The cells were finally plated down in 6-well plates at a seeding density of 1.0 x10^4 cells/cm^2.

2.2.3. Whole calvarial organ culture

Calvariae were dissected from 3 days old C57BL/6 wild-type (WT) mice under sterile conditions according to published literature (Mohammad et al., 2008, Orriss et al., 2012). Calvaria were transferred to pre-warmed calvaria culture media (α-MEM containing 0.2% w/v bovine serum albumin (BSA) and 0.05 mg/ml gentamycin) in a 12-well plate. Subsequently, the calvariae were cut mid-sagittal and the two hemi-Sections were cultured in calvaria culture media for 24 hours prior to experimentation. Calvaria hemi-Sections were cultured in a humidified incubator maintained at 37^0C and 5.0% CO_2 for up to 2 days.

2.3. FGF-2 treatments

When MC3T3 and calvaria primary osteoblasts were 100% confluent (approx. 72 h) the culture media was removed from the wells and the cells washed in PBS. In the initial experiments, media containing variable concentrations (0 – 50 ng/ml) of FGF-2 (PeproTech -USA) in α-MEM supplemented with 1% v/v FBS and 0.05 mg/ml gentamycin was added to each well. The vehicle diluent for the FGF-2 (0.1% w/v BSA in PBS) was added to 1% v/v FBS containing media and served as the control culture.

After 4 and 24 h FGF-2 incubation, the media was removed and the cells washed with sterile ice-cold PBS to remove excess media. The cells were scraped and processed for RNA extraction and protein assay (see Sections 2.4.1 and 2.5.2, respectively). For all further experiments, FGF-2 was used at 10 ng/ml to treat cells over short and long time periods (see results for precise details) and 0.1% w/v BSA in 1% v/v FBS media served as the negative control. Each experimental condition was completed in triplicate. For calvaria cultures, FGF-2 at 10 ng/ml concentration (0.1% w/v BSA as negative control) was added to appropriate wells.

2.4. RNA methods

2.4.1 Isolation of RNA from cells

Cell monolayers were scraped with 1 ml ice-cold PBS, pelleted by centrifugation and stored at -80^{0}C freezer. The RNA was later extracted with Qiagen RNeasy Mini kit (Qiagen, Manchester, UK), following manufacturer's instructions and as reported previously (Genetos et al., 2011). In summary, this involved homogenising the sample in lysing and denaturing buffer. Ethanol (70%) was added for the efficient binding of RNA precipitates to the silica-gel-based membrane. Contaminants were removed with washing buffers and centrifugation, while DNAse treatment was used to digest any DNA present. The RNA was subsequently eluted though the membrane with RNase free water. The quantity of RNA in ng/ul was measured with a NanoDrop spectrophotometer (ThermoScientific, Paisley, U.K.). The level of purity was evaluated by determining the ratio of absorbancies at 260/280 nm wavelengths, and

values ~2.0 was taken as optimal. The samples were diluted with RNase free water and stored at -80^{0}C for later analysis.

2.4.2 Isolation of RNA from tissues

RNA was extracted using a RNeasy mini kit, following the manufacturer's instruction (Qiagen) as previously published (Reno et al., 1997) . The bone and calvaria were homogenised in 1 ml Qiazol (Qiagen, Germany) for cell lysis, and left at room temperature for 5 min to promote disociation of nucleoprotein complexes. Chloroform (200 ul) was added and thoroughly mixed to enhance phase separation, which was then undertaken by centrifugation at 9300 g for 15 min at 4^{0}C. After centrifugation, 3 phases were visible: an upper colourless aqueous phase containing RNA; white interphase; and lower red phase containing organic matter. The upper colourless phase was carefully aspirated to avoid contamination with the other phases. Seventy percent ethanol (600 ul), was added for efficient binding of RNA precipitates to the silica-gel-based membrane. Contaminants were removed with washing buffers and centrifugation, while DNAse treatment was used to digest any DNA present. The RNA was assessed for quantity and purity by spectrophotmometry as described above (Section 2.4.1). The RNA was stored at -80^{0}C.

2.4.3. Reverse transcription

DNA polymerase enzyme - reverse transcriptase was used to convert the diluted RNA samples to complementary DNA (cDNA). The RNA was diluted to 5 ng/ul with nuclease free water (NFW) and the diluted RNA (10 ul) was incubated with 2 ul of random primers (0.05 ug/ul) and loaded onto the Dyad PCR Thermal Cycler (MJ

Research, Canada) and incubated at 70^0C for 10 min. A master mix of 2 ul 10X PCR reaction buffer, 2 ul dithiotheitol (DTT) (0.1 M), 1 ul deoxyribonucleotide triphosphate (dNTP) mix (10mM) and 1 ul Superscript II RNase H enzyme was prepared and added to each sample. The samples were reverse transcribed to cDNA using the following thermal profile in the Dyad PCR thermal cycler: 25^0C for 10 min; 42^0C for 50 min; 70°C for 15 min and held at 4^0C. The cDNA produced was stored at -20^0C.

2.4.4. Optimisation of qPCR primers

Primer efficiency was tested with serial dilutions of cDNA (known to express the gene of interest) and a standard line drawn. Primers were considered satisfactory if the amplification efficiency was within the range of 93-107%, with an R^2 value between 0.98 and 1.00 indicating a perfect linear correlation, and an amplification curve with sigmoid curves at regular intervals along the dilution series. Primer specificity was demonstrated by the formation of a single peak in the disociation curve.

2.4.5. Quantitative polymerase chain reaction (qPCR)

The cDNA samples were all diluted to 5 ng/ul with NFW. A master mix, consisting of 10 ul 2xqPCR master mix with SYBR green (PrimerDesign, UK), 1 ul primer mix (detailed in Appendix, Table 1), and NFW (4 ul) was made up. Primers were deigned to span an intron to avoid amplifying any contaminating genomic DNA. Fifteen microlitres of the master mix was added to 5 ul of diluted cDNA, and loaded into the MX3000p Stratagene qPCR machine (Agilent technologies, Santa Clara, USA). Amplification of the cDNA was as follows: 10 min at 95^0C, 45 cycles of 15 s at 95^0C

and 1 min at 60°C, and a final cycle of 1 min at 95^{0}C, 30 s at 60^{0}C, and 15 s at 95^{0}C and 30 s at 25^{0}C to provide dissociation curves. The cycle threshold (Ct) values for the samples were normalised to that of *Atp5b* in MC3T3 cell lines and mice primary osteoblasts, or *Gapdh* in whole mice calvaria as previously reported (Kyono et al., 2012, Huesa et al., 2015, Houston et al., 2016) , and the relative expression of each gene was calculated using the 2ΔCt method (Livak and Schmittgen, 2001). NFW instead of cDNA was amplified as a negative control.

2.5. Protein methods

2.5.1. Protein isolation

To enable fast efficient lysis of the cell and protein solubilisation, 100 ul of Radioimmunoprecipitation assay (RIPA) buffer (ThermoScientific, UK) solution containing protease inhibitor cocktail (Roche, Germany) was added to the cell monolayers. The cells were scraped with a sterile filter tip and an additional 100 ul of RIPA buffer was used to wash the well. Samples were vortexed and lysates in a total volume of 200 ul were stored at -20^{0}C.

2.5.2. DC protein assay

The protein concentration of each sample was determined using a detergent compatible (DC) protein assay (Bio-Rad, Watford, UK) based on the Lowry assay (Lowry et al., 1951). Protein samples were thawed, vortexed and centrifuged at 9300 g for 5 min and 5 ul of sample was pipetted in duplicate into a 96-well micro titre plate alongside standard dilutions of a protein assay standard (lyophilised bovine plasma gamma globulin 0 – 2 mg/ml). To all standards and samples, 25 ul Bio-Rad

DC protein assay Reagent A (Bio-Rad, Hertfordshire, UK) and 200 ul of Bio-Rad DC protein assay Reagent B (Bio-Rad, Hertfordshire, UK), were added and the plates were allowed to incubate for 15 min. Absorbance was analysed using a BioTek Synergy microplate reader (Winooski, Vermont, USA), at 690 nm. Protein concentration in each sample was determined using the standard curve generated from the standard dilutions.

2.5.3 Western blotting

Protein lysates were denatured in a pre-heated block at 70^0C for 10 min. An equal quantity of the denatured protein (8-12 ug), was loaded into 10% SDS-polyacrylamide gel wells (NuPAGE- Life tech. UK), which were subsequently placed in a electrophoresis gel tank (Xcell Surelock, Invitrogen, UK) containing MOPS (3-*N*-morpholino propanesulfonic acid) and SDS (sodium dodecyl sulfate). The gel tank was connected to a Bio-Rad power pack (Pac300; Bio-Rad). Five percent MOPS running buffer (Appendix), in water was poured into the tank chamber, while antioxidant (NuPAGE, UK) was added to the inner chamber of the gel tank to preserve the reduced proteins. Electrophoresis was completed at 200 V for 50 min at room temperature (RT).

Protein was transferred to a nitrocellulosse (NC) membrane (GE Healthcare, Buckinghamshire, U.K.). Briefly, the NC membrane was sandwiched between Tris-buffered saline (1X TBS) soaked filter paper and sponges creating a wet transfer within a transfer module (Invitrogen). Transfer was carried out on ice at 30V for

90min. The NC membrane was blocked in appropriate buffer dissolved in TBS/Tween-20 (TBS/T) and incubated over night at 4^0C.

The NC block solution was washed off the membrane in TBS/T (3 x 10 min) and incubated for 1 h at RT with the appropriate primary antibody (see Appendix, Table 2). After further washing in TBS/T (3 x 10 min) at RT, the NC membrane was incubated for 1 h at RT with species appropriate peroxidase labelled secondary antibody (see Appendix, Table 3), (Dako, Denmark) diluted in 5% w/v Marvel in TBS/T buffer. The NC membrane was finally washed with TBS/T (4 x 10 min), before bound antibody was detected with enhanced chemiluminescence (ECL) (GE-Healthcare) according to the manufacturer's recommendation. In brief, the ECL mixture was pipetted on to the NC membrane, allowed to stand for 1min and placed in an X-ray cassette sandwiched between two transparencies. In the dark room, the film was placed in the same cassette for 30 s, removed and loaded into the X-OGRAPH medical film processor (Konica Minolta, SRX-101A, Banbury, UK) and allowed to develop in the dark(Mahmood and Yang, 2012). The films were scanned and saved and densitometric analysis of protein expression was performed using Image J (https://imagej.nih.gov/ij/) (Baldari et al., 2015).

2.5.4. Stripping NC membrane for additional western blotting

The NC membrane was stripped in Restore Plus western blot stripping buffer (Thermo- Scientific), for 30 min at RT, and then washed in 1xTBS/T (3x10 min). The NC membrane was blocked in 5% w/v Marvel or 5% w/v BSA in TBS/T and incubated overnight at 4^0C. Subsequently it was washed in 1xTBS/T (3 x 10 min). For the

detection of the loading control, NC membrane was treated with the stripping buffer (Appendix) to clear all bands which was confirmed with ECL. The stripped NC membrane was incubated for 1 h at RT with an antibody to peroxidase tagged β-actin (Appendix, Table 2). Subsequently the NC membrane was washed in 1xTBS/T (3 x 10 min) and the peroxidase label was detected with ECL as previously described. The films were scanned and saved, while densitometric analysis of protein expression was performed using Image J as previously described.

2.6. Immunofluorescence of cultured cells

Immunofluorescence localisation of target proteins was carried out as published (Anastasiadis et al., 2000), on MC3T3 osteoblast-like cells that had been cultured on sterilised glas coverslips at a density of 6.3 x 10^3 cells/cm^2. Following treatment with FGF-2 (Section 2.3), the cells were fixed with 4% paraformaldehyde (PFA) for 15 min and washed 3 times (5 min each) with 1 ml of PBS. A blocking buffer (1X PBS, 5% v/v normal serum from an appropriate animal species (donor of secondary antibody) and 0.3% v/v Triton X-100) was added to each well and incubated at RT for 1 h. After removal of the blocking buffer the primary antibody (Appendix, Table 2) diluted in antibody dilution buffer (1X PBS, 0.3% v/v Triton X-100 and 1% w/v BSA), was added to each well. The negative control consisted of an identical concentration of IgG from the same animal species as the primary antibody. The cells were incubated on a shaker, overnight at 4°C after which the primary antibody was discarded and the monolayers were washed 3 times with PBS, for 5 min each. AlexaFluor-conjugated secondary antibodies (Table 3) diluted in antibody dilution buffer, was added to each

well. The cells were incubated for a further 2 h in the dark at RT. The monolayers were subsequently rewashed 3 times with PBS after which the cover slips (containing the cell monolayers) were carefully turned upside down onto a microscope slide with ProLong Gold antifade reagent with DAPI (Life Tech, USA) for nuclei staining. The slides were then visualised using a Leica DMRB fluorescence microscope and images were taken with a Leica DFC300 digital colour camera (Leica, Milton Keynes, UK).

2.7. Phalloidin staining of cultured cells

MC3T3 osteoblast-like cells were stained for filamentous (F)-actin using the Phalloidin (Liu et al., 2011). The cells were seeded at 1.0 $x10^4$ cells/ cm^2 in 6-well plates and were maintained in reduced serum medium (Section 2.2.1). Following treatment with FGF-2 (Section 2.3), the cells were fixed in 4% PFA for 15 min after which they were rinsed 3 X PBS, permeabilised in 0.1% w/v trypsin (Sigma-Aldrich, Poole, UK) in PBS for 10 min and then rinsed again with 3 X PBS. The cells were incubated in 30ul of Alexa Fluor 488-conjugated phalloidin (Life Tech, Oregon, USA) (5 uM in PBS with 2% w/v BSA) in the dark at RT for 3 h. They were then rinsed 3 X PBS and imaged on a Zeis Axiovert 25s inverted microscope and digital imaging system (Carl Zeis Microscopy, LLC, USA).

2.8. Transfection of MC3T3 cells with E11 siRNA

E11 small interfering ribonucleic acid (E11 siRNA) and scrambled siRNA stocks were obtained from Qiagen, UK, and diluted to 10 nM. MC3T3 osteoblast-like cells were expanded, seeded at 8.0 x 10^3 cells/cm^2 in 12 well plates and maintained in reduced serum medium (1% v/v FBS). The use of siRNA has been described also in literature

to deplete RNA post transcriptionally (Genetos et al., 2011, Garufi et al., 2014). This was carried out according to manufacturer's instruction and involves gentle transfection of cells with a mix of 5.4% v/v of 10 nM E11 siRNA or scrambled siRNA for study or scrambled groups respectively; 84% v/v of serum free media; and 10.7% v/v of HiPerFect transfection agent, which was added drop-wise to the cells as per manufacturer's instructions (Qiagen, UK). Mock cells were transfected gently with a mix of 89.3%v/v serum free media and 10.7%v/v HiPerFect transfection reagent. After 24 h incubation in a $37^0C/5\%CO_2$ incubator, FGF-2 at 10 ng/ml was added to appropriate wells whereas 0.1% w/v BSA served as the negative control. The cells were scraped after 24 h of FGF-2 treatment (Section 2.3) for downstream gene and protein analysis (Sections 2.4 and 2.5).

2.9. RhoA activity assay

MC3T3 cell monolayers were scraped in a G-LISA lysis buffer supplied with the GLISA assay kit (Cytoskeleton, Denver, USA), after 4, 6, 24 and 48 h culture with FGF-2 (Section 2.3). Lysates were immunoblotted for E11 (Section2.5) to ensure FGF-2 stimulation of E11. Subsequently, using a GLISA assay which precisely identifies active GTP-bound RhoA, the quantification of RhoA activation was carried out by luminometry and expressed in relative light units (RLU) as per the manufacturer's instructions (Staines et al., 2016).

2.10 Alamar Blue Cell Viability Assay

This was carried out according to published literature (White et al., 1996, Nakayama et al., 1997). MC3T3 cells were cultured in 6-well plates as described in Section 2.2.1.

Cells were treated with FGF-2 (10 ng/ul) and 0.1% w/v BSA as positive control at confluency (Section 2.3). After 24 h FGF-2 stimulation, the media was removed and 700 ul of fresh media added to each well. To each well, 70 ul Alamar Blue reagent was added, then the plate was wrapped in aluminium foil to prevent light contact and placed in a humidified incubator maintained at 37^0C and 5.0% CO_2 for 3 h. Fresh media plus FGF-2 or BSA was used as a negative control. The Alamar blue fluorescence were read at 530/25, 590/35 nm on Bioteck plate reader.

2.11 Lactate Dehydrogenase (LDH) Assay

MC3T3 cells were cultured in 6-well plates as described in Section 2.2.1. Cells were treated with FGF-2 (10 ng/ul) and 0.1% w/v BSA as positive control at confluency (Section 2.3). After 24 h FGF-2 stimulation, the media was removed and an LDH assay kit used according to the manufacturer's instructions (Promega, Southampton, UK). Briefly, the Assay Buffer was thawed, and 12 ml taken out, wrapped in aluminium foil to protect from light and warmed to room temperature. This 12 ml of room temperature Assay Buffer was added to a bottle of Substrate Mix to form the CytoTox96 Reagent. It was inverted and shaken gently to disolve the substrate. Fifty micro litres aliquots from all test and control wells was transferred to a fresh 96-well flat clear bottom plate. Fifty microlitres of the CytoTox96 Reagent was added to each sample. The plate was covered with foil to protect it from light and incubated for 30 min at room temperature. Fifty microlitres of Stop Solution was added to each well of the 96-well plate. Using Biotek plate reader, absorbance was read at 490 nm within 1 h after adding the Stop Solution.

2.12. Histological Studies

2.12.1 Paraffin embedded tissue

The knee joints of *Fgf*-2 global KO (Zhou et al., 1998) and WT mice (kind gift from Prof. Tonia Vincent, The Kennedy Institute of Rheumatology, Oxford University) were fixed for 48 h in 10% neutral buffered formalin and preserved subsequently in 70% ethanol. The joints were decalcified in 10% w/v EDTA at 4^0C with regular changes for approximately 4 weeks. An automated tissue processor (Leica microssystems, Wetzlar, Germany) was used to prepare all of the samples. Briefly, the samples were passed through an increasing series of ethanol baths until dehydrated in 100% ethanol; they were then infiltrated with paraffin wax. The samples were then manually placed in paraffin wax blocks. The surface of the paraffin wax blocks were cooled with an ice block and 5μm sections were cut using a Leica RM 2235 microtome (Leica, Milton Keynes, UK). The sections were finally mounted onto microscope slides coated with poly-l-lysine.

2.12.2 Immunohistochemistry

For immunohistochemical analysis of target proteins, the Vectastain ABC kit (Vector Laboratories, Peterborough, UK) was used according to the manufacturer's instructions. This was carried out on paraffin embedded Sections (Section 2.12.1). Sections were first de-waxed in xylene and rehydrated though a series of graded alcohols to distilled H_2O. Antigen unmasking was carried out with 0.1% v/v trypsin in PBS for 30 min at 37^oC using water bath (Cattoretti et al., 1993). Endogenous peroxidase activity was blocked by treatment with 0.03% v/v H_2O_2 in methanol for 30

min at RT. After 3 x 5 min washes in PBS the sections were blocked in normal blocking buffer (1:50 dilution of the appropriate normal serum in PBS) for 20 min at RT. The test sections were then incubated in primary antibody (see Appendix 1, Table 2), while the control sections were incubated in appropriate immunoglobulin G (IgG). They were diluted to an appropriate concentration in normal blocking buffer at 4^0C overnight. Unbound primary antibody was removed by 3 x 5 min washes in PBS. The sections were subsequently incubated in biotinylated secondary antibody (Appendix, Table 3) diluted with normal blocking buffer at RT for 30 min. After 3 x 5 min washes in PBS, sections were incubated with Vectastain ABC reagents 2A and 2B (2 drops of avidin and 2 drops of biotin complex) in 5ml PBS for 30 minutes at RT. They were later washed for 3 x 5 min in PBS. Staining was then developed in diaminobenzidine (DAB) solution (0.06% v/v DAB in 0.1% v/v H_2O_2 in PBS) for about 2 minutes. The sections were rinsed in tap water and counterstained with haematoxylin using Leica Autostainer XL (Leica, Milton Keynes, UK). Finally, sections were dehydrated though graded alcohols, cleared with xylene and mounted in DePeX. Images were captured with Nikon Eclipse Ni microscope (Nikon, UK), fitted with Zeis Axiocam 105 colour camera (Carl Zeis, UK).

2.12.3 Frozen tissue

Tibia from *Fgf-2* KO and WT mice were decalcified in 10% w/v EDTA at 4^0C with regular changes for 4 weeks. They were then subjected to increasing concentrations of sucrosse from 10% to 30% w/v for cryoprotection and then subsequently coated in 5% w/v polyvinyl acetate and snap frozen in a cooled hexane bath for 30 s (Bradbeer

et al., 1988, Ruan et al., 2013). The tissue was finally stored at -80°C until use. Frozen tissue was embedded in optimal cutting temperature (OCT) embedding medium (Brights) and attached to a metal chuck. Following trimming of excess OCT, 10 uM sections were cut at -30°C using a cryostat (OTF500/HS-001, Brights, Huntingdon, UK) with the knife blade angle set to 22°. The sections were placed in a slide tray, covered in aluminium foil, and stored at -80°C.

2.12.4 Phalloidin staining for cryosections

The slides (Section 2.10.3) were removed from -80°C freezer and kept on the bench for 45 min to bring them to RT before the removal of the tin foil. They were subsequently washed twice in PBS before incubation in 0.1% v/v triton X-100 in PBS for 30 min at RT. After extensive washing in PBS the sections were incubated in a solution containing 0.05% v/v phalloidin/1% w/v BSA/PBS at RT in the dark for one h. The slides were then washed 3 x PBS and finally mounted in Dako fluorescence mounting medium (Dako, USA). The slides were stored in the dark at RT and subsequently imaged on a Zeis Axiovert 25 Phase/Fluorescent microscope fitted with Zeis Axiocam 503 high resolution colour camera/Zen software, single eGFP semrock filter block + multiple bandpas Semrock DAPI/AF488/TRITC (Carl Zeis, UK).

2.13. Data analysis

Data are presented as mean ± S.E.M. for n≥3 observations. Using GraphPad Prism 6 (GraphPad Software, Inc., USA), differences unless otherwise stated were assessed by one or two-way analysis of variance (ANOVA) for which Tukey's post-tests for multiple comparisons were conducted. $P<0.05$ was considered to be significant. Tests

for assumptions of ANOVA done included tests on equality or homogeneity of variance such as Brown-Forsythe test.

Chapter 3

Regulation of E11 expression by FGF-2

3.1. Introduction

The protein E11 is a mucin type transmembrane glycoprotein of about 38-42 kDa with several regulatory functions spanning from cell development and differentiation, epithelial-mesenchymal transition (EMT), oncogenesis and invasiveness (Thiery, 2002, Wicki and Christofori, 2007, Martín-Villar et al., 2009, Astarita et al., 2012). Fundamental studies by Bonewald and colleagues identified E11, a mucin-type transmembrane glycoprotein, as the earliest osteocyte marker protein expressed during osteocytogenesis (Zhang et al., 2006). Furthermore, E11 triggers actin cytoskeletal dynamics (Staines et al., 2016), which are required for dendrite formation and transient E11 knockdown blocks dendrite elongation (Zhang et al., 2006). E11 has also been reported to be up-regulated during mechanical loading with associated extensions of the osteocyte dendrites in the mineralized matrix, suggesting a possible role in aiding biochemical communication amongst osteocytes, and other bone cells in their microenvironment (Zhang et al., 2006). Despite this, how E11 expression is regulated and the precise mechanisms by which E11 promotes dendrite formation are poorly understood.

Nonetheless, clues from other model systems have indicated that basic fibroblast growth factor (bFGF) or FGF-2 is able to change chondrocyte gene expression *in vitro*, including that of E11 (Chong et al., 2013). Specifically, E11 expression was found to be FGF-2 dependent following injury to cartilage *in vitro* and to joint tissues *in vivo* (Chong et al., 2013). FGF-2 is a member of the FGF large family of polypeptide growth factors involved in several developmental mechanisms, including skeletal

development, in several multicellular organisms (Itoh and Ornitz, 2004, Thisse and Thisse, 2005). In addition to chondrocytes, FGF-2 expressed by osteoblasts and stored in the extracellular matrix (ECM), where it regulates bone formation via influence on progenitor cell lineage commitment and/or osteoblast differentiation (Sabbieti et al., 1999, Montero et al., 2000, Hurley et al., 2002, Xiao et al., 2010a). FGF-2 is also involved in normal bone formation as highlighted by its absence in KO mice being associated with poor bone formation and mass (Coffin et al., 1995, Montero et al., 2000). *In vitro*, FGF-2 down regulates osteoblast markers such as collagen type 1 and also regulates genes controlling mineralisation during osteoblast differentiation (Fang et al., 2001, Kyono et al., 2012). FGF-2 is involved in regulation of bone matrix protection by inducing the expression of tissue inhibitors of metalloproteinases – TIMPs (Varghese et al., 1995).

In view of the published role of FGF-2 in stimulating E11 expression in cartilage explants and osteoblast-like cells, it is therefore likely that FGF-2 may have an impact on osteoblast expression of E11 and the acquisition of the dendritic osteocyte phenotype (Gupta et al., 2010, Chong et al., 2013). Hence, the aim of this Chapter is to elucidate the nature of FGF-2 regulation of E11 during osteocytogenesis.

3.2. Hypothesis

FGF-2 stimulates the expression of E11 in MC3T3 osteoblast like cell lines and primary osteoblasts, promoting the acquisition of the osteocyte phenotype.

3.3. Aims

I To examine the effect of FGF-2 on E11 expression in MC3T3 osteoblast cell lines and primary osteoblasts.

II To establish the effect of FGF-2 on the attainment of the osteocyte phenotype in osteoblast cell lines and primary osteoblasts.

III To evaluate the effect of FGF-2 on E11 expression in SCB osteocytes from mice deficient in *Fgf-2.*

3.4. Materials and methods

3.4.1 MC3T3 cells

As outlined in Section 2.2.1, MC3T3 cells were cultured at a density of 6×10^4 cells/cm^2 in a humidified atmosphere (37°C, 5% CO_2) for up to 15 days. When confluent, cells were initially supplemented with FGF-2 at increasing concentrations from 0 – 50 ng/ml or 0.1% w/v BSA as negative control. For subsequent experiments, FGF-2 was added at 10 ng/ml with 0.1% w/v BSA as negative control. The medium was changed every 2-3 days.

3.4.2 RNA analysis of MC3T3 cells

RNA was isolated from MC3T3 cells at specific time points using a Qiagen RNeasy kit according to the manufacturer's instructions and cDNA was prepared (Section 2.4.1). For qPCR analysis, cDNA was used at 5 ng/ul, as detailed in Section 2.4.5. Results were normalised to the *Atp5b* housekeeping gene. Primers used are detailed in Appendix I Table 1.

3.4.3 Protein extraction from MC3T3 cells and western blotting

At defined time points, protein was extracted from MC3T3 cells in RIPA buffer as detailed in Section 2.5.1. Protein samples were quantified (Section 2.5.1) and appropriate quantities were used for western blot analysis (Section 2.5.3). E11 protein expression was determined using a goat anti-mouse anti-E11 antibody at a dilution of 1:1000 and a HP-labelled rabbit anti-goat secondary antibody (1:3000). Antibody labelling was visualised using the ECL detection kit. Uniform protein loading was confirmed by re-probing the membrane with mouse monoclonal HP-labelled anti-β actin antibody (1:70000).

3.4.4. Immunofluorescence

Immunofluorescence for localisation of E11 after treatment of MC3T3 with FGF-2 at 10 ng/ml concentration or 0.1% w/v BSA as negative control was as described in Section 2.6. E11 protein expression was localised using a goat anti-mouse anti-E11 antibody at a dilution of 1:900 and a donkey anti-goat AlexaFluor-conjugated secondary antibodies HP-labelled rabbit anti-sheep secondary antibody (1:250). The slides were subsequently stained with ProLong Gold antifade reagent with DAPI for nuclei staining, before imaging with microscope.

3.4.5 Transfection of MC3T3 cells with E11 siRNA

Functional studies using E11 siRNA transfection was carried out on MC3T3 cells as described in Section 2.8. Two control groups were used, one treated with scrambled siRNA while the mock group was treated with only the HiPerFect transfection agent. RNA was extracted and reverse transcribed (Sections 2.4.1 and 2.4.3). For qPCR

analysis, Section2.4.5. Western blotting on extracted protein was done as described in Section 2.5.3. Immunofluorescence for localisation of E11 after transfection was as described in Section 2.6. E11 protein expression was localised using a goat anti-mouse anti-E11 antibody at a dilution of 1:900 and donkey anti-goat AlexaFluor-conjugated secondary antibodies (1:250).

3.4.6 Primary osteoblasts

Primary osteoblasts were extracted from the calvaria of 3 days old WT mice as detailed in Section 2.2.2. Cells were cultured for 2 days at 37°C in cell culture media before treatment with FGF-2 at 10 ng/ml concentration or 0.1% w/v BSA as negative control in appropriate wells. RNA was extracted and reverse transcribed (Sections 2.4.1 and 2.4.3 respectively). For qPCR analysis, cDNA was used at 5 ng/ul, as detailed in Section 2.4.5. RT-qPCR results were normalised to the *Atp5b* housekeeping gene. Primers used are detailed in Appendix I, Table 1. Proteins were extracted as described (Sections 2.5.1), and western blotting was done as described above in Section 3.4.3 and β-actin served as loading control.

3.4.7 Whole calvaria

Whole calvariae were dissected from 3-day-old C57BL/6 wild-type mice as detailed in Section 2.2.3. Cavaria hemiSections were incubated in calvaria culture media for 2 days after treatment with FGF-2 at 10 ng/ml concentration or 0.1% w/v BSA as negative control in appropriate wells. After 6, 24 and 48 h of FGF-2 stimulation, RNA was extracted and reverse transcribed as described in Section 2.4.2 and 2.4.3 respectively). For qPCR analysis, cDNA was used at 5 ng/ul, as detailed in Section

2.4.5. Results were normalised to the *Gapdh* housekeeping gene. Primers used are detailed in Appendix I Table 1.

3.4.8 Immunohistochemical staining of the murine tibias

Tibias of 10-week old *Fgf-2* KO and wild type mice (Section 2.10.1) were immunostained for E11 and sclerostin as described in Section 2.10.2. Immunohistochemical staining of 5 um-thick tibiae paraffin embedded decalcified sections was performed using antibodies for E11 (1:500), and sclerostin (1:500), and the Vectastain ABC kit, as outlined in Section 2.10.2 and Appendix 1 Table 1. Immunohistochemical labelling was visualised using DAB chromogen. Goat IgG concentrations at same concentrations were used instead of the primary antibodies as negative controls. The labels on the slides were masked by tape to allow blind assessment of the staining. For analysis of the percentage of positively stained E11 or sclerostin osteocytes, the Grid/Collection Stitching Plugin within Fiji was use to merge the several images of the Section afterwards positive staining and total osteocytes were counted (Schindelin et al., 2012).

3.4.9 Measuring osteocyte cell volume and dendrite parameters in mouse tibiae

Histological Sections of longitudinally cut mouse tibiae were stained with Phalloidin-Fluorescein Isothiocyanate to demonstrate F-actin (Section 2.12.4).

Sections were imaged on a Zeis LSM 710 Laser Scanning Confocal Microscope with 488nm laser excitation and detection settings from 493 to 634 nm. Z-stacks were produced with optimal Nyquist overlap settings using a 63x/1.4 na oil immersion lens. Voxel sizes were 0.1x0.1x1.00 um in x,y,z planes respectively.

Images were analysed using Bitplane Imaris software as previously published (Staines et al., 2017). This essentially involved importing the image stacks into Bitplane Imaris 9.2.0 software. Imaris Filament Tracer was used to create algorithms to render and measure canalicular processes; while surface rendering was used for osteocyte cell body measurements. Algorithm settings were set constant and applied to all images (see Appendix Algorithm 1.). Histological sections were blinded to the operator/analyst by masking with tape, later divided into 2 unknown groups (Group 1 and Group 2) to allow comparisons in the Imaris Vantage software module. Imaging and analysis with the Bitplane Imaris software was done by Mr Robert Fleming. Statistics were carried out in Minitab 17 software.

3.5 Results

3.5.1. Dose-response of FGF-2 on the expression of *E11* gene and protein by MC3T3 osteoblast-like cells.

To ascertain the optimum concentration of FGF-2 for use in future experiments, a dose-response study was conducted in MC3T3 osteoblast-like cells. Increasing concentrations of FGF-2 (1, 10, 25 and 50 ng/ml) were examined for their effects on E11 expression. After 4 h of incubation with 1, 10, 25 and 50 ng/ml of FGF-2, there was an upward trend of higher *E11* gene expression when compared to control cultures (no FGF-2 supplementation) (Fig. 3.1A). The differences did not reach significance. There was also an upward trend in E11 gene expression with stimulation by FGF-2 for 24 h at all concentrations studied (Fig. 3.1B). Similarly, after 24 h, the FGF-2 treated cells synthesized more E11 protein and this was particularly notable in the 10, 25, and 50 ng/ml treated cells. This increase in E11 protein expression was not apparent after

4 h of FGF-2 treatment (all concentrations tested) (Fig. 3.1C). Since FGF-2 at 10 ng/ml promoted E11 gene, albeit not significantly, and protein expression, this concentration was chosen based on optimal induction and cost effectivenesss for subsequent studies.

3.5.2 Effect of FGF-2 10 ng/ml over a short time-course on E11 expression and osteocyte/osteoblast gene markers in MC3T3 osteoblast-like cells.

Cells were stimulated with FGF-2 at 10 ng/ml for 4, 6, and 24 h. RT-qPCR showed that *E11* gene expression was significantly up-regulated after 4 ($P<0.001$) and 6h ($P<0.001$) exposure to FGF-2 but there was a lessened response after 24 h ($P<0.05$) when compared with untreated control cells (Fig. 3.2A). This confirms the gene expression data shown in Figure 3.1. Although in this experiment, statistical significance was reached whereas trends were only previously observed. Further confirmation was observed at the protein level where western blotting showed that at 4, 6 and 24 h time points, E11 protein expression was increased in FGF-2 stimulated cells when compared to control cells (Fig. 3.2B).

FGF-2 also induced the up-regulation of osteocyte markers *Phex* and *Dmp1* ($P<0.01$; Fig. 3.2C & D) and down regulation of the osteoblast markers *Col1a1*, *Bglap*, *Alpl*, with *Postn* ($P<0.01$; Fig. 3.2E - H). The down regulation of *Col1a1*, *Bglap* and *Alp* and upregulation of *E11, Phex* and *Dmp1* by FGF-2 after 24 h, strongly suggests that FGF-2 promotes the differentiation of pre-osteoblast/osteoblast to the osteocyte phenotype. *Sost* Ct values were high with almost flat dissociation curve as MC3T3 cells are not known to expresss *Sost* especially in early time points.

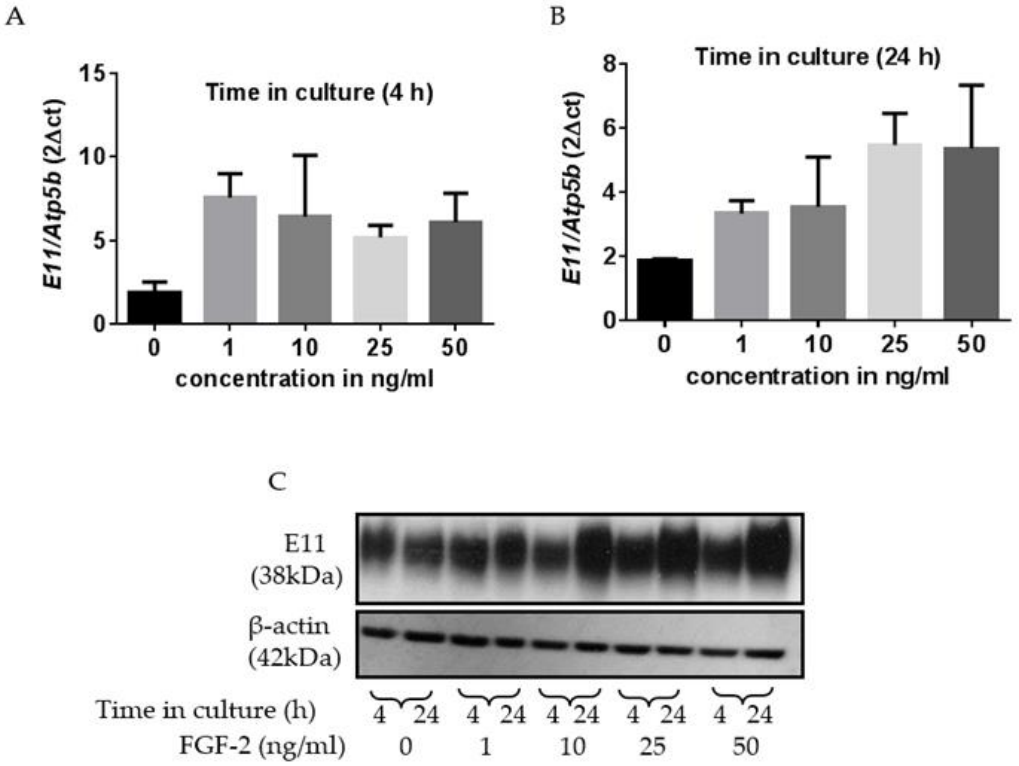

Figure 3.1 Temporal expression of E11 by MC3T3 cells cultured in increasing concentrations of FGF-2.

The effects of FGF-2 (0 – 50 ng/ml) on E11 gene (**A** & **B**), and protein (**C**) expression after 4 and 24 h incubation was assessed by RT-qPCR and western blotting, respectively. Data (**A** & **B**) are presented as mean ± S.E.M (n=3).

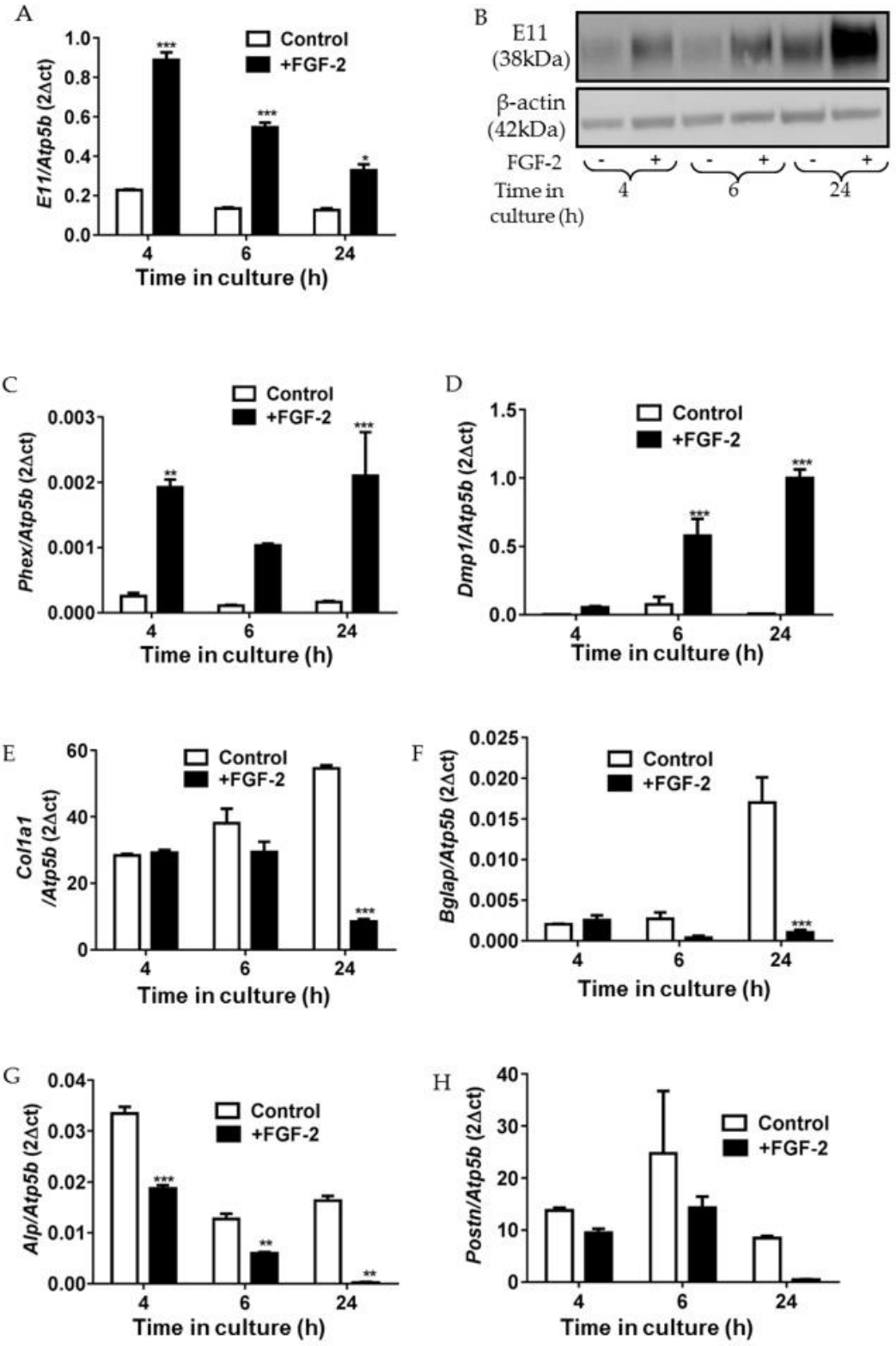
A
E11/Atp5b (2Δct)
Control
+FGF-2
Time in culture (h)
B
E11
(38kDa)
β-actin
(42kDa)
FGF-2
Time in culture (h)
C
Phex/Atp5b (2Δct)
D
Dmp1/Atp5b (2Δct)
E
Col1a1 /Atp5b (2Δct)
F
Bglap/Atp5b (2Δct)
G
Alp/Atp5b (2Δct)
H
Postn/Atp5b (2Δct)

(Previous page) Figure 3.2 Temporal expression of E11 and osteocyte/osteoblast gene markers by MC3T3 cells cultured in FGF-2 10 ng/ml over short time course.

The effect of FGF-2 on (**A**) E11 gene and (**B**), E11 protein expression after 4, 6 and 24 h stimulation. Note the effect on other osteocyte markers (**C**) *Phex*, and (**D***) Dmp1* gene expression; and osteoblast gene markers (**E**) *Col1a1,* (**F***) Bglap* (**G**) *Alpl*, and (**H**) *Postn* gene expression after same time points. Data are presented as mean ± S.E.M (n=3); *p<0.05; **p<0.01; ***p<0.001 compared to control cells.

3.5.3 Effect of FGF-2 over a long time-course on osteocyte gene markers in MC3T3 osteoblast-like cells.

MC3T3 osteoblast-like cells were stimulated with FGF-2 at 10 ng/ml for 2, 5, 9, 12 and 15 days to evaluate its long term effects on *E11* and osteocyte gene markers. At all-time points studied, *E11* expression was not significantly increased by FGF-2 stimulation (Fig. 3.3A). Interestingly, western blotting showed that E11 protein synthesised by MC3T3 cells from day 9 onwards, was lower in FGF-2 stimulated cells when compared with time-matched controls (Fig. 3.3B). There was however a robust up-regulation of two late osteocyte marker genes *Phex* and *Dmp1* ($P<0.001$) by day 15 (Fig. 3.3C & D). *Sost* expression was not significantly altered at any time points studied by FGF-2 treatment (Fig. 3.3E).

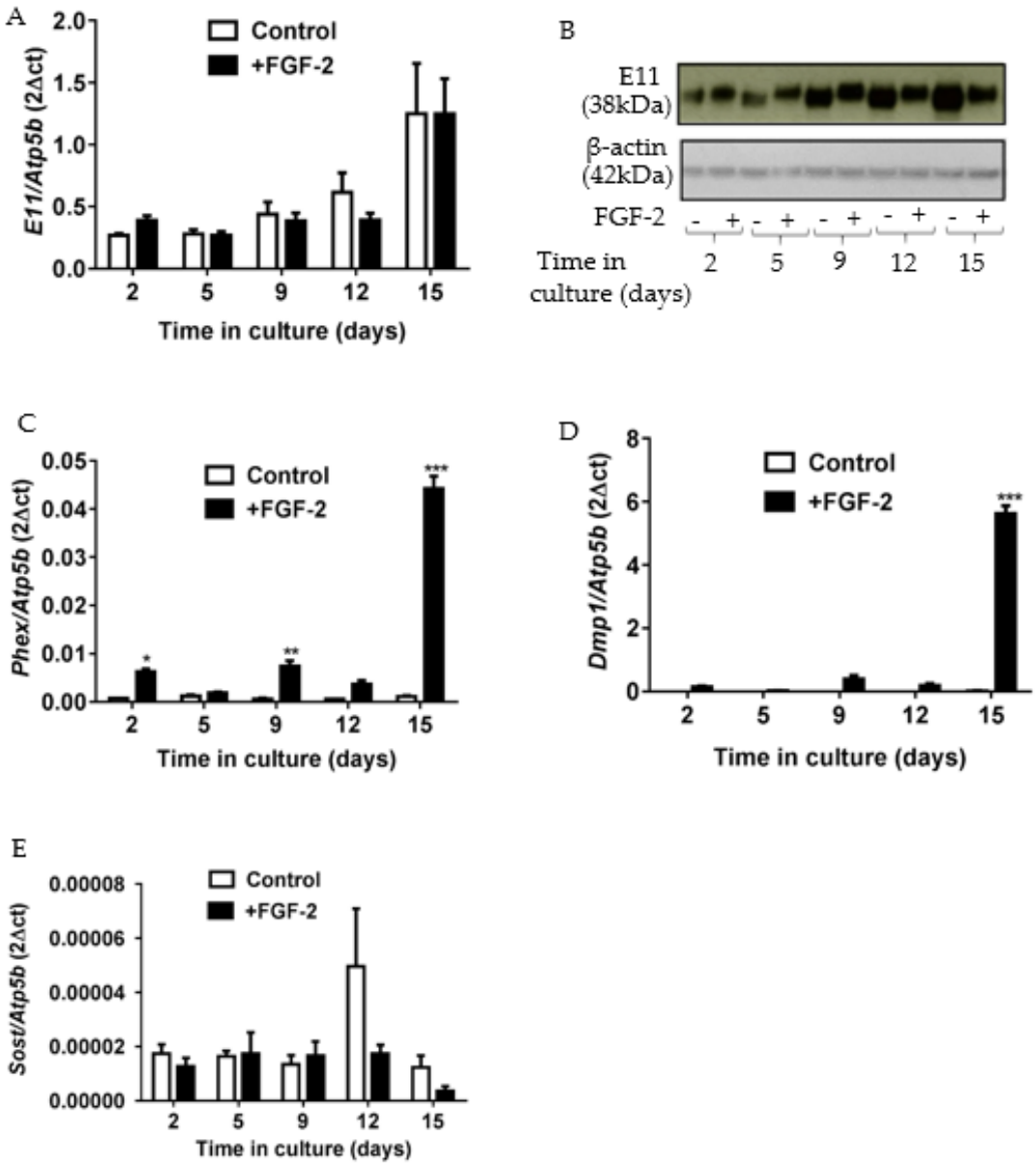

Figure 3.3 Temporal expression of osteocyte gene markers by MC3T3 cells cultured in FGF-2 10 ng/ml over long time course.

The effect of FGF-2 10 ng/ml on (**A**) E11 gene and *(***B***),* E11 protein expression after 2 – 15 days stimulation. Note the effect on other osteocyte markers (**C**) *Phex*, (**D***) Dmp1,* and (**E**) *Sost* gene expression after same time points. Data are presented as mean ± S.E.M (n=3); *p<0.05; **p<0.01; ***p<0.001 compared to control cells.

3.5.4 Effect of FGF-2 on the spatial expression of E11 in MC3T3 osteoblast-like cells

The above data has shown that FGF-2 was able to induce E11 expression and other markers of the osteocyte phenotype. To extend these data, I investigated the spatial expression of E11 in MC3T3 osteoblast-like cells treated with FGF-2 at 10 ng/ml for 6, 24, 48 and 72 h by phase contrast microscopy and E11 immunostaining. Phase contrast microscopy revealed that after 14 days in culture, the control cells were still ovoid/cuboidal shape (Fig. 3.4A), while the treated cells had the prominent elongated dendrites typical of osteocytes (Fig. 3.4B). The immunofluorescence microscopy of the cells after 6 h FGF-2 treatment showed little alterations to E11 expression or cell morphology (data not shown), whereas FGF-2 treatment for 24 - 72 h resulted in a stark change in cell morphology with the appearance of many dendritic processes radiating from the cell membrane when compared to control cells (Figs. 3.4C-H & I-N). Furthermore, the distribution of intra-cellular E11 expression was also altered by FGF-2 treatment. In the control cells, E11 expression was more generally uniformly located within the cytoplasm with a more perinuclear location whereas in the FGF-2 treated cells E11 was associated with the dendrite projections at the cell membrane (Figs. 3.4C-H & I-N). The control, non FGF-2 treated cells also trended towards a similar appearance with time in culture, but this accelerated with FGF-2 treatment. Together, these data are consistent with altered E11 expression and distribution (in response to FGF-2) driving the acquisition of the dendritic phenotype in differentiating osteoblasts.

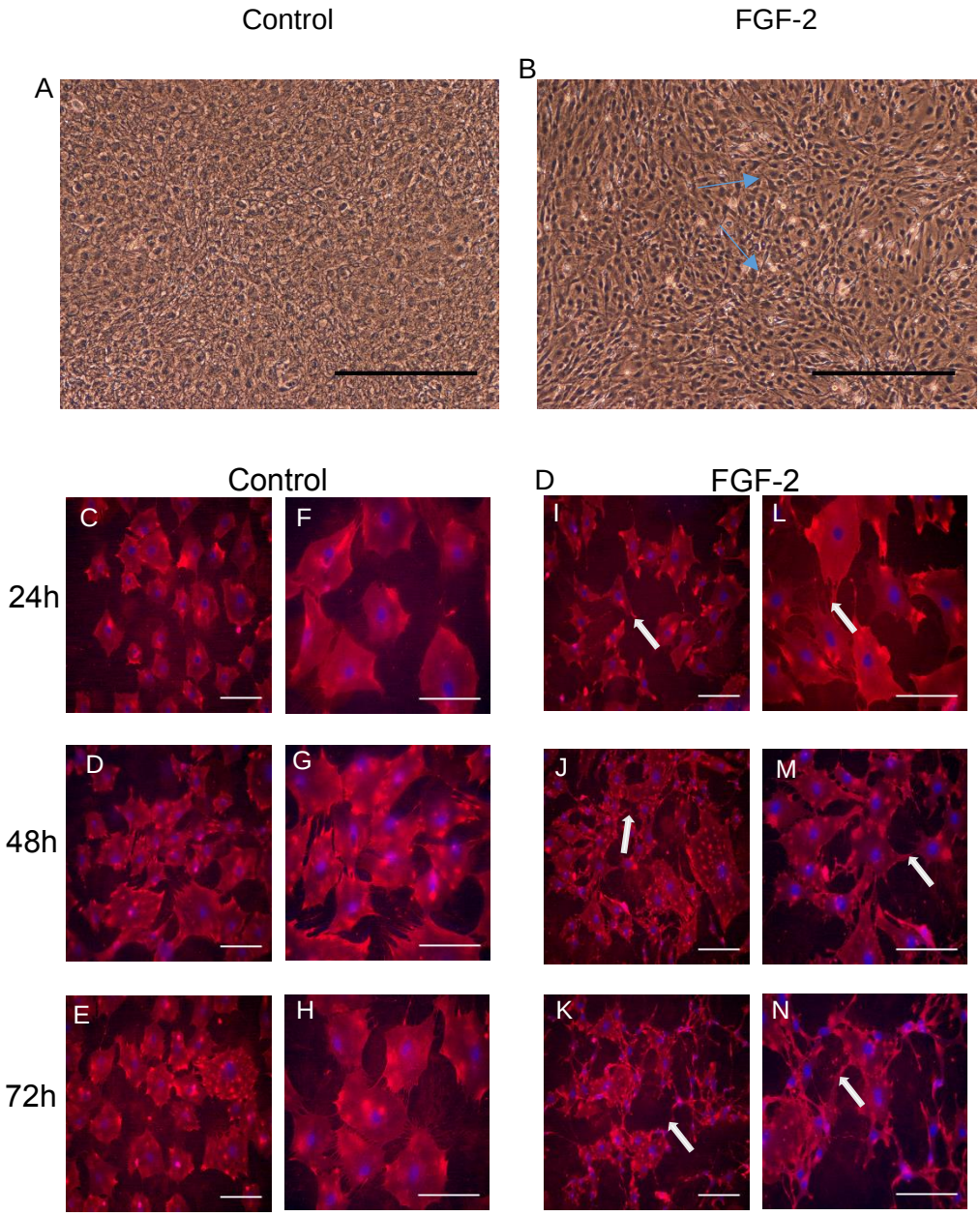

Figure 3.4 Spatial expression of E11 in MC3T3 osteoblast-like cells cultured in FGF-2

Phase contrast microscopy showing phenotypic change from cuboidal osteoblast shape in control (**A**); to a dendritic osteocyte phenotype in FGF-2 treated cells (**B**). Immunofluorescence microscopy showing E11 expression and distribution in control cells (**C-H**), and FGF-2 stimulated cells (**I-N**), for 24, 48 and 72 h time points. Note the blue arrows pointing at long dendrites, white arrows point to E11 accumulations at sites of dendritic projections. Images are representative of three separate experiments. Scale bar, A, **B**, **C-E** & **I-K** (vii-ix) = 200 um; **F-H** & **L-N** = 150 um).

3.5.5 Effect of 24 h FGF-2 treatment on the spatial distribution of F-actin in MC3T3 osteoblast-like cells

Phalloidin staining was used to observe the phenotypic distribution of the microfilament F-actin in FGF-2 treated MC3T3 cells (Wulf et al., 1979). This is important, as intra-cellular F-actin organisation is associated with the formation of dendrite formation during the acquisition of the osteocyte phenotype. Phalloidin staining revealed that the control cells had a typical rounded morphology with fewer and shorter dendrites (Fig. 3.5A), while FGF-2 treated MC3T3 cells expressed more numerous, and longer dendrites, intertwining with one another (Fig. 3.5B).

3.5.6. Cell Viability Assay and LDH Assay

The Alamar Blue Cell Viability assay and the LDH assay were carried out according to manufacturer's instruction (Section2.10). This was conducted to validate the biological life of the cells under study and to investigate if the treatments were having toxic effects on the cells during the study. The results for cell viability showed no differences between FGF-2 treated and control MC3T3 cell cultures (Fig. 3.6A); and the blue colour of the Alamar Blue dye were all reduced to red in both control and treated cultures, thus confirming the cells were viable. The LDH assay revealed that FGF-2 treated MC3T3 cells release les LDH than the control cultures, thereby indicating les cell death in these cultures ($P<0.05$, Fig. 3.6B).

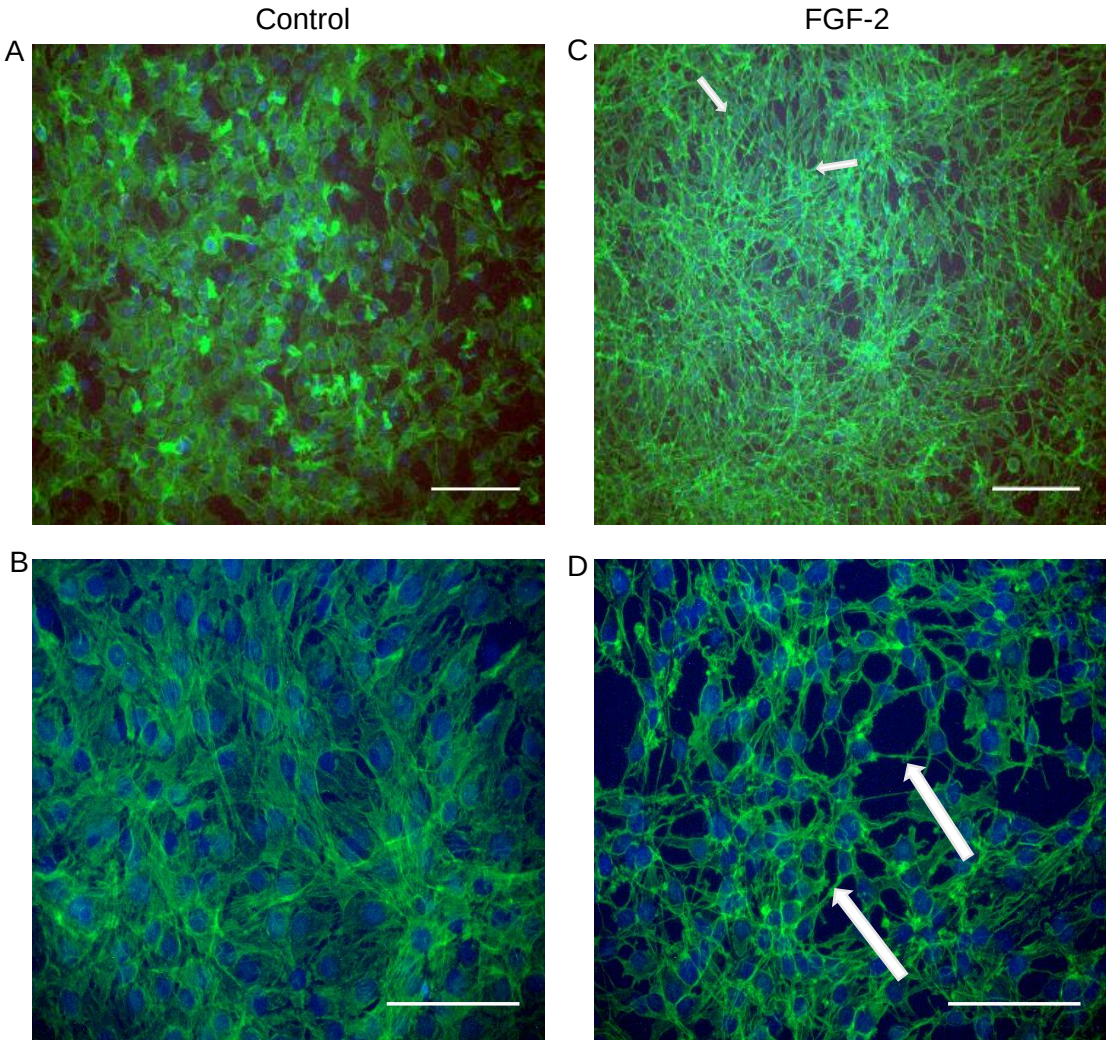

Figure 3.5. Spatial distribution of F-actin in MC3T3 osteoblast-like cells cultured in FGF-2

The effect of FGF-2 10 ng/ml on MC3T3 osteoblast-like cell morphology after phalloidin staining for F-actin after 24 h in control (**A** and **B**), and treated cells (**C** and **D**). Note the white arrows pointing at the dendrites F-actin in the treated cells. Images are representative of three separate experiments. Scale bar (**A** and **C**) = 200 um; (**B** and **D**) = 150 um.

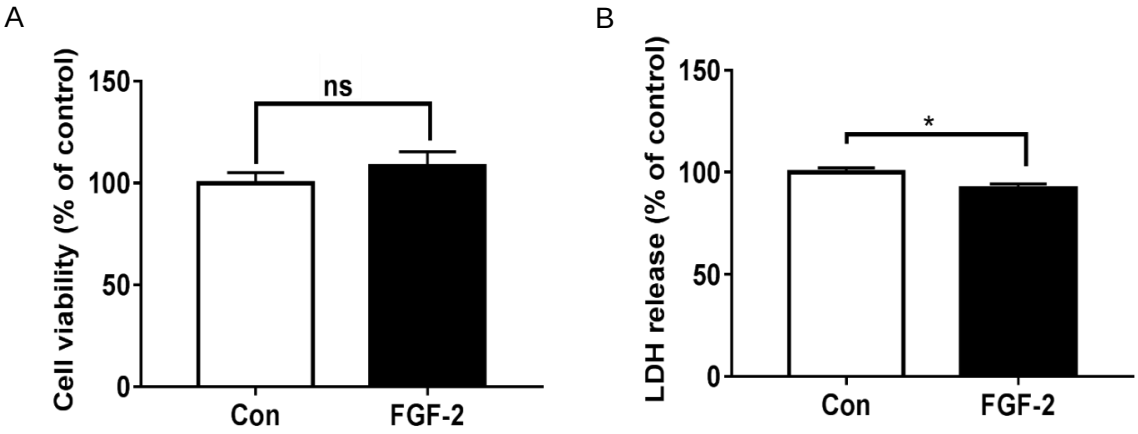

Figure 3.6. Cell Viability and Lactate Dehydrogenase (LDH) profile of MC3T3 cells cultured in FGF-2 10 ng/ml for 24 h.

(**A**) Alamar Blue cell viability assay showing no difference between the FGF-2 treated and control cultures. (**B**) LDH release from FGF-2 treated cultures was significantly lower than the control cultures. Data are presented as mean ± S.E.M (n=3); *$p<0.05$; ns = not significant.

3.5.7 Effect of E11siRNA transfection on FGF-2 stimulation of E11 expression and F-actin distribution by MC3T3 cells

To investigate if the effects of FGF-2 on MC3T3 osteoblast-osteocyte differentiation is mediated by E11, the cells were transfected with E11siRNA and incubated for 24 h by FGF-2. *E11* gene (77% knockdown vs. mock control, 70% knockdown vs. scrambled control; $P<0.05$; Fig. 3.7A) and protein (Fig. 3.7B) expression were silenced successfully by E11 siRNA transfection. After 24 h of FGF-2 treatment, FGF-2 stimulated *E11* gene expression in scrambled and mock treated groups but not in the E11 siRNA transfected cells (Fig. 3.7A). Gene expression analysis of the other osteocytes makers showed the significant up-regulation of *Phex* ($P<0.01$; Fig. 3.7C) and *Dmp1* ($P<0.001$; Fig. 3.7D), in the FGF-2 treated cells when compared to the control samples of E11siRNA, scrambled and mock groups. Immunofluorescence intensity of E11 expression in siRNA treated cells (Fig. 3.8A & B) was less than that observed in the scrambled (Fig. 3.8C & D) and mock (Fig. 3.8E & F) treated cells. Moreover, whilst FGF-2 promoted dendrite formation in all groups of cells, their number appeared les in those pre-treated with E11siRNA (Fig. 3.7A & B) when compared to the scrambled (Fig. 3.8 & D) and mock (Fig. 3.8E & F) treated cells. F-actin distribution after 24 h FGF-2 stimulation showed similar trend with shorter dendrites seen in the E11siRNA pre-treated cells with retained osteoblast cuboidal shape (Fig. 3.8G & H), when compared to scrambled (Fig.3.8I & J), and mock (Fig.3.8K & L) that showed more spindle osteocyte like shape in the FGF-2 stimulated cells.

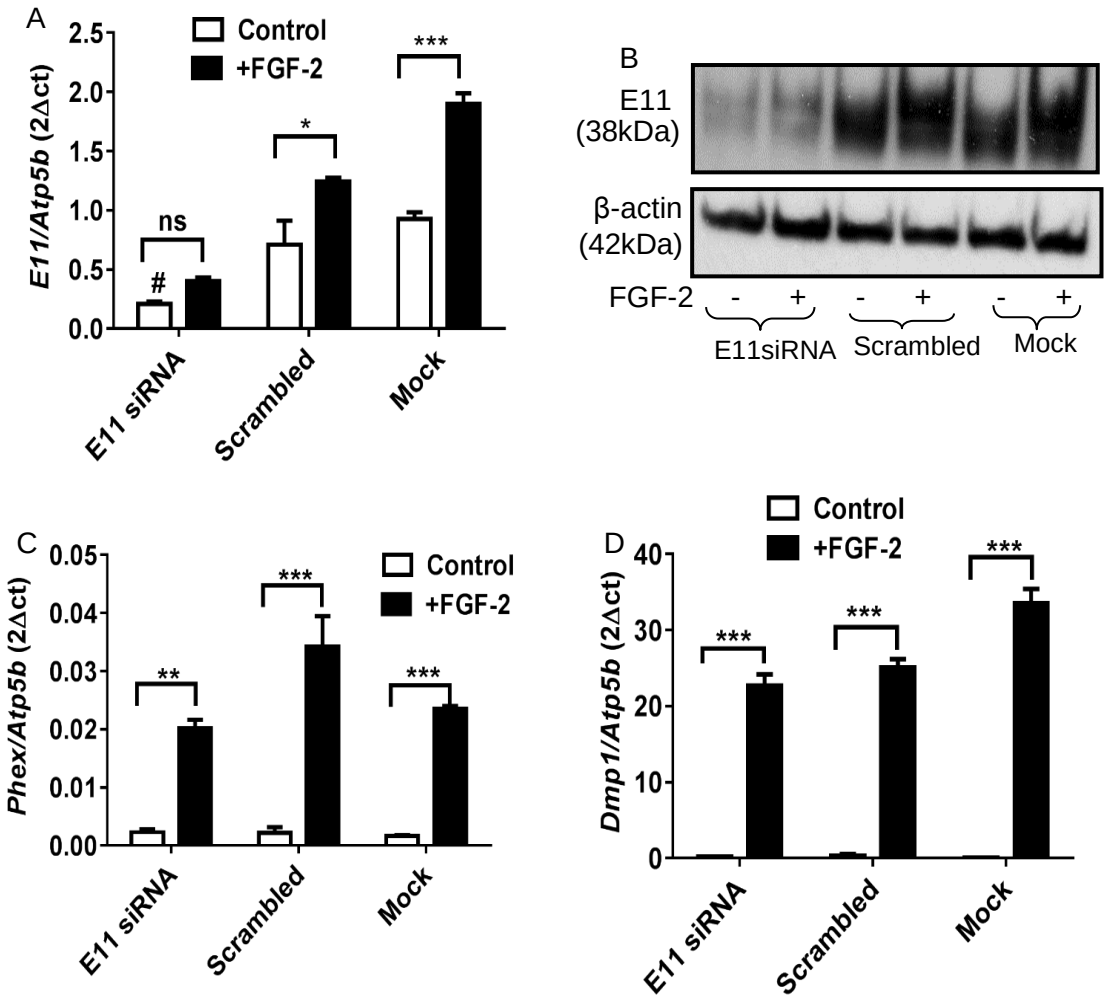

Figure 3.7 Temporal expression of E11, *Phex and Dmp1* by FGF-2 stimulated MC3T3 cells after E11 siRNA transfection

The effect of E11siRNA transfection on FGF-2 10 ng/ml stimulation of (**A**) E11 gene and (**B**), E11 protein expression after 24 h stimulation. Note the effect on other osteocyte markers (**C**) *Phex*, and (**D**) *Dmp1* gene expression after same time point. Results are normalised to the Atp5b housekeeping gene. Data are presented as mean ± S.E.M (n=3); *p<0.05; **p<0.01; ***p<0.001 compared to control cells; #p<0.05 of E11siRNA control cells compared of scrambled control cells.

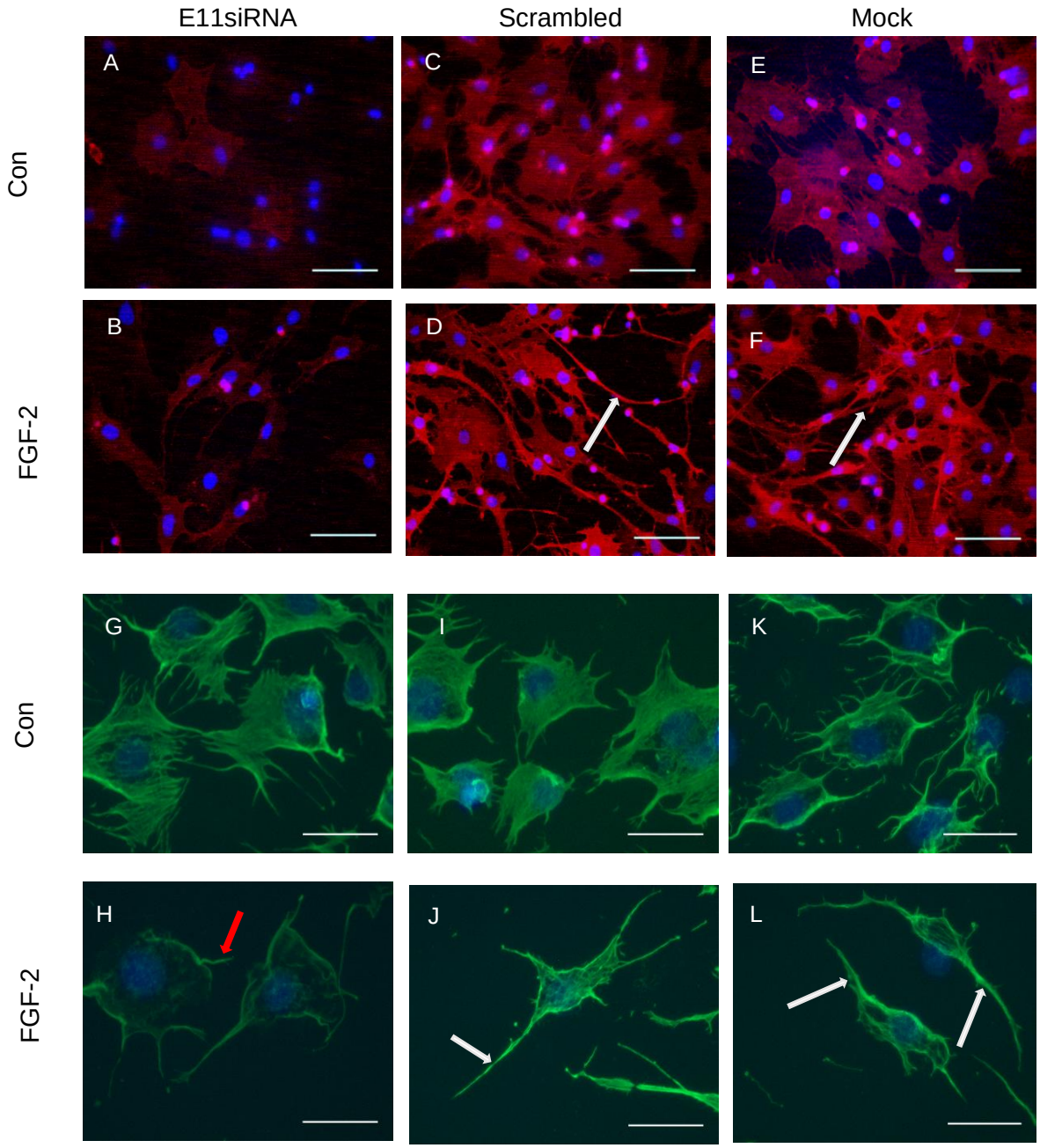

Figure 3.8 Spatial expression of E11 and F-actin distribution by MC3T3 cells cultured in FGF-2 after E11siRNA transfection

Immunofluorescence of E11 localisation (**A-F)** revealed loss of dendrite formation in the E11siRNA groups (**A** & **B**) when compared to the scrambled (**C** & **D**) and mock (**E** & **F**). Phalloidin staining for F-actin (**G-L**) showing similar trend as seen E11siRNA groups (**G** & **H**), when compared to the scrambled (**I** & **J**) and mock (**K** & **L**). Note longer and prominent dendrites in FGF-2 treated scrambled and mock cultures (white arrow), and retained flattened shaped cell (red arrow) in E11siRNA phalloidin staining. Scale bar (**A-F**) = 150 um; (**G-L**) = 100 um.

3.5.8 The effect of FGF-2 on the expression of E11 gene and protein expression by primary calvarial osteoblasts

Primary osteoblasts isolated from the calvaria of 3-day old wild type mice were used. An FGF-2 concentration-response experiment was first completed to optimise further studies with primary osteoblasts and therefore the temporal analysis of *E11* gene expression in the presence of a range of FGF-2 concentrations was carried out as previously described in MC3T3 osteoblast-like cells (Fig 3.1). After 4 h treatment with FGF-2 at 1, 10, 25 and 50 ng/ml, there was a small but consistent trend of higher E11 gene expression when compared to control cells (Fig. 3.9A). This up regulation of E11 protein expression was more marked after 24 h FGF-2 treatment (Fig. 3.9B). Analysis of E11 protein expression revealed that E11 expression was higher in control cells (no FGF-2 treatment) cultured for 24 h than in cells cultured for 4 h (Fig. 3.9C). This suggests that prolonged culture length induced E11 expression. After 4 h, the FGF-2 treated cells expressed more E11 protein and this was particularly notable in the 25, and 50 ng/ml treated cells (Fig. 3.9C).

Similarly, after 24 h, the FGF-2 treated cells expressed more E11 protein and this was most noticeable in the 10, 25, and 50 ng/ml treated cells (Fig. 3.8C). A 10 ng/ml concentration of FGF-2 was chosen for future experiments to reflect optimum expression and cost effectiveness.

3.5.9 Effect of FGF-2 10 ng/ml over a short time-course on (1) E11 expression and (2) osteocyte/osteoblast gene markers in primary osteoblasts

E11 expression was significantly up-regulated after 6 ($P<0.05$) and 24 h ($P<0.001$) exposure to FGF-2 when compared with untreated control cells (Fig. 3.10A). Western blotting also indicated that FGF-2 induced E11 protein expression and this was particularly evident after 24 h FGF-2 exposure (Fig. 3.10B). FGF-2 at 10 ng/ml also induced the up-regulation of osteocyte markers *Phex* ($P<0.001$, Fig. 3.10C) and *Dmp1* ($P<0.01$, Fig. 3.10D) whilst down regulating osteoblast markers, *Col1a1, Bglap, Alpl*, *Postn* (Fig. 3.10E - H). The down regulation of *Col1a1*, *Alp, Postn and Bglap* and upregulation of *E11, Phex* and *Dmp1* by FGF-2 after 24 h, indicates that FGF-2 is inducing differentiation of primary preosteoblast/osteoblasts to the osteocyte phenotype.

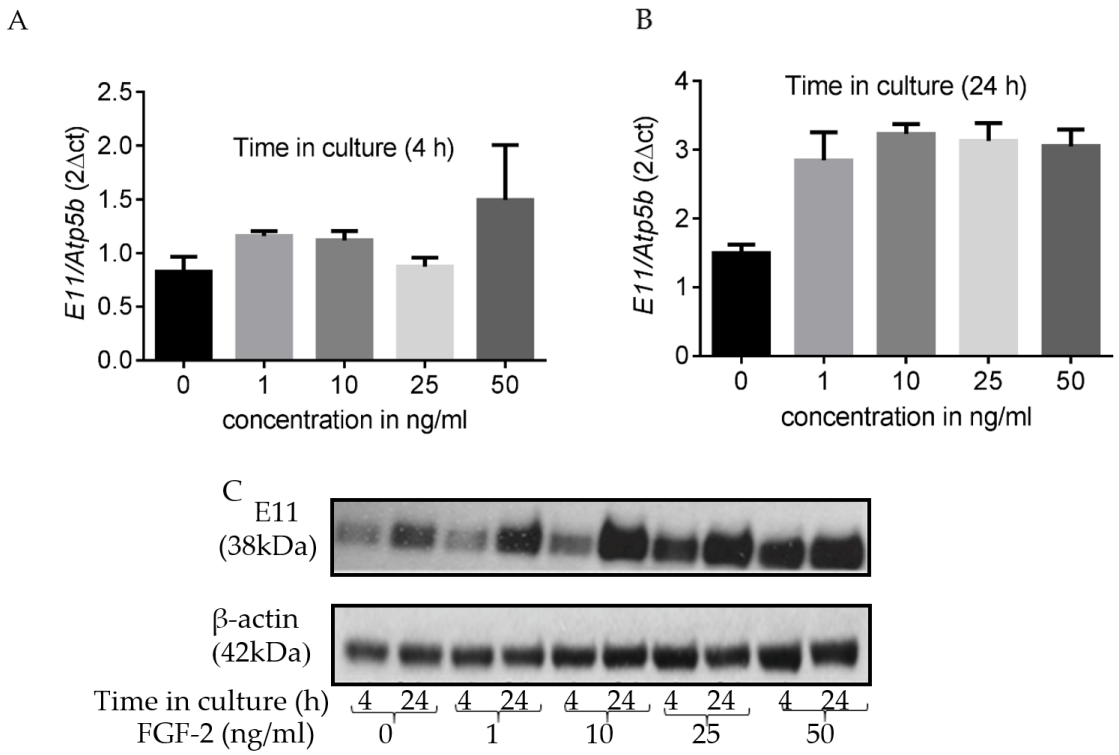

Figure 3.9 Temporal expression of E11 by primary osteoblasts cultured in increasing concentrations of FGF-2.

Temporal gene expression of E11 by primary osteoblasts cultured in increasing concentrations of FGF-2. The effects of FGF-2 (0 - 50 ng/ml) on E11 gene expression at (**A**) 4 h and (**B**) 24 h. (C) E11 protein expression was also examined after FGF-2 treatment for 4 and 24 h by western blotting. Data are presented as mean ± S.E.M (n=3).

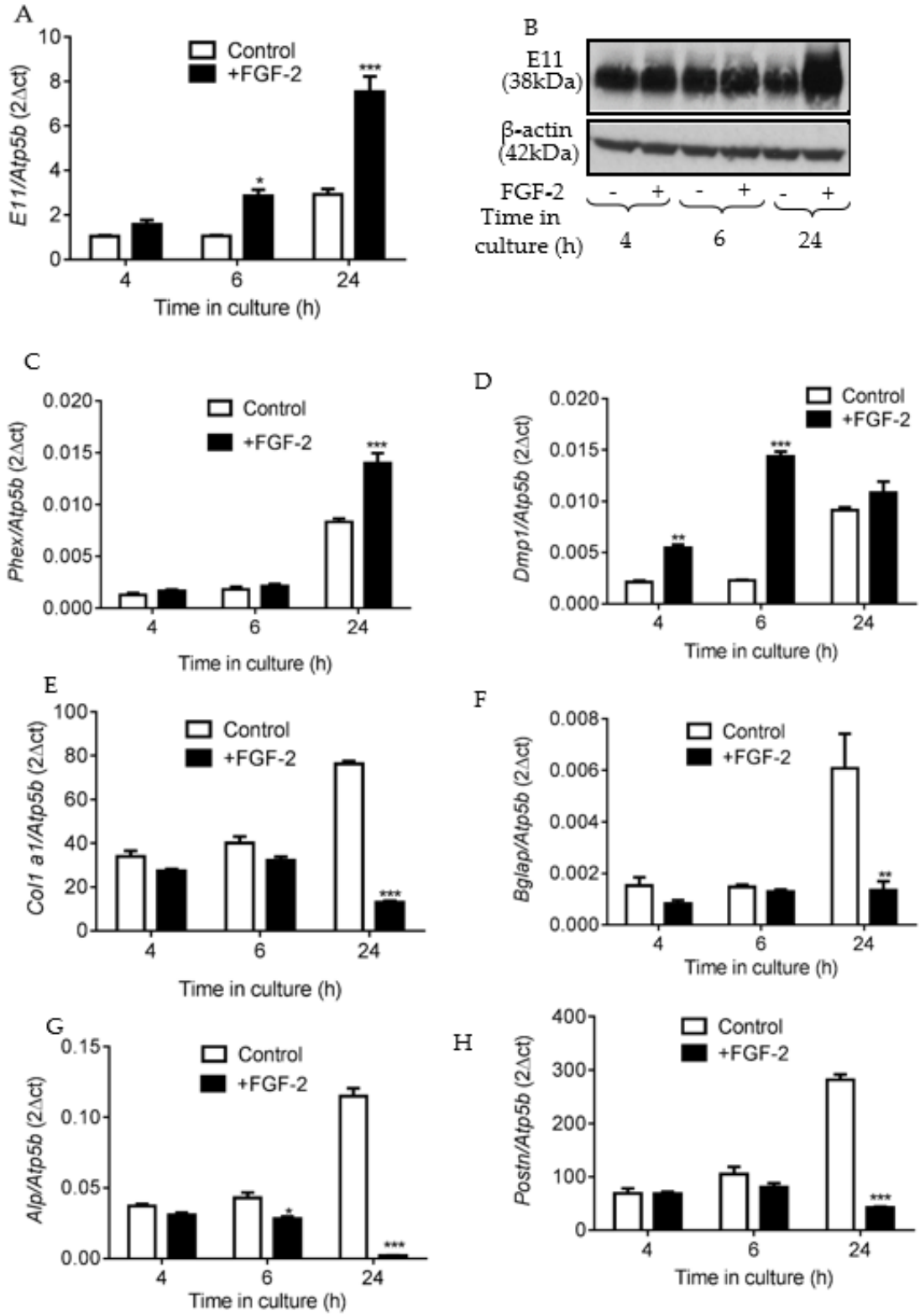
A
E11/Atp5b (2Δct)
Control
+FGF-2
Time in culture (h)
B
E11
(38kDa)
β-actin
(42kDa)
FGF-2
Time in
culture (h)
C
Phex/Atp5b (2Δct)
D
Dmp1/Atp5b (2Δct)
E
Col1 a1/Atp5b (2Δct)
F
Bglap/Atp5b (2Δct)
G
Alp/Atp5b (2Δct)
H
Postn/Atp5b (2Δct)

(Previous page) Figure 3.10 Temporal expression of E11 and osteocyte/osteoblast gene markers by primary osteoblasts cultured in FGF-2 10 ng/ml.

The effect of FGF-2 10 ng/ml on (**A**) E11 gene and (**B**), E11 protein expression after 4, 6 and 24 h stimulation. Note the effect on other osteocyte markers (**C**) *Phex*, and (**D***) Dmp1* gene expression; and osteoblast gene markers (**E**) *Col1a1,* (**F***) Bglap* (**G**) *Alpl*, and (**H**) *Postn* gene expression after same time points. Data are presented as mean ± S.E.M (n=3); *p<0.05; **p<0.01; ***p<0.001 compared to control cells.

3.5.10 Effect of FGF-2 on the osteocyte phenotypic appearance of primary osteoblasts

The previous data using immunofluorescence microscopy indicated that FGF-2 was able to increase E11 expression and promote greater dendritic cytoplasmic projects in MC3T3 cells. In this present study, primary osteoblasts were similarly investigated to ases the cellular distribution of E11 during the osteocytogenesis. The control cells showed a similar cuboidal shape at all stages of differentiation with little evidence of dendritic formation at the membrane surface (Fig. 3.11A-F). After treatment with FGF-2, there was clear evidence for the formation of dendrites from the primary cells at all-time points (Fig. 3.11G-L).

3.5.11 Effect of FGF-2 10 ng/ml *E11* expression and osteocyte/osteoblast gene markers in cultured whole calvaria.

To investigate if FGF-2 drives *E11* expression in more physiological condition i.e. compared with cultured cells as done previously, an *ex-vivo* study was completed on whole calvaria. This model will replicate possible interactions between the ECM and both *E11* and FGF-2, which was absent in both the cell line and the primary osteoblast models used previously. Changes in gene expression in this model were limited. There was however a small but significant increase in *E11* ($P<0.05$, Fig. 3.12A) and *Dmp1* ($P<0.001$, Fig. 3.12B) expression by FGF-2 after at 6h but not at the other time points. No changes in the expression of osteoblast marker genes (*Phex* (Fig. 3.12C), *Alp* (Fig. 3.12D), *Bglap* (Fig. 3.12E), *and Postn* (Fig. 3.12F)) by FGF-2 were noted at any of the time points studied.

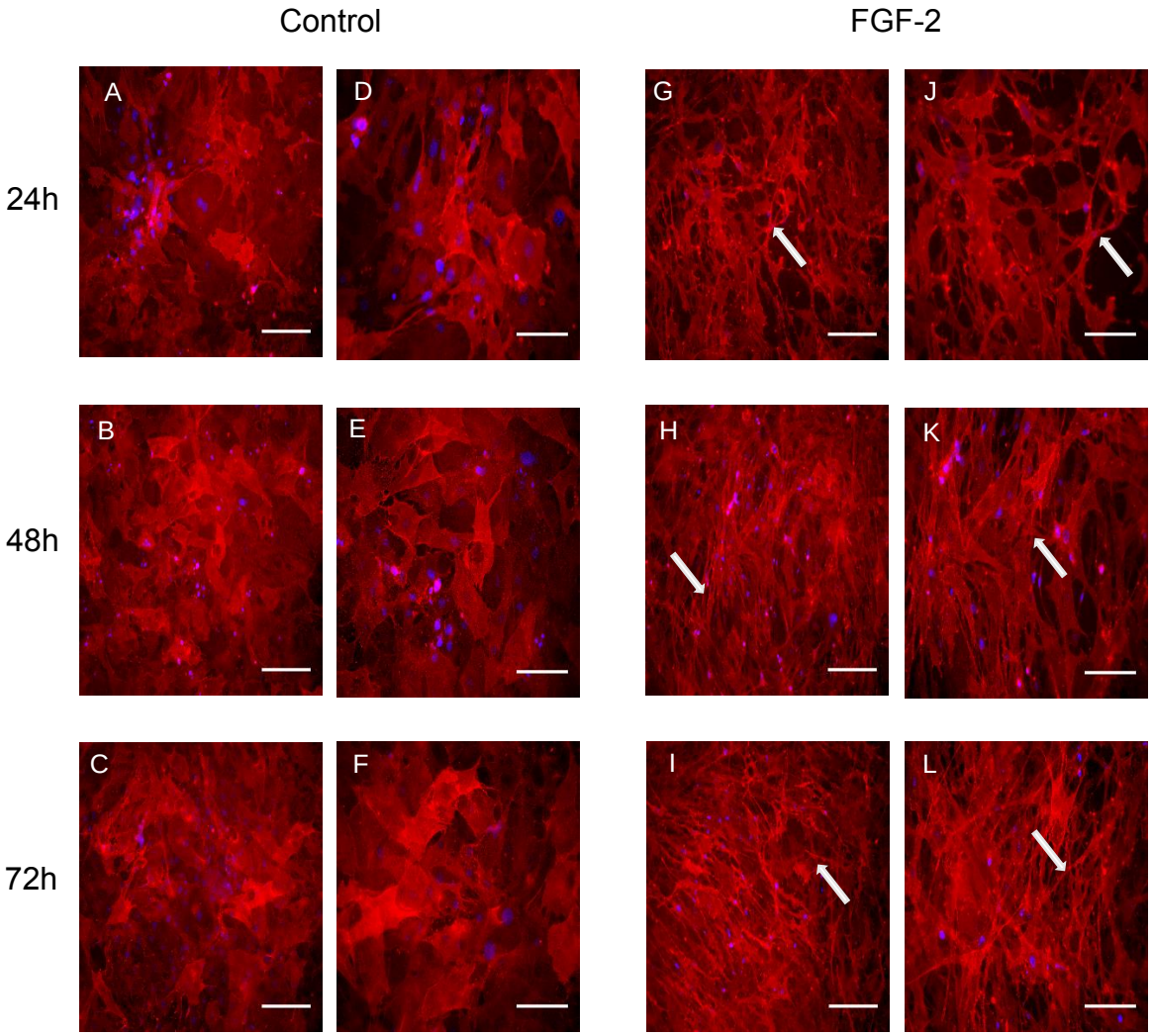

Figure 3.11 Spatial expression of E11 in primary osteoblasts cultured in the presence of FGF-2.

The effect of FGF-2 10 ng/ml on E11 expression and distribution in primary cells assessed by immunofluorescence microscopy of control cells (**A**); and cells treated by FGF-2 (**B**) at 24, 48 and 72 h time points. Note the arrows pointing at the dendrites. Images are representative of three separate experiments. Scale bar, **A-C** & **G-I** = 200 um; **D-F** & **J-L** = 150 um).

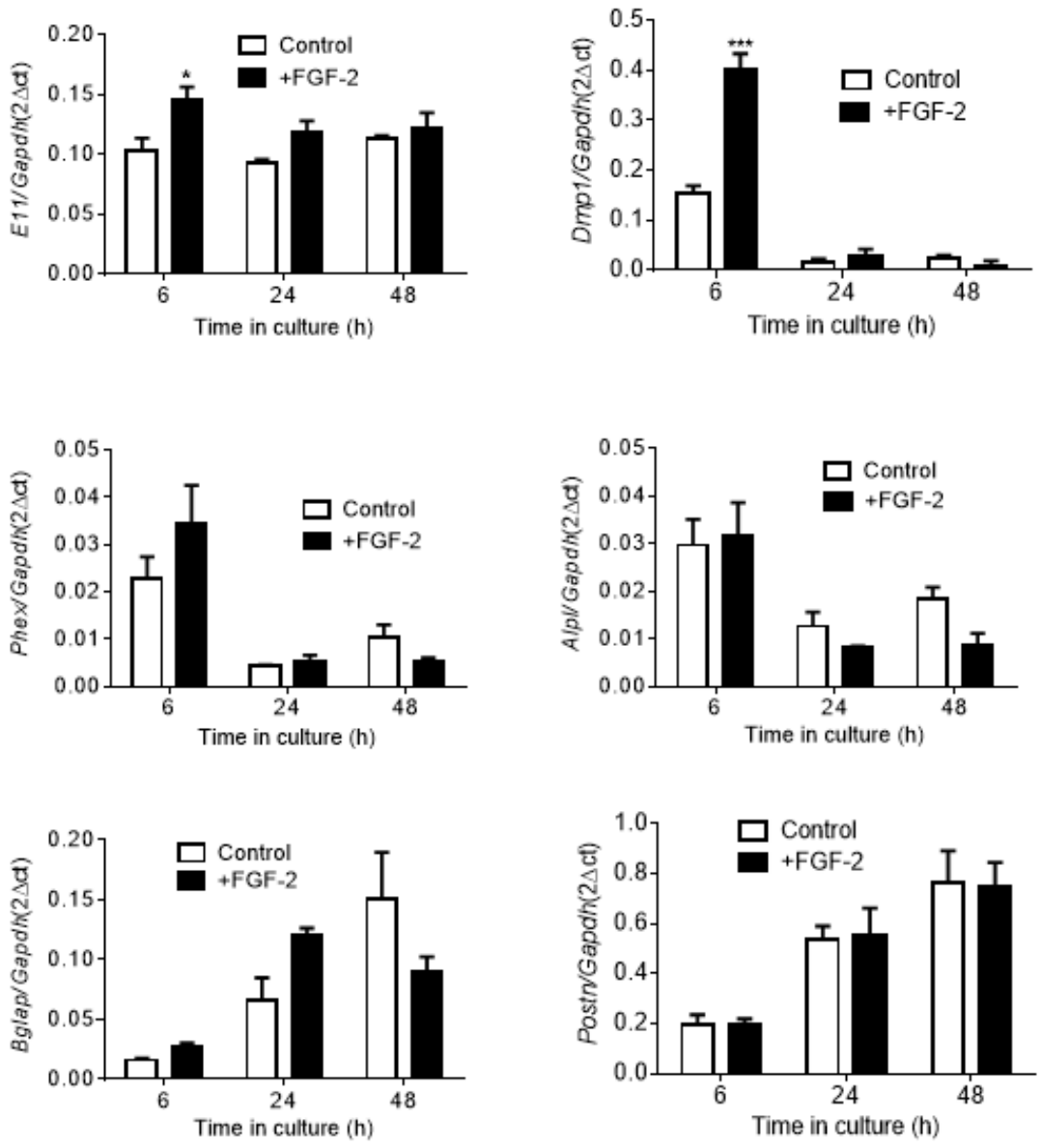

Figure 3.12 Temporal expression of *E11* and osteocyte/osteoblast gene markers in whole calvaria cultured in the presence of FGF-2 10 ng/ml.

Temporal gene expression of whole calvaria cultured with FGF-2 10 ng/ml 6- 48 h. RT-qPCR assessed expression *of* (**A**) *E11* (**B**) *Dmp1* (**C**) *Phex* (**D**) *Alp*, (**E**) *Bglap,* and (**F**) *Postn*. Data are presented as mean ± S.E.M for n=3 observations; *p<0.05; ***p<0.001.

3.5.12. Investigating if deletion of *Fgf-2* in vivo affect E11 and Sclerostin expression in osteocytes.

Having shown the up-regulation of *E11* expression by FGF-2 in MC3T3 osteoblast-like cell line, primary osteoblasts and whole calvaria, the next study was designed to investigate the relationship between FGF-2 and both E11 and sclerostin expression *in vivo*. Immunohistochemistry was employed to examine whether bones from *Fgf-2* KO mice exhibited altered E11 and sclerostin expression. Osteocytes of subchondral, trabecular and cortical bone from *Fgf-2* KO stained positively for E11, and this osteocyte staining appeared larger and stronger when compared to the same in osteocytes from WT mice (Figs. 3.13, 3.14, and 3.15). However, the quantification of the number of E11 positive cells in all three bone regions was similar in samples from both *Fgf-2* KO and WT mice (Fig. 3.15E). Sclerostin osteocyte immunostaining was similar in cortical, trabecular and subchondral bone of *Fgf-2* KO and WT mice as was the quantification of the number of sclerostin positive osteocytes in all three bone regions (Figs. 3.16, 3.17, and 3.18). Hypertrophic chondrocytes of the articular cartilage stained positive to sclerostin immunostaining (Fig. 3.16A & B). IgG control Sections were negative (Fig. 3.19).

3.5.13. Investigating if deletion of *Fgf-2* in vivo affects osteocyte dimension in mice.

Having observed larger osteocytes in *Fgf-2* KO mice relative to those in WT mice (Figs. 3.14A & C), osteocyte phalloidin staining was performed in the cortical bone of *Fgf-2* KO and WT mice (Fig. 3.20A & B) to confirm this. There was a significant increase in cell body volume ($P<0.05$, Fig. 3.20C), but no differences in cell sphericity

were observed (Fig. 3.20D). In addition, the total number of dendrites (Fig. 3.20E) and dendrite volume (Fig. 3.20F) were unchanged between *Fgf-2* KO and WT mice. There was, however, a significant decrease in average dendrite volume in *Fgf-2* KO mice compared with WT mice ($P<0.01$; Fig. 3.20G).

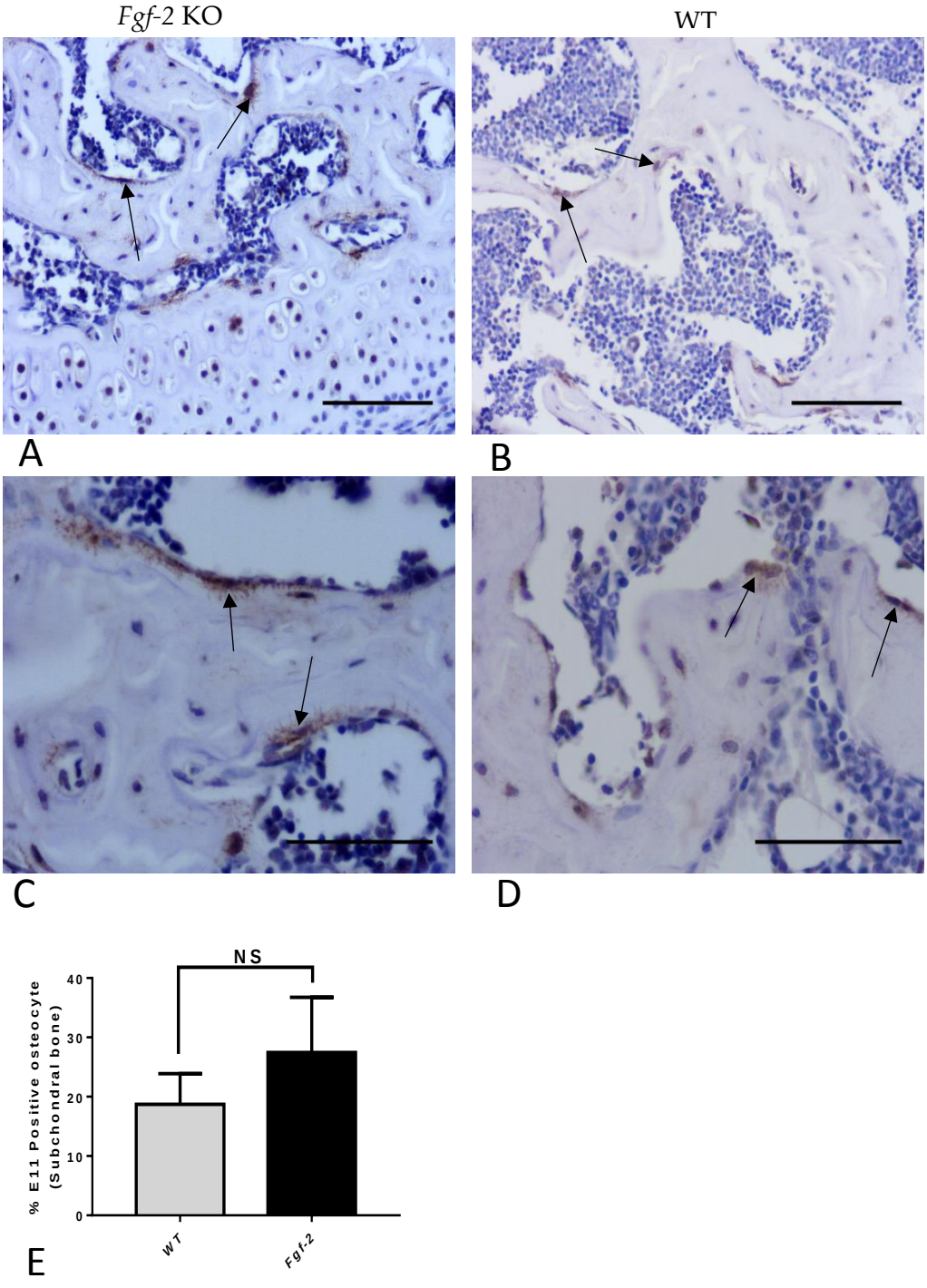

Figure 3.13 E11 immunostaining of tibial subchondral bone osteocytes from *Fgf-2* KO and WT mice.

Sections of subchondral bone osteocytes (black arrow) in both *Fgf-2* KO (**A & C)** and WT (**B & F**) showing E11 localisation to osteocytes and their dendritic processes., Quantification of E11 positive osteocytes was similar in both WT and *Fgf-2* KO subchondral bone (**E**). Data are presented as mean ± S.E.M for n=3 observations, NS= not statistically significant. Scale Bar (**A & B**) =150 um; (**C & D**) =100 um

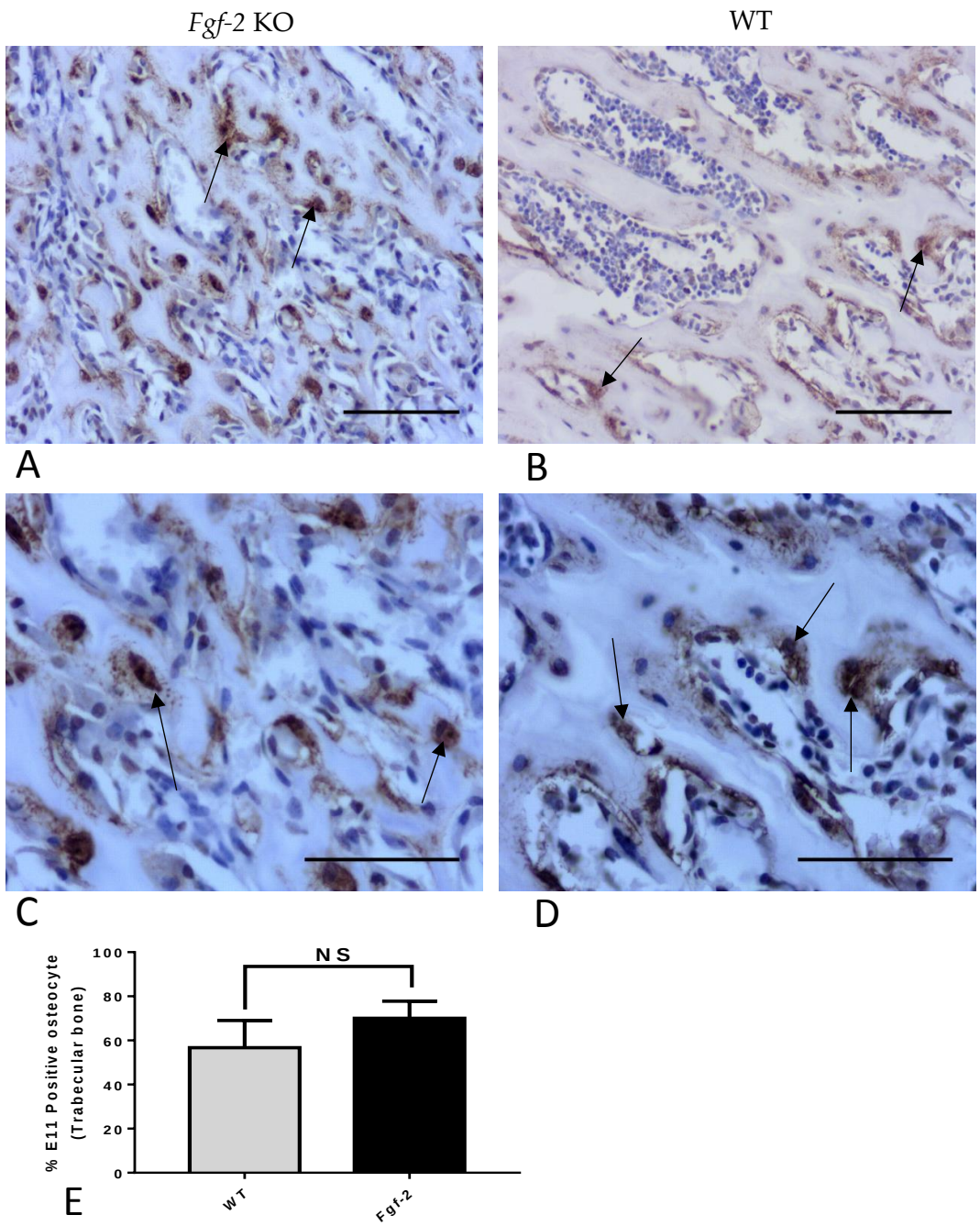

Figure 3.14 E11 immunostaining of tibial trabecular bone osteocytes from *Fgf-2* KO and WT mice.

Section of trabecular bone osteocytes (black arrow) in both *Fgf-2* KO (**A & C)** and WT (**B & F**) showing E11 localisation to osteocytes and their dendritic processes., Quantification of E11 positive osteocytes was similar in both WT and *Fgf-2* KO trabecular bone (**E**). Note the larger osteocytes in the *Fgf-2* KO (**A & C**). Data are presented as mean ± S.E.M for n=3 observations, NS= not statistically significant. Scale Bar (**A & B**) =150 um; (**C & D**) =100 um

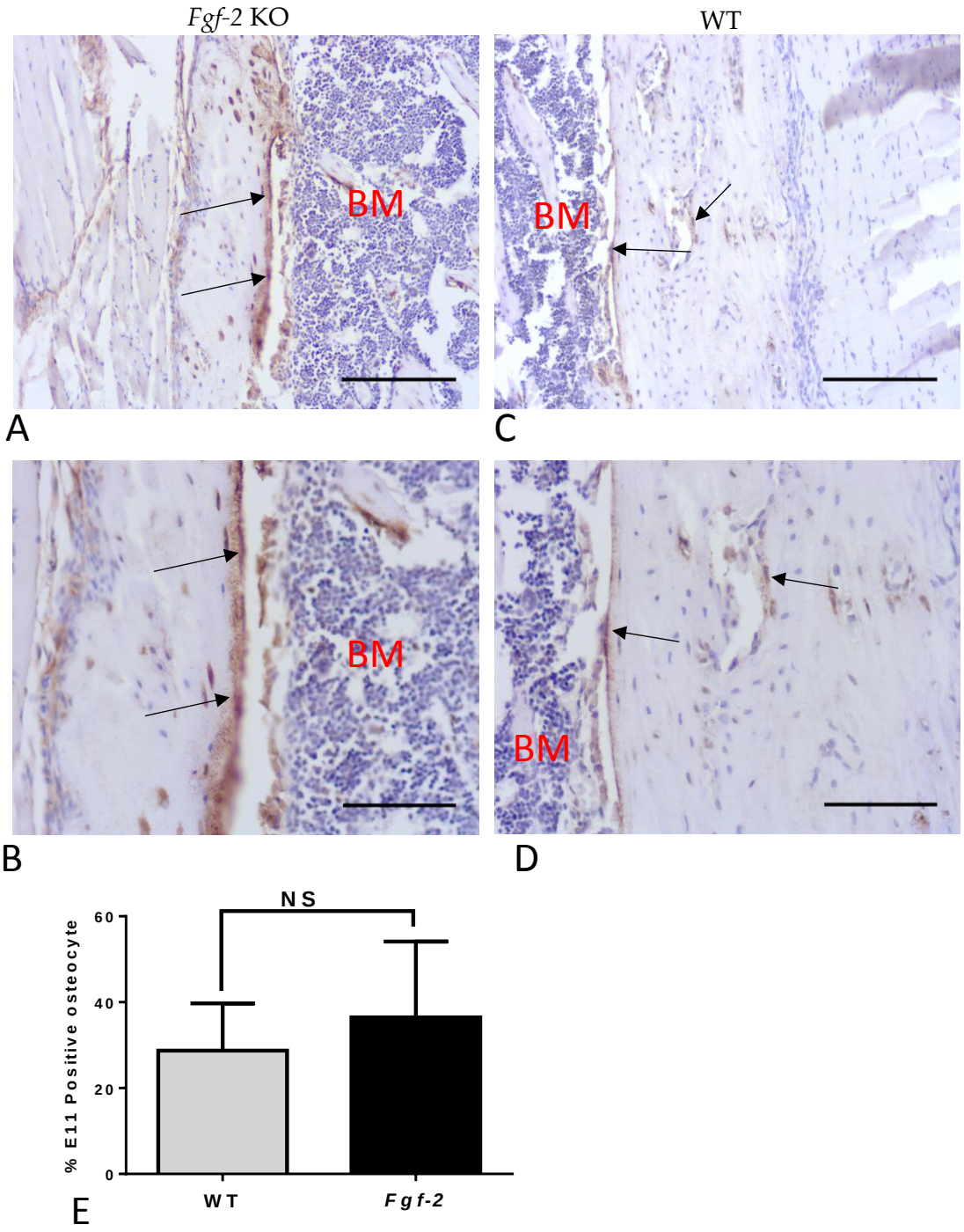

Figure 3.15 E11 immunostaining of tibial cortical bone osteocytes *of Fgf-2* KO and WT mice

Section of cortical bone osteocytes (black arrow) in both *Fgf-2* KO (**A & B**) and WT (**C & D**), showing E11 localisation to osteocytes and their dendritic processes., Quantification of E11 positive osteocytes was similar in both WT and Fgf-2 KO cortical bone (**E**). Note the bone marrow, BM. Data are presented as mean ± S.E.M for n=3 observations, NS = not statistically significant. Scale bar (**A & C**) = 300 um; (**B & D**) =150 um.

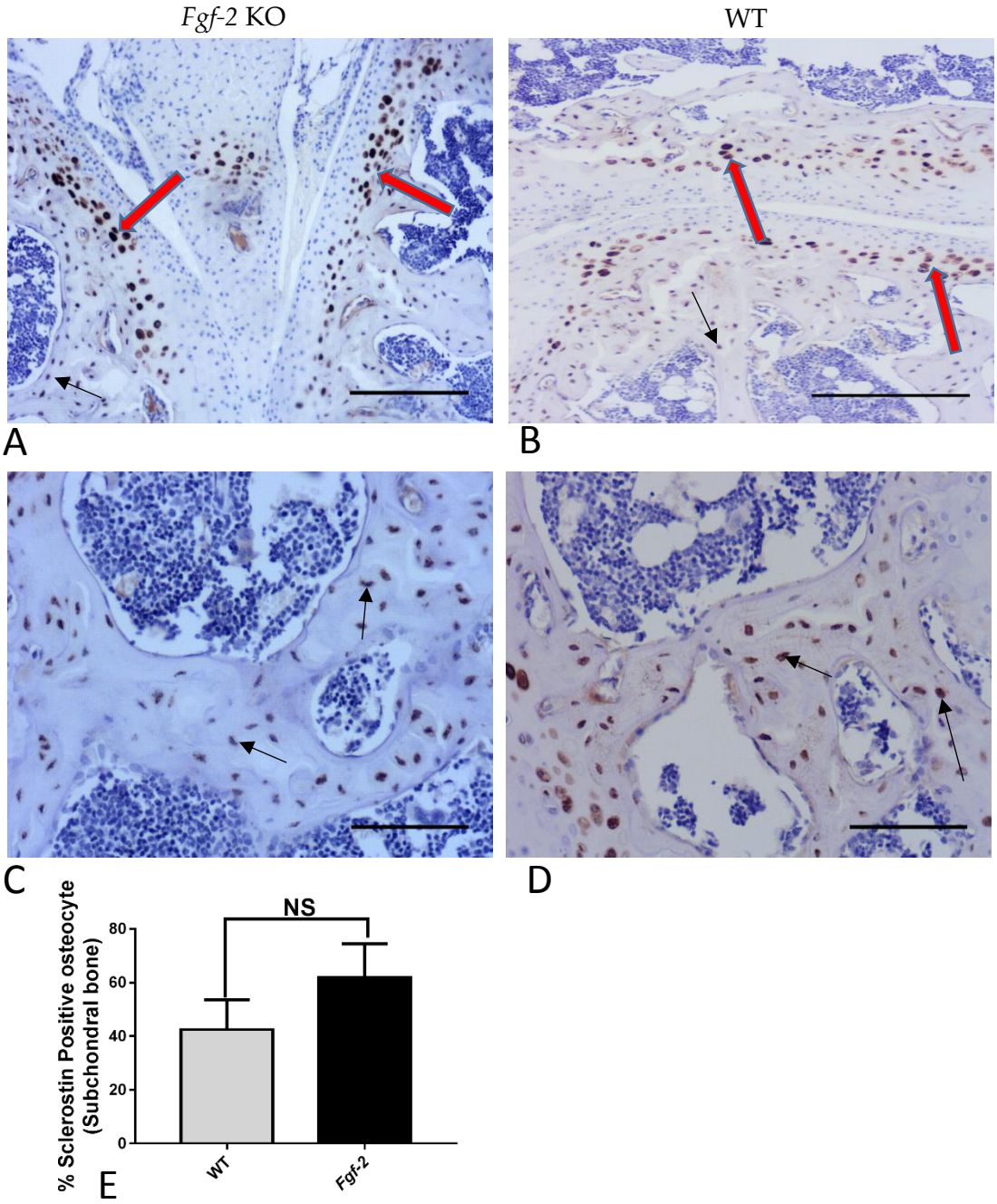

Figure 3.16 Sclerostin immunostained *Fgf-2* KO and WT mice tibial articular cartilage and subchondral bone.

Section of subchondral bone osteocytes (black arrow) in both *Fgf-2* KO (**A & B**) and WT (**C & D**), showing no difference in Sost immunostaining, as was also shown from quantification of sclerostin positive osteocytes (**E**). Note the positive staining of hypertrophic chondrocytes of the articular cartilage (red arrow). Data are presented as mean ± S.E.M for n=3 observations. NS= not statistically significant. Scale bar (**A & C**) = 300 um; (**B & D**) =150 um.

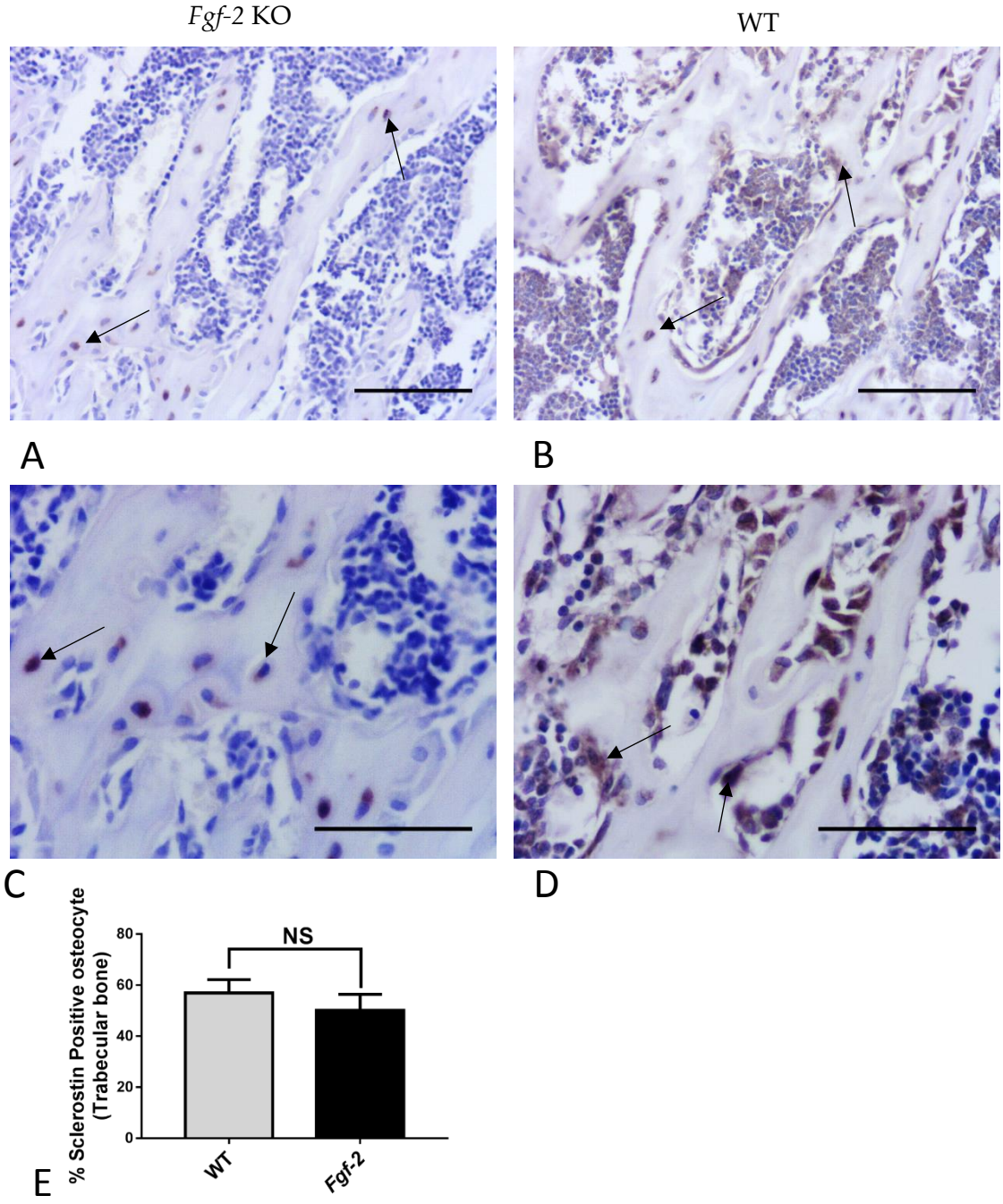

Figure 3.17 Sclerostin immunostained *Fgf-2* KO and WT mice tibial trabecular bone osteocytes

Section of trabecular bone osteocytes (black arrow) in both *Fgf-2* KO (**A & C)** and WT (**B & F**) showing no difference in sclerostin immunostaining, as was also shown from quantification of sclerostin positive osteocytes (**E**). Data are presented as mean ± S.E.M for n=3 observations, NS = not statistically significant. Scale Bar (**A & B**) =150 um; (**C & D**) =100 um

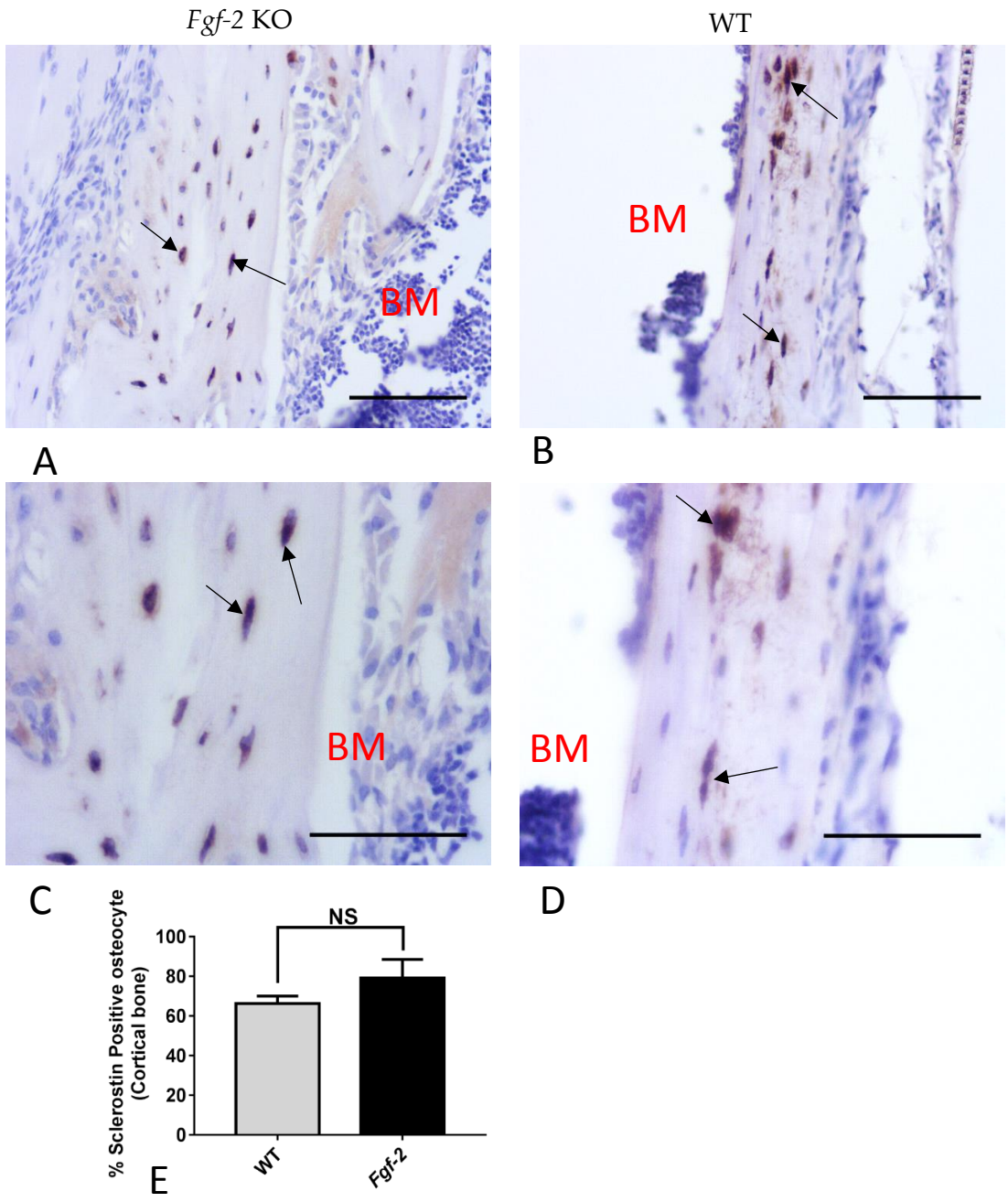

Figure 3.18 Sclerostin immunostained *Fgf-2* KO and WT mice tibial cortical bone osteocytes

Section of cortical bone osteocytes (black arrow) in both *Fgf-2* KO (**A & C)** and WT (**B & F**) showing no difference in sclerostin immunostaining, as was also shown from quantification of sclerostin positive osteocytes (**E**). Note the bone marrow, BM. Data are presented as mean ± S.E.M for n=3 observations, NS = not statistically significant. Scale Bar (**A & B**) =150 um; (**C & D**) =100 um

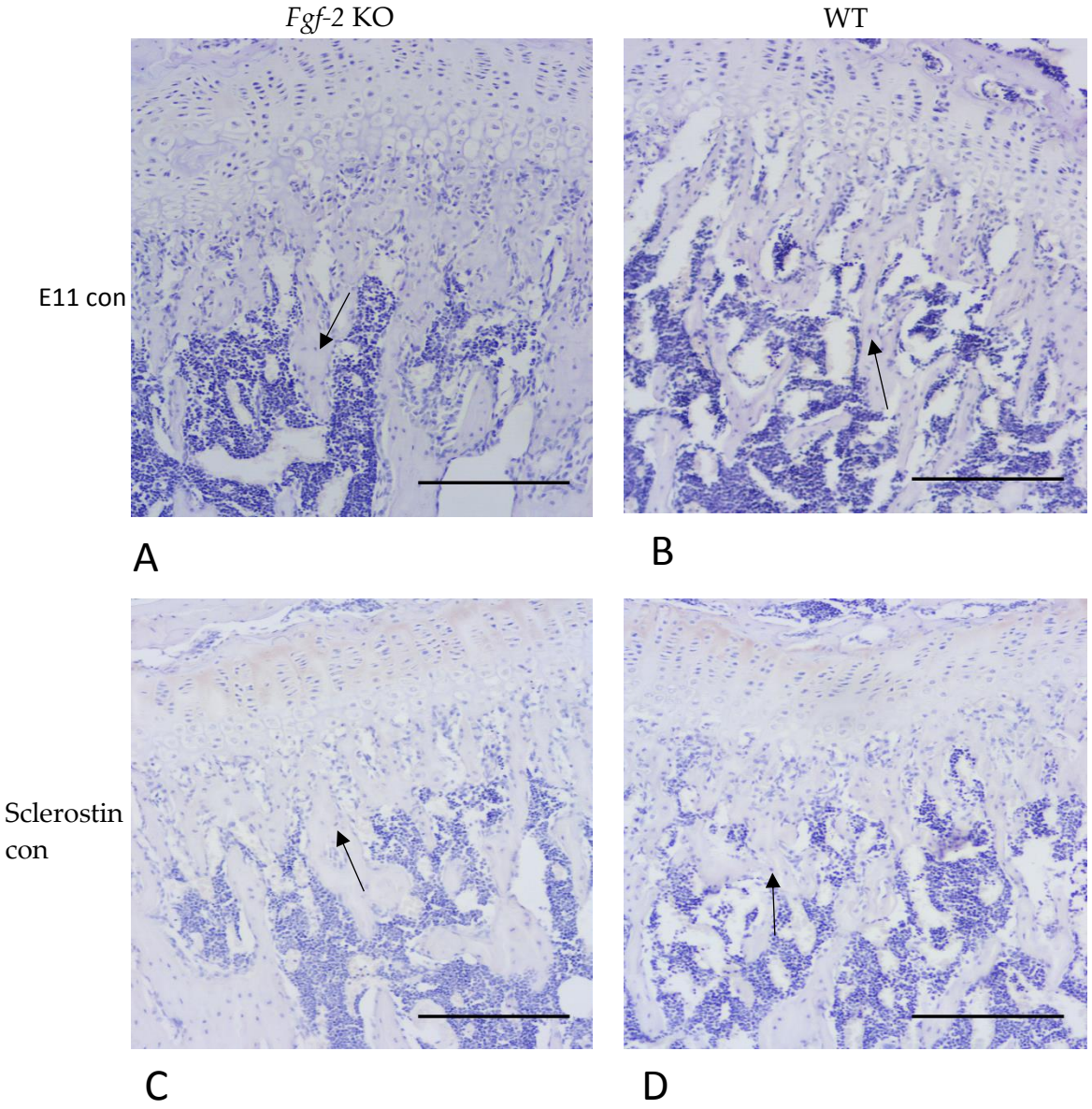

Figure 3.19 IgG control sections of tibial trabecular bone osteocytes of *Fgf-2* KO and WT mice.

Section of trabecular bone osteocytes (black arrow) in both *Fgf-2* KO (**A & B**) and WT (**C & D**) showing no positive staining in the absence of the primary antibodies. This confirms the specificity to the sclerostin and E11 antibodies. Scale bar=300 um

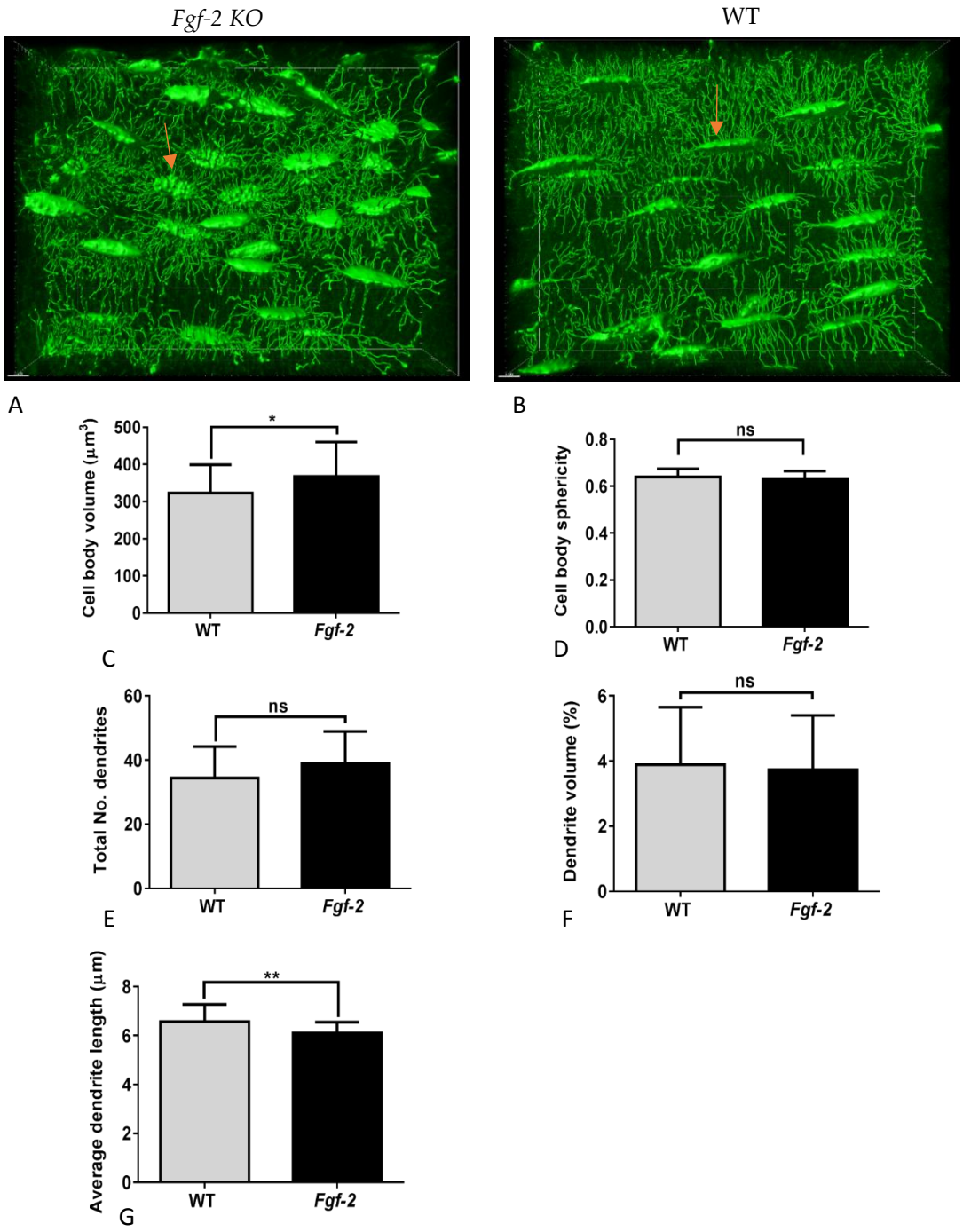

Figure 3.20 Phalloidin stained *Fgf-2* KO and WT mice tibial cortical bone osteocytes

Section of cortical bone osteocytes in both *Fgf-2* KO (**A**) with larger cell body volume than the WT (**B**) as was confirmed by quantification (**C**), but same cell spherical shape (**D**). While the total dendrite number and volume (**E & F**), were same, the average length of the WT was longer than the *Fgf-2* KO (**G**). Note the dendrites (pink arrow) emerging from the osteocyte cell body. Data are presented as mean ± S.E.M for n=3 observations; *p<0.05, **p<0.01. Scale bar = 7 um.

3.5 Discussion

The transmembrane glycoprotein E11, has long been recognised to be an early driver of the osteoblast to osteocyte transition and the acquisition of the dendritic appearance (Zhang et al., 2006, Gupta et al., 2010). Consistent with this, the data in this study, which used a number of osteoblast and organ culture models, showed that FGF-2 is able to increase E11 expression and that this is likely to lead to the observed increase in osteocyte dendrite formation.

A previous brief report has shown that FGF-2 treatment of osteoblast-like cells was able to induce an increase in E11 expression and the appearance of the osteocyte phenotype (Gupta et al., 2010, Miyagawa et al., 2014), this present study, has confirmed these observations in both MC3T3 and primary osteoblasts. The significant up-regulation of *E11*, *Phex* and *Dmp1* and down-regulation of *Col1*, *Bglap, Alp and Postn* in the FGF-2 treated cultures suggests that FGF-2 is inducing the differentiation of the osteoblast to the osteocyte phenotype. This was demonstrated further by the lack of difference in E11 expression after prolonged treatment with FGF-2, suggesting that the osteocyte had differentiated beyond this early gene marker threshold. This study has also extended these observations to show that E11 is an early osteocyte marker, is also regulated by FGF-2 at the protein level, just like the osteoblast/osteocyte gene markers (Paic et al., 2009, Gupta et al., 2010, Stern et al., 2012). The similar stimulatory effect of FGF-2 on E11 expression in both cell types, especially the primary osteoblasts, suggests the possibility of a similar effect *in vivo*,

as down-regulation of E11 has been reported in *Fgf-2* KO mice in an injured joint model study (Chong et al., 2013).

The whole calvaria study was aimed at providing an *ex vivo* environment to extend the understanding on FGF-2-E11 interactions, having established a positive stimulatory effect on E11 expression by FGF-2 in MC3T3 osteoblast like cells and primary osteoblasts. This system replicates a near physiological environment, maintaining cell plurality and ECM interactions (Mohammad et al., 2008, Kyono et al., 2012), hence it is commonly used to investigate the regulatory mechanisms of bone formation (Mohammad et al., 2008, Dallas et al., 2013). FGF-2 up-regulated *E11* gene expression, as well as known osteocyte marker gene *Dmp1*, in the early time points. This stimulatory effect was abolished in the later time points. This loss in stimulation may be due to the differentiated state of the cells after prolonged culture. It is possible that following attainment of the osteocyte phenotype, these cells do not respond to further FGF-2 stimulation as the requirement for E11 to promote dendrite formation is past. Other explanations may also exist and include the degradation rate of FGF-2 where it possesses a half-life of 7.6 h *in vivo* (Beenken and Mohammadi, 2009). It is also possible that as FGF-2 saturates the ECM and its pro-differentiating effects were diminished as different cell types in the calvaria such as mesenchymal cells and fibroblasts responded to it stimulation. Worthy of note is that the concentration of 10 ng/ml may be too low to maintain physiological adequacy as 1-10 ng/ul has been reported to induce bone formation and maturation in mice study (Nakamura et al., 2005). The up-regulation of early osteocyte genes in the whole calvaria model here

corroborates with the data from the cell line and primary osteoblasts, strongly supporting a role for FGF-2 in the stimulation of E11 expression in normal physiological conditions.

Fluorescence microscopy also disclosed altered E11 expression and localisation within the differentiating osteoblasts. E11 was found to be concentrated at the base of the dendritic spikes of the osteocytes after 24-72 h of FGF-2 treatment and it is likely that this redistribution of E11 within the cell is necessary for the transformation of the osteoblast from a cuboidal shape to the osteocytic phenotype characterised by a stellate-like cell with long dendritic processes (Zhang et al., 2006). The presence of more E11 in the cytoplasm than the plasma membrane projections of control cells suggests that FGF-2 not only stimulates up-regulation of E11, but also facilitates the translocation of the E11 towards the cell membrane. This ability of FGF-2 to alter subcellular protein distribution is supported by a previous finding in mesenchymal stem cells (MSCs), in relation to the expression of Twist and Spry4 proteins from peri-nuclear to nucleus as regards Twist, but Spry4 was translocated to the cytoplasmic surface of the plasma membrane (Lai et al., 2011). While fluorescence microscopy revealed increase in length and number of dendrites, this was not readily appreciated by phase contrast microscopy, a feature that may be associated with higher cell density and low colour resolution. Further evaluation with quantification tools like Imaris software should be done to ascertain if this increased dendricity in the FGF-2 treated cells is of a significant size compared to control cultures.

The intracellular signalling mechanisms by which FGF-2 promotes E11 cytoplasmic redistribution and dendrite formation is likely to involve interactions with the cell cytoskeleton. Cytoskeletal actin reorganisation is associated with aiding cell movement and serves as a sensory cell membrane projection (Lamouille et al., 2014). The use of phalloidin staining to detect F-actin, confirmed that this microfilament, is an abundant member of the osteoblast cytoskeleton and is involved in FGF-2 mediated cell shape changes. Further studies are warranted, however to investigate if the distribution of other cytoskeletal proteins such as microtubules and intermediate filaments are also modified by FGF-2 treatment (Fletcher and Mullins, 2010). The F-actin filaments concentrated at the dendritic spikes may serve as a sensory function. This view is supported by published work where the dendrites served as mechanoreceptors in osteocytes during a loading experiment (Zhang et al., 2006). Some actin-rich cell projections reported include filopodia, lamelliopodia and invadopodia (Ridley, 2011, McNiven, 2013). The observed E11 immunofluorescence localisation at osteocyte dendritic spikes has been reported previously in MLO-Y4 osteocyte-like cells and primary osteocytes isolated from long bones (Stern et al., 2012).

Here the utilisation of E11 siRNA to firstly successfully knock down E11 expression in MC3T3 cells, and secondly to examine the effects of FGF-2 on osteoblast to osteocyte transition in the absence of E11. The resultant data revealed that the E11 siRNA cells had fewer and shorter dendrites after treatment with FGF-2. These data when combined with the immunofluoresence and phalloidin data support the

growing model of evidence that E11 is very important in the acquisition of the dendritic morphology of osteocytes though actin, thus very suggestive that E11 plays a crucial role in the early events of osteocytogenesis (Zhang et al., 2006). A notable finding with the E11 siRNA knockdown was the ability of FGF-2 to still upregulate *Phex* and *Dmp1* expression. This suggests that the effects of FGF-2 on osteoblasts are not all mediated via E11 expression.

The *in vitro* studies herein have shown FGF-2 promotes E11 expression in osteoblast like-cell line (MC3T3), murine primary osteoblasts and calvaria. It was therefore quite surprising to observe that E11 and sclerostin protein expression by osteocytes was similar in Sections of bone (cortical, trabecular and subchondral) from *Fgf-2* deficient and WT mice. This observation differs from published data that reported the down-regulation of E11 in these *Fgf-2* KO mice chondrocytes as assessed by mRNA quantification (Chong et al., 2013). This difference in E11 expression may be due to different tissue types or the effect of surgery (DMM) stress in the earlier report while the tissue used in this study were from out on naïve mice. Additionally, the age of the mice studied may have had a bearing on the E11 expression data. Young mice (6 weeks-old) were used in this study, whereas a study with adult mice revealed skeletal abnormalities in the bone of *Fgf-2* deficient mice including abnormal osteoblast differentiation and bone volume loss associated with decreased bone formation and mineralization (Montero et al., 2000, Fei et al., 2011). This suggests that the loss of FGF-2 signalling was not compensated for in older mice by other members of the FGF family of polypeptides, as redundancy between them has been previously reported

(Kan et al., 1999, Behr et al., 2010). In contrast, another study has shown no obvious skeletal developmental abnormality in *Fgf-2* KO adult mice, a result attributed to effect of redundancy in the FGF family (Ortega et al., 1998, Su et al., 2014).

The similar E11 and sclerostin protein expression by osteocytes from *Fgf-2* deficient and WT mice maybe a consequence of the significantly increased cell body volume observed in *Fgf-2* KO osteocytes as revealed by phalloidin staining. Indeed FGF-2 has been reported to decrease chondrocyte hypertrophy in a murine metatarsal organ culture model and as such, may play a similar role in the formation of the osteocyte (Mancilla et al., 1998). Also the phalloidin staining revealed a significant decrease in average dendrite length in *Fgf-2* KO mice compared to WT mice; a phenotype that has been previously reported in bone specific E11 conditional knockout mice (Staines et al., 2017). This therefore suggests that lack of FGF-2 *in vivo* results in dysregulated osteocytogenesis.

In conclusion, in this Chapter, has shown that FGF-2 promotes E11 expression and redistribution within the differentiating osteoblast (Fig. 3.21), but further studies are required to show the signalling mechanism underlying this FGF-2 induced increased E11 expression.

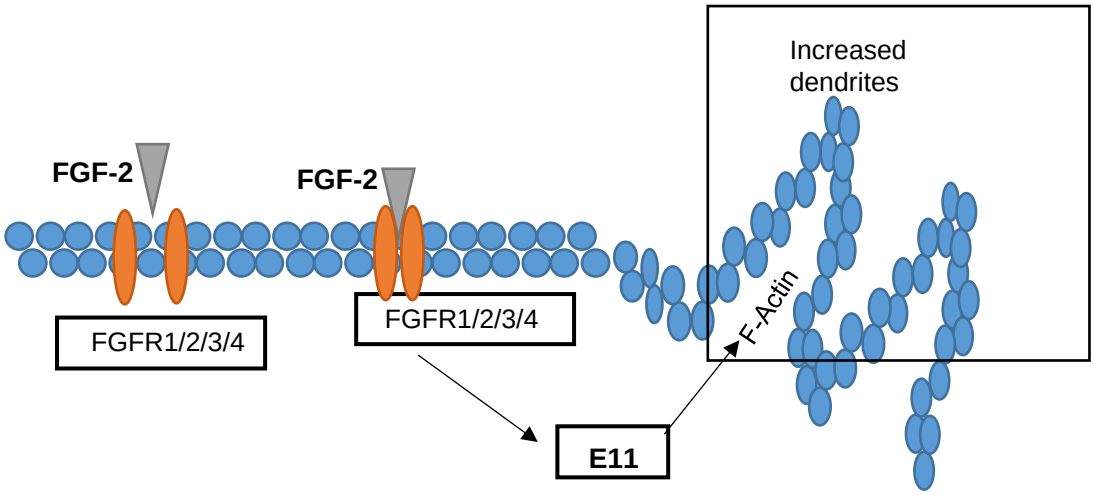

Fig. 3.21 Schematic of Chapter 3 results

In this chapter, I have revealed that FGF-2 increases E11 expression and this influences the F-actin cytoskeleton to promote osteocyte dendrite formation.

Chapter 4

Understanding the signalling mechanisms underpinning FGF-2 regulation of E11 expression

4.1. Introduction

In Chapter 3 it was revealed that FGF-2 stimulates *E11* mRNA expression in MC3T3 osteoblast-like cells, primary osteoblasts and whole calvaria. This increased *E11* expression was associated with increased expression of osteocyte marker genes (*Phex* and *Dmp1*), downregulation of osteoblast marker genes (*Col1a1, Bglap and Alpl),* promotion of E11 protein synthesis and the acquisition of the osteocytic dendritic morphology. To better understand the mechanistic role of FGF-2 in mediating osteocytogenesis, it is necessary to understand the signalling events that are up- and down-stream of raised E11 expression in response to FGF-2.

The FGF-2 signalling cascade is activated after the ligand FGF-2 binds to the appropriate FGF receptor (FGFR), a Receptor Tyrosine Kinase (RTK), for which there are four well documented different types (FGFR 1-4). After FGF induced dimerisation of the FGFR, upstream molecules such as the adaptor proteins phospholipase C-ɣ (PLC-ɣ), and FGF receptor substrate 2 (FRS-2), are phosphorylated (see Fig. 1.7) (Turner and Grose, 2010). The PLC-ɣ downstream cascade involves hydrolysis of phosphatidylinositol-4,5-diphosphate to inositol-1,4,5-triphophate and diacylglycerol; and subsequent activation of protein kinase C (PKC) by diacylyglycerol (Bottcher and Niehrs, 2005). FGF-2 activation of PKC is involved in the upregulation of N-cadherin expression, differentiation, early apoptosis and sodium-dependent phosphate transport in human and murine osteoblasts (Suzuki et al., 2000, Debiais et al., 2001, Marie et al., 2002).

FRS-2 phosphorylation is central to a series of signalling complexes that involve Shp2, Grb2, GAB1, Ras (Jackson et al., 2006), which together promote various downstream signalling pathways including mitogen activated protein kinase (MAPK), signal transducer and activator of transcription (STAT), phosphatidylinositol 3-kinase/Protein Kinase B (PI3K/Akt), and canonical WNT (Kevin and Stuart, 1997, Yao et al., 2015). The Ras/MAPK is the major signalling pathway activated upon FGFR dimerisation (Thisse and Thisse, 2005). There is evidence that while its effects can be dose dependent, it can also be stage dependent following activation of a specific receptor, even though promiscuity has been reported amongst the FGFRs in the mature skeleton (Jackson et al., 2006, Soltanoff et al., 2009).

During the FGF signalling cascade, MAPK family members phosphorylate nuclear transcription factors such as E26 transformation-specific (Ets), activator protein 1 (AP-1), and Activating transcription factor/cAMP response element-binding proteins for appropriate gene regulation (Dailey et al., 2005, Thisse and Thisse, 2005, Marie, 2012). The members of the MAPK family include ERK1/2, p38 MAPK and JNK (Matsuguchi et al., 2009). There is a fourth member of the family referred to as ERK5 (Chang and Karin, 2001). The activation of this MAPK family of molecules is associated with cell proliferation, cell survival and protection from apoptosis, differentiation and cell cycle arrest (Kevin and Stuart, 1997, Matsuguchi et al., 2009).

Whilst the role of these downstream signalling pathways in the proliferation and differentiation of some cells have been documented, their role in mediating FGF-2

driven osteocytogenesis though increased E11 expression is largely unknown. Similarly, how E11 modifies cytoskeletal re-organisation is not clear. Evidence from other cell types suggests that E11 associates with the ezrin, radixin and meosin (ERM) family of proteins to induce cytoskeletal re-organisation via activation of the small GTPase RhoA (Martín-Villar et al., 2006). However whether FGF-2 mediates this process is unclear. Therefore, the aim of this Chapter was to decipher the signalling molecules and the nature of their actions associated with FGF-2 mediated osteocytogenesis.

4.2 Hypothesis

FGF-2 regulates E11 expression principally though MAPKs signalling pathways and influences cytoskeletal re-organisation though ERM.

4.3 Aims

I Decipher the intracellular signalling molecules activated in MC3T3 osteoblast-like cells by FGF-2 treatment.

II Determine the importance of these signalling molecules for the promotion of E11 expression after FGF-2 stimulation of MC3T3

III Examine the role of ERM and the small GTPase RhoA in FGF-2 mediated osteocytogenesis.

4.4 Materials and Methods

4.4.1 MC3T3 osteoblast-like cells

As outlined in Section 2.2.1, MC3T3 cells were cultured at a density of 6×10^4 cells/cm^2 in a humidified atmosphere (37°C, 5% CO_2) for up to 15 days. When confluent, cells were supplemented with FGF-2 at a concentration of 10 ng/ml, or 0.1% BSA as negative control. The culture medium was changed every 2-3 days.

4.4.2 Signalling inhibitors

MC3T3 cells were incubated for with appropriate concentrations (specific details in results) of the MEK inhibitors, PD98059 (Millipore, Hertfordshire, UK) and U0126 (InvivoGen, Toulouse, France); PI3K inhibitor, LY294002 (InvivoGen, Toulouse, France); p38 MAPK inhibitor, SB203580 (Cell Guidance System, UK); and FGFR1/2/3 inhibitor, AZD4547 (Stratech Scientific Ltd, Suffolk, UK). These inhibitors have been reported to be selective for these molecules (Hotokezaka et al., 2002, Macrae et al., 2007, Choi et al., 2008, Shimada et al., 2016). Control cultures were incubated with the inhibitor vehicle (0.1% DMSO) only. After a pre-incubation with the inhibitors for 1 h except AZD4547 which was 3 h, the cells were subsequently treated with FGF-2 at 10 ng/ml concentration, or 0.1% BSA. These experiments were carried out in triplicates and three independent experiments unless otherwise stated.

4.4.3 RNA analysis of MC3T3 cells

RNA was isolated from MC3T3 cells at specific time points using a Qiagen RNeasy kit according to the manufacturer's instructions and cDNA was prepared (Section 2.4.1). For qPCR analysis, cDNA was used at 5 ng/ul, as detailed in Section 2.4.5. Results were normalised to the *Atp5b* housekeeping gene and the relative gene expression level was calculated using the ΔΔCt method (Livak and Schmittgen, 2001). Primers used are detailed in Appendix I, Table 1. The housekeeping gene Atp5b was stable

4.4.4 Protein extraction from MC3T3 cells and western blotting

At defined time points, protein was extracted from MC3T3 cells in RIPA buffer as detailed in Section 2.5.1. Protein samples were quantified (Section 2.5.1) and subsequently were used for western blot analysis (Section 2.5.3). Protein expression was determined using appropriate primary and HP-linked secondary antibodies (Appendix, Tables 2 & 3). Antibody labelling was visualised using ECL detection. Equal protein loading was confirmed by probing the membrane with mouse monoclonal HP-labelled anti-β actin antibody (1:70000). Densitometry analysis of protein was performed using Image J (https://imagej.nih.gov/ij/) (Baldari et al., 2015).

4.4.5 RhoA activity assay

MC3T3 cell monolayers were scraped in a G-LISA lysis buffer supplied with the GLISA assay kit (Cytoskeleton, Denver, USA), after 4, 6, 24 and 48 h culture with FGF-

2 (Section 2.3). Lysates were immunoblotted for E11 (Section 2.5) to confirm FGF-2 stimulation of E11. Subsequently, using a G-LISA assay which precisely identifies active GTP-bound RhoA, the quantification of RhoA activation was carried out by luminometry and expressed in relative light units (RLU) as per the manufacturer's instructions (Staines et al., 2016).

4.5. Results

4.5.1 Evaluation of *FGFR* expression by MC3T3 cells following FGF-2 stimulation.

To undertake receptor profiling in MC3T3 cells following FGF-2 stimulation, mRNA from treated and control cultures were analysed by RT-qPCR at 0.25, 4 and 24 h after FGF-2 stimulation. The results revealed no significant change in *Fgfr1* expression at all-time points studied (Fig. 4.1A). However, the expression of *Fgfr2* and *Fgfr3* were both similarly affected by FGF-2 treatment, with a decrease in their expression noted after 4 and 24 h stimulation (Fig. 4.1B &C). *Fgfr4* was not found to be expressed by MC3T3 cells using several primer pairs from the published literature and primer banks. The expression levels of *Fgfr1* were however 12-fold higher over a 24 h time period, while the expression levels of *Fgfr2* and *Fgfr3* presented a significant decrease especially in the treated cultures over same time period. Therefore, one can speculate on a more prominent involvement of FGFR1 in mediating the FGF-2 mediated transition from osteoblast to osteocyte.

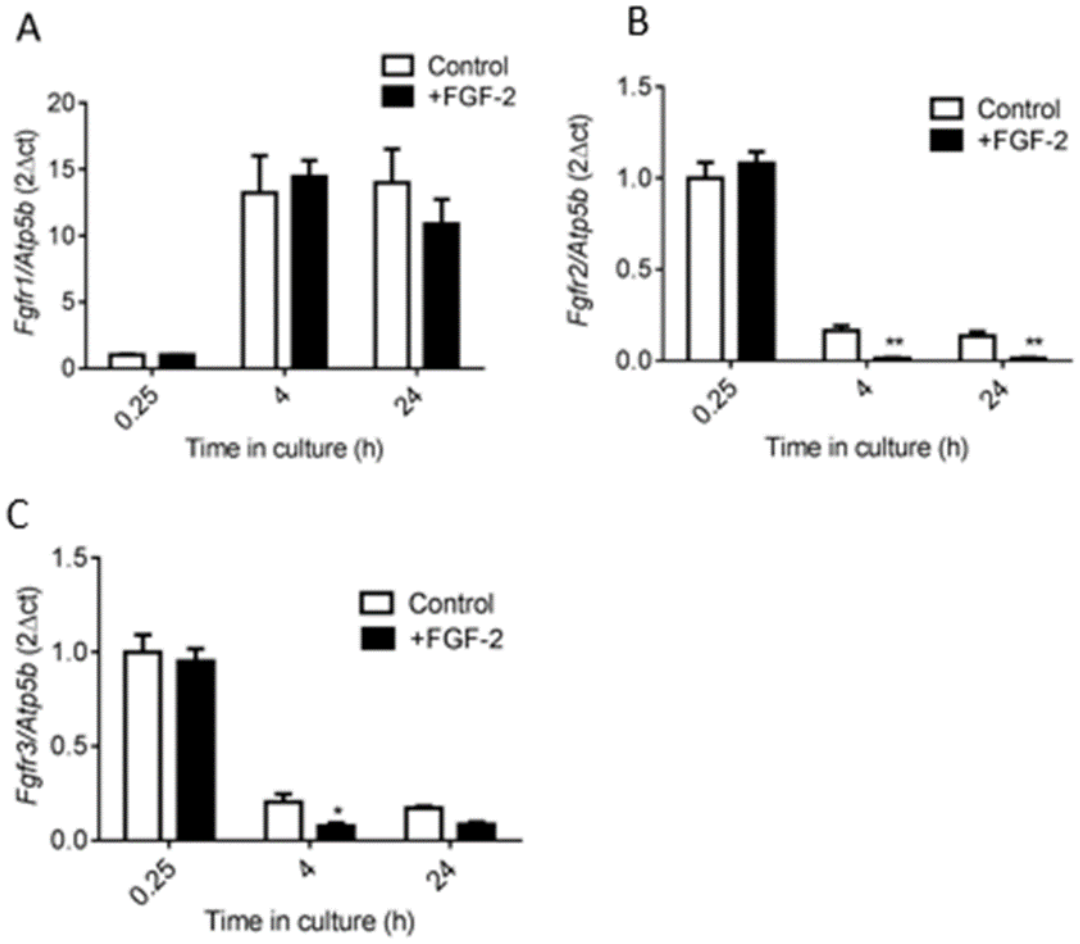

Figure 4.1 Temporal *Fgfr* gene expression of MC3T3 cells cultured with FGF-2 for 15 min, 4 h and 24 h.

RT-qPCR assessed expression *of* (**A**) *Fgfr1* (**B**) *Fgfr2* (**C***) Fgfr3* after FGF-2 stimulation. After several attempts with different *Fgfr4* primer sequences obtained from primer banks and published papers no amplified product was obtained suggesting that MC3T3 cells do not express *Fgfr4*. Data are presented as mean ± S.E.M for n=3 observations; *p<0.05; **p<0.01.

4.5.2. Identification of the downstream intracellular signalling pathways driving FGF-2 stimulation of E11 expression in MC3T3 osteoblast-like cell

FGF-2 stimulation resulted in increased phosphorylated ERK1/2 (ERK1/2), Akt and p38 MAPK when compared to BSA treated control cells (Fig. 4.2A). Densitometry quantification revealed a significant increase in phosphorylated ERK1/2 ($P<0.001$, Fig. 4.2B); p38 MAPK ($P<0.05$, Fig. 4.2C); and Akt ($P<0.01$. Fig 4.2D) in FGF-2 treated samples compared to BSA controls. No significant increase in JNK activity was seen in samples treated with FGF-2 (Fig. 4.2A & E).

4.5.3. Temporal effects of FGF-2 on ERK1/2 activation in MC3T3 cells

The duration and intensity of ERK1/2 signalling can be used to evaluate if a growth factor is driving cellular proliferation or differentiation (Murphy et al., 2003, Chen et al., 2005, Pellegrino and Stork, 2006). In this experiment, ERK1/2 signalling was examined after treating cells with FGF-2 for 5 min, 15 min, 30 min , 1 h, 4 h, 8h, 24 h, and 48 h. Cells treated with 1% BSA for the same duration served as a negative control. Western blotting showed clear and sustained activation of phosphorylated ERK1/2 in treated cells at all-time points when compared with the control cultures (Fig. 4.3).

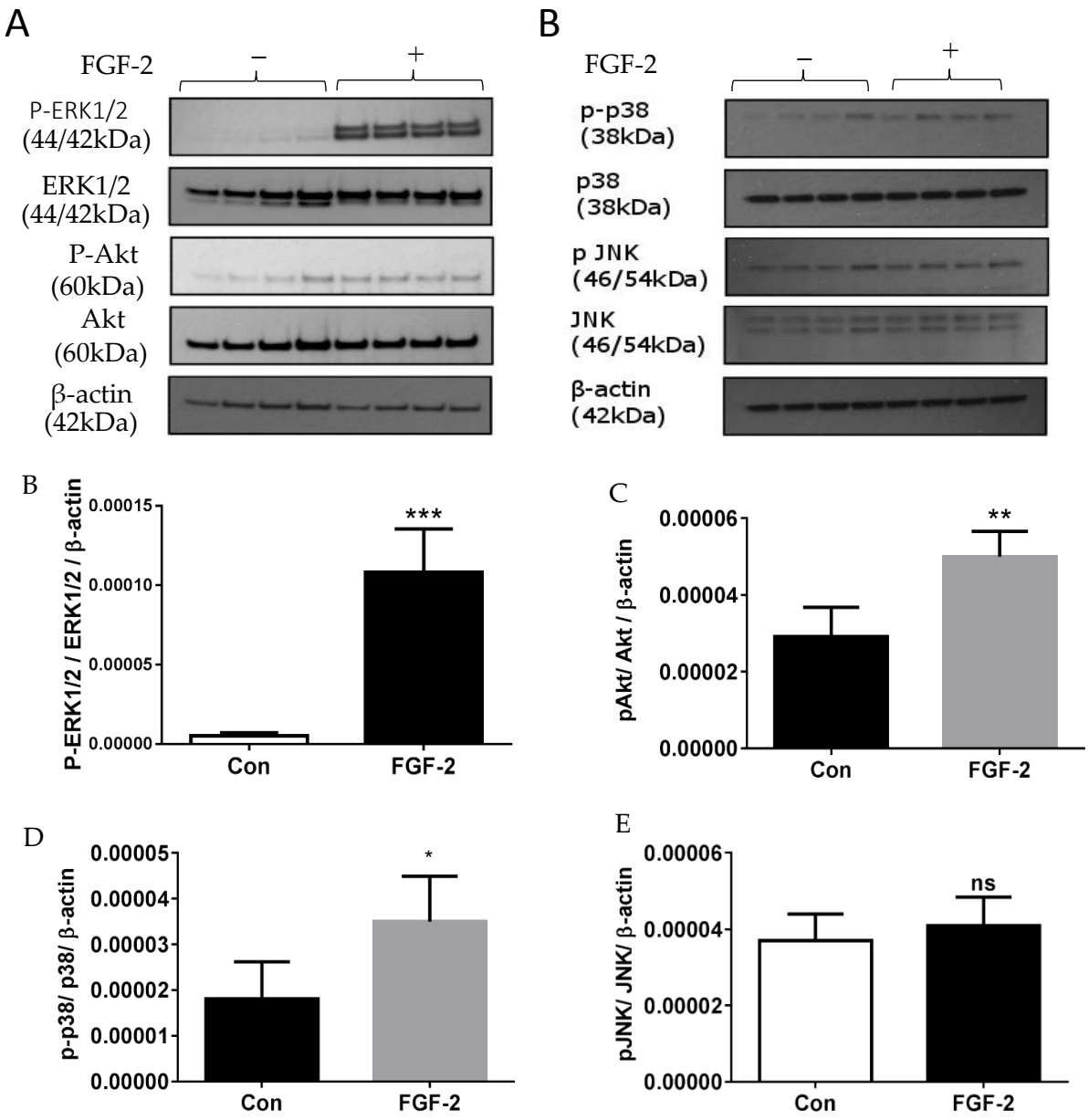

Figure 4.2 Investigating the downstream signalling pathways involved in FGF-2 stimulation of E11 expression in MC3T3 cells.

Western blotting analysis of MC3T3 cells for phosphorylated and total ERK1/2, Akt, p38 MAPK, and JNK (**A**). Densitometry analysis of Western blotting revealed significant upregulation of (**B**) activated ERK1/2, (**C**) Akt, and (**D**) p38 MAPK in MC3T3 cells treated with FGF-2 when compared to control cells. There was no significant increase in (**E**) JNK expression. Samples were normalised to β-actin for loading control. Data are presented as mean ± S.E.M for n=3. *p<0.05; **p<0.01; ***p<0.001.

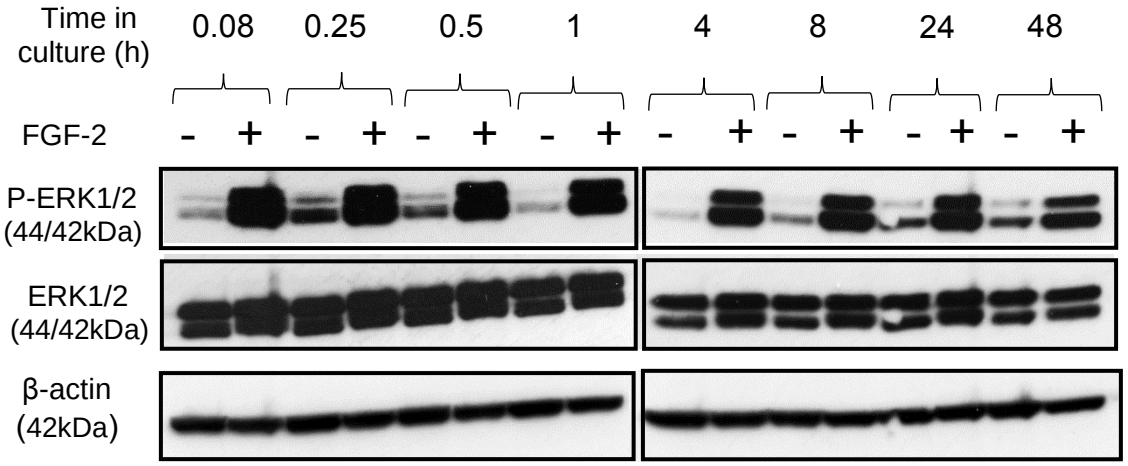

Figure 4.3 ERK1/2 signalling in MC3T3 cells stimulated with FGF-2 for variable amounts of time

Western blotting analysis of MC3T3 cells for phosphorylated and total ERK1/2, in MC3T3 cells treated with FGF-2 when compared to control cells. Note the increase in phosphorylated ERK1/2 in the treated cells at all-time points studied. Total ERK1/2 and β-actin were similar at all-time points and treatments suggesting consistent loading of all samples.

4.5.4. Investigating the effect of ERK1/2 inhibition on the promotion of E11 protein expression by FGF-2 in MC3T3 cells

From the previous study (Section 4.5.1), ERK1/2 was identified as the signalling molecule that was most highly activated by FGF-2 suggesting that its activation may be central to FGF-2's ability to stimulate E11 expression. Therefore, the effect of inhibiting ERK1/2 phosphorylation on E11 expression was carried out using PD98059 a highly selective inhibitor of MEK, which is an upstream activating kinase of ERK1/2 (Kevin and Stuart, 1997). Consistent with previous data (Fig 4.2), FGF-2 stimulation for 15 min promoted ERK1/2 activation ($P<0.001$, Fig. 4.4A & B), and subsequently increased *E11* mRNA/protein expression after both 4 and 24 hours ($P<0.001$, Fig. 4.4C-E). However, western blotting also revealed that 1 h pre-incubation with the inhibitor PD98059 (10 uM) a concentration chosen from previous studies (Macrae et al., 2007), it did not reduce ERK1/2 activation in the presence of FGF-2 and the stimulation of E11 mRNA/protein expression by FGF-2 was not consistently reduced by PD98059 treatment (Fig. 4.4A-E). This suggests that the effect of the inhibitor may be time dependent as the inhibition of *E11* mRNA expression seen at 4 h were abolished after 24 h period.

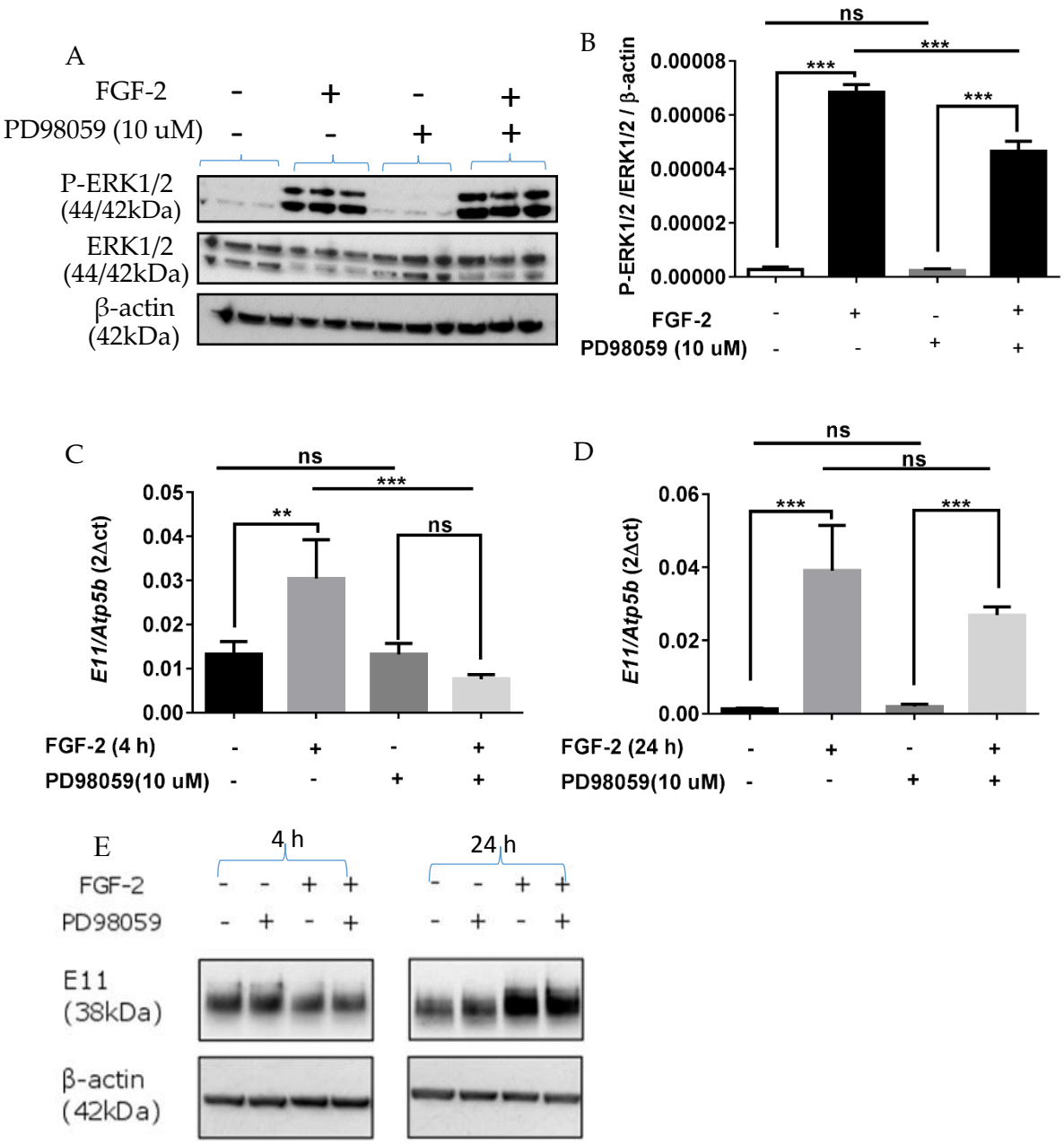

Fig. 4.4. Effect of PD98059 (10 uM) inhibition on ERK1/2 signalling and *E11* gene expression on MC3T3 cells stimulated with FGF-2.

Western blots result for (**A**), ERK1/2 expression after 15 min of FGF-2 stimulation; and (**B**), densitometry analysis showing the significant upregulation of ERK1/2. RT-qPCR analysis of *E11* expression from cells stimulated with FGF-2 for (**C**) 4 h, and (**D**) 24 h in the presence or absence of the inhibitor PD98059. (**E**), western blots for E11 protein expression. Samples were normalised to *Atp5b* for RT-qPCR. β-actin was used for western blotting loading control. Data are represented as mean ± S.E.M for n=3. **p<0.01; ***p<0.001; ns = not significant.

In light of this result, an increased concentration of PD98059 (25 uM) was tried in an attempt to confirm the importance of ERK1/2 activation to mediate FGF-2's ability to enhance E11 expression. However, the incubation for 1 h with PD98059 (25 uM) did not reduce FGF-2's ability to enhance ERK1/2 activation and E11 protein expression (Figs. 4.5A -C).

4.5.5 Examining the effects of an alternative MEK inhibitor (U0126) on E11 expression in MC3T3 cells

From the previous studies, the MEK inhibitor PD98509 did not significantly reduce ERK1/2 phosphorylation and therefore U0126 another commonly used MEK inhibitor was used in further studies (Hotokezaka et al., 2002, Macrae et al., 2007). Increasing concentrations of U0126 were pre-incubated with MC3T3 cells for 1 h, after which the cells were treated with FGF-2 or BSA for 0.25, 4 and 24 h. Consistent with previous data (Figs 4.4A & 4.5A), FGF-2 stimulated a significant increase in ERK1/2 phosphorylation after 15 min ($P<0.001$, Figs. 4.6A & B), and *E11* gene and protein expression after 4 h ($P<0.01$, Figs. 4.6C & E) and 24 h ($P<0.01$, Fig. 4.6D & E) treatment. U0126 at 10 uM however did not blunt ERK1/2 activation (Figs. 4.6A & B) or alter E11 expression (Figs 4.6C-E) and therefore further studies using a higher concentration of U0126 (25 uM) were warranted. This was the highest concentration tested as off-target effects and toxicity have been reported in studies employing higher concentrations of U0126 (Dokladda et al., 2005, Wauson et al., 2013).

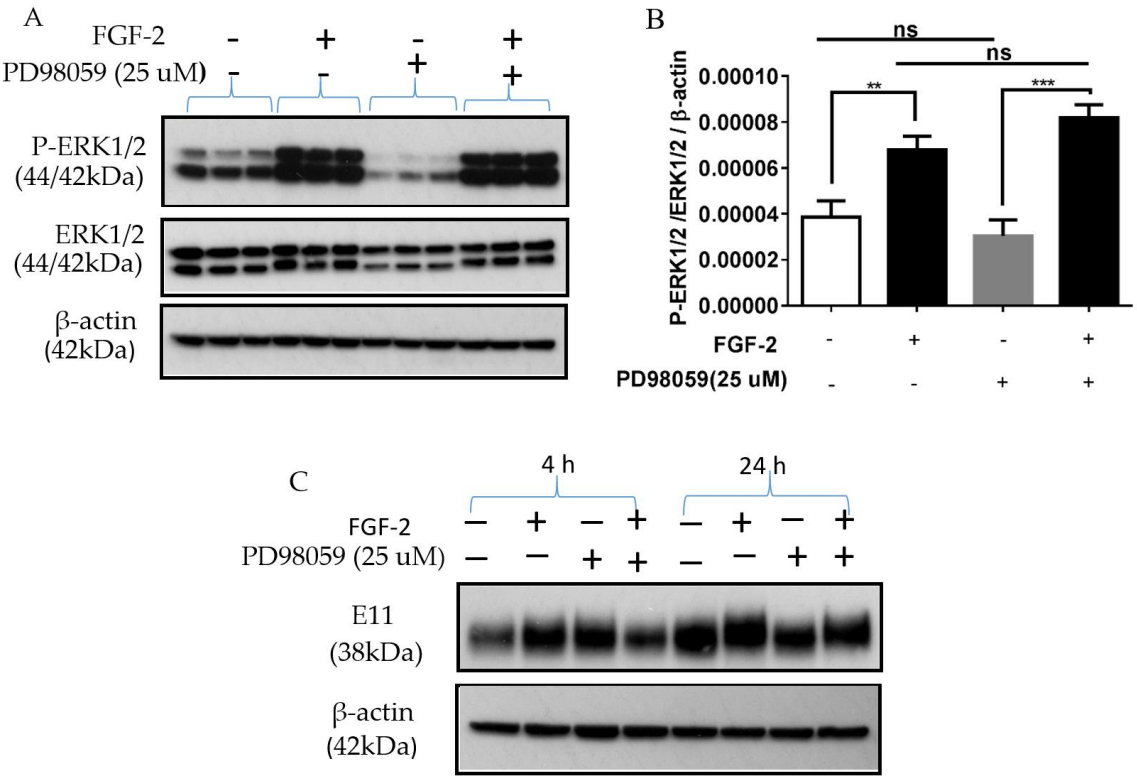

Figure 4.5 Effect of PD98059 (25 uM) on FGF-2 stimulation of ERK1/2 activation and *E11* gene and protein expression in MC3T3 cells.

Western blots result for (**A**), ERK1/2 expression; and (**B**), densitometry analysis of gel showing the stimulation of ERK1/2 phosphorylation in the presence or absence of PD98059. (**C**), Western blot analysis of E11 protein expression. Samples were normalised to β-actin in western blots for loading control. Data are represented as mean ± S.E.M for n=3. **p<0.01; **p<0.001; ns = not significant.

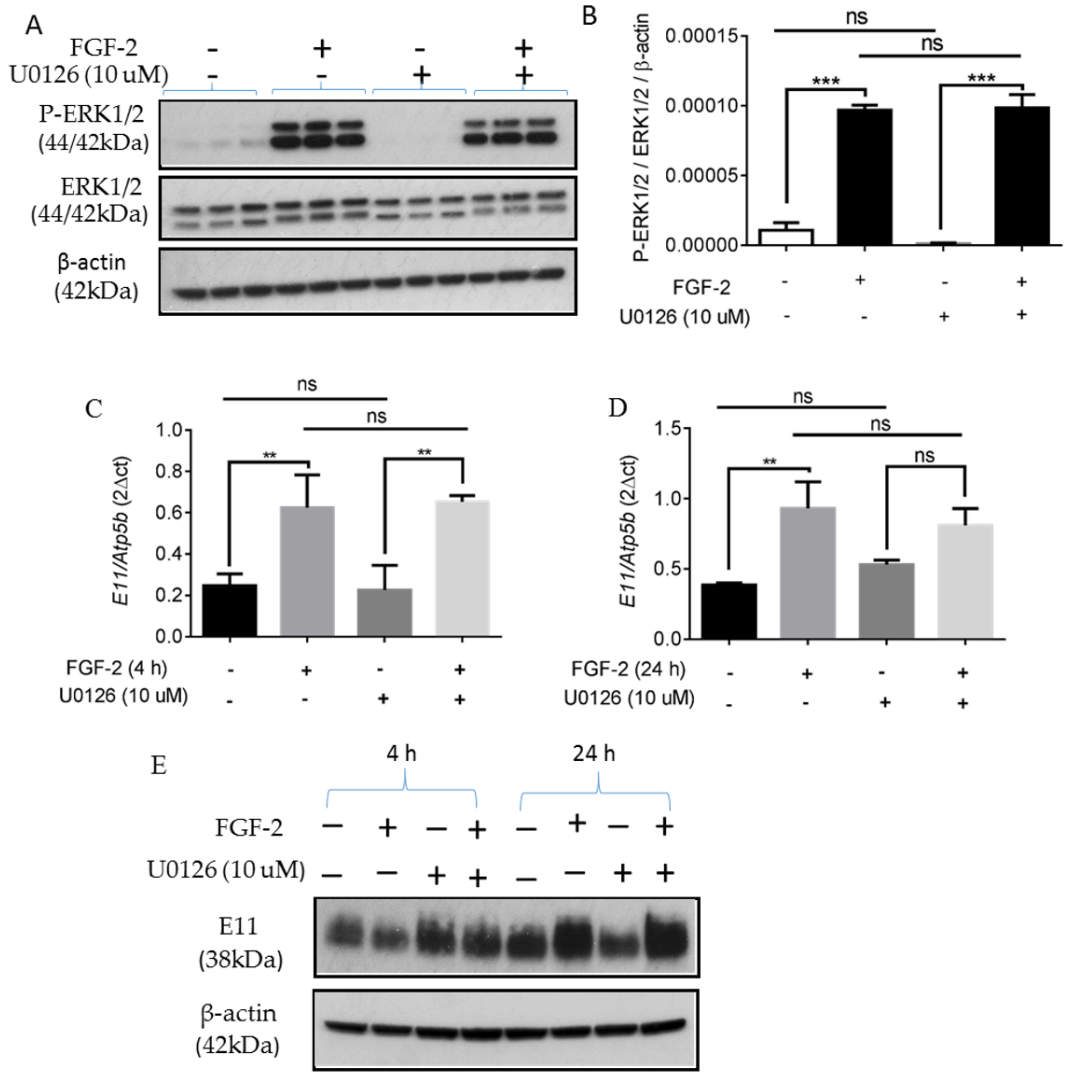

Figure 4.6 Effect of U0126 (10 uM) on FGF-2 stimulation of ERK1/2 phosphorylation and *E11* gene expression and protein expression in MC3T3 cells.

Western blots result for (**A**), ERK1/2 expression ; and (**B**), densitometry analysis showing the significant upregulation of ERK1/2 phosphorylation by FGF-2 in the presence or absence of U0126 RT-qPCR and Western analysis of *E11* expression by cells stimulated with FGF-2 for (**C,E)** 4 h, and (**D,E**) 24 h in the presence or absence of the inhibitor. Samples were normalised to *Atp5b* in RT-qPCR, while in western blots, β-actin was used for loading control. Data are represented as mean ± S.E.M for n=3. *p<0.05;**p<0.01; ***p<0.001; ns = not significant.

At this higher inhibitor concentration, U0126 did partially blunt FGF-2s ability to phosphorylate ERK1/2 ($P<0.001$) but despite this the resultant ERK1/2 activation remained significantly higher than control cells ($P<0.001$, Figs. 4.7A & B). The stimulation of E11 gene and protein expression by FGF-2 was unaffected by 25 um U0126 (Figs 4.7C-E).

4.5.6 Investigating the effects of U0126 (25 uM) ERK1/2 inhibitor on p38 MAPK and Akt signalling

Due to the sustained promotion of E11 expression even when ERK1/2 phosphorylation was slightly inhibited (Figs 4.7A & B) by the ERK1/2 inhibitor U0126 (25 um), it is possible that other compensatory signalling pathways are activated to overcome this reduction in ERK1/2 activation. As reported earlier, FGF-2 also promoted p38 MAPK and Akt phosphorylation in MC3T3 cells (Section4.5.2) and therefore it was of interest to note if the addition of U0126 could alter FGF-2 effect on these signalling molecules.

FGF-2 stimulated p38 MAPK phosphorylation which is in agreement with previous results (Fig. 4.2D) but this increased phosphorylation was not influenced by the pre-treatment with U0126 (Figs 4.8A & B). FGF-2 also increased Akt phosphorylation which is in agreement with previous experiments (Fig.4.2C), however unlike p38 MAPK the addition of U0126 resulted in an increase in Akt activation by FGF-2 (Fig. 4.8 C & D)

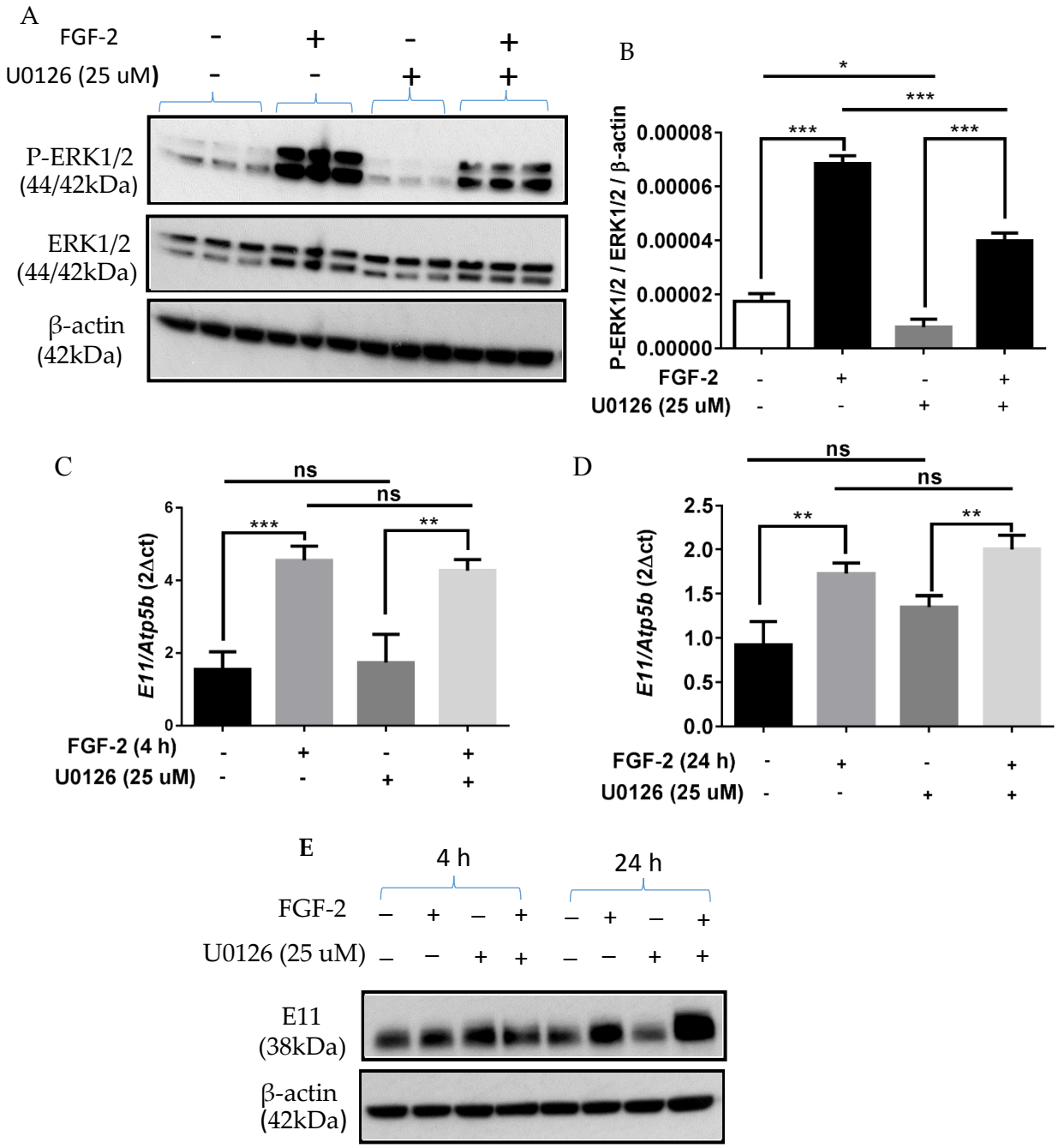

Figure 4.7 Effect of U0126 (25 uM) on FGF-2 stimulation of ERK1/2 phosphorylation and *E11* gene and protein expression in MC3T3 cells.

Western blots result for (**A**), active ERK1/2; and (**B**), densitometry analysis showing the significant upregulation of ERK1/2 phosphorylation by FGF-2 in the presence or absence of U0126. RT-qPCR and Western blot analysis of *E11* expression by cells stimulated with FGF-2 for 4 h, and 24 h (**C - E**) in the presence or absence of the inhibitor. Samples were normalised to *Atp5b* in RT-qPCR, while in western blots, β-actin was used for loading control. Data are represented as mean ± S.E.M for n=3. **p<0.01; ***p<0.001; ns = not significant.

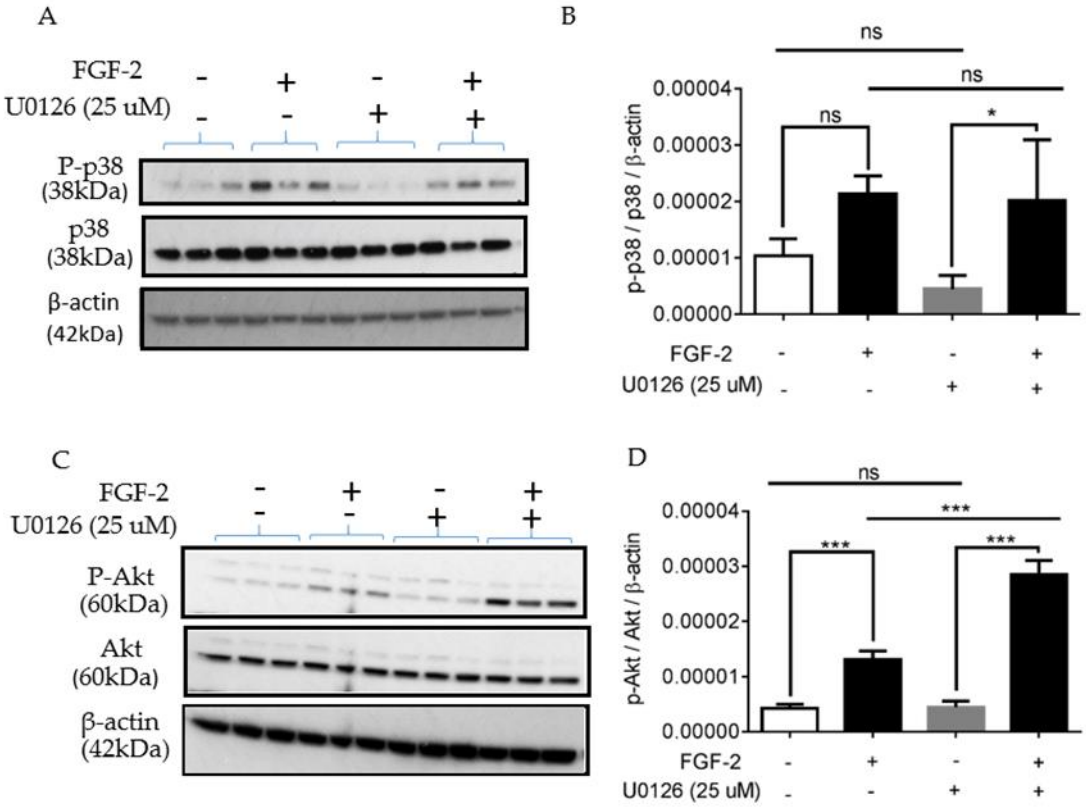

Figure 4.8 Effect of U0126 (25 uM) on p38 MAPK and Akt phosphorylation after FGF-2 stimulation in MC3T3

Western blot showing p38 MAPK phosphorylation in the presence and absence of FGF-2 and U0126 (**A**), and densitometry analysis showing its significant increase in the FGF-2 treated cultures in the presence of inhibitor U0126 (**B**). Western blot showing FGF-2 driven increased P-Akt expression in the presence of the U0126 inhibitor (**C**), which was significantly upregulated as assessed by densitometry analysis (**D**). Samples were normalised to β-actin for loading control. Data are represented as mean ± S.E.M for n=3. *p<0.05; ***p<0.001; ns = not significant.

4.5.7 Investigating the combined effects of U0126 (25 uM) ERK1/2 inhibitor and LY294002 Akt inhibitor on E11 expression

As a result of the above study suggesting a possible Akt signalling compensation mechanism following ERK1/2 inhibition the next approach was to pre-treat cells with both LY294002 (10 uM) and U0126 (25 uM) to potentially inhibit Akt and ERK1/2 phosphorylation, respectively. The effects on ERK1/2 and Akt phosphorylation and E11 expression would then be determined. Prior to this, however, a range of LY294002 concentrations at 1 h incubation were tested to determine the optimum inhibitor concentration for these proposed experiments. All LY294002 concentrations tested (10 - 100 uM) resulted in the complete inhibition of Akt activation (Fig. 4.9). From this result, 10 uM was chosen as the optimum concentration, as it was the lowest inhibitor concentration to get maximum inhibition of Akt phosphorylation and thereby reducing the potential toxic off target effects on the cells. Thereafter the cells were subjected to a 1 h pre-incubation with the inhibitors, followed by treatment with FGF-2 (or 0.1% BSA for control cultures) for 15 min, 4 and 24 h.

After 15 min of FGF-2 stimulation, phosphorylated ERK1/2 levels were significantly increased from control levels but were not influenced by the presence of both U0126 and LY294002 (Figs. 4.10A, B). FGF-2 caused a small but non-significant increase in Akt phosphorylation and whilst the addition of U0126 and LY294002 caused a reduction (non-significant) in basal Akt activation levels, the effect of both inhibitors together resulted in increased Akt activation in response to FGF-2 ($P<0.001$). This

response was also higher than the equivalent Akt activation levels seen with FGF-2 in the absence of both inhibitors ($P<0.05$; Figs. 4.10A& C). E11 expression in response to FGF-2 at the gene and protein level was relatively unaffected by the addition of both U0126 and LY294002 (Fig. 4.10D-F).

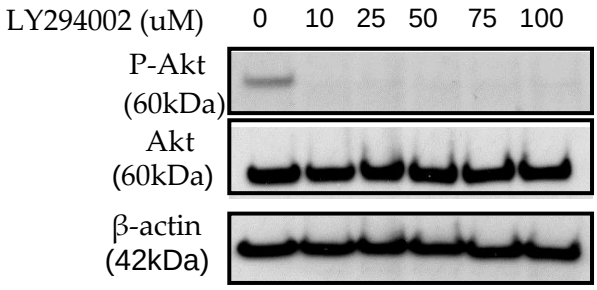

Figure 4.9 Effect of various concentrations of the inhibitor LY294002 on phosphorylated Akt expression.

Western blotting for p-Akt and total Akt in MC3T3 cells treated with increasing concentrations of the Akt inhibitor LY294002 for 15 min. Note that all concentrations used were effective in inhibiting Akt activation. Samples were normalised to β-actin for loading control.

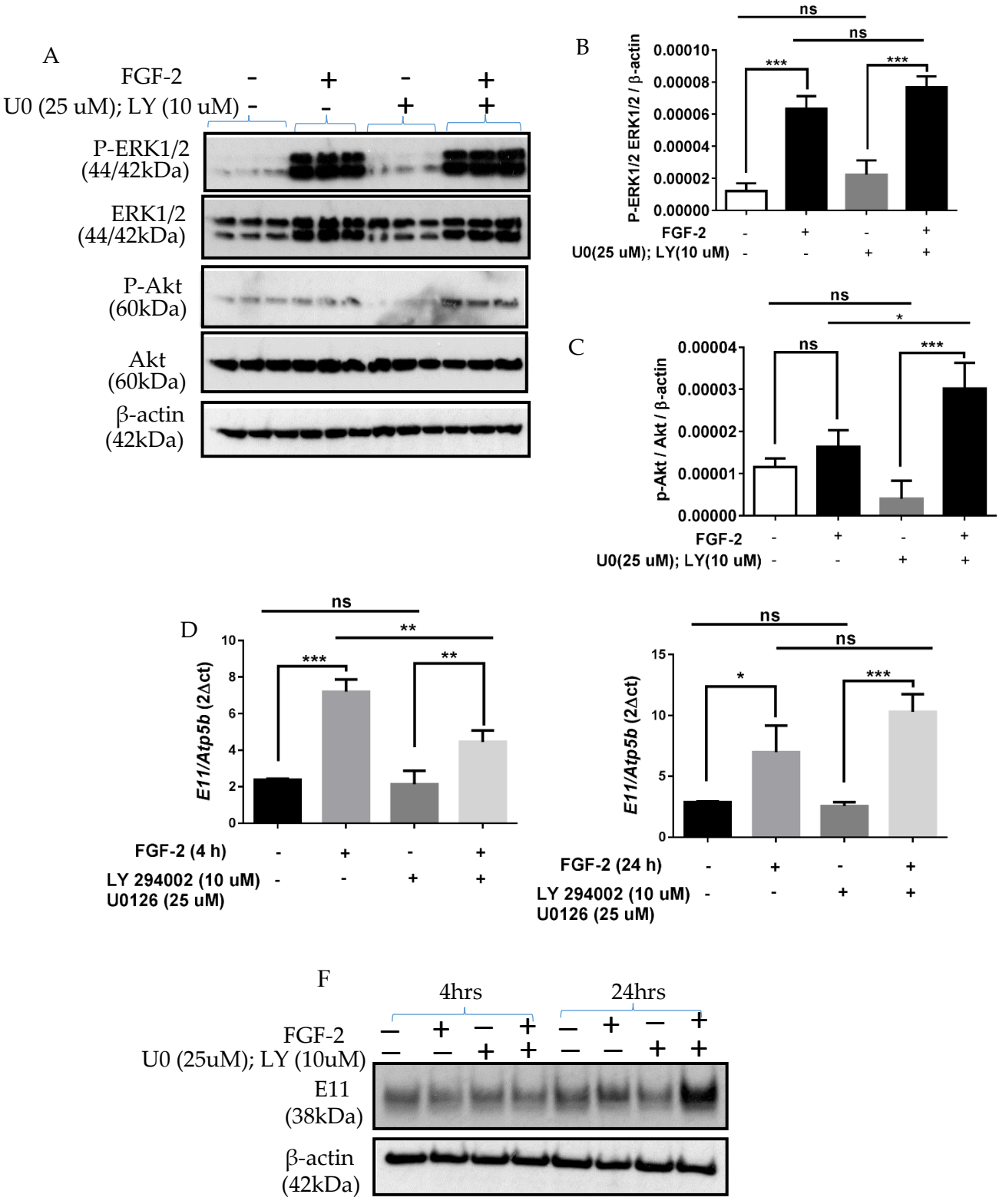
A
FGF-2
U0 (25 uM); LY (10 uM)
P-ERK1/2 (44/42kDa)
ERK1/2 (44/42kDa)
P-Akt (60kDa)
Akt (60kDa)
β-actin (42kDa)
B
P-ERK1/2 ERK1/2 / β-actin
FGF-2
U0(25 uM); LY(10 uM)
C
p-Akt / Akt / β-actin
D
E11/Atp5b (2Δct)
FGF-2 (4 h)
LY 294002 (10 uM)
U0126 (25 uM)
FGF-2 (24 h)
F
4hrs
24hrs
FGF-2
U0 (25uM); LY (10uM)
E11 (38kDa)
β-actin (42kDa)

(Previous page) Figure 4.10 Effect of both U0126 and LY294002 on FGF-2 induced phosphorylation of ERK1/2, Akt, and E11 gene and protein expression in MC3T3 cells.

FGF-2 stimulated both ERK1/2 (**A &** B) and Akt (**A** & **C**) phosphorylation. ERK1/2 activation by FGF-2 was not influenced by the presence of both U0126 and LY294002 (**B**) whereas Akt activation was increased when both U0126 and LY294002 were present (**C**). Gene (**D** & **E**) and protein (**F**) expression of E11 was not influenced by the presence of both U0126 and LY294002. Samples were normalised to β-actin for loading control. Data are represented as mean ± S.E.M for n=3. *p<0.05; ***p<0.001; ns = not significant.

4.5.8 Examination of the possible cross-talk between ERK1/2 and Akt activation during FGF-2 stimulated E11 expression and MC3T3 differentiation

As the stimulation of E11 expression by FGF-2 was maintained despite with the presence of both U0126 (25 uM) and LY294004 (10 uM) (Figs. 4.10D, E & F); the singular effect of LY294002 (10 uM) was investigated for the existence of possible cross-talk between phosphorylated ERK1/2 and Akt molecules after FGF-2 stimulation. This was important as earlier results (see Figs. 4.8C & D) revealed that phosphorylated Akt was significantly upregulated in the presence of U0126 (25 uM). After a 1 h pre-incubation in LY294002 (10 uM), the cells were stimulated with FGF-2 for 15 min, 4 and 24 h. After 15 min in the presence of the inhibitor, FGF-2 was not, as expected, able to promote the phosphorylation of Akt as observed in the cultures with FGF-2 alone ($P<0.001$; Figs. 4.11A & B). In contrast, LY294002 (10 uM) was unable to stop the activation of ERK1/2 by FGF-2 (Figs. 4.11A & C). E11 expression at the gene and protein level were increased by FGF-2 after 4 and 24 h, which was unaffected in the presence of LY294002 (Figs. 4.11D-F).

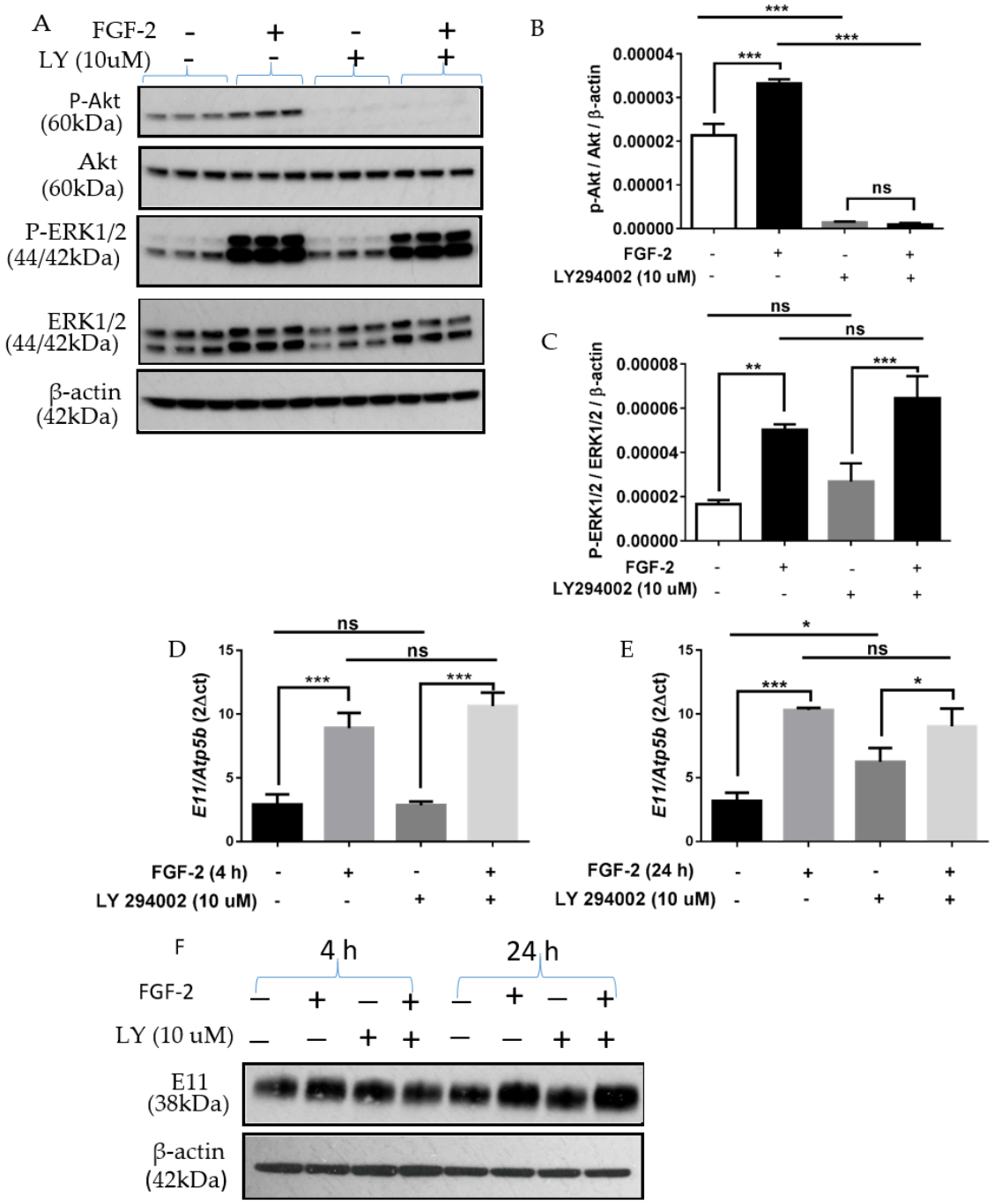
A
FGF-2
LY (10uM)
P-Akt (60kDa)
Akt (60kDa)
P-ERK1/2 (44/42kDa)
ERK1/2 (44/42kDa)
β-actin (42kDa)
B
p-Akt / Akt / β-actin
FGF-2
LY294002 (10 uM)
C
P-ERK1/2 / ERK1/2 / β-actin
D
E11/Atp5b (2Δct)
FGF-2 (4 h)
LY 294002 (10 uM)
E
FGF-2 (24 h)
F
4 h
24 h
LY (10 uM)
E11 (38kDa)
β-actin (42kDa)

(Previous page) Figure 4.11 Examination of the cross-talk between ERK1/2 and Akt activation during FGF-2 stimulated E11 expression in MC3T3 cells.

Western blot result disclosing the effect of the PI3K inhibitor LY294002 (10 uM) on FGF-2 stimulation of Akt and ERK1/2 phosphorylation (**A**). Densitometry showed that in the presence of the inhibitor, FGF-2 did not upregulate P-Akt activation (**B**) but there was no effect of the inhibitor on P-ERK1/2 activation by FGF-2 (**C**). RT-qPCR and Western blot analysis of *E11* expression from cells stimulated with FGF-2 were unaffected by the presence of LY294002 (D-F). Samples were normalised to *Atp5b* in RT-qPCR and β-actin served as a loading control in western blot. Data are represented as mean ± S.E.M for n=3. *p<0.5; **p<0.01; ***p<0.001; ns = not significant.

4.5.9. Investigating the effect of p38 MAPK inhibition on E11 protein expression in MC3T3 cells

Having determined that E11 expression was still stimulated by FGF-2 in the presence of ERK1/2 and Akt phosphorylation inhibitors (Section 4.5.9), the next study was designed to determine whether inhibition of p38 MAPK phosphorylation (one of the MAPKs upregulated by FGF-2; Section4.5.2) blunted FGF-2s ability to promote E11 expression. The compound SB203580 is a known p38 MAPK inhibitor (Jarnicki et al., 2008, Ferreiro et al., 2010). This inhibitor SB203580 at 10 uM for 1 h pre-incubation (Lali et al., 2000), was used to ases the effect of p38 MAPK signalling on E11 expression in both treated and control cells. E11 expression at the gene and protein level was increased by FGF-2 after 4 and 24 h but expression levels were unaffected by the presence of SB203580 (Figs. 4.12A-C).

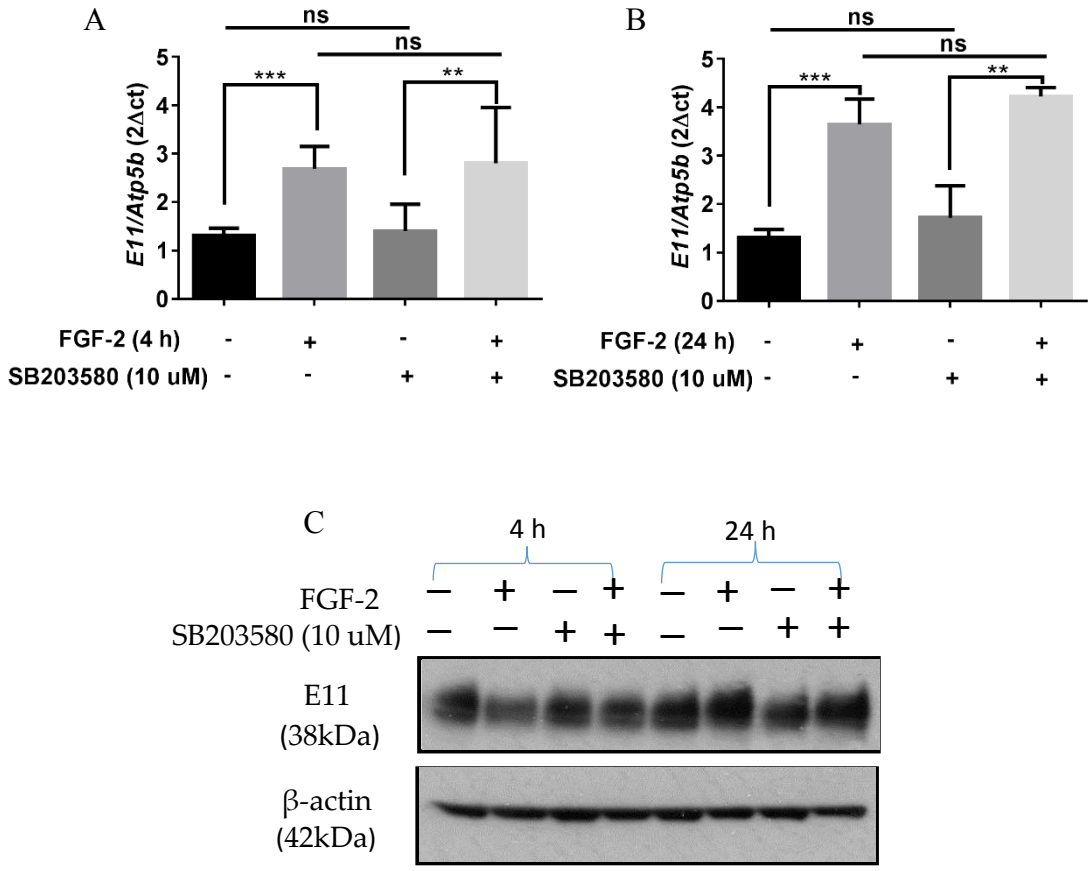

Figure 4.12 Effect of SB203580 (10 uM) on FGF-2 induced E11 expression in MC3T3 cells

RT-qPCR and Western blot analysis of *E11* expression by MC3T3 cells stimulated with FGF-2. Expression was unaffected by the presence of SB203580 at 10 uM (A-C). Samples were normalised to *Atp5b* in RT-qPCR, and β-actin served as a loading control in western blot. Data are represented as mean ± S.E.M for n=3. *p<0.5; **p<0.01; ***p<0.001; ns = not significant.

4.5.10. Effect of FGF receptor inhibition on FGF-2 mediated ERK1/2 activation and E11 expression in MC3T3 cells.

Having previously detailed the expression of *Fgfr1/2/3* in MC3T3 cells, the effect of inhibiting FGF function on FGF-2's ability to stimulate ERK1/2 activation and E11 expression was next studied. AZD4547 (0-1 uM), a recognised FGFR1/2/3 inhibitor (Yao et al., 2015, Zhang et al., 2015, Shimada et al., 2016), was incubated with the cells for 3 h prior to treatment with FGF-2 for an additional 15 min to determine the desired concentration of AZD4547 for further studies. In these pilot experiments, the read-out used was ERK1/2 phosphorylation. The result of the ERK1/2 western blots showed a dose response relationship with increasing concentrations of AZD4547, inhibiting ERK1/2 activation which was completely inhibited at 1 uM (Fig. 4.13A). Further experiments used this concentration of AZD4547 but also a lower concentration (100 nM) which was also effective in blocking FGF-2 signalling but would potentially have less off-target effects on the cells.

In a subsequent more long-term experiment (15 min – 24 h), both inhibitor concentrations blocked ERK1/2 activation but less effect on inhibiting E11 expression by FGF-2 (Figs 4.13B & C).

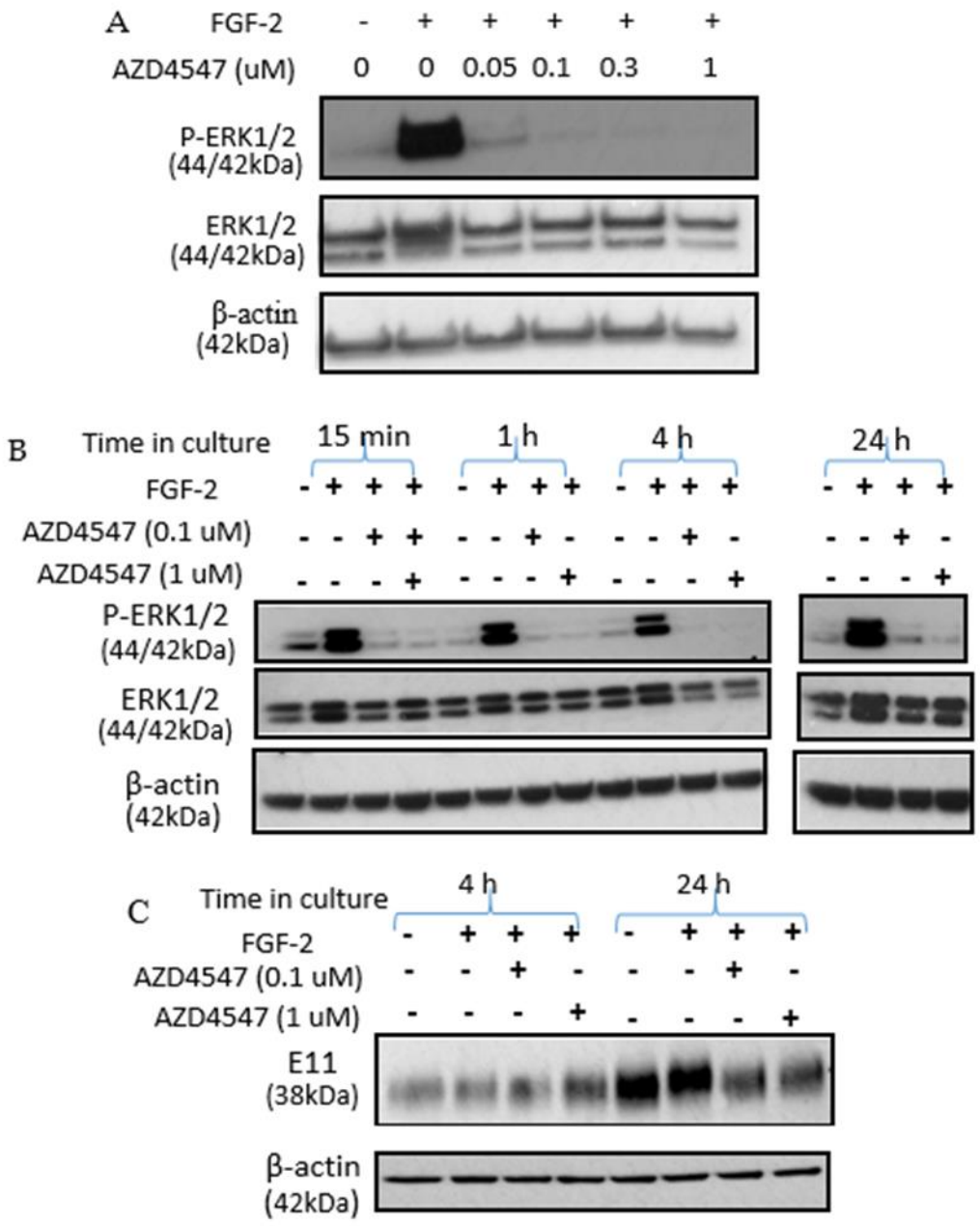

Figure 4.13 Effects of the FGFR1/2/3 inhibitor AZD4547 on the ability of FGF-2 to promote ERK1/2 activation and E11 expression in MC3T3 cells.

Note the dose inhibitory response of AZD4547 on ERK1/2 activation after 15 min FGF-2 treatment (**A**). Both 0.1 uM and 1 uM concentrations of AZD4547 were used to block FGF-2 signalling and the effects on ERK1/2 activation (B), and E11 expression (C), were examined over an extended period (15 min – 24 h). Samples were normalised to β-actin for loading control.

4.5.11 Effect of FGF-2 treatment on activation of RhoA in MC3T3 cells

To investigate further the mechanism by which FGF-2 is able to drive changes towards the acquisition of the osteocytic morphology and increased dendrite formation via cytoskeletal re-organisation (as seen previously in Figs. 3.4B & D), the ability of FGF-2 to activate the small GTPase RhoA was next investigated. After 4, 6, 24, and 48 h of FGF-2 treatment, the expression of the E11 protein was, as expected, increased in the treated cultures which was most notable at the 24 h time point (Fig. 4.14A). This rise in E11 expression by FGF-2 was not however associated with any significant difference in RhoA activation at the time points that FGF-2 promoted E11 expression (Fig. 4.14B).

4.5.12 Effect of FGF-2 treatment on activation of ERM in MC3T3 cells

Having observed no significant differences in the activation of RhoA by FGF-2 a further study was carried out to ascertain if FGF-2 was able to influence the activation of the ERM family of proteins, which in other cell types can alter cytoskeletal re-organisation via activation of RhoA. Consistent with the Rho A data the western analysis of ERM phosphorylation showed no differences in phosphorylation of ERM at all-time points studied (Fig. 4.15).

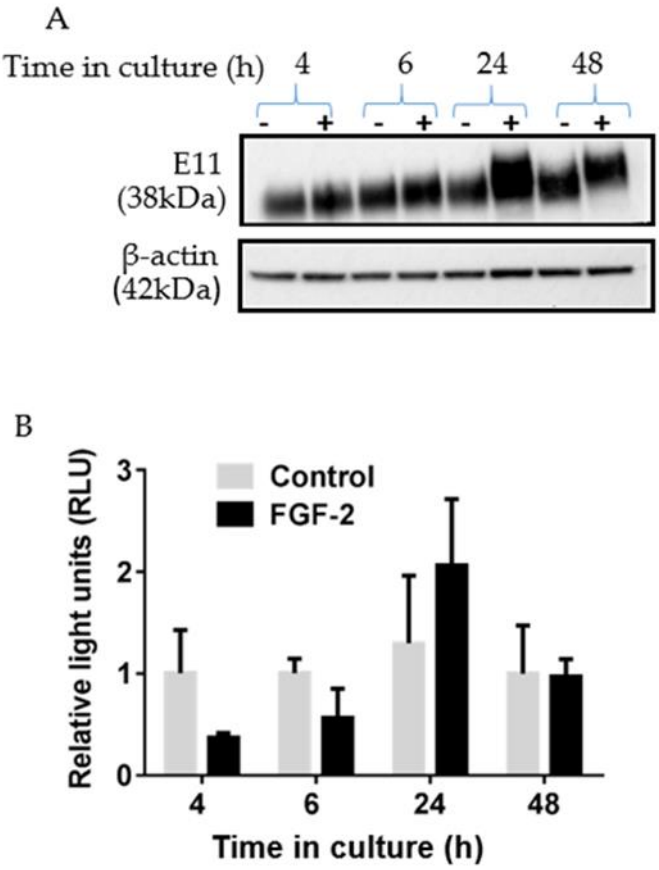

Figure 4.14 Activation of RhoA in FGF-2 treated MC3T3 cultures

(**A**) Western blot analysis of E11 expression after treatment of cells with FGF-2 for 4, 6, 24 and 48 h. The increase in E11 expression was most obvious after 24 h of FGF-2 treatment. Samples were normalised to β-actin for loading control. (**B**), RhoA activation levels were similar between the FGF-2 treated and control cultures at all-time points investigated.

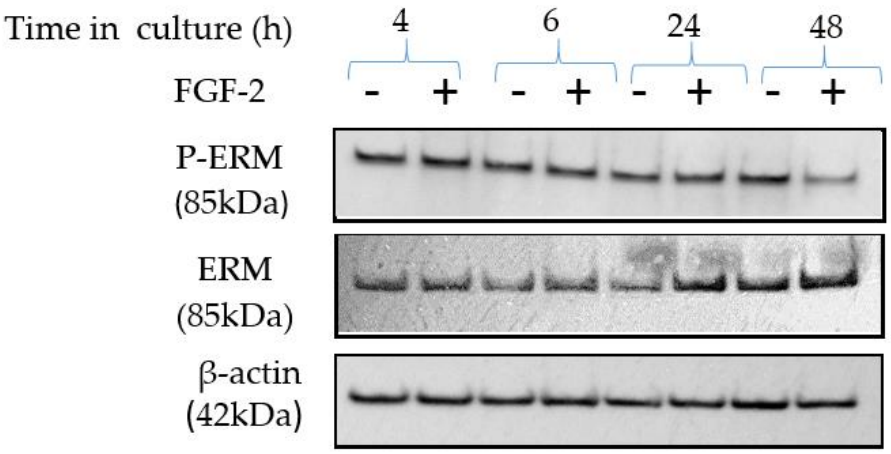

Figure 4.15 Activation of ERM proteins in FGF-2 treated MC3T3 cultures

Western blot analysis of ERM phosphorylation by FGF-2 treatment for 4, 6, 24 and 48 h showing no difference in phosphorylated ERM proteins at all-time points studied. Samples were normalised to β-actin as loading control.

4.5 Discussion

The intracellular molecules that mediate FGF-2's intracellular effects are activated upon FGF-2 binding to its RTK receptors - the FGFRs. The downstream signalling molecules include ERK1/2, p38 MAPK, Akt and PKC (Turner and Grose, 2010). In this study, activation of the ERK1/2 signalling pathway appeared to be the principal pathway activated by FGF-2 in osteoblast-like cells. This finding of dominant ERK1/2 signalling is in agreement with an earlier report where FGF-2 was shown to drive the upregulation of an osteocyte expression gene *Dmp1* in MLO-Y4 osteocyte-like cells (Kyono et al., 2012). Phosphorylation of ERK1/2 has also been shown to mediate cell proliferation, differentiation, and matrix mineralisation in human osteoblast culture (Lai et al., 2001, Marie et al., 2012). These results taken together highlight the importance of ERK1/2 signalling in mediating FGF-2s effects in osteoblasts including osteocytogenesis.

ERK1/2 signalling duration and strength are linked to its precise function in determining cell fate during growth and development (Murphy et al., 2003, Pellegrino and Stork, 2006). Sustained phosphorylated ERK1/2 signalling for 24 h or more following treatment with a growth factor is associated with cell differentiation, whereas reversal of phosphorylated ERK1/2 to baseline levels after 30 min post-treatment, which is referred to as transient signalling, is characteristic of a role in promoting cell proliferation (Chen et al., 2005, Pellegrino and Stork, 2006). In this study, the sustained activation of ERK1/2 by osteoblasts over long time periods (>24 h) was associated with an up-regulation of osteocyte markers and a down-regulation

osteoblast markers, as was shown in Chapter 3, thereby confirming its central role in osteoblast terminal differentiation under FGF-2 stimulation. Others have also reported the importance of ERK1/2 signalling in osteoblast initiation and commitment to the differentiation process (Lai et al., 2001).

An explanation for the various differentiation and proliferation responses of cells to sustained or transient ERK1/2 activation is unclear. However, this may be due to the different cell types and growth factors studied, the subcellular localisation of the phosphorylated ERK1/2 and the activation of different transcription factors, which are reported to serve as duration sensors (Murphy et al., 2002, Murphy et al., 2003, Chen et al., 2005, Pellegrino and Stork, 2006). Another explanation may involve the induction of various 'immediate early genes of which *E11* will be the prime immediate early gene candidate to be induced by FGF-2 for the terminal differentiation of osteoblasts to the osteocyte.

In addition to ERK1/2 activation by FGF-2 in osteoblast-like cells, there was significant activation of p38 MAPK and Akt by FGF-2. Activation of p38 MAPK has been reported by others to be involved in osteoblast differentiation in an ERK1/2 independent manner (Hu et al., 2003) whereas Akt activation has been reported to stimulate the proliferation of bone marrow derived osteoprogenitor cells, as well as osteoblast differentiation in synergy with ERK1/2 pathway (Choi et al., 2008).

Establishing which specific signalling molecules mediates the increased E11 expression after FGF-2 stimulation can be achieved by strategies that involve

inhibition of the selected signalling pathway. The use of chemical inhibitors in pathway elucidation has become popular because they are commercially available, inexpensive, extensively validated and can be used in mammalian models *in vivo*, hence the growing promise of optimising them for therapeutic uses (Alessi et al., 1995). PD98059 is a known inhibitor of MEK1/2 (Kevin and Stuart, 1997), which is an upstream activator to ERK1/2 (Pang et al., 1995). PD98059 treatment of cells to inhibit ERK1/2 phosphorylation in this study had little effect on E11 gene or protein expression and this may be due to the inability of PD98059 (at the concentrations used in this study) to ablate ERK1/2 activation in the osteoblast-like cells. Indeed, in other studies PD98059 has been shown to be ineffective in blocking the activities of MEK1/2 which is itself activated by c-Raf (Alessi et al., 1995). Furthermore it has been reported in previous studies using NIH3T3 cells that PD98059 only reduced MEK1/2 activation by 50-80% (Kevin and Stuart, 1997). This disadvantage of using PD98050 has also been reported with Swiss 3T3 cells, where ERK1/2 was still activated in these cells incubated with high concentrations (50 uM) of the inhibitor. Trying higher concentration of PD98059 was not considered for this study because apart from possible off target effects, it has poor solubility in aqueous media and it may also activate c-Raf which lies directly upstream of MEK1/2 (Alessi et al., 1995).

Due to these disappointing results using PD98059, another MEK1/2 inhibitor, U0126 (Fukazawa et al., 2002), which has about 100 fold greater affinity for MEK1/2 than PD98059, was used to enhance understanding of the role ERK1/2 activation in mediating the effects of FGF-2 on E11 expression (Favata et al., 1998). Similar to the

PD98059 experiments, little inhibition of ERK1/2 phosphorylation was observed with the concentrations of U0126 used (10 and 25 uM) although at the latter concentration the stimulation of ERK1/2 phosphorylation was dampened a little. This may possibly help to explain the lack of effect of U0126 on FGF-2 induced E11 gene and protein expression. Despite the significant decrease in ERK1/2 activation by U0126 (25 uM), it is likely that the level of activation remained above threshold levels to stimulate normal amounts of E11 expression. However, another possibility is that compensatory pathways exist to up-regulate E11 expression, since the inhibition of ERK1/2, Akt and p38 MAPK had no effect on E11 expression. Cross talk between ERK1/2 and other MAPK signalling molecules has been reported *e.g.* the upregulation of p38 MAPK phosphorylation in the presence of U0126 (Hotokezaka et al., 2002). It is also possible that the inhibitors used in this study, PD98059 and U0126 may be inducing off target effects on cell proliferation and cellular homeostasis (Hotokezaka et al., 2002). Also SB203580 has been shown to induce the upregulation of ERK1/2 at high concentrations (Birkenkamp et al., 2000). Therefore, the interpretation of the results obtained from the use of these inhibitors should be treated with caution (Dokladda et al., 2005, Wauson et al., 2013). In addition, to be noted is the possibility of beta actin changing with dendricity during FGF-2 driven osteocytogenesis, but the uniform bands of total proteins in these experiments validates the observed changes seen after FGF-2 stimulation.

FGF-2 mediated downstream effects are activated by its attachment to the FGFR receptor tyrosine kinase, which in turn induces receptor dimerisation. In this study,

FGF-2 stimulation of E11 expression by osteoblast-like cells is possibly mediated though F*gfr1* because its level of expression is over ten-fold higher in the 24 h time period, while a significant decrease was seen in the expression of *Fgfr2*/3 in the treated cultures. The relative importance of *Fgfr1* has been documented to drive osteoblast differentiation (Iseki et al., 1999), as a fivefold difference between *Fgfr1* expression and F*gfr2*/3/4 in MC3T3 osteoblast-like cells has been reported (Niger et al., 2012). It is of interest to note, however that the expression levels of *Fgfr1* expression were not altered in the presence of its ligand whereas prolonged incubation with FGF-2 caused a significant decrease in the expression of *Fgfr2/3*, a feature that is associated with switch from proliferation to differentiation in calvarial osteoblasts (Cowan et al., 2003). The relevance of these observations are unclear for FGF-2s ability to stimulate E11 expression , however it has been reported that FGF-2 treatment of` cells results in an increase in *Fgfr1* expression , and down regulation of *Fgfr2* and *Fgfr3* expression during calvarial suture development, where *Fgfr1* stimulates osteoprogenitor differentiation and suture union, while *Fgfr2*/3 induces proliferation (Teven et al., 2014). Nonetheless, it is important that further confirmatory tests like receptor dimerisation activity or cellular localisation of Fgfr1 be completed to confirm the role of *Fgfr1* in this study.

The importance of the relatively high levels of *Fgfr1* expression after 24 h by MC3T3 osteoblast-like cells, is underscored by published works reporting that FGFR1 mediates specific stages of osteogenesis and bone mass regulation (Zhang et al., 2014). It also induces mature osteoblast to differentiate upon stimulation with FGF-2 a

function that is central to driving increased osteocytogenesis (Jacob et al., 2006). In addition, FGFR1 has been shown to be the most important FGF-1 receptor during induction of neurite outgrowth of PC12 cells (Lin et al., 1996), a phenotypic switch that is key in the adoption of the osteocyte dendritic phenotype.

It is interesting to note that *Fgfr4* was not found to be expressed in these cells despite the use of several primer pairs from primer banks, published literature and commercial companies. This is consistent with a previous study in which calvaria bone has been reported not to express F*gfr4* (Partanen et al., 1991).

The use of AZD4547 for the inhibition of FGFR kinase has also been well reported (Zhang et al., 2012, Gavine et al., 2012, Xie et al., 2013). Its action attenuates the activation effects of FGFR1/2/3 on FRS-2 and subsequent down-regulation of the downstream signalling pathways such as the MAPKs and PI3K/Akt (Yao et al., 2015, Katoh, 2016). The relative level of phosphorylated ERK1/2 expression was employed to measure the degree of FGFR activation by FGF-2 after incubation with AZD4547. This approach has also been carried out in previous published studies using non-small-cell lung cancer cells (Marek et al., 2009). In this study, AZD4547 decreased the expression of ERK1/2 activation in a dose dependent manner. This effect has been seen in FGFR-expressing colorectal cancer cells (Yao et al., 2015). In this study, the inhibitor AZD4547 blunted FGF-2s ability to stimulate ERK1/2 expression, but had little effect on blocking E11 protein expression. It may reflect time dependent ability of the inhibitor AZD4547 to effectively prevent receptor dimerisation, hence

molecules upstream like ERK1/2 were blunted out but more studies should be done, as FGF-2 appears to be having little effect on E11 expression.

One of the functions of the E11 protein in modulating the early events of osteocytogenesis includes the acquisition of the osteocyte (dendritic) morphology. This feature was detailed in FGF-2 treated MC3T3 cell lines and primary osteoblasts in Chapter 3. A potential mechanism underlying this function of E11 protein in modifying cell shape is via the up-regulation of RhoA activation (Staines et al., 2016). RhoA is associated with regulating the ERM/CD44 complex, which is important in plasma membrane shape modification, cell migration and invasiveness (Hirao et al., 1996, Scholl et al., 1999, Martín-Villar et al., 2006). In this study, FGF-2 treated cells showed no RhoA activation. This may be due to the upregulation of other members of the Rho family of small GTPases such as Rac1 or Cdc42, which have been reported to also serve as molecular linkers during cytoskeletal protein activation and plasma membrane modification into structural extension such as filipodia (Nakamura et al., 2000, Jeon et al., 2010). The lack of activation of RhoA as seen in this study is supported by previous published work where E11 induced filipodia-like processes in MCF7 carcinoma cells formed despite inactivation of RhoA (Orriss et al., 2014). Nevertheless, this result is at variance with reported up-regulation of RhoA activation by E11 in MLO-A5 late osteoblast-like cells and MDCK type-II epithelial cells (Martín-Villar et al., 2006, Staines et al., 2016). This observed difference in the ability of E11 to induce cell morphology changes towards including the adoption of cell membrane

extensions or processes with or without activation of RhoA may be due to cell type, stage of cellular differentiation or even species variation (Martín-Villar et al., 2006).

Despite the lack of RhoA activation, the data presented in Chapter 3 supports the growing body of evidence that E11 is critical for the acquisition of the dendritic morphology characteristic of osteocytes (Zhang et al., 2006).

In addition to the RhoA data, the amount of phosphorylated ERM proteins were unaffected by FGF-2 stimulation, which may suggest the existence of another pathway to induce cell shape and dendrite formation that is independent of ERM proteins (Nakamura et al., 2000).

In conclusion, the results of this Chapter has indicated that the promotion of the osteocyte phenotype by FGF-2 is possibly via *Fgfr1* activation and increased E11 expression (Fig. 4.16). The signalling pathway(s) involved however, remains unclear but may involve phosphorylation of signalling molecules such as ERK1/2, Akt and p38 MAPK. With this knowledge, further studies will enable the determination of the significance of FGF-2/E11 interactions in subchondral bone thickening in the aetiology of osteoarthritis.

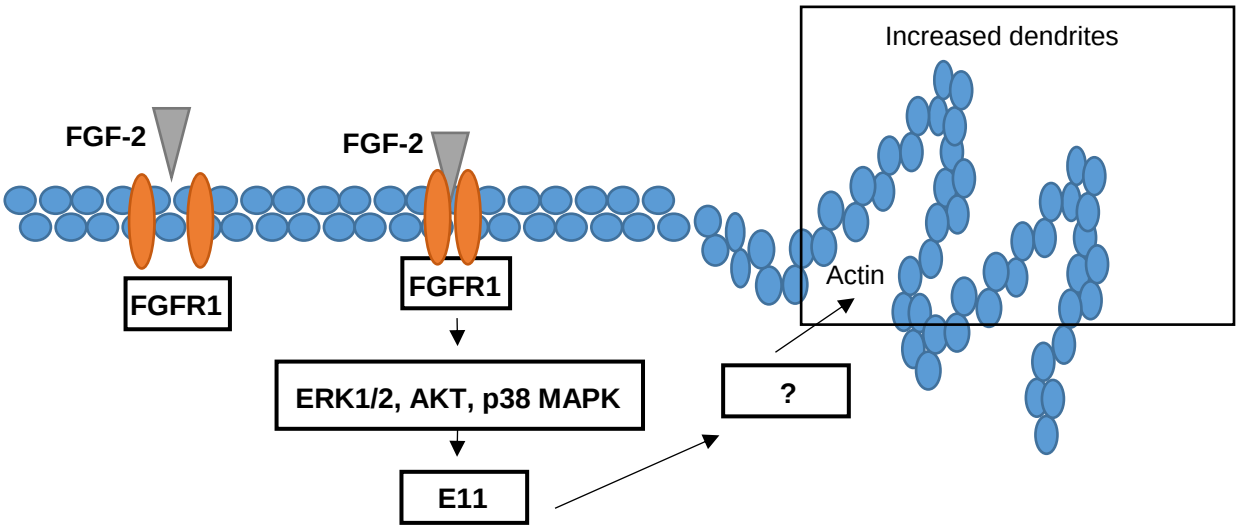

Fig. 4.16 Schematic of Chapter 4 results

This chapter has revealed that FGF-2 increases E11 expression possibly through ERK1/2 activation and compensatory Akt signalling, and this influences the actin cytoskeleton to promote osteocyte dendrite formation.

Chapter 5

Investigating the expression of E11 in OA pathogenesis

5.1. Introduction

Osteoarthritis (OA) is a degenerative and painful joint disease, and a worldwide healthcare burden in animals and man. OA is a disease of the whole joint and, perhaps rightly, research has largely sought to target the articular cartilage (AC) as this tissue undergoes severe deterioration (Goldring and Goldring, 2010, Sharma et al., 2013, Poulet and Staines, 2016). Subchondral bone (SCB) thickening in OA joints –although often considered secondary – is however one of the earliest detectable changes which many now consider to be a potential trigger for subsequent AC degeneration and OA progression (Li et al., 2013). There remains much speculation regarding the mechanism underpinning this modified SCB:AC relationship in OA, with cellular cross-talk and modified SCB stiffness proposed to exert a vital role (Goldring and Goldring, 2010, Sharma et al., 2013). Indeed, reports of altered SCB mineralisation and stiffness in OA have led to proposals that joint loading engenders greater AC deformation and OA degeneration (Findlay and Atkins, 2014, Im and Kim, 2014). Whilst the role of SCB in OA pathogenesis is unclear, it is undeniable that its modified remodelling contributes to sclerosis – a further OA defining feature. Despite this, the cellular/molecular mechanisms are not fully understood and therefore current clinical strategies remain limited.

Like cortical and trabecular bone, the SCB contains an abundance of osteocytes which are essential to its structure and function. In OA, the osteocytes of the SCB have an abnormal morphology, with both fewer and disorganised dendritic processes (Jaiprakash et al., 2012). In addition, there are many reports of disrupted expression

of the mature osteocyte marker sclerostin in OA SCB (Albisetti et al., 2013, Wu et al., 2016). This therefore suggests that the osteocyte may play a central role in the pathogenesis of the SCB in OA. Furthermore, the dendritic morphology of the osteocyte may be essential for maintaining healthy SCB. Published data and data reported in this thesis has shown that osteocyte dendrite formation is one of the early key events of osteocytogenesis and is associated with the expression of the osteocyte early marker gene *E11* (Zhang et al., 2006). Increased whole joint E11 expression has been reported in OA mice following surgical destabilisation of the medial meniscus (DMM), and in an *in vitro* cartilage injury assay using RT-qPCR (Burleigh et al., 2012, Chong et al., 2013). Despite these observations, the biological importance of altered E11 expression in OA has not been progressed further but it may be related to its known function in osteocyte biology.

Various animal models have been established to enable temporal studies on the pathogenesis of OA in the joint. The availability of these models help overcome the constraint of OA diagnosis and study on human patients, which often present at late stages of OA when pain and radiographic features become very apparent (Lorenz and Richter, 2006). These models have become an integral part of the armoury in the evaluation of either disease modifying therapy or studies towards understanding the cellular and molecular mechanisms underlying OA pathogenesis (Goldring and Goldring, 2010). The animal species reportedly used in OA studies include mice, rat, rabbit, guinea pig, goat, sheep, dog, cat and horses (Radin et al., 1995, Burleigh et al., 2012, Gregory et al., 2012, McCoy, 2015).

DMM, an OA instability model, is one of the most commonly used OA models. DMM involves transecting the anterior attachment of the medial meniscus to the tibial plateau, releasing a small portion of the medial meniscal anterior horn, hence the OA is induced by increased loading on the tibia. While the sham operated control mouse undergoes similar surgery the meniscus is not cut; the non-operated mouse control undergoes no surgery (Inglis et al., 2008, Botter et al., 2009, Malfait et al., 2010). This model of OA has the advantage of the gradual development over a long time, which replicates the human condition. Importantly, it allows the study of OA pathophysiology from the early to late stages (Inglis et al., 2008, Botter et al., 2009, Li et al., 2012). It also simulates human OA as the mouse develops OA features like SCB sclerosis after surgery, joint damage and degeneration long before any evidence of pain (Kamekura et al., 2005, Inglis et al., 2008, Malfait et al., 2010). However, there is discontent on the presence of SCB thickening observed in both the ipsilateral knee (ascribed to the OA process), and the control contralateral knee (ascribed to overloading with lamenes) (Loeser et al., 2013, Fang and Beier, 2014). In addition, DMM is an invasive procedure, which in itself may be associated with additional inflammation and cartilage damage (Fang and Beier, 2014, Miller et al., 2015).

Previously in this thesis, it was shown that FGF-2 upregulates E11 expression and increases osteocyte dendrite formation. Hence, extending my study for clinical relevance, this Chapter will help to elucidate the nature of E11 expression in SCB osteocytes of OA samples using WT and *Fgf-2* KO mice after DMM and sham surgeries. In addition, expression of E11 in a number of animal species and human OA samples will were also completed for comparative studies.

5.2. Hypothesis

E11 protein is differentially expressed in SCB osteocytes in comparative animal and human OA samples. The absence of FGF-2 decreases the expression of E11 protein in SCB osteocytes of OA samples.

5.3. Aims

I Quantify E11 protein expression in SCB osteocytes of WT mice with DMM induced OA.

II Examine E11 protein expression in SCB osteocytes of *Fgf-2* KO mice with DMM induced OA samples.

III Evaluate E11 protein expression in SCB osteocytes of OA samples from human and domestic animals.

5.4. Materials and methods

5.4.1 Human and animal samples

The human SCB samples were obtained from patients undergoing total knee replacement of two females and one male aged 63-75 year OA patients. Mr Amish Amin (University of Edinburgh) based on clinical and radiographic OA features diagnosed OA. Samples are obtained with patient consent and all procedures with ethical approval by NHS Lothian in collaboration with Mr. Anish Amin. The collection, storage, and subsequent use of human tissues are regulated in Scotland by The Human Tissue Act (Scotland) 2006. The study of these tissues was in compliance with all necessary UK licenses and ethical approvals.

The OA samples from SCB of domestic animals were kindly donated by Dr Dylan Clements, while Dr Katherine Staines donated the WT DMM samples. The samples were residual tissues collected from pets undergoing surgical for the treatment of disease with informed consent (OA samples), or which had died of unrelated disease (feline samples, ovine samples and equine samples and healthy canine samples) consent for use was obtained from the animal owners, and ethical approval for their collection and use given by the Veterinary Ethical Review Committee of the University of Edinburgh (VERC; approval 23/12 (canine), 23/12 (ovine), 7/5/09 (feline). The canine and feline samples were from elbow joints, the ovine samples from hip joints and the equine samples from the proximal metatarsal joint. In all cases, the joints were macroscopically evaluated for signs of disease as OA samples, while the healthy joints will be referred to as control in this thesis. The DMM and sham tibias of 14 weeks old *Fgf-2* KO and WT mice were donated by Prof. Tonia Vincent, were sampled 4 weeks post-surgery.

5.4.2 Toluidine Blue/Fast Green staining of the murine tibias

Toluidine blue dye is used extensively in cartilage staining as it binds to the negatively charged proteoglycans (Appleyard et al., 1999, Schmitz et al., 2010). The 5 uM thick tibiae paraffin embedded decalcified Sections were first de-waxed in xylene and rehydrated though a series of graded alcohols to distilled H_2O. They were incubated in 0.4% Toluidine Blue dissolved in sodium acetate buffer (see Appendix I). After washing in distilled H_2O, they were counterstained in 0.02% Fast Green in distilled H_2O. They were subsequently rinsed in distilled H_2O, blot dried and quickly

mounted. Images were captured with a Nikon Eclipse Ni microscope (Nikon, UK), fitted with Zeis Axiocam 105-colour camera (Carl Zeis, UK).

5.4.3. E11 and sclerostin protein sequencing alignment

Species-specific amino acid sequences for E11 and sclerostin were obtained from NCBI protein database (**https://www.ncbi.nlm.nih.gov/guide/proteins/**) while Clustal Omega was used to perform alignment and comparison of the species sequences under study including mouse, human, sheep, dog, cat, and horse (Sievers et al., 2011, McWilliam et al., 2013). The sequences were then uploaded into the online Clustal Omega alignment tool hosted on EMBL-EBI website (**https://www.ebi.ac.uk/Tools/msa/clustalo/**) to perform alignment and compute sequence similarity/identity between the different species. The level of homology between amino acid sequences for two different species was expressed as mean percent identity, which was calculated by dividing the degree of identity matching in the sequence alignment (pairs of identical letters) by the span of the alignment, where gaps are regarded as mismatches (Spalding and Lammers, 2004).

5.4.4 Immunohistochemical staining of the murine tibias

Murine tibias of same reference points from DMM and sham groups (Section 2.12.1) were immunostained for E11 and sclerostin as described in Section 2.12.2. Immunohistochemical staining of 5 um thick tibiae paraffin embedded decalcified sections was performed using E11 and sclerostin primary antibodies at (1:500) dilution, while secondary antibody was at (1:200) dilution using Vectastain ABC kit

as outlined in Section 2.12.2 and Appendix I Table 1. Immunohistochemical labelling was visualised using DAB chromogen. For control Sections, goat IgG at the same concentrations as primary antibody (1:500) was used instead of the primary antibodies. The percentage of positively stained E11 or sclerostin osteocytes was calculated (Section 3.4.8).

5.4.5 Immunohistochemical staining of comparative human and animal studies with anti-mouse E11 and sclerostin antibodies.

Sections of SCB from mouse, human, dog, cat, sheep and horse joints were immunostained with anti-mouse E11 and sclerostin antibodies as described in Section 5.4.1. Quantification was by means of counting sclerostin positively immunostained osteocytes across all microscopic fields and expressed as a percentage of the total number of osteocytes present.

5.4.6 Immunohistochemical staining of comparative human and animal studies with anti-human E11 antibodies.

Sections of SCB from mouse, human, dog, cat, sheep and horse joints were first de-waxed in xylene, and rehydrated though a series of graded alcohols to distilled H_2O. Antigen unmasking was carried out with 0.1% trypsin in PBS for 30 min at 37^{o}C using a water bath (Cattoretti et al., 1993). Endogenous peroxidase activity was blocked by treatment with 0.03% H_2O_2 in methanol for 30 minutes at RT. After 3 x 5 min washes in PBS the sections were blocked in normal donkey serum buffer (1:5 dilution of the appropriate normal serum in PBS) for 20 min at RT. The Sections were then incubated

in sheep anti-human E11 primary antibody (1:100 in PBS) at 4^0C overnight. Sheep IgG (1:200 in PBS) was used instead of the primary antibodies as a negative control. Unbound primary antibody was removed by 3 x 5 min washes in PBS. The Sections were subsequently incubated in donkey anti-sheep secondary antibody (1:200 in PBS) at RT for 1 h. They were later washed for 3 x 5 min in PBS. Staining was then developed in DAB solution for about 2 minutes. The Sections were rinsed in tap water and counterstained with haematoxylin using a Leica Autostainer XL (Leica, Milton Keynes, UK). Finally, Sections were dehydrated though graded alcohols, cleared with xylene and mounted in DePeX. Images were captured with Nikon Eclipse Ni microscope (Nikon, UK), fitted with Zeis Axiocam 105 colour camera (Carl Zeis, UK). Quantification triplicates per group was by means of counting E11 positively immunostained osteocytes across all microscopic field and expressed as a percentage of the total number of osteocytes present as done in Section 3.4.8.

5.4.7 Immunohistochemical staining of Human OA samples

Human OA samples were immunostained for E11 protein with anti-human E11 antibody (Section 5.4.6), and sclerostin protein with anti-mouse sclerostin antibody (Section 5.4.4).

5.4.8. Optimising anti-human E11 antibodies for immunostaining canine SCB samples.

Dog SCB samples were immunostained as described in Section 5.4.4 providing encouraging results. However, for full optimisation a range of antigenic epitope retrieval buffers were used. They include EDTA (1 mM at pH of 8.0), Tris/EDTA

(10 mM/1m M at pH of 9.0) and citrate buffer (10 mM at pH of 6.0) for 90min at 70^{o}C using a water bath. In addition, the concentrations of the primary antibody was varied 1:100; 1:50; 1:20; while secondary was varied to include 1:100 and 1:200 dilutions.

5.4.9. Measuring SCB thickness in tissue Sections via a histological tool (2D)

The thickness of the mice SCB was measured using the Fiji program (Schindelin et al., 2012). Bright field microscopic images of the Sections were sequentially captured with a Nikon Eclipse Ni2 microscope (Nikon, UK), fitted with Zeis Axiocam 105 colour camera (Carl Zeis, UK), and analysed on Zen Imaging software. Using a Fiji program, the images were fused to form a composite picture, while a calibrated rule measured SCB length distally from the SCB plate to the dorsal border of the nearest bone marrow. This measurement was completed at five points uniformly across the SCB of each tissue Section.

5.5. Results

5.5.1 Investigating E11 and sclerostin expression in DMM induced OA samples from tibias of WT mice

The expression of E11 and sclerostin in tibial SCB osteocytes of the DMM and sham operated WT mice was assessed by immunostaining. Despite there being an upward trend in the percentage of E11 positively stained osteocytes the results revealed the absence of a significant difference between sham and DMM groups in both the lateral and medial aspects of the tibia, (Figs. 5.1A - F). In addition, the percentage of sclerostin positively stained osteocytes were similar in both tibial condyles from the two groups (Figs. 5.2A-F).

5.5.2 Analyses of SCB sclerosis in WT mouse tibias after DMM surgery

Having observed no differences in the number of E11 and sclerostin positively stained osteocytes in the SCB of DMM mouse knee joints, there was a need to investigate the development of the SCB sclerotic phenotype to try and explain these unexpected results. This becomes imperative as no AC loss was noticed in both sham and DMM samples (Fig. 5.3A & B). 2D measurements of SCB thickness in sham and DMM samples (Figs. 5.3A & B), showed no overt differences in the thickness of the SCB (Fig. 5.3C). This lack of SCB sclerosis may therefore explain the unaltered E11 and sclerostin expression in this model.

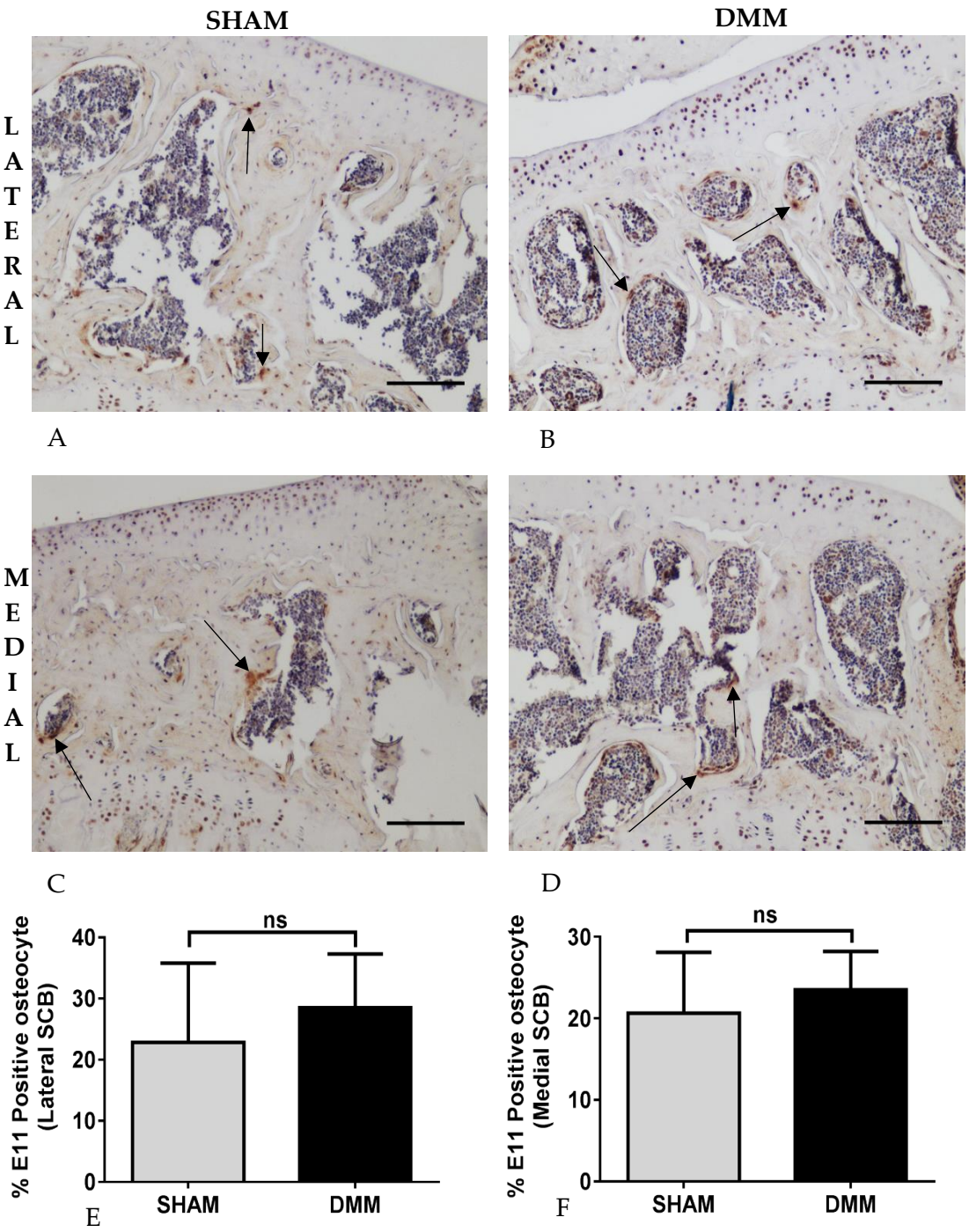

Figure 5. 1 E11 immunostained WT DMM and SHAM mice tibial subchondral bone osteocytes

Section of WT subchondral bone osteocytes (black arrow) in both SHAM (**A & C)** and DMM (**B & D**) no difference in E11 immunostaining in both groups was shown from quantification of E11 positive osteocytes in both lateral (**E**), and medial (**F**) sections of the DMM and SHAM groups. Data are presented as mean ± S.E.M (n=6); ns = not significant. Scale Bar =300 um.

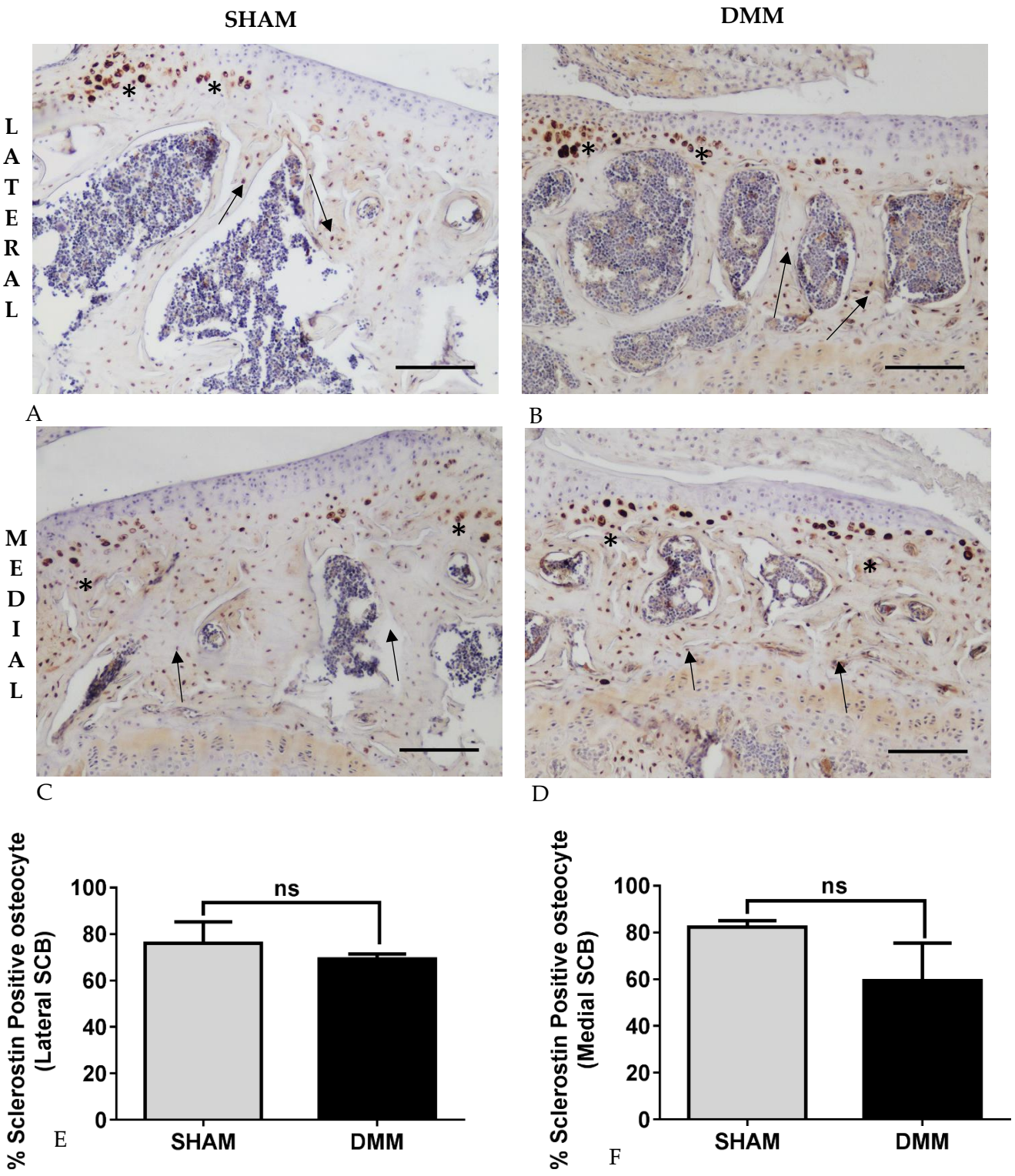

Figure 5. 2 Sclerostin immunostained WT DMM and SHAM mice tibial subchondral bone osteocytes

Section of WT subchondral bone osteocytes (black arrow) in both SHAM (**A & C)** and DMM (**B & D**) showing no difference in sclerostin immunostaining in both groups, as was shown from quantification of sclerostin positive osteocytes in both lateral (**E**), and medial (**F**) sections of the DMM and SHAM groups. Note the positive staining of hypertrophic chondrocytes of the articular cartilage (*). Data are presented as mean ± S.E.M (n=6); ns = not significant. Scale Bar = 300 um.

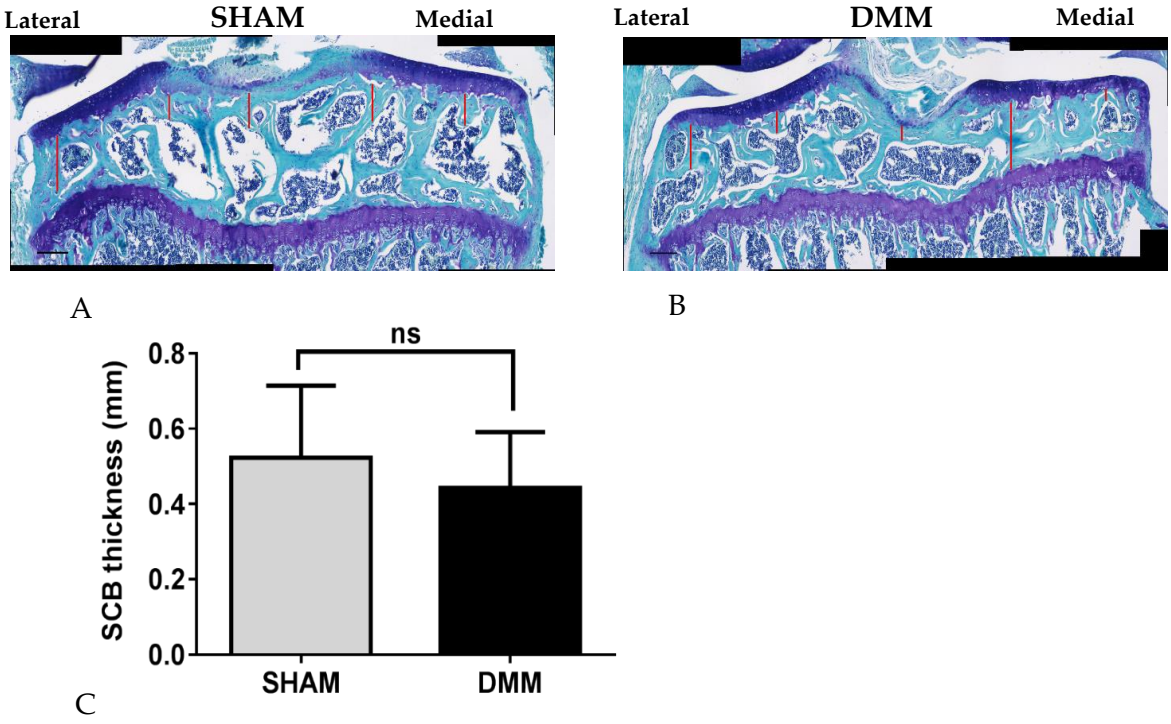

Figure 5. 3 Measuring tibial SCB thickness of WT mice after DMM using histological (2D) tool

Section of WT subchondral bone thickness (red lines) measured at 5 points distally from the subchondral plate to the dorsal border of the nearest bone marrow in both SHAM (**A)** and DMM (**B**), showing no difference in between them, as was shown from quantification (**C**). Data are presented as mean ± S.E.M (n=3); ns = not significant. Scale Bar = 300 um.

5.5.3 E11 and Sclerostin expression in SCB of human tibia OA samples

The percentage of E11 positive osteocytes in OA and control samples of human tibial SCB were quantified. There was no difference in the percentage of E11 positive and total osteocytes between the control and OA samples (Figs. 5.4 A –F). Anti-mouse sclerostin antibody was used to immunostain human tibial SCB Sections from OA and control patients (Figs. 5.5A-D). The percentage sclerostin positive- and total-osteocytes showed no difference and were similar in OA and control samples (Figs. 5.5E & F).

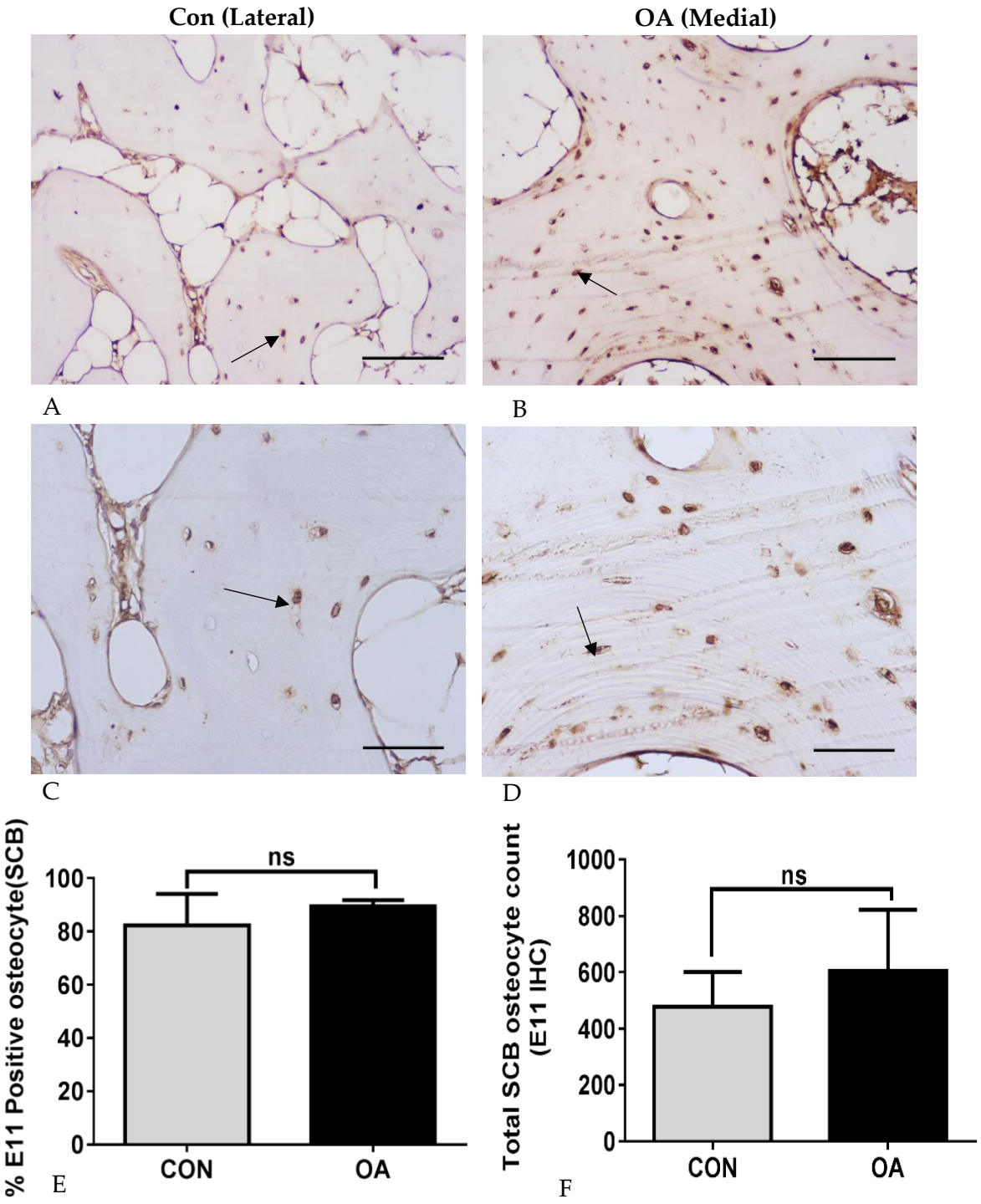

Figure 5.4 E11 immunostained OA and control human tibial SCB osteocytes

Section of human tibial SCB osteocytes (black arrow) in both Con (**A & C**) and OA (**B & D**) samples. Quantification of percentage E11 positive osteocytes and total osteocytes indicated no differences between control and OA samples (**E & F**). Data are presented as mean ± S.E.M (n=3). Scale Bar (**A & B**) =300 um; (**C & D**) = 150 um.

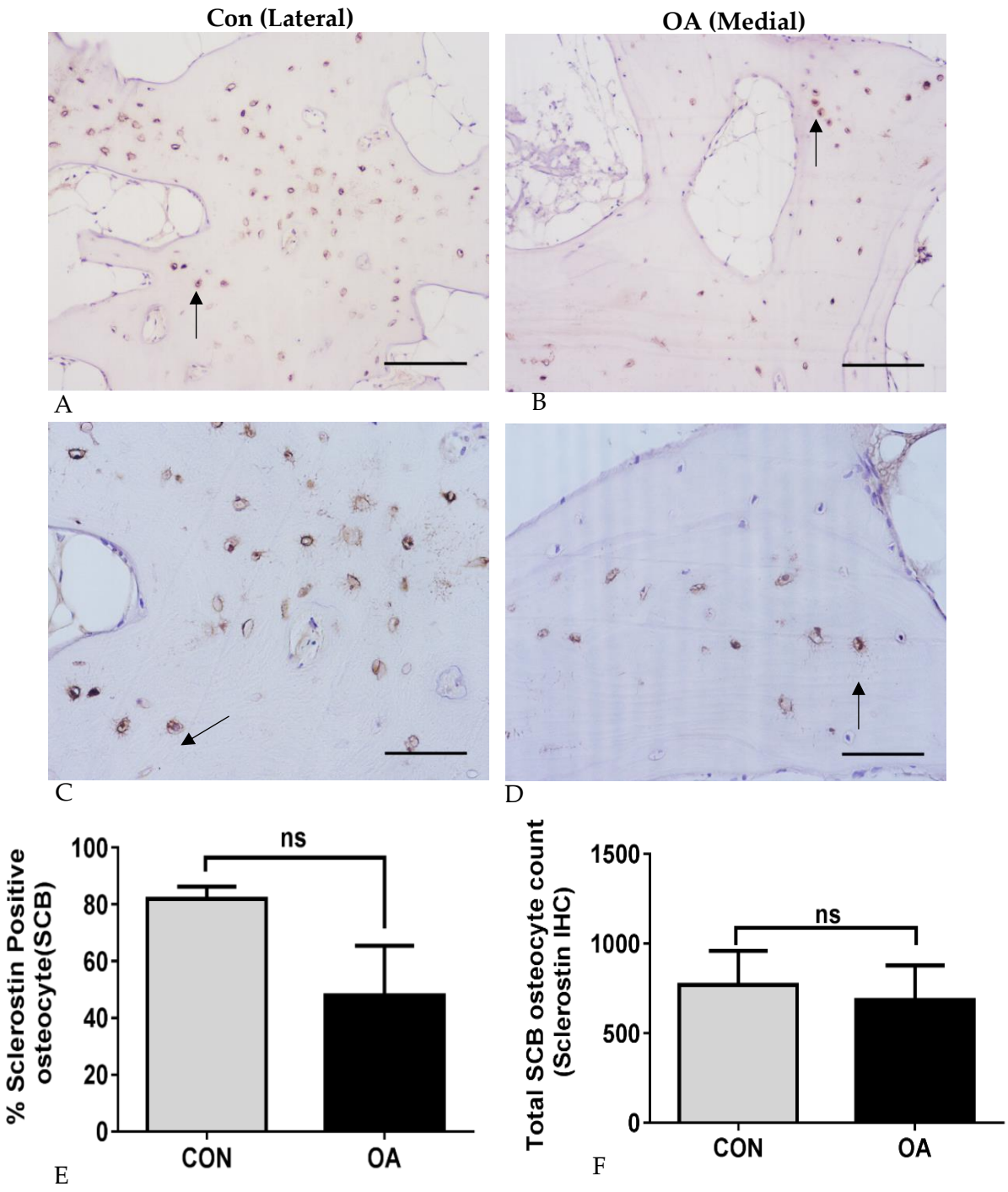

Figure 5.5 Anti-mouse sclerostin immunostained human tibial SCB sections from OA and control patients

Sclerostin localisation to human tibial SCB osteocytes (black arrow) in both Con (**A & C)** and OA (**B & D**) samples. Quantification of percentage sclerostin positive osteocytes and total osteocytes indicated no differences between control and OA samples (**E & F**). Data are presented as mean ± S.E.M (n=3 for OA; n=2 for con). Scale Bar (**A & B**) =300 um; (**C & D**) = 150 um.

5.5.4 E11 and sclerostin comparative protein sequence homology

As antibodies for dog, cat, horse and sheep E11 and sclerostin are not commercially available, E11 and sclerostin protein sequence homology in these species was completed using clustal omega programme (Sievers et al., 2011), as a guide to gauge potential cross-reactivity with mouse or human antibody.. The E11 protein of human, mouse, dog, horse, sheep and cat showed variable amino (N)-terminal homology, but increased homology was found at the carboxyl (C)-terminal (Fig. 5.6). The percent identity matrix between all species is shown in Table 5.1. The sclerostin protein of human, mouse, dog, horse, sheep and cat showed strongest sequence homology at the N terminal (Fig. 5.7). The percent identity matrix between all species is shown in (Table 5.2).

Figure 5.6 E11 protein sequence homology by Clustal Omega programme

E11 protein sequence homology of man, domestic and lab animals showed poor homology at the N-terminal. Homology was stronger at conserved C-terminal. This is illustrated by the relative number of asterix (*) below each sequence alignment.

Table 5.1 Percent Identity Matrix (E11) - created by Clustal 2.1

	Mouse	Human	Dog	Cat	Horse	Sheep
1: Mouse	100.00	47.53	53.70	48.77	47.22	42.76
2: Human	47.53	100.00	64.81	57.76	58.39	53.95
3: Dog	53.70	64.81	100.00	67.86	61.49	49.68
4: Cat	48.77	57.76	67.86	100.00	55.41	41.03
5: Horse	47.22	58.39	61.49	55.41	100.00	45.14
6: Sheep	42.76	53.95	49.68	41.03	45.14	100.00

Figure 5.7 Sclerostin protein sequence homology by Clustal Omega programme

Sclerostin protein sequence homology of man, domestic and lab animals showed well conserved N-terminal and poor homology in the C-terminal as was expressed in the relative number of asterix (*) below each sequence alignment.

Table 5.2 Percent Identity Matrix (Sclerostin) - created by Clustal 2.1

	Mouse	Human	Dog	Horse	Sheep	Cat
1: Mouse	100.00	88.15	91.00	65.77	60.87	69.57
2: Human	88.15	100.00	95.77	74.17	66.35	74.64
3: Dog	91.00	95.77	100.00	74.17	66.35	76.08
4: Horse	65.77	74.17	74.17	100.00	55.48	68.71
5: Sheep	60.87	66.35	66.35	55.48	100.00	58.94
6: Cat	69.57	74.64	76.08	68.71	58.94	100.00

5.5.5 Optimisation of antibodies for immunohistochemistry (IHC) protocol in domestic animals using anti-mouse and anti-human E11 antibodies

Taking into account the protein sequence homology data (Section 5.5.4), immunostaining with anti-mouse E11 antibodies was carried out on select animals including dog, cat, sheep, and horse. The results showed positive E11 staining in "positive control" mouse samples (Fig. 5.8A), but no cross reactivity in the Sections from the various animals tested (Figs. 5.8C, E & Figs. 5.9A, C, E). The results of anti-human E11 antibodies showed similar positive E11 immunostaining in human SCB osteocytes (Fig. 5.10A), and lack of cross reactivity in most of the other animals (Figs. 5.10C, E & Figs. 5.11C, E). However, in the canine Sections, which showed the highest percent identity homology with human (64.81%, Table 5.1), osteocyte cell bodies (but not dendrites) were detected although this was accompanied with strong non-specific background staining (Fig. 5.11A). These results were promising, hence the need to optimise anti-human E11 antibodies for use in further staining of the canine samples.

Subsequently, different epitope retrieval buffers were trialled with the anti-human E11 antibody on canine samples (Section 5.4.6). However, this revealed that the use of these new three buffers did not enhance the identification of E11 in canine SCB osteocytes (Figs. 5.12A-C).

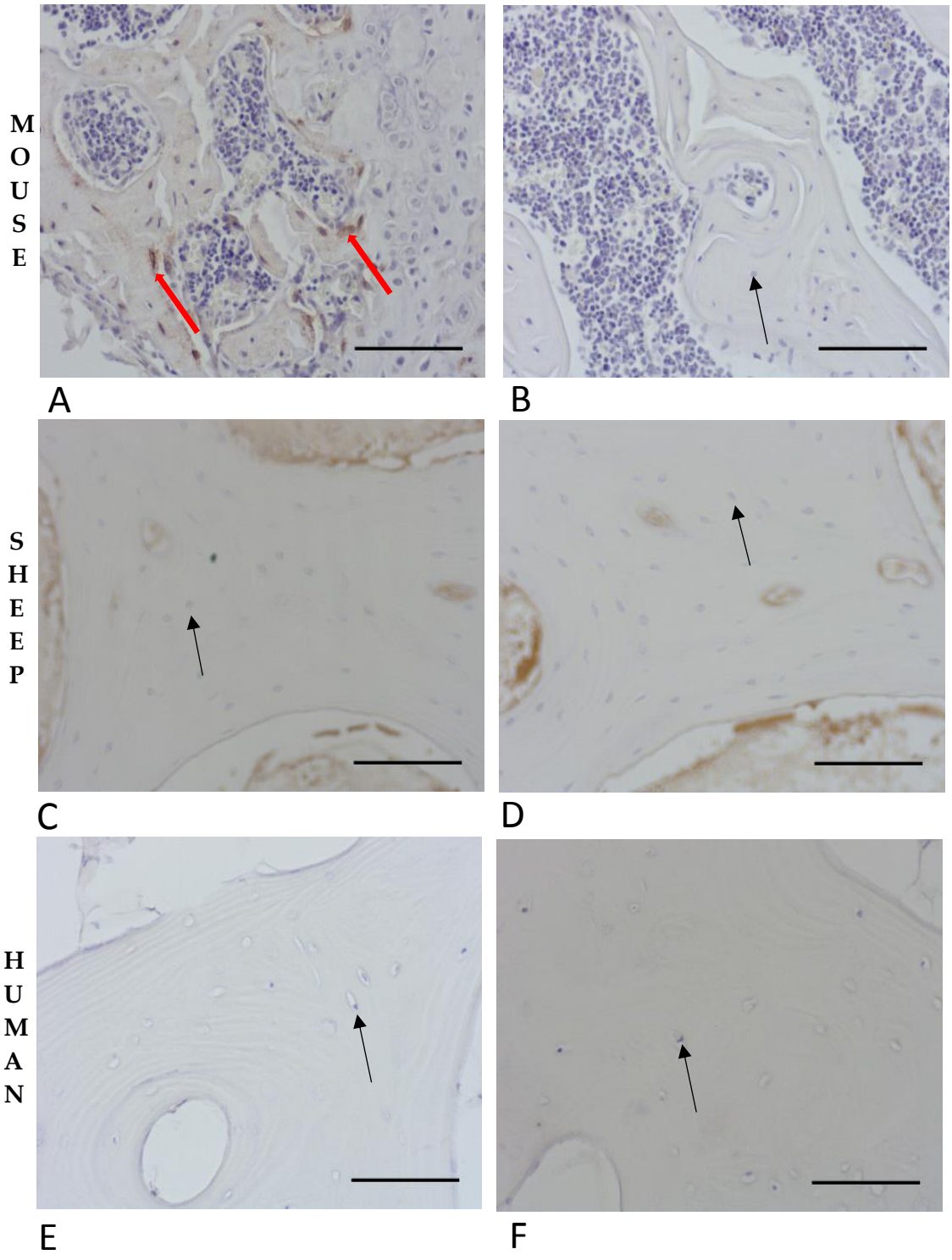

Fig. 5.8. Immunostaining of mouse, sheep and human SCB osteocytes with anti-mouse E11 antibodies

Subchondral bone sections of mouse, sheep and human SCB incubated with anti-mouse E11 antibodies (test) or appropriate IgG control (con); **A** -test & **B** –control of mouse knee joints; **C** -test & **D** –control of sheep samples; **E** -test, and **F** -control of human samples. Note, red arrows indicate positive E11 stained osteocytes in the mouse test samples whereas black arrows indicate non-stained osteocytes. Scale bar = 150 um.

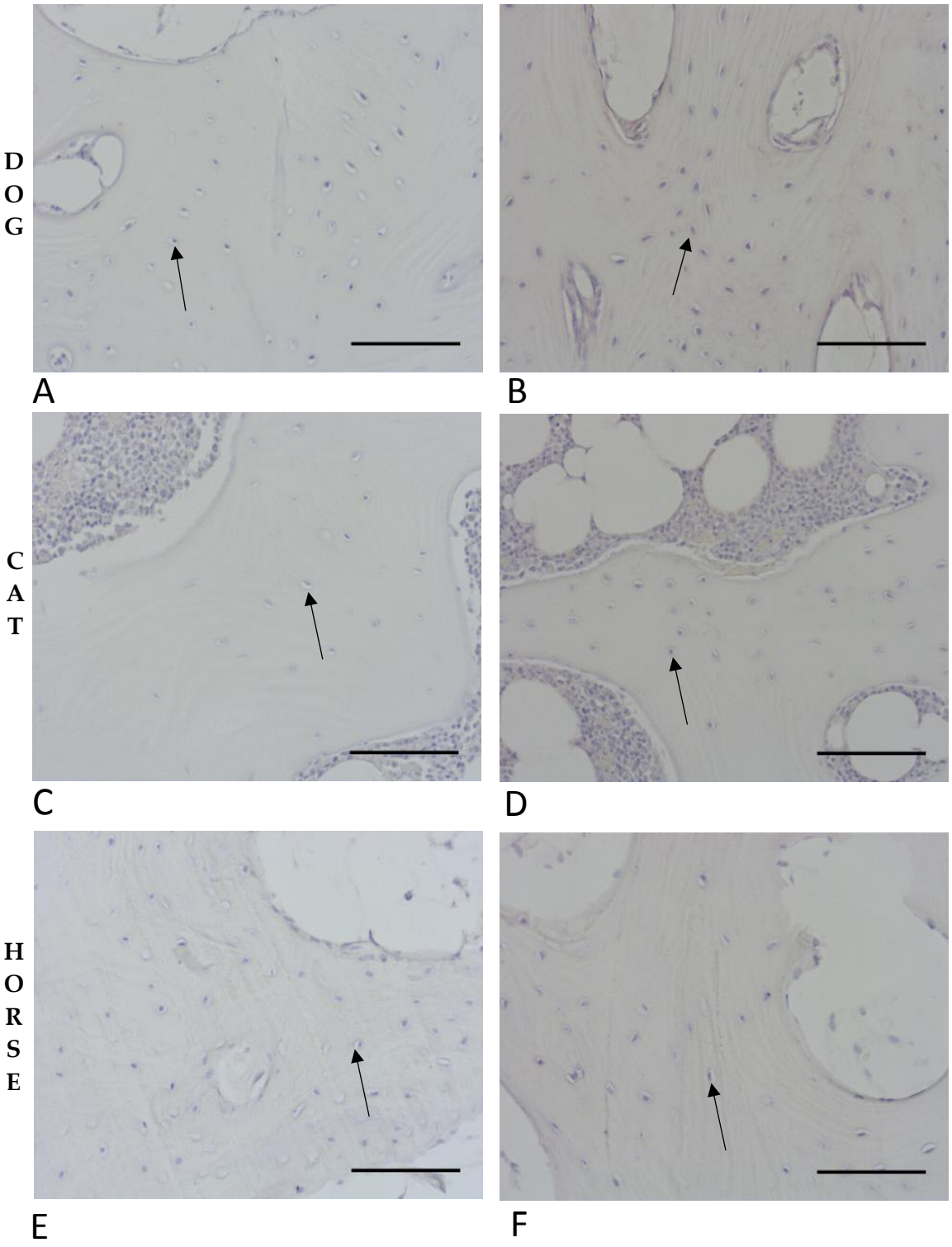

Fig. 5.9. Immunostaining of dog, cat, and horse SCB with anti-mouse E11 antibodies

Subchondral bone sections of dog, cat and horse reacted with anti-mouse E11 antibodies; A -test, **B** -control of dog samples; **C** -test and **D** -control of cat samples; **E**-test, and **F**-control of horse samples. Note, black arrows indicate non-stained osteocytes. Scale bar =150 um.

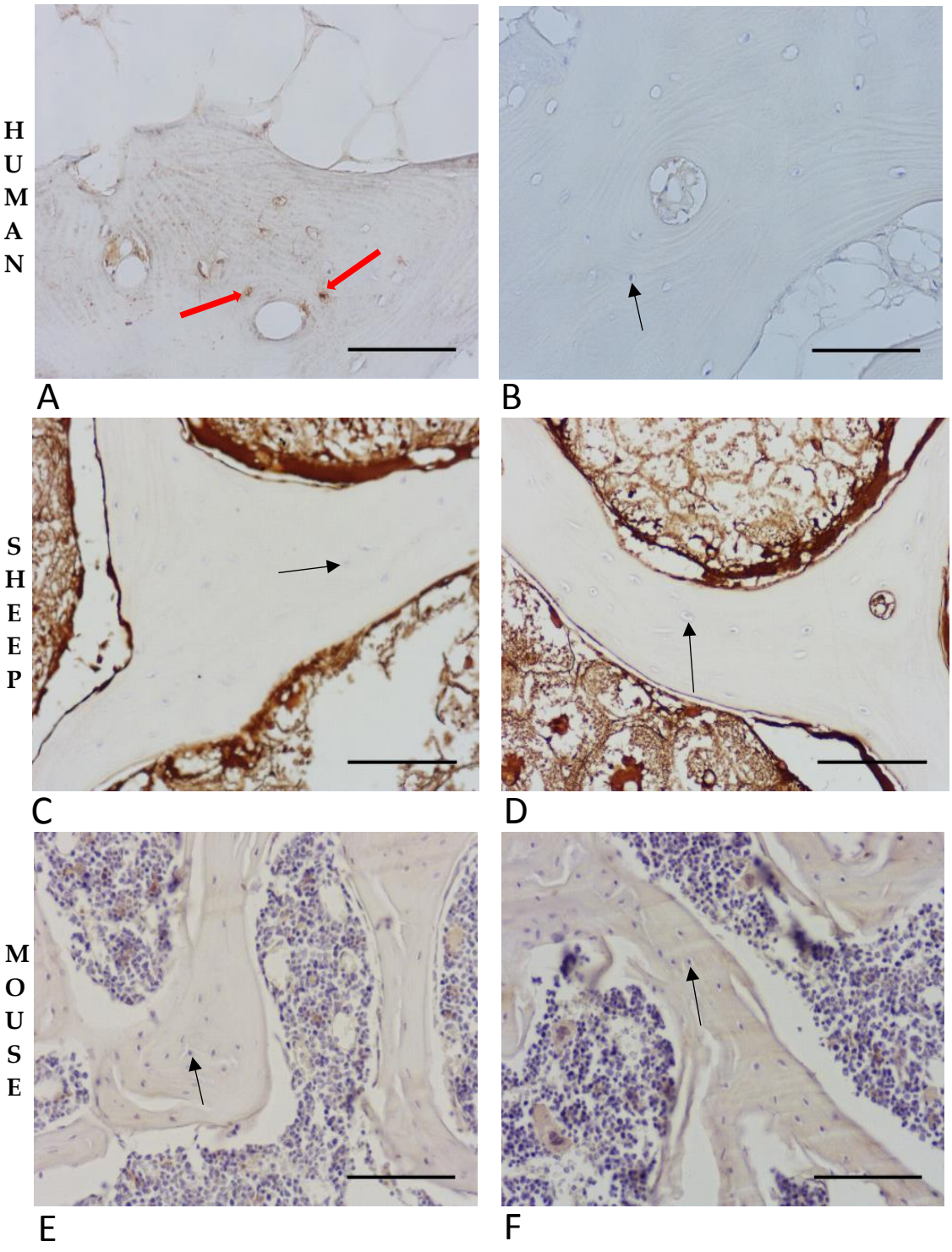

Fig. 5.10. Immunostaining of human, sheep and mouse SCB with anti-human E11 antibodies

Subchondral bone sections of human, sheep and mouse reacted with anti- human E11antibodies; **A** -test & **B** –control are human samples; **C**-test & **D** -control, are sheep samples; **E** -test, and **F** -control are mouse samples. Note red arrows indicate osteocyte positive to anti-human E11 whereas black arrows indicate non-stained osteocytes. Scale bar = 150 um.

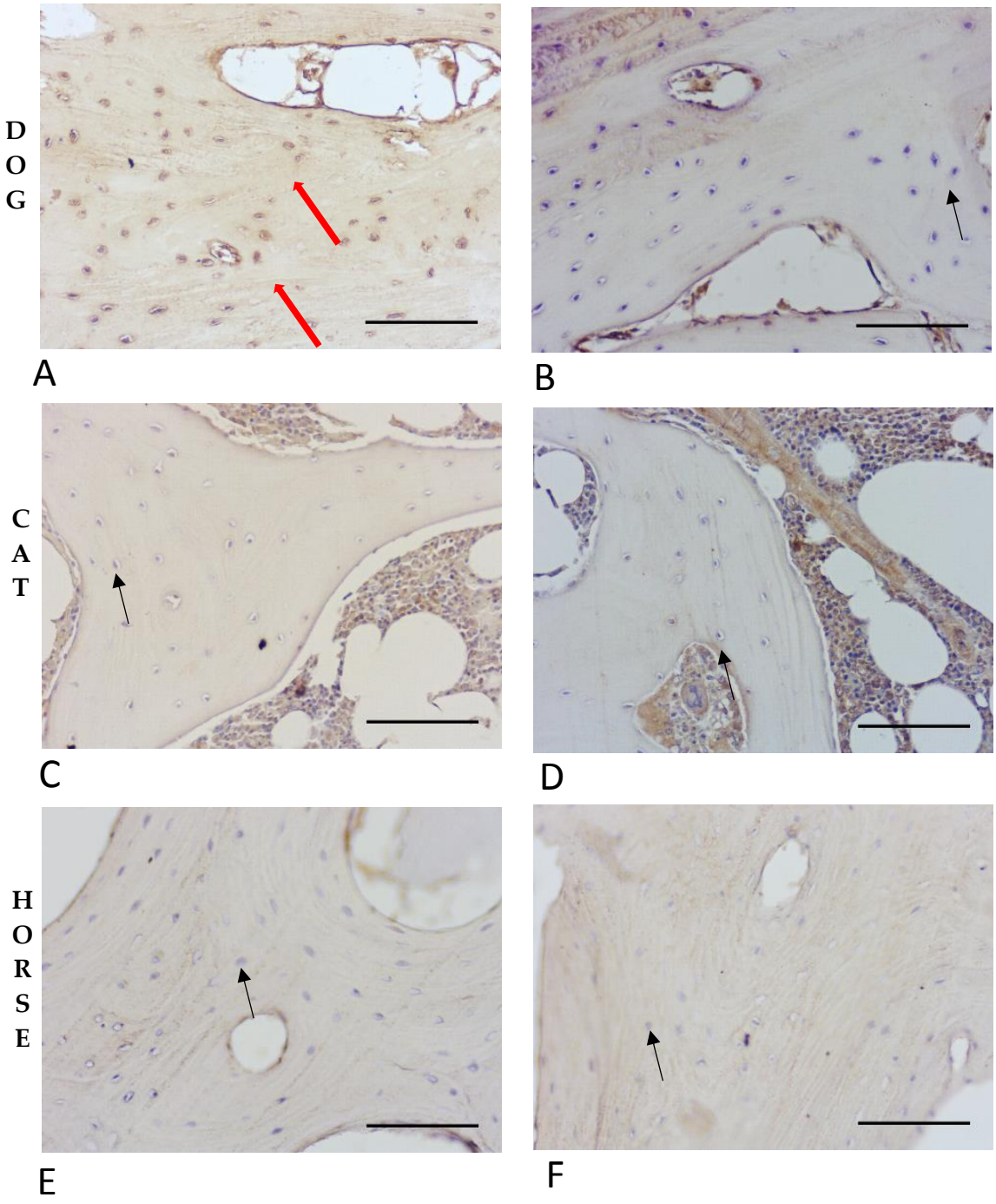

Fig. 5.11. Immunostaining of dog, cat and horse SCB with anti-human E11 antibody

Normal subchondral bone sections of dog, cat and horse reacted with anti-human E11 antibodies; **A** -test, **B** -control are dog samples; **C** -test and **D** -control are cat samples; **E**-test, and **F**-control are horse samples. Note, dog osteocytes look positively stained (red arrows), whereas black arrows indicate non-stained osteocytes. Scale bar =150 um.

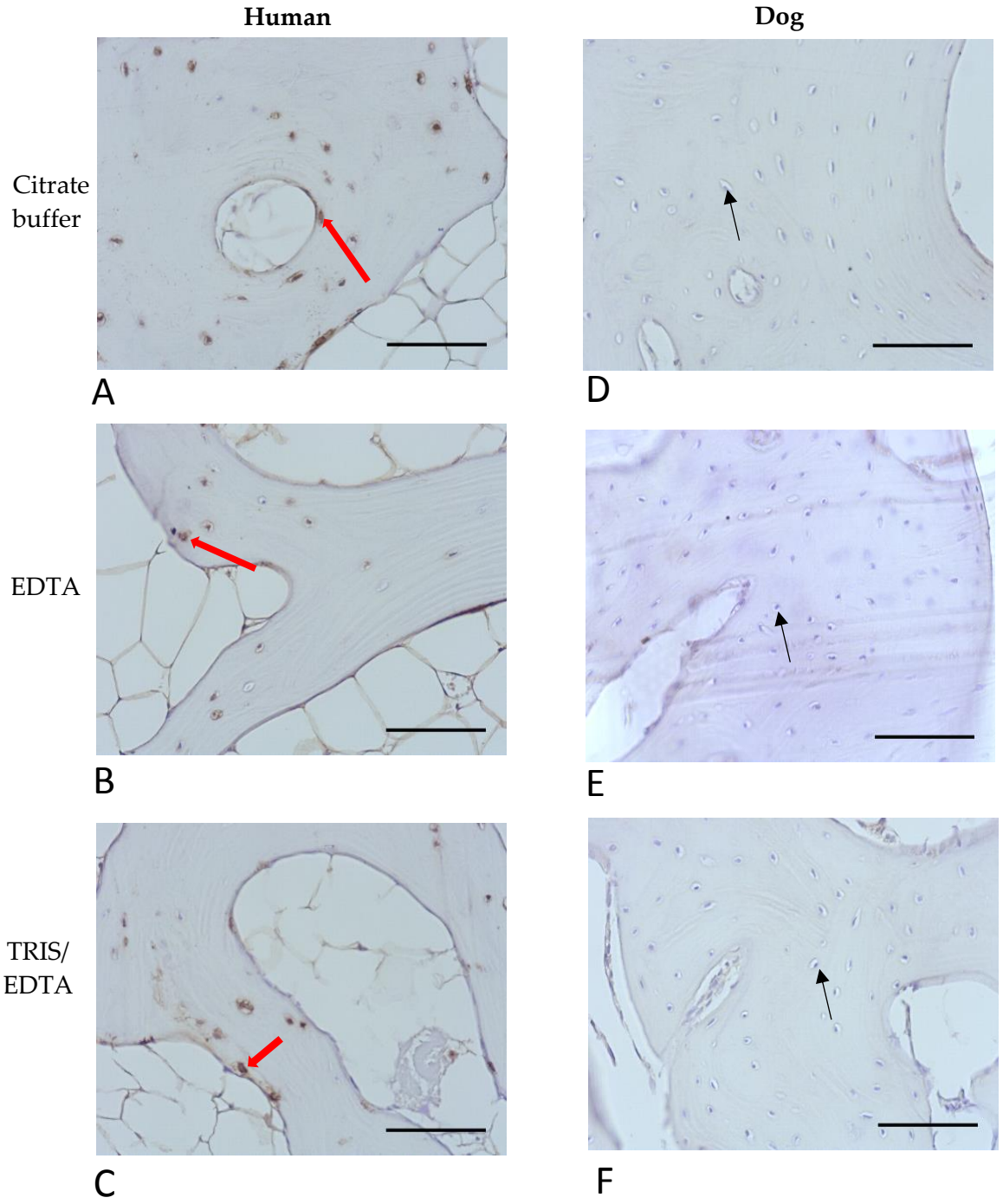

Figure 5.12 Optimisation of anti-human E11 immunostaining of canine SCB sections using different antigen retrieval buffers.

Subchondral bone sections of human (**A-C**), and canine (**D-F**) immunostained with anti-human E11 antibodies after pre-treatment with antigen retrieval buffers including citrate buffer (**A & D**); EDTA (**B & E**); and TRIS/EDTA (**C & F**). Note red arrows indicate osteocyte positive cells whereas black arrows indicate non-stained osteocytes. Scale bar = 150 um.

5.5.6 E11 expression in canine OA samples using anti-human E11 antibody

E11 expression in canine tibial SCB osteocytes from OA, and healthy samples that will be referred to as control samples was investigated using a anti-human E11 antibody after trypsin antigen retrieval. The percentage of E11 positive osteocytes was significantly greater (Fig. 513E; $P<0.01$) in OA canine samples (Figs. 5.13B & D), in comparison to non-OA samples (Figs. 5.13A & C). It also appeared that the dendrites radiating from the stained osteocyte bodies were more obvious in the OA samples.

5.5.7. Optimisation of anti-mouse sclerostin antibody protocol for IHC staining of SCB Sections from domestic animals

The osteocytes within SCB Sections from sheep, dog, cat and horse were also reacted with anti-mouse sclerostin antibody to test for potential cross reactivity. As expected, positive sclerostin immunostaining was observed in mouse and human SCB samples (Figs. 5.14A & C), but no cross reactivity in the other animals tested (Figs. 5.14E & Figs 5.15 A, C, E). It is worthy to note that in the horse, there were some osteocytes which labelled positive, but the vast majority were negative (data not shown).

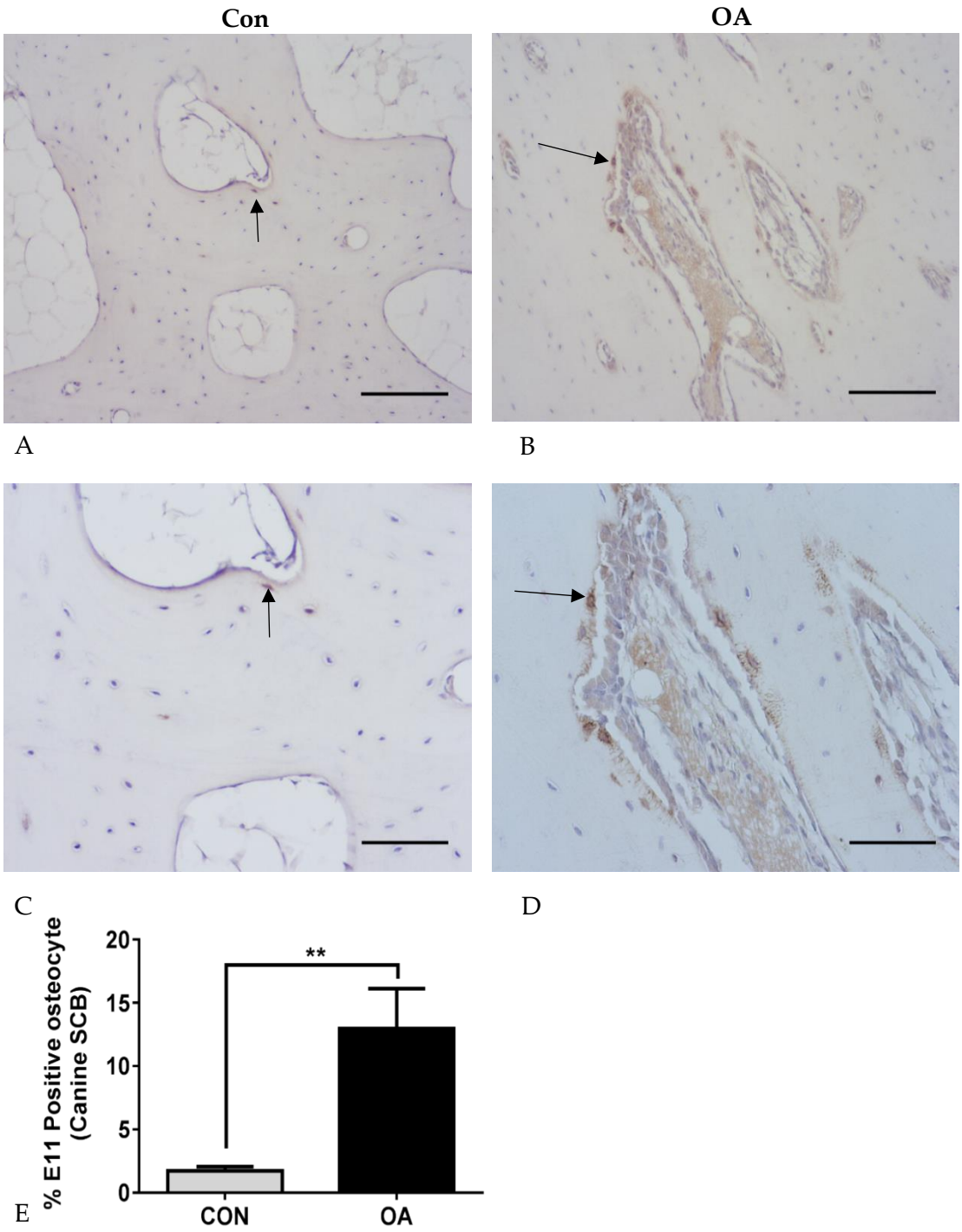

Figure 5.13 Control and OA canine tibial SCB osteocytes immunostained with anti-human E11 antibodies.

Section of canine tibial SCB showing E11 expression in osteocytes (black arrow) in both Con (**A & C)** and OA (**B & D**) samples. Quantification of E11 positive osteocytes indicated a significantly greater number in the OA samples compared with control samples (**E**). Data are presented as mean ± S.E.M (n=3); **p<0.01. Scale Bar (**A & B**) = 300 um; (**C & D**) = 150 um.

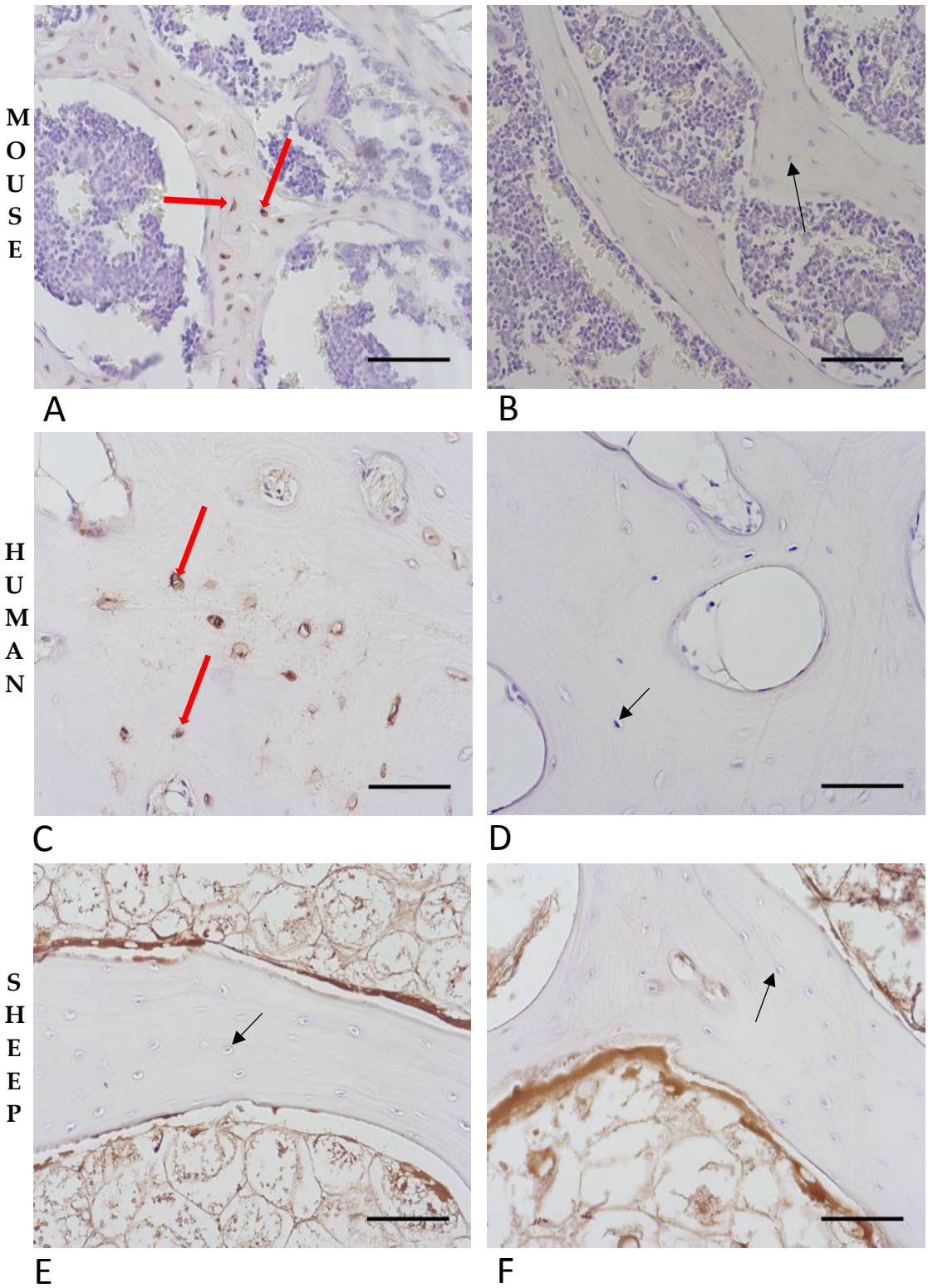

Fig. 5.14. Immunostaining of mouse, human and sheep SCB with anti-mouse sclerostin antibodies

Subchondral bone sections of mouse and human all stained with anti-mouse sclerostin antibodies; **A** -test & B –control are mouse samples; **C** -test & **D** -control are human samples; **E** -test, and **F** -control are sheep samples. Note red arrows indicate positive osteocyte staining in the mouse and human test samples, while black points at non-stained osteocytes. Scale bar = 150 um.

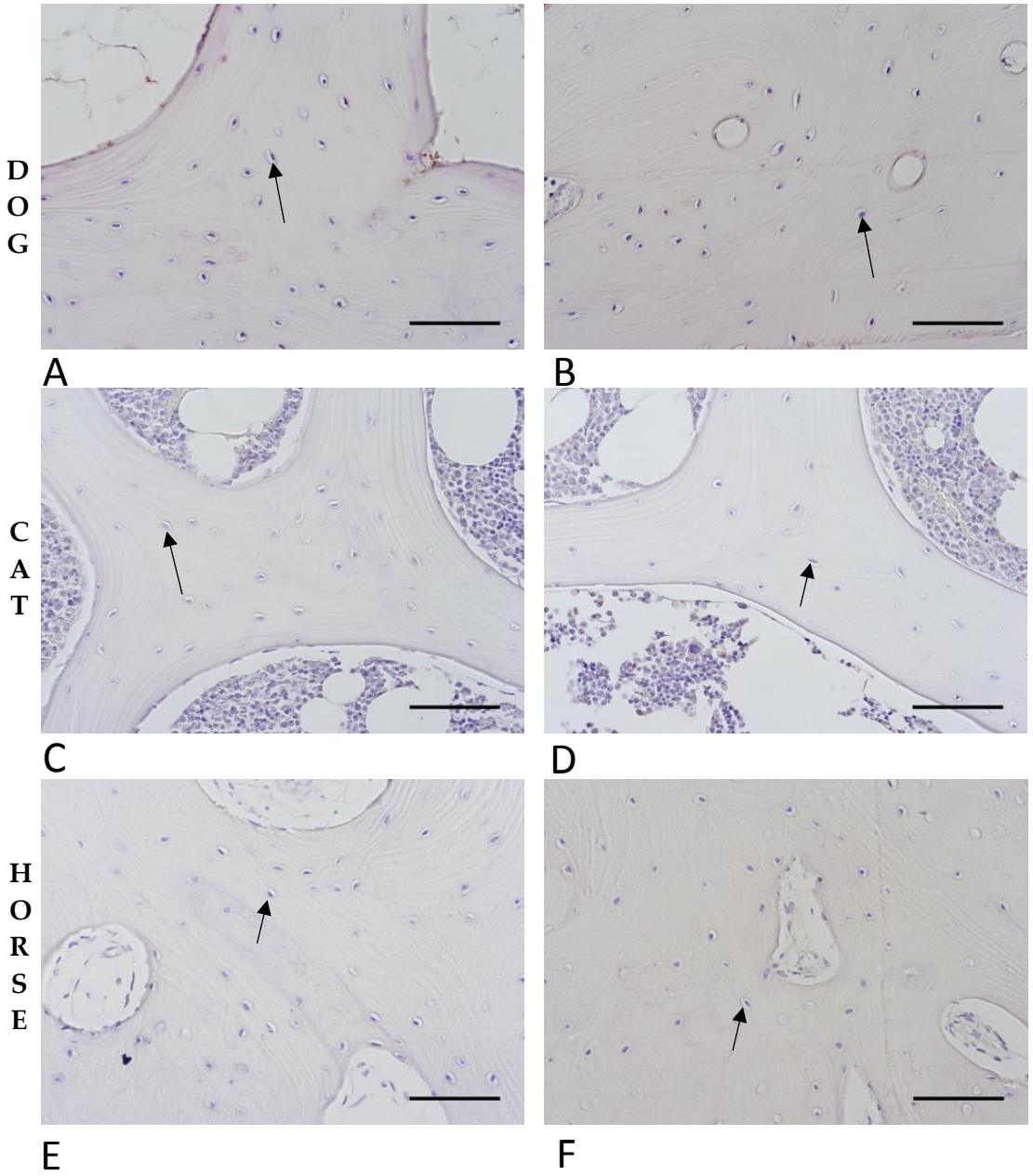

Fig. 5.15. Immunostaining of dog, cat, and horse SCB with anti-mouse sclerostin antibodies

Subchondral bone sections from dog, cat and horse, all reacted with anti-mouse sclerostin antibodies; A -test, **B** -control are dog samples; **C** -test and **D** –control are cat samples; **E**-test, and **F**-control are horse samples. Note black arrows indicating non-stained osteocytes in test and control sections. Scale bar =150 um.

5.5.8 E11 and sclerostin expression in OA (DMM induced) and control samples from tibias of *Fgf-2* KO and WT mice

To extend this project to understand the role of FGF-2 in regulating E11 and sclerostin expression during OA pathology, DMM and sham (control) mice from *Fgf-2* KO and WT samples were investigated. The use of toluidine blue staining showed normal AC in the control samples (Figs. 5.16A & B), while the DMM samples (Figs. 5.16C & D) confirmed focal AC loss and development of OA in both WT and *Fgf-2* KO groups as previously reported (Chia et al., 2009).

E11 immnunostaining on the lateral condyle of the tibia (Figs. 5.17A-D), showed an increase in the number of E11 positively stained osteocytes in the *Fgf-2* KO mice compared with their respective controls ($p<0.05$; Fig. 5.17E). However, the number of E11 positively stained osteocytes was not affected by the presence of DMM induced OA (Fig. 5.17E). In the medial tibia condyle, (Figs. 5.18A-D), a significant increase in the number of E11 positively stained osteocytes was noted in the *Fgf-2* KO sham joints when compared with WT control mice ($p<0.01$; Fig. 5.18E). However, as noted with the lateral condyle, the number of E11 positively stained osteocytes was not affected by the presence of DMM induced OA (Fig. 5.18E).

Sclerostin immunolabelling revealed no difference in the number of sclerostin positively stained osteocytes between genotypes and OA induction in either the lateral (Figs. 5.19A-E), or medial (Figs. 5.20A-E) aspect of the tibia.

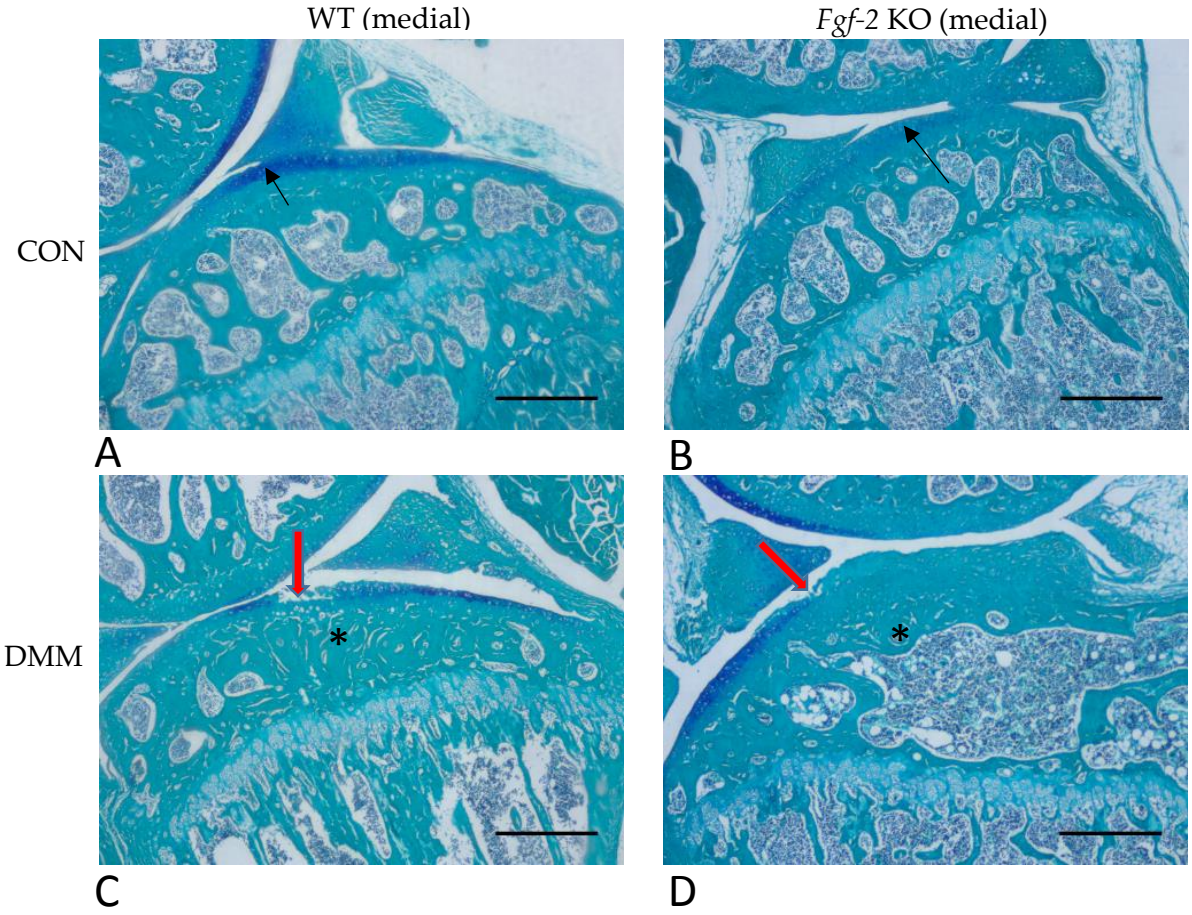

Figure 5.16 Histological assessment of DMM induced OA in *Fgf-2* KO and WT mice tibia using Toluidine blue staining

Section of tibial SCB showing normal AC (black arrow) in control (non-operated) in both WT (A) and *Fgf-2* KO (B). Note OA signs of AC lesion (red arrow) and SCB thickening with reduced bone marrow (*) in both WT (C) and *Fgf-2* KO (D). Scale bar = 600 um.

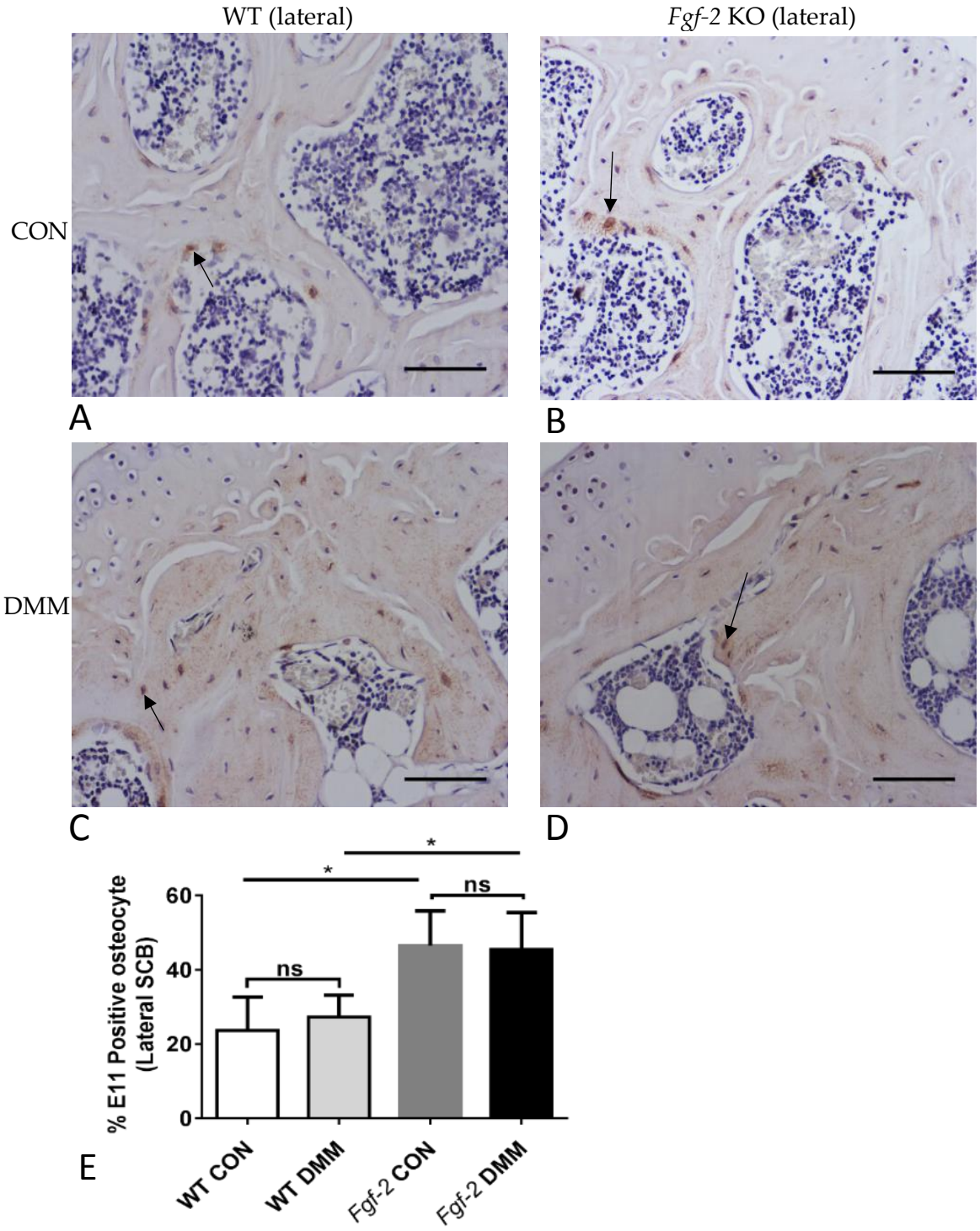

Figure 5.17 E11 immunostained *Fgf-2* KO/WT DMM and CON (non-operated) mice. Lateral tibial subchondral bone osteocytes

Sections of lateral tibial SCB osteocytes (black arrow) in both WT control and DMM (**A & C),** and *Fgf-2* KO control and DMM (**B & D**). Quantification of E11 positive osteocyte number showed an increase in E11 positive osteocytes in the *Fgf-2* KO DMM when compared to WT DMM (**E)**. This increase in the number of E11 positive osteocytes was also noted in controls of *Fgf-2* KO Con when compared to WT Con (**E**). Data are presented as mean ± S.E.M (n=4); *p<0.05; ns = not significant. Scale bar = 150 um.

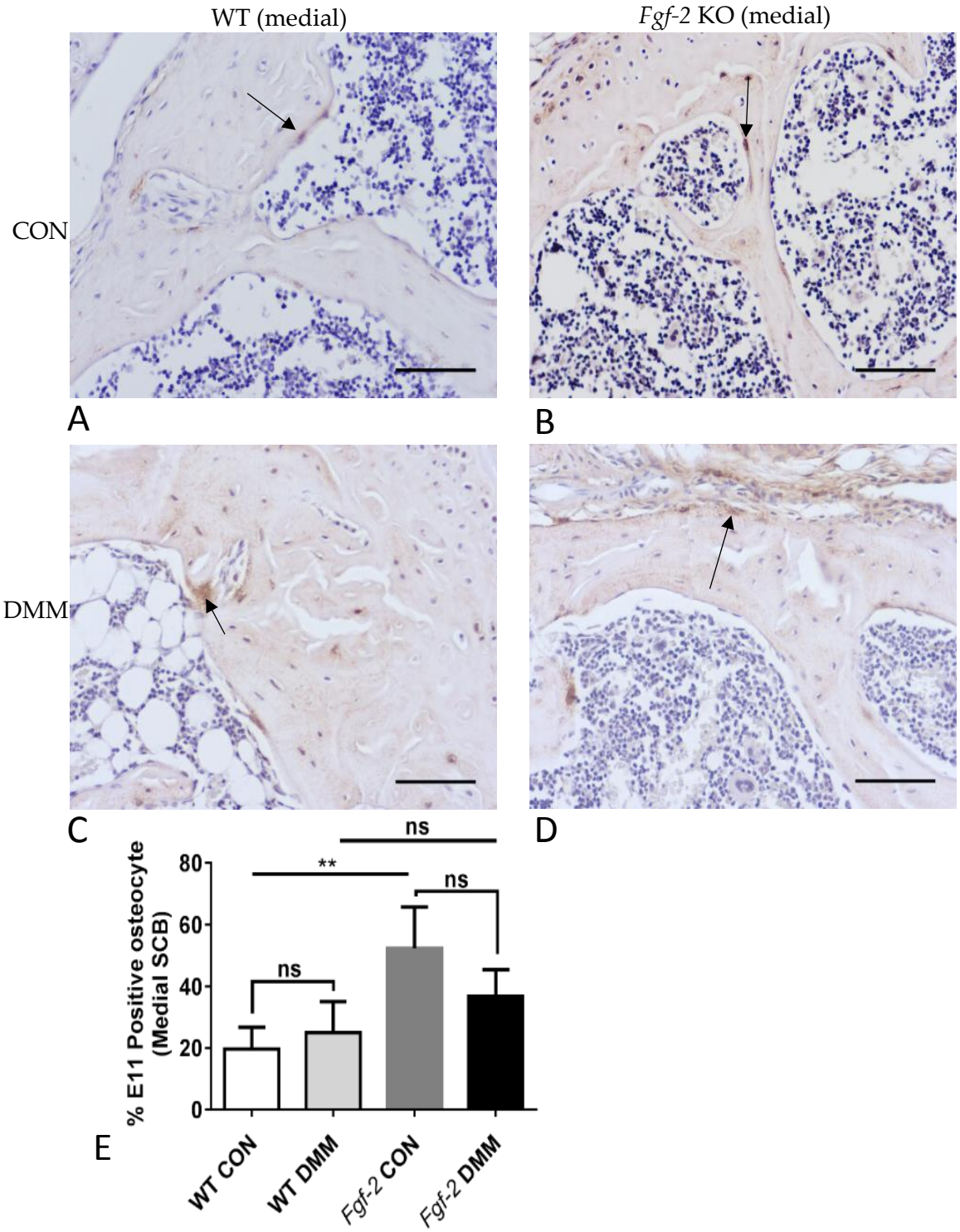

Figure 5.18 E11 immunostained *Fgf-2* KO/WT DMM and CON (non-operated) mice. Medial tibial subchondral bone osteocytes

Sections of medial tibial SCB osteocytes (black arrow) in both WT control and DMM (**A & C),** and *Fgf-2* KO control and DMM (**B & D**). Note, increase in the number of E11 positive osteocytes in *Fgf-2* KO controls when compared to WT Con samples (**E**). Data are presented as mean ± S.E.M (n=4); *p<0.05; **p<0.01; ns = not significant. Scale bar = 150 um.

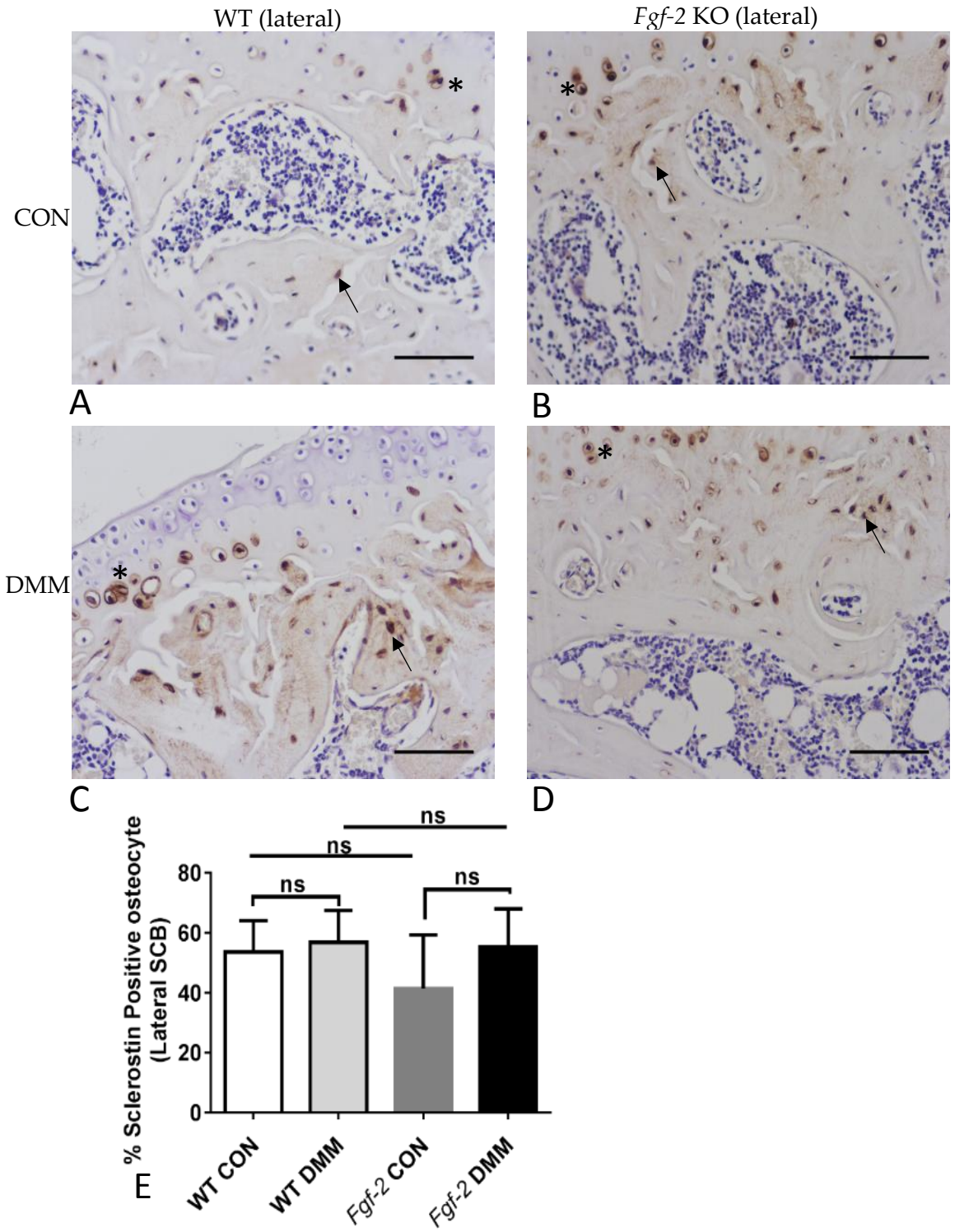

Figure 5. 19 Sclerostin immunostained Fgf-2 KO/WT DMM and CON (non-operated) mice. Lateral tibial SCB osteocytes

Sections of lateral tibial SCB osteocytes (black arrow) in both WT control and DMM (**A & C),** and *Fgf-2* KO control and DMM (**B & D**). Quantification of the number of sclerostin positive osteocytes showed no difference in the DMM tibias of both WT and *Fgf-2* KO groups (**E**). Data are presented as mean ± S.E.M (n=4); ns = not significant. Scale Bar = 150 um.

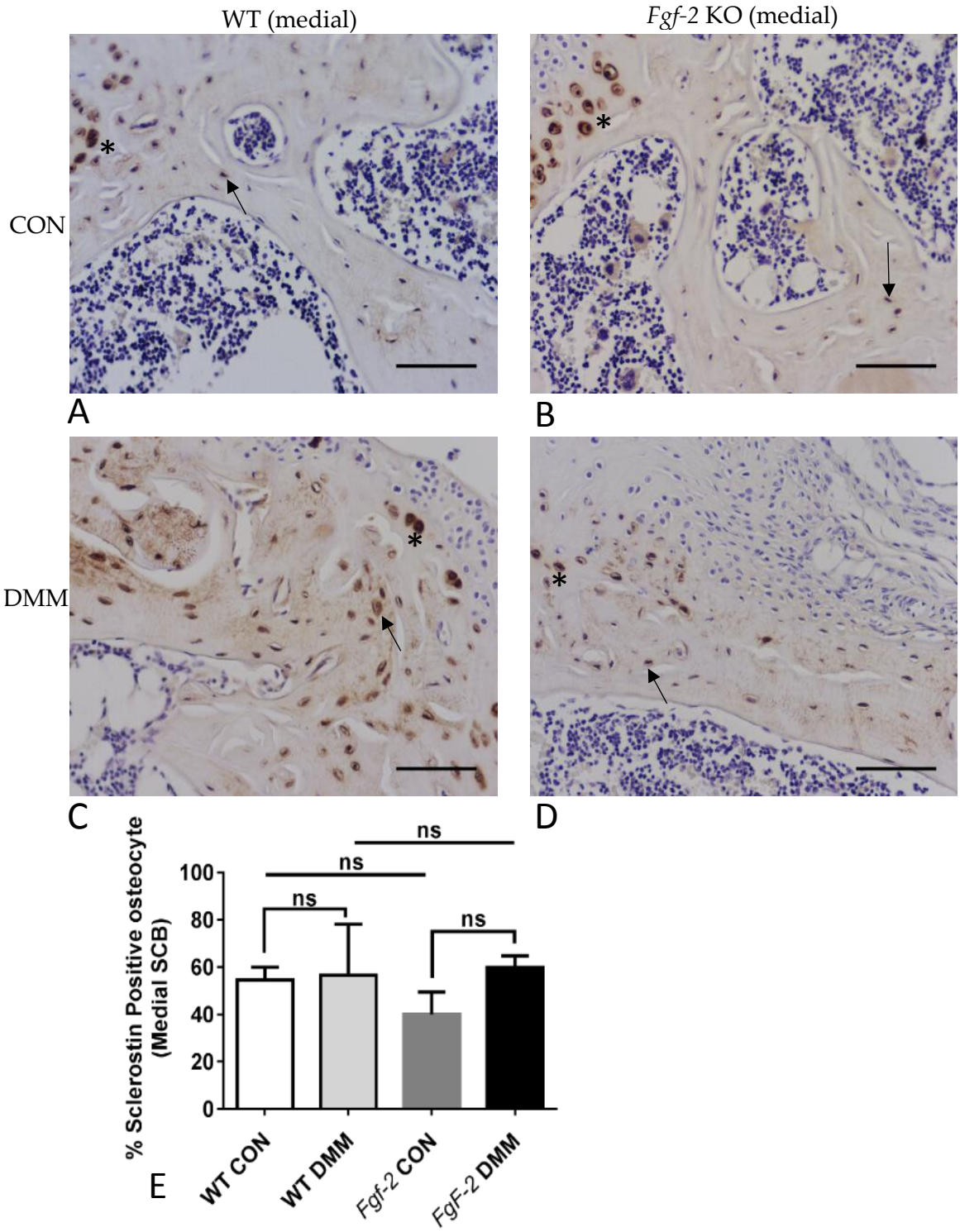

Figure 5. 20 Sclerostin immunostained Fgf-2 KO/WT DMM and CON (non-operated) mice. Medial tibial subchondral bone osteocytes

Sections of medial tibial SCB osteocytes (black arrow) in both WT control and DMM (**A & C),** and *Fgf-2* KO control and DMM (**B & D**). Quantification of the number of sclerostin positive osteocytes showed no difference in the DMM tibias of both WT and *Fgf-2* KO groups (**E**). Data are presented as mean ± S.E.M (n=4); ns = not significant. Scale Bar = 150 um.

5.5 Discussion

Bone remodelling is an integral process to bone health, but is dysregulated during OA pathophysiology (Burr and Gallant, 2012, Baker-LePain and Lane, 2012). In OA, it varies temporally from early bone resorption, to late stage-associated increased bone formation and subsequent sclerosis. Spatially, differences also occur in the medial and lateral Sections of the joint (Findlay, 2013). In addition, some osteocyte-expressed molecules including E11, Phex, Dmp1, and sclerostin that are involved in bone remodelling are dysregulated during OA pathology (Appleton et al., 2007, Jaiprakash et al., 2012, Chong et al., 2013, Bouaziz et al., 2015). In this Chapter, two osteocyte markers, E11 and sclerostin were immunohistochemically localised to SCB osteocytes in a number of OA samples. The first investigation compared WT mice after sham and DMM surgery and no differences in both E11 and sclerostin immunostaining between the DMM and sham control mice was noted. This may be due to the absence of obvious OA pathology such as AC loss and absence of SCB sclerosis. This was unexpected but there is a need to confirm these data in the 3D context by micro computed tomography (micro-CT) analysis as 2D results are highly inconsistent mostly due to Sectioning protocols of angle and region (Jia et al., 2017).

Histological studies of human OA samples are mostly limited to tissues obtained via joint replacement therapy and cadaver specimens (Lorenzo et al., 2004, Wallace et al., 2017). While these sources may present a wide pool of tissues, it has a major limitation of representing mostly late stage OA (Lorenzo et al., 2004). In this Chapter, OA samples were sourced from patients undergoing total knee replacement, and they

showed no obvious differences in osteocyte E11 and sclerostin immunostaining compared with control samples. This may reflect that the number of osteocytes expressing E11 and sclerostin were not altered during this stage of OA, or that the sample size was not big enough to reflect any variation. Another suggestion may be the effect of differences in loading on specific sections of the bone. In addition, the fact that both samples are from the same disease joint may reflect this similar E11 expression. Nevertheless, a significant decrease in the number SCB osteocyte positively immunolabelled for sclerostin in human OA samples has been reported and it was related to the observed sclerosis (Jaiprakash et al., 2012).

In our domestic animals, the burden of naturally occurring OA is also a major concern as documented in sheep, horses, cats and dogs (Clarke et al., 2005, Clements et al., 2009, Robin et al., 2013, Vandeweerd et al., 2013). Hence, an insight into the molecular profile of the SCB during OA pathology of these animals will be very relevant for their therapeutic management. This becomes important as there is variation in gene expression between human and dogs during OA pathology including the tissue inhibitor of matrix metalloproteinase -2 (Kevorkian et al., 2004, Stoker et al., 2006, Clements et al., 2009). In this Chapter, the increased number of E11 stained SCB osteocytes in the canine OA samples relative to the control samples was a novel result and may be attributed to newly formed osteocytes in the sclerotic bone; a cardinal feature of OA.

Protein sequence similarity searching has become an integral aspect of determining homologous sequence of new proteins (Pearson, 2013). This process widely employs

programs like BLAST, FASTA, PSI-BLAST, HMMER3, SEARCH, CLUSTAL OMEGA and PEARSON (Smith and Waterman, 1981, Pearson and Lipman, 1988, Pearson, 1991, Altschul et al., 1997, Sievers et al., 2011). The resulting information enables correlation of structures, function and common ancestry for highly similar sequences. Applying the 30% identity rule as the minimum for two sequences to be accepted as homologous (Pearson, 2013), the results from E11 sequence alignment analysis suggest that the E11 gene from mouse, human, cat, dog, sheep and horse can be described as homologous. This agrees with other authors that have reported the E11 gene to be highly conserved between species (Astarita et al., 2012).

Nevertheless, with exception of dog samples, the SCB osteocytes of the species under study did not cross-react with anti-mouse or anti-human E11 antibodies. This might reflect the specific nature of the E11 epitope that the antibody was raised against (Kaneko et al., 2016). It may also reflect low reliability and accuracy of the percent identity analysis in sequence homology determination (Pearson, 2013); and the use of sequence homology as a tool in predicting antibody cross-reactivity (Sankian et al., 2005).

Sclerostin sequence alignment analysis also suggested that the sclerostin gene from mouse, human, cat, dog, sheep and horse could be described as homologous However, only the SCB osteocytes from human Sections with 88% identity cross-reacted with anti-mouse sclerostin. This may be due to poor alignment of the antigenic epitopes specific to this antibody, as dog sclerostin was >90% identical to the mouse sequence and did not cross react. Also some authors have suggested that

antibody cross-reactivity potential can be influenced by factors like sequence similarity, analogous antigenic determinants, and structural compatibility like charges and shape (McClain, 2017).

Tissue processing activities such as formalin fixation, EDTA decalcification, paraffin embedding and even Sectioning has been suggested to deleterious affect the quality of immunostaining (Hadjiargyrou et al., 2001). These processes especially formalin fixation cause tissue structure modification like protein cross-linking that have the tendency to massk antigenic epitopes. In addition to using proteolytic enzymes such as trypsin to break formalin induces bonds, several aqueous salts or known protein denaturing agents such as Tris-HCl, EDTA-NaOH and citrate buffer can also be used at high temperatures (Morgan et al., 1994, Pileri et al., 1997). In this Chapter, trypsin, EDTA, Tris EDTA and citrate buffers were used in an attempt to unmassk epitope site on canine SCB Sections for optimising anti-human E11 antibodies. Only trypsin treated SCB Sections resulted in osteocytes that were positively immunostained.

Earlier in this thesis (Chapter 3), FGF-2 showed capacity to regulate E11 in MC3T3 osteoblast-like cells *in vitro*, but this correlation was not observed in the *in vivo* studies using *Fgf-2* KO mice. Redundancy amongst other members of the FGF family of growth factors was suggested as being responsible for this lack of FGF-2 effect. Extending the study further to determine if FGF-2 regulates osteocyte, E11 expression during OA was carried out on *Fgf-2* KO mice using the DMM model. Joint instability models of OA induction such as DMM has become a widely recognised procedure as it produces focal AC lesions, SCB sclerosis, osteophyte formation and pain (Inglis et

al., 2008, Little et al., 2009, Zhang et al., 2016). In this project, the DMM samples from *Fgf-2* KO and WT mice showed robust AC lesion; while the WT SCB showed sclerosis and reduced bone marrow, thus establishing that these samples indeed developed OA as has been previously published (Chia et al., 2009). The number of E11 positive osteocytes within SCB osteocytes was however not altered after DMM in the *Fgf-2* KO mice. This result is not consistent with earlier findings of E11 gene down-regulation as measured by RT-PCR in the AC of *Fgf-2* KO mice after DMM surgery (Chong et al., 2013). This may reflect differences method of calculating E11 expression as positive cells were counted here while Chong et al measured mRNA. In addition, the differences in tissue types, as studies by Chong et al., involved the AC, rather than the SCB. While the possibility of AC contamination with some SCB tissue may be the source of E11 in the Chong et al study, as chondrocytes are not show not cytoplasmic extension such as dendrites or invadopodia that is a classical function of E11, but some authors have also E11 expression in foetal chondrocytes(Smith and Melrose, 2011).

It is worthy to note the significant increase in the number of E11 positive osteocytes within the SCB of *Fgf-2* KO mice compared to the WT mice observed in the control joints. In Chapter 3, no differences in the number of E11 positive osteocytes between naïve *Fgf-2* KO and WT mice was noted. This discrepancy may reflect an adjustment to loading on the contralateral knee in the non-operated knee joints. This raises the concern on the appropriateness of using the sham surgery or non-operated contralateral limb as a control during studies on DMM induced OA models in mice.

Specifically, the SCB sclerosis phenotype has been reported in both experimental and control limbs in the DMM model (Loeser et al., 2012, Fang and Beier, 2014, Miller et al., 2015).

In this Chapter, whilst WT mice displayed SCB sclerosis after DMM, little sclerosis was observed in the *Fgf-2* KO mice. The absence of sclerosis in the *Fgf-2* KO is consistent with a previous finding of reduced bone formation and fewer trabeculae with increased inter-trabeculae space in mice with *Fgf-2* loss of function mutation (Montero et al., 2000). The authors attributed this structural feature to an imbalance in bone resorption than formation. Sclerostin is a well-recognised inhibitor of bone formation and acts via of the Wnt canonical pathway. Sclerostin expression by osteocytes is down-regulated during loading which is likely to contribute to the bone anabolic response (Robling et al., 2008). During OA pathology, sclerostin expression is also down-regulated leading to the clasical SCB sclerosis (Jaiprakash et al., 2012). In this present, work the number of sclerostin positive osteocytes in the SCB osteocytes of WT and *Fgf-2* KO mice after DMM surgery was similar. This lack of differential sclerostin expression in the WT mice after DMM on both lateral and medial sides has however also been previously noted in a study on SCB osteocyte during OA pathology (Jia et al., 2017). In the unoperated group, the lack of any difference in the sclerostin positive SCB osteocytes was quite intriguing and further studies are required to allow for quantification sclerostin positive SCB osteocytes in chronic OA samples.

In conclusion, the results of this Chapter have shown that E11 and sclerostin proteins from dog, cat, horse, sheep, man and mouse can be considered homologous. E11 expression was altered during OA. Specifically, the number of osteocytes expressing E11 was increased in the contralateral knee after DMM in *Fgf-2* KO mice. This may reflect increased loading in the limb due to gait adjustment post-surgery. In canine SCB osteocytes, an increased number of osteocytes positive for E11 suggests a role for this bone inhibitory protein in OA disease progression and this aspect is worthy of further examination.

Chapter 6

Final discussion

6.1 General discussion

The osteocyte is emerging as an important bone cell, with vital roles in regulating skeletal function both mechanically and biochemically (Bonewald, 2011, Plotkin and Bellido, 2016). Recent evidence has confirmed that bone is an endocrine organ regulating phosphate homeostasis (Karsenty and Ferron, 2012, Dallas et al., 2013). This emerging function of bone is also attributed to the osteocyte and its lacuna-canaliculi dendrite network that enables the osteocytes to communicate with itself, osteoblasts, osteoclasts and other body organs, though secreted factors such as sclerostin, RANKL/OPG and FGF-23 (Bonewald, 2011, Compton and Lee, 2014, Guo and Yuan, 2015). The development of this dendrite network is regulated by E11, an early osteocyte marker gene and the focus of this thesis (Zhang et al., 2006, Bonewald, 2008).

Whilst the stability of this dendrite linked lacuna-canaliculi network ensures effective bone homeostasis; its disruption is associated with adverse effects on bone architecture and skeletal health (Dallas et al., 2013, van Dijk et al., 2013, Staines et al., 2017). High bone material quality has been correlated with dense dendrite networks, while the reverse is observed in loose networks (Kerschnitzki et al., 2013). Indeed there are a number of disorders associated with disrupted osteocyte dendrites including; osteoporosis presenting poorly oriented dendrites towards the vasculature with reduced interconnectivity; osteomalacia with an elevated number of dendrites that are hyper-connected; and osteoarthritis in which the dendrites are characterised by decreased number and morphology (Knothe Tate et al., 2004, Bonewald, 2004,

Bonewald, 2008, Jaiprakash et al., 2012). The data gathered in this thesis, will add to the body of knowledge in designing therapies related to dysregulated osteocyte communication networks in pathology.

One of the predisposing factors to fracture is reduced bone quality and structural alteration (Rachner et al., 2011). Recent studies have revealed the relative importance of dendrites as regards to osteocyte viability, as a significant reduction in dendrite number is observed prior to decreases in cell density during ageing (Tiede-Lewis et al., 2017). Moreover, a positive correlation has been established between the absence of dendrite development and bone fragility (Plotkin and Bellido, 2016). Ageing osteoporotic bones are characterised by reduced cortical thickness with enlarged diameter, elevated cortical porosity, and reduced trabecular bone volume to total volume (Kerschnitzki et al., 2013, Tiede-Lewis et al., 2017). This poor quality bone architecture is related to the reduced osteocyte dendritic network, which would reduce the bone's mechanosensing ability and impair its response to loading (Noble et al., 2003, Tatsumi et al., 2007, Adachi et al., 2009, Staines et al., 2017). From the work of this thesis, it can be speculated that the upregulation of E11 expression may reverse the osteocyte dendrite reduction in the ageing population - especially in female osteoporosis patients who are more at risk of bone fractures (Seeman, 2013, Black and Rosen, 2016, Tiede-Lewis et al., 2017). This suggestion builds on the emerging function of osteocyte being the master regulator of bone remodelling and imbalances lead to diseases such as osteoporosis and OA.

The osteocyte is able to regulate bone mineral homeostasis though its expression of FGF-23, a growth factor that has conferred on bone being ascribed the function as an endocrine organ (Teti and Zallone, 2009, Bonewald, 2011, Dallas et al., 2013, Plotkin

and Bellido, 2016). FGF-23 regulates phosphate reabsorption in the kidney tubules (Razzaque, 2009). Another mechanism central to whole body mineral regulation is the phenomenon of perilacunar remodelling, also referred to as osteocytic osteolysis (Bélanger et al., 1967, Teti and Zallone, 2009, Dallas et al., 2013). In this process, the osteocyte expresses known osteoclast makers like TRAP and cathepsin K, and dissolves mineral deposits in its lacuna (Wergedal and Baylink, 1969, Nakano et al., 2004, Qing et al., 2012). This action releases minerals such as calcium into the circulation during lactation that is associated with high calcium demand (Kwiecinski et al., 1987, Qing et al., 2012). What is very remarkable about this mechanism is the ability of the osteocyte to exploit its huge surface area to have access to a large mineral deposit in the bone matrix (Kerschnitzki et al., 2013). Hence, the maintenance of the abundant dendrite network is key in the osteocyte regulation of body mineral balance; and the results from this thesis suggest that increased E11 expression may play a vital role in this.

FGF-2 is one of the many growth factors described to be important for skeletal health where it has mitogenic potential in several types of mesenchymal cells (Rifkin and Moscatelli, 1989). In addition, FGF-2 plays a key role in the differentiation of skeletal cells such as osteoblasts during growth and development (Kyono et al., 2012). Therapeutically, the use of recombinant FGF-2 to manage traumatic bone injuries like fractures has provided a glimmer of hope for its use in other skeletal disorders (Einhorn and Gerstenfeld, 2015). In this thesis, FGF-2 upregulation of *E11* expression and osteocytogenesis is suggestive of a possible physiological application for the

therapeutic use of FGF-2 in disorders of the osteocyte dendritic network previously discussed. This thesis speculatively revealed a strong influence of FGFR1 on FGF-2 induced osteocytogenesis (Chapter 4), despite the published literature indicating a lack of consensus as to which FGFR is the most appropriate receptor to FGF-2 (Yang, 2013). The implication of this is that it may be difficult to identify an appropriate target receptor for therapeutic evaluation in loss or gain of FGFR function with FGF-2 signalling. It may also portend an advantage for using exogenous FGF-2, as more emphasis may be on the downstream signalling pathway to target when evaluating outcomes. This suggested emphasis on the downstream molecules may help circumvent the cautious opinion of some investigators on the potential difficulties of FGF-2 in biological therapeutics due to intricacy in receptor action profiles (Li et al., 2012). However, studies in human OA articular chondrocytes have made convincing arguments for the use of FGFR1 antagonist in designing OA therapeutic drugs. This suggestion was supported by findings that FGFR1 was the most expressed FGFR; and was associated with severe catabolic actions in the human OA articular cartilage when stimulated by both endogenous and exogenous FGF-2 (Yan et al., 2011, Nummenmaa et al., 2015). The discrepancy between my suggestion and the authors' on therapeutic potential for FGFR1 may be related to difference in species, cell types and health status of the cells.

The role of the SCB in the pathophysiology of OA is becoming more widely accepted (Kwan Tat et al., 2010). This may be a reflection of better tools for investigation/detection such as magnetic resonance imaging, microCT, and more

advanced animal models (Kwan Tat et al., 2010, Fang and Beier, 2014). Animal models have enabled the simulation of various human OA phenotypes for detailed investigation including spontaneously occurring, trauma induced, loading induced, and genetic manipulation. In OA pathology, SCB sclerosis is underpinned by dysregulated bone remodelling, potentially due to altered osteocytogenesis. In early OA, excessive remodelling results in a shift towards more bone resorption, however in late OA a switch to increased bone formation is seen, therefore resulting in SCB sclerosis (Bettica et al., 2002, Bouaziz et al., 2015).

Sclerostin, a late osteocyte marker protein and Wnt signalling inhibitor, is down regulated during mechanical loading and OA pathophysiology (Poole et al., 2005, Bezooijen et al., 2005, Robling et al., 2008, Chan et al., 2011, Albisetti et al., 2013, Wu et al., 2016, Zarei et al., 2017). In view of the established role of the Wnt canonical pathway in regulating osteoblast differentiation and bone remodelling (Macsai et al., 2008, Jin et al., 2015), it can be postulated that sclerostin modulation of Wnt signalling pathway in early OA may be a good target in reducing the development of sclerosis associated with late OA. The need for this approach has also been highlighted by other researchers including the possible use of recombinant sclerostin protein (Baker-LePain and Lane, 2012, Wu et al., 2016). This becomes imperative as encouraging results are emerging from the use of sclerostin neutralising antibody in reversing bone loss (Eddleston et al., 2009, Li et al., 2009).

Similarly, this thesis examined the possibility of E11 as a target for the prevention of OA pathology. Currently, the expression of E11 in OA is largely unknown. As a

reduced number of osteocyte dendrites has been observed, it is plausible that the expression of E11 may be decreased (Jaiprakash et al., 2012). This reduction may dampen the bone's response to loading during OA due to the known role of the osteocyte in this physiological process (Zhang et al., 2006). One can therefore speculate on the use of recombinant FGF-2 to induce increased dendrite number, with a possible focal reprogramming to normal osteocytogenesis in early OA. Whilst no differences were observed in E11 expression in the mouse and human samples, E11 was significantly increased in canine OA samples in this thesis (Chapter 5). This therefore highlights the need to extend the study to ascertain if species differences or sample size (human), or methods of OA induction (mouse), and other variables such as stage of disease, inflammatory response, sex, age, and sample anatomic location in the joint may all be contributing to these contrasting observations.

In conclusion, this thesis has identified FGF-2 as a regulator of increased E11 expression and osteocytogenesis speculatively though FGFR1. While the increased expression of E11 upregulated osteocyte dendrite formation was established in this thesis and corroborated by previous workers, the data on FGFR1 speculatively mediating this expression has added to the ongoing debate on the precise FGF-2 receptor. Nevertheless, the upregulation of some downstream molecules like ERK1/2, Akt and p38 MAPK during this process of osteocytogenesis, confers on FGF-2 the ability to play a crucial role in the maintenance of the osteocyte network. However, some questions remain largely unanswered including if a specific downstream molecule like ERK1/2, Akt and p38 MAPK or combination mediates this effect on

increased E11 expression and increased dendrite formation. Also unresolved is the actual nature of E11 expression during OA pathology. The findings of this thesis adds to our body of knowledge on the potential of recombinant FGF-2 as a therapeutic agent targeting osteocyte network related bone disorders such as osteoporosis and osteoarthritis.

6.2 Directions for future research

The results presented in this thesis have identified a role for FGF-2 in regulating osteocytogenesis. They have pinpointed this functional role to be mediated though the expression of E11. However, further work is necessary to fully elucidate the signalling mechanisms underpinning this, and the functional role, which this may play in OA.

Certainly, the investigation of other FGF-2 responsive signalling pathways in osteoblasts would be of great benefit in furthering our understanding of FGF-2 mediated osteocytogenesis. The activation of Runx2 in response to FGF-2 stimulation of MC3T3 osteoblast-like cells is associated with upregulation of the gap junction protein connexion 43 that activates ERK1/2 and PKC δ pathways. PKC signalling, which is also associated with RhoA/ERM, has been seen to regulate cell membrane protrusion and eventual cell motility (Revenu et al., 2004). This makes a case for further studies investigating PKC δ ability to mediate FGF-2 stimulation of E11 expression and osteocytogenesis (Lima et al., 2009, Hebert and Stains, 2013, Capulli et al., 2014). In this thesis, *Fgfr1* had over a 10-fold increase in expression after

stimulation with FGF-2 in comparison with other receptors. Therefore, more studies using specific *Fgfr1* inhibitors will help decipher its relative importance. In addition, primary osteoblasts from *Fgfr1* loss of function mutation could be stimulated with FGF-2 to observe its effect on E11 expression and dendrite formation.

Previous studies have shown that FGF-2 upregulates *Dmp1* though ERK1/2 (Kyono et al., 2012). This may help explain the upregulation of Dmp1 by FGF-2 in this thesis despite E11 knock down using E11 siRNA (Chapter 3), as the two genes are possibly stimulated though the same ERK1/2 pathway (Kyono et al., 2012). In addition, it is possible that residual expression of E11 is enough to drive the up-regulation of other osteocyte markers (Staines et al., 2017). To help establish further the role of E11 in osteoblast to osteocyte transition *in vitro,* the use of gene editing tools like Clustered Regularly Interspersed Palindromic Repeats (CRISPR)/ CRISPR-associated protein-9 nuclease (Cas9), generally referred to as CRISPR/Cas9, may be of immense benefit (Sander and Joung, 2014). Also, it will important to induce OA in E11 conditional knock out (E11 cKO) mice as the results from our study using the hypomorphic conditional deletion of E11 in bone revealed a reduction in osteocyte dendrite volume, length, and response to loading (Staines et al., 2017).

As reported in this thesis, the induction of OA with the use of the DMM model as showed no differences in SCB osteocyte immunolabelling of E11 and sclerostin in *Fgf-2* KO and WT mice. However, the results from E11 immunolabelling showed contrasting results in the WT mice in Chapters 3 & 5; E11 was increased in the WT versus *Fgf-2* KO sham mice in the DMM study, while the naïve mice showed no

difference. This discrepancy may reflect an adjustment to loading on the contralateral knee in the unoperated knee joints. It would therefore be interesting to adopt a loading method in the *Fgf-2* KO mice to examine the effects of *Fgf-2* deletion on the bones response to loading, and loading induced OA. This may then also provide key insights into the role of E11 in these processes.

Reference list

ADACHI, T., AONUMA, Y., TANAKA, M., HOJO, M., TAKANO-YAMAMOTO, T. & KAMIOKA, H. 2009. Calcium response in single osteocytes to locally applied mechanical stimulus: Differences in cell process and cell body. *Journal of Biomechanics,* 42**,** 1989-1995.

ALBISETTI, W., GIARRATANA, L. S., VIGANÒ, C., CASTIGLIONI, S. & MAIER, J. A. 2013. Sclerostin: A Novel Player Regulating Bone Mass in Inflammation? *European Journal of Inflammation,* 11**,** 345-352.

ALESSI, D. R., CUENDA, A., COHEN, P., DUDLEY, D. T. & SALTIEL, A. R. 1995. PD 098059 is a specific inhibitor of the activation of mitogen-activated protein kinase kinase in vitro and in vivo. *Journal of Biological Chemistry,* 270**,** 27489-27494.

ALLAN, L. A., MORRICE, N., BRADY, S., MAGEE, G., PATHAK, S. & CLARKE, P. R. 2003. Inhibition of caspase-9 through phosphorylation at Thr 125 by ERK MAPK. *Nature Cell Biology,* 5**,** 647-654.

ALTSCHUL, S. F., MADDEN, T. L., SCHÄFFER, A. A., ZHANG, J., ZHANG, Z., MILLER, W. & LIPMAN, D. J. 1997. Gapped BLAST and PSI-BLAST: a new generation of protein database search programs. *Nucleic Acids Research,* 25**,** 3389-3402.

ANASTASIADIS, P. Z., MOON, S. Y., THORESON, M. A., MARINER, D. J., CRAWFORD, H. C., ZHENG, Y. & REYNOLDS, A. B. 2000. Inhibition of RhoA by p120 catenin. *Nature Cell Biology,* 2**,** 637-644.

ANDERSON, H. C. 2003. Matrix vesicles and calcification. *Current Rheumatology Reports,* 5**,** 222-226.

ANDERSON, H. C., HSU, H. H., MORRIS, D. C., FEDDE, K. N. & WHYTE, M. P. 1997. Matrix vesicles in osteomalacic hypophosphatasia bone contain apatite-like mineral crystals. *The American Journal of Pathology,* 151**,** 1555-1561.

ANDERSON, H. C., SIPE, J. B., HESSLE, L., DHAMYAMRAJU, R., ATTI, E., CAMACHO, N. P. & LUIS MILLÁN, J. 2004. Impaired Calcification Around Matrix Vesicles of Growth Plate and Bone in Alkaline Phosphatase-Deficient Mice. *The American Journal of Pathology,* 164**,** 841-847.

APPLETON, C. T. G., PITELKA, V., HENRY, J. & BEIER, F. 2007. Global analyses of gene expression in early experimental osteoarthritis. *Arthritis & Rheumatism,* 56**,** 1854-1868.

APPLEYARD, R. C., GHOSH, P. & SWAIN, M. V. 1999. Biomechanical, histological and immunohistological studies of patellar cartilage in an ovine model of osteoarthritis induced by lateral meniscectomy. *Osteoarthritis and Cartilage,* 7**,** 281-294.

ARMELIN, H. A. 1973. Pituitary extracts and steroid hormones in the control of 3T3 cell growth. *Proceedings of the National Academy of Sciences of the United States of America,* 70**,** 2702-2706.

ARRINGTON, A. K., HEINRICH, E. L., LEE, W., DULDULAO, M., PATEL, S., SANCHEZ, J., GARCIA-AGUILAR, J. & KIM, J. 2012. Prognostic and predictive roles of KRAS mutation in colorectal cancer. *International Journal of Molecular Sciences,* 13**,** 12153-12168.

ASHRAF, S., MAPP, P. I. & WALSH, D. A. 2011. Contributions of angiogenesis to inflammation, joint damage, and pain in a rat model of osteoarthritis. *Arthritis & Rheumatology,* 63**,** 2700-2710.

ASTARITA, J. L., ACTON, S. E. & TURLEY, S. J. 2012. Podoplanin: emerging functions in development, the immune system, and cancer. *Frontiers in Immunology,* 3**,** 283.

BAKER-LEPAIN, J. C. & LANE, N. E. 2012. Role of Bone Architecture and Anatomy in Osteoarthritis. *Bone,* 51**,** 197-203.

BAKKER, A. D., SOEJIMA, K., KLEIN-NULEND, J. & BURGER, E. H. 2001. The production of nitric oxide and prostaglandin E2 by primary bone cells is shear stress dependent. *Journal of Biomechanics,* 34**,** 671-677.

BALDARI, S., UBERTINI, V., GARUFI, A., D'ORAZI, G. & BOSSI, G. 2015. Targeting MKK3 as a novel anticancer strategy: molecular mechanisms and therapeutical implications. *Cell Death & Disease,* 6**,** e1621.

BANCROFT, L. W., PETERSON, J. J. & KRANSDORF, M. 2004. Cysts, geodes, and erosions. *Radiologic Clinics of North America,* 42**,** 73-87.

BARON, R. & KNEISSEL, M. 2013. WNT signaling in bone homeostasis and disease: from human mutations to treatments. *Nature Medicine,* 19**,** 179-192.

BEENKEN, A. & MOHAMMADI, M. 2009. The FGF family: biology, pathophysiology and therapy. *Nature Reviews Drug Discovery,* 8**,** 235-253.

BEHR, B., PANETTA, N. J., LONGAKER, M. T. & QUARTO, N. 2010. Different endogenous threshold levels of Fibroblast Growth Factor-ligands determine the healing potential of frontal and parietal bones. *Bone,* 47**,** 281-294.

BÉLANGER, L. F., BÉLANGER, C. & SEMBA, T. 1967. Technical approaches leading to the concept of osteocytic osteolysis. *Clinical Orthopaedics and Related Research,* 54**,** 187-196.

BENITO, M., VEALE, D., FITZGERALD, O., VAN DEN BERG, W. B. & BRESNIHAN, B. 2005. Synovial tissue inflammation in early and late osteoarthritis. *Annals of the Rheumatic Diseases,* 64**,** 1263-1267.

BERTOZZI, C. C., SCHMAIER, A. A., MERICKO, P., HESS, P. R., ZOU, Z., CHEN, M., CHEN, C.-Y., XU, B., LU, M.-M., ZHOU, D., SEBZDA, E., SANTORE, M. T., MERIANOS, D. J., STADTFELD, M., FLAKE, A. W., GRAF, T., SKODA, R., MALTZMAN, J. S., KORETZKY, G. A. & KAHN, M. L. 2010. Platelets regulate lymphatic vascular development through CLEC-2–SLP-76 signaling. *Blood,* 116**,** 661-670.

BETTICA, P., CLINE, G., HART, D. J., MEYER, J. & SPECTOR, T. D. 2002. Evidence for increased bone resorption in patients with progressive knee osteoarthritis: Longitudinal results from the Chingford study. *Arthritis & Rheumatism,* 46**,** 3178-3184.

BEZOOIJEN, R. L. V., DIJKE, P. T., PAPAPOULOS, S. E. & G.M. LÖWIK, C. W. 2005. SOST/sclerostin, an osteocyte-derived negative regulator of bone formation. *Cytokine & Growth Factor Reviews,* 16**,** 319-327.

BHATIA, A., ALBAZZAZ, M., ESPINOZA ORÍAS, A. A., INOUE, N., MILLER, L. M., ACERBO, A., GEORGE, A. & SUMNER, D. R. 2012. Overexpression of DMP1 Accelerates Mineralization and Alters Cortical Bone Biomechanical Properties in Vivo. *Journal of the Mechanical Behavior of Biomedical Materials,* 5**,** 1-8.

BI, W., DENG, J. M., ZHANG, Z., BEHRINGER, R. R. & DE CROMBRUGGHE, B. 1999. Sox9 is required for cartilage formation. *Nature Genetics,* 22**,** 85-89.

BIRKENKAMP, K. U., TUYT, L. M. L., LUMMEN, C., WIERENGA, A. T. J., KRUIJER, W. & VELLENGA, E. 2000. The p38 MAP kinase inhibitor SB203580 enhances nuclear factor-kappa B transcriptional activity by a non-specific effect upon the ERK pathway. *British Journal of Pharmacology,* 131**,** 99-107.

BLACK, D. M. & ROSEN, C. J. 2016. Postmenopausal Osteoporosis. *New England Journal of Medicine,* 374**,** 254-262.

BLANEY DAVIDSON, E. N., VAN DER KRAAN, P. M. & VAN DEN BERG, W. B. 2007. TGF-beta and osteoarthritis. *Osteoarthritis Cartilage,* 15**,** 597-604.

BLOM, A. B., BROCKBANK, S. M., VAN LENT, P. L., VAN BEUNINGEN, H. M., GEURTS, J., TAKAHASHI, N., VAN DER KRAAN, P. M., VAN DE LOO, F. A., SCHREURS, B. W., CLEMENTS, K., NEWHAM, P. & VAN DEN BERG, W. B. 2009. Involvement of the Wnt

signaling pathway in experimental and human osteoarthritis: prominent role of Wnt-induced signaling protein 1. *Arthritis & Rheumatism,* 60**,** 501-512.

BODINE, P. V., ZHAO, W., KHARODE, Y. P., BEX, F. J., LAMBERT, A. J., GOAD, M. B., GAUR, T., STEIN, G. S., LIAN, J. B. & KOMM, B. S. 2004. The Wnt antagonist secreted frizzled-related protein-1 is a negative regulator of trabecular bone formation in adult mice. *Molecular Endocrinology,* 18**,** 1222-1237.

BONEWALD, L. 2006. Osteocytes as multifunctional cells. *Journal of musculoskeletal & neuronal interactions,* 6**,** 331-333.

BONEWALD, L. F. 2004. Osteocyte biology: its implications for osteoporosis. *Journal of Musculoskeletal and Neuronal Interactions,* 4**,** 101-104.

BONEWALD, L. F. 2008. CHAPTER 8 - Osteocytes A2 - MARCUS, ROBERT. *In:* FELDMAN, D., NELSON, D. A. & ROSEN, C. J. (eds.) *Osteoporosis (Third Edition).* San Diego: Academic Press.

BONEWALD, L. F. 2011. The Amazing Osteocyte. *Journal of Bone and Mineral Research,* 26**,** 229-238.

BONEWALD, L. F. & JOHNSON, M. L. 2008. Osteocytes, Mechanosensing and Wnt Signaling. *Bone,* 42**,** 606-615.

BOTTCHER, R. T. & NIEHRS, C. 2005. Fibroblast growth factor signaling during early vertebrate development. *Endocrine Reviews,* 26**,** 63-77.

BOTTER, S. M., GLASSON, S. S., HOPKINS, B., CLOCKAERTS, S., WEINANS, H., VAN LEEUWEN, J. P. & VAN OSCH, G. J. 2009. ADAMTS5-/- mice have less subchondral bone changes after induction of osteoarthritis through surgical instability: implications for a link between cartilage and subchondral bone changes. *Osteoarthritis Cartilage,* 17**,** 636-645.

BOUAZIZ, W., FUNCK-BRENTANO, T., LIN, H., MARTY, C., EA, H. K., HAY, E. & COHEN-SOLAL, M. 2015. Loss of sclerostin promotes osteoarthritis in mice via beta-catenin-dependent and -independent Wnt pathways. *Arthritis Research & Therapy,* 17**,** 24.

BRADBEER, J. N., DUNHAM, J., FISCHER, J. A., NAGANT DE DEUXCHAISNES, C. & LOVERIDGE, N. 1988. The metatarsal cytochemical bioassay of parathyroid hormone: validation, specificity, and application to the study of pseudohypoparathyroidism type I. *Journal of Clinical Endocrinology and Metabolism,* 67**,** 1237-1243.

BRANDI, M. L. 2009. Microarchitecture, the key to bone quality. *Rheumatology,* 48**,** iv3-iv8.

BREITENEDER-GELEFF, S., MATSUI, K., SOLEIMAN, A., MERANER, P., POCZEWSKI, H., KALT, R., SCHAFFNER, G. & KERJASCHKI, D. 1997. Podoplanin, novel 43-kd membrane protein of glomerular epithelial cells, is down-regulated in puromycin nephrosis. *The American Journal of Pathology,* 151**,** 1141-1152.

BRIGHTON, C. T. & ROBERT, M. H. 1986. Histochemical localization of calcium in the fracture callus with potassium pyroantimonate: possible role of chondrocyte mitochondrial calcium in callus calcification. *The Journal of Bone and Joint Surgery,* 68-A**,** 703-715.

BRIGHTON, C. T. & ROBERT, M. H. 1991. "Early histological and ultrastructural changes in medullary fracture callus",. *The Journal of Bone and Joint Surgery,* 73-A**,** 832-847.

BRUNKOW, M. E., GARDNER, J. C., VAN NESS, J., PAEPER, B. W., KOVACEVICH, B. R., PROLL, S., SKONIER, J. E., ZHAO, L., SABO, P. J., FU, Y.-H., ALISCH, R. S., GILLETT, L., COLBERT, T., TACCONI, P., GALAS, D., HAMERSMA, H., BEIGHTON, P. & MULLIGAN, J. T. 2001. Bone Dysplasia Sclerosteosis Results from Loss of the SOST Gene Product, a Novel Cystine Knot–Containing Protein. *American Journal of Human Genetics,* 68**,** 577-589.

BUCKWALTER, J. A. & MARTIN, J. A. 2006. Osteoarthritis. *Advanced Drug Delivery Reviews,* 58**,** 150-167.

BURKE, D., WILKES, D., BLUNDELL, T. L. & MALCOLM, S. 1998. Fibroblast growth factor receptors: lessons from the genes. *Trends in Biochemical Sciences,* 23**,** 59-62.

BURLEIGH, A., CHANALARIS, A., GARDINER, M. D., DRISCOLL, C., BORUC, O., SAKLATVALA, J. & VINCENT, T. L. 2012. Joint immobilization prevents murine osteoarthritis and reveals the highly mechanosensitive nature of protease expression in vivo. *Arthritis & Rheumatism,* 64**,** 2278-2288.

BURR, D. B. 2004. Anatomy and physiology of the mineralized tissues: Role in the pathogenesis of osteoarthrosis. *Osteoarthritis and Cartilage,* 12**,** 20-30.

BURR, D. B. & GALLANT, M. A. 2012. Bone remodelling in osteoarthritis. *Nature Reviews Rheumatology,* 8**,** 665-673.

BURRA, S., NICOLELLA, D. P., FRANCIS, W. L., FREITAS, C. J., MUESCHKE, N. J., POOLE, K. & JIANG, J. X. 2010. Dendritic processes of osteocytes are mechanotransducers that induce the opening of hemichannels. *Proceedings of the National Academy of Sciences of the United States of America,* 107**,** 13648-13653.

CAPULLI, M., PAONE, R. & RUCCI, N. 2014. Osteoblast and osteocyte: games without frontiers. *Archives of Biochemistry and Biophysics,* 561**,** 3-12.

CARRINO, J. A., BLUM, J., PARELLADA, J. A., SCHWEITZER, M. E. & MORRISON, W. B. 2006. MRI of bone marrow edema-like signal in the pathogenesis of subchondral cysts. *Osteoarthritis Cartilage,* 14**,** 1081-1085.

CATTORETTI, G., PILERI, S., PARRAVICINI, C., BECKER, M. H. G., POGGI, S., BIFULCO, C., KEY, G., D'AMATO, L., SABATTINI, E., FEUDALE, E., REYNOLDS, F., GERDES, J. & RILKE, F. 1993. Antigen unmasking on formalin-fixed, paraffin-embedded tissue sections. *The Journal of Pathology,* 171**,** 83-98.

CHAN, B. Y., FULLER, E. S., RUSSELL, A. K., SMITH, S. M., SMITH, M. M., JACKSON, M. T., CAKE, M. A., READ, R. A., BATEMAN, J. F., SAMBROOK, P. N. & LITTLE, C. B. 2011. Increased chondrocyte sclerostin may protect against cartilage degradation in osteoarthritis. *Osteoarthritis Cartilage,* 19**,** 874-885.

CHANG, L. & KARIN, M. 2001. Mammalian MAP kinase signalling cascades. *Nature.,* 410**,** 37-40.

CHAUDHARY, L. R. & HRUSKA, K. A. 2001. The Cell Survival Signal Akt is Differentially Activated by PDGF-BB, EGF, and FGF-2 in Osteoblastic Cells. *Journal of Cellular Biochemistry,* 81**,** 304-311.

CHEN, F., GUO, R., ITOH, S., MORENO, L., ROSENTHAL, E., ZAPPITELLI, T., ZIRNGIBL, R. A., FLENNIKEN, A., COLE, W., GRYNPAS, M., OSBORNE, L. R., VOGEL, W., ADAMSON, L., ROSSANT, J. & AUBIN, J. E. 2014. First Mouse Model for Combined Osteogenesis Imperfecta and Ehlers-Danlos Syndrome. *Journal of Bone and Mineral Research,* 29**,** 1412-1423.

CHEN, J. R., PLOTKIN, L. I., AGUIRRE, J. I., HAN, L., JILKA, R. L., KOUSTENI, S., BELLIDO, T. & MANOLAGAS, S. C. 2005. Transient versus sustained phosphorylation and nuclear accumulation of ERKs underlie anti-versus pro-apoptotic effects of estrogens. *Journal of Biological Chemistry,* 280**,** 4632-4638.

CHIA, S. L., SAWAJI, Y., BURLEIGH, A., MCLEAN, C., INGLIS, J., SAKLATVALA, J. & VINCENT, T. 2009. Fibroblast growth factor 2 is an intrinsic chondroprotective agent that suppresses ADAMTS-5 and delays cartilage degradation in murine osteoarthritis. *Arthritis & Rheumatology,* 60**,** 2019-2027.

CHOI, S. C., KIM, S. J., CHOI, J. H., PARK, C. Y., SHIM, W. J. & LIM, D. S. 2008. Fibroblast growth factor-2 and -4 promote the proliferation of bone marrow mesenchymal stem cells by the activation of the PI3K-Akt and ERK1/2 signaling pathways. *Stem Cells and Development,* 17**,** 725-736.

CHONG, K. W., CHANALARIS, A., BURLEIGH, A., JIN, H., WATT, F. E., SAKLATVALA, J. & VINCENT, T. L. 2013. Fibroblast growth factor 2 drives changes in gene expression following injury to murine cartilage in vitro and in vivo. *Arthritis and Rheumatism,* 65**,** 2346-2355.

CLARKE, B. 2008. Normal Bone Anatomy and Physiology. *Clinical Journal of the American Society of Nephrology,* 3**,** S131-S139.

CLARKE, S. P., MELLOR, D., CLEMENTS, D. N., GEMMILL, T., FARRELL, M., CARMICHAEL, S. & BENNETT, D. 2005. Prevalence of radiographic signs of degenerative joint disease in a hospital population of cats. *Veterinary Record,* 157**,** 793-799.

CLEMENTS, D. N., FITZPATRICK, N., CARTER, S. D. & DAY, P. J. R. 2009. Cartilage gene expression correlates with radiographic severity of canine elbow osteoarthritis. *The Veterinary Journal,* 179**,** 211-218.

COFFIN, J. D., FLORKIEWICZ, R. Z., NEUMANN, J., MORT-HOPKINS, T., DORN, G. W., LIGHTFOOT, P., GERMAN, R., HOWLES, P. N., KIER, A. & O'TOOLE, B. A. 1995. Abnormal bone growth and selective translational regulation in basic fibroblast growth factor (FGF-2) transgenic mice. *Molecular Biology of the Cell,* 6**,** 1861-1873.

COMPTON, J. T. & LEE, F. Y. 2014. A Review of Osteocyte Function and the Emerging Importance of Sclerostin. *The Journal of Bone and Joint Surgery. American Volume,* 96**,** 1659-1668.

COWAN, C. M., QUARTO, N., WARREN, S. M., SALIM, A. & LONGAKER, M. T. 2003. Age-related Changes in the Biomolecular Mechanisms of Clvarial Osteoblast Biology Affect Fibroblast Growth Factor-2 Signaling and Osteogenesis. *Journal of Biological Chemistry,* 278**,** 32005-32013.

CUENDA, A. & ROUSSEAU, S. 2007. p38 MAP-Kinases pathway regulation, function and role in human diseases. *Biochimica et Biophysica Acta (BBA) - Molecular Cell Research,* 1773**,** 1358-1375.

DAILEY, L., AMBROSETTI, D., MANSUKHANI, A. & BASILICO, C. 2005. Mechanisms underlying differential responses to FGF signaling. *Cytokine & Growth Factor Reviews,* 16**,** 233-247.

DALLAS, S. L. & BONEWALD, L. F. 2010. Dynamics of the transition from osteoblast to osteocyte. *Annals of the New York Academy of Sciences,* 1192**,** 437-443.

DALLAS, S. L., PRIDEAUX, M. & BONEWALD, L. F. 2013. The Osteocyte: An Endocrine Cell … and More. *Endocrine Reviews,* 34**,** 658-690.

DE VERNEJOUL, M. C. 1998. Bone Structure and Function. *In: Geusens P. (eds) Osteoporosis in Clinical Practice. Springer, London***,** 1-4.

DEBIAIS, F., LEFEVRE, G., LEMONNIER, J., LE MEE, S., LASMOLES, F., MASCARELLI, F. & MARIE, P. J. 2004. Fibroblast growth factor-2 induces osteoblast survival through a phosphatidylinositol 3-kinase-dependent, -beta-catenin-independent signaling pathway. *Experimental Cell Research,* 297**,** 235-246.

DEBIAIS, F., LEMONNIER, J., HAY, E., DELANNOY, P., CAVERZASIO, J. & MARIE, P. J. 2001. Fibroblast growth factor-2 (FGF-2) increases N-cadherin expression through protein kinase C and Src-kinase pathways in human calvaria osteoblasts. *Journal of Biological Chemistry,* 81**,** 68-81.

DECKER, R. S., KOYAMA, E. & PACIFICI, M. 2014. Genesis and morphogenesis of limb synovial joints and articular cartilage. *Matrix Biology,* 39**,** 5-10.

DOKLADDA, K., GREEN, K. A., PAN, D. A. & HARDIE, D. G. 2005. PD98059 and U0126 activate AMP-activated protein kinase by increasing the cellular AMP:ATP ratio and not via inhibition of the MAP kinase pathway. *FEBS Letters,* 579**,** 236-240.

DUCY, P. 2000. Cbfa1: a molecular switch in osteoblast biology. *Developmental Dynamics,* 219**,** 461-471.

DUCY, P., DESBOIS, C., BOYCE, B., PINERO, G., STORY, B., DUNSTAN, C., SMITH, E., BONADIO, J., GOLDSTEIN, S., GUNDBERG, C., BRADLEY, A. & KARSENTY, G. 1996. Increased bone formation in osteocalcin-deficient mice. *Nature,* 382**,** 448-452.

DUCY, P., ZHANG, R., GEOFFROY, V., RIDALL, A. L. & KARSENTY, G. 1997. Osf2/Cbfa1: A Transcriptional Activator of Osteoblast Differentiation. *Cell,* 89**,** 747-754.

DUDLEY, H. R. & SPIRO, D. 1961. The fine structure of bone cells. *Journal of Biophysical and Biochemical Cytology,* 11**,** 627-649.

EDA, H., AOKI, K., MARUMO, K., FUJII, K. & OHKAWA, K. 2008. FGF-2 signaling induces downregulation of TAZ protein in osteoblastic MC3T3-E1 cells. *Biochemical and Biophysical Research Communications,* 366**,** 471-475.

EDDLESTON, A., MARENZANA, M., MOORE, A. R., STEPHENS, P., MUZYLAK, M., MARSHALL, D. & ROBINSON, M. K. 2009. A Short Treatment With an Antibody to Sclerostin Can Inhibit Bone Loss in an Ongoing Model of Colitis. *Journal of Bone and Mineral Research,* 24**,** 1662-1671.

EIMAR, H., TAMIMI, F., RETROUVEY, J. M., RAUCH, F., AUBIN, J. E. & MCKEE, M. D. 2016. Craniofacial and Dental Defects in the Col1a1Jrt/+ Mouse Model of Osteogenesis Imperfecta. *Journal of Dental Research,* 95**,** 761-768.

EINHORN, T. A. & GERSTENFELD, L. C. 2015. Fracture healing: mechanisms and interventions. *Nature reviews. Rheumatology,* 11**,** 45-54.

EKWALL, A. K., EISLER, T., ANDERBERG, C., JIN, C., KARLSSON, N., BRISSLERT, M. & BOKAREWA, M. I. 2011. The tumour-associated glycoprotein podoplanin is expressed in fibroblast-like synoviocytes of the hyperplastic synovial lining layer in rheumatoid arthritis. *Arthritis Research & Therapy,* 13**,** R40.

ENGLISH, J., PEARSON, G., WILSBACHER, J., SWANTEK, J., KARANDIKAR, M., XU, S. & COBB, M. H. 1999. New insights into the control of MAP kinase pathways. *Experimental Cell Research,* 253**,** 255-270.

ESWARAKUMAR, V. P., MONSONEGO-ORNAN, E., PINES, M., ANTONOPOULOU, I., MORRISS-KAY, G. M. & LONAI, P. 2002. The IIIc alternative of Fgfr2 is a positive regulator of bone formation. *Development.,* 129**,** 3783-3793.

FAKHRY, A., RATISOONTORN, C., VEDHACHALAM, C., SALHAB, I., KOYAMA, E., LEBOY, P., PACIFICI, M., KIRSCHNER, R. E. & NAH, H. D. 2005. Effects of FGF-2/-9 in calvarial bone cell cultures: differentiation stage-dependent mitogenic effect, inverse regulation of BMP-2 and noggin, and enhancement of osteogenic potential. *Bone,* 36**,** 254-266.

FANG, H. & BEIER, F. 2014. Mouse models of osteoarthritis: modelling risk factors and assessing outcomes. *Nature Reviews Rheumatology,* 10**,** 413.

FANG, M. A., GLACKIN, C. A., SADHU, A. & MCDOUGALL, S. 2001. Transcriptional Regulation of Alpha 2(I) Collagen Gene Expression by Fibroblast Growth Factor-2 in MC3T3-E1 Osteoblast-like Cells. *The Journal of Cellular Biochemistry,* 80**,** 550-559.

FARR, A., NELSON, A. & HOSIER, S. 1992. Characterization of an Antigenic Determinant Preferentially Expressed by Type I Epithelial Cells in the Murine Thymus. *The Journal of Histochemistry and Cytochemistry,* 40**,** 651-664.

FAVATA, M. F., HORIUCHI, K. Y., MANOS, E. J., DAULERIO, A. J., STRADLEY, D. A., FEESER, W. S., VAN DYK, D. E., PITTS, W. J., EARL, R. A., HOBBS, F., COPELAND, R. A., MAGOLDA, R. L., SCHERLE, P. A. & TRZASKOS, J. M. 1998. Identification of a novel inhibitor of mitogen-activated protein kinase kinase. *The Journal of Biological Chemistry,* 273**,** 18623-18632.

FEI, Y. & HURLEY, M. M. 2012. Role of fibroblast growth factor 2 and Wnt signaling in anabolic effects of parathyroid hormone on bone formation. *The Journal of Cellular Physiology* 227**,** 3539-3545.

FEI, Y., XIAO, L., DOETSCHMAN, T., COFFIN, D. J. & HURLEY, M. M. 2011. Fibroblast growth factor 2 stimulation of osteoblast differentiation and bone formation is mediated by modulation of the Wnt signaling pathway. *The Journal of Biological Chemistry,* 286**,** 40575-40583.

FELSON, D. T., GALE, D. R., ELON GALE, M., NIU, J., HUNTER, D. J., GOGGINS, J. & LAVALLEY, M. P. 2005. Osteophytes and progression of knee osteoarthritis. *Rheumatology (Oxford),* 44**,** 100-104.

FENG, J. Q., WARD, L. M., LIU, S., LU, Y., XIE, Y., YUAN, B., YU, X., RAUCH, F., DAVIS, S. I., ZHANG, S., RIOS, H., DREZNER, M. K., QUARLES, L. D., BONEWALD, L. F. & WHITE, K. E. 2006. Loss of DMP1 causes rickets and osteomalacia and identifies a role for osteocytes in mineral metabolism. *Nature Genetics,* 38**,** 1310-1315.

FENG, X. 2009. Chemical and Biochemical Basis of Cell-Bone Matrix Interaction in Health and Disease. *Current Chemical Biology,* 3**,** 189-196.

FERNÁNDEZ-MUÑOZ, B., YURRITA, M. M., MARTÍN-VILLAR, E., CARRASCO-RAMÍREZ, P., MEGÍAS, D., RENART, J. & QUINTANILLA, M. 2011. The transmembrane domain of podoplanin is required for its association with lipid rafts and the induction of epithelial-mesenchymal transition. *The International Journal of Biochemistry & Cell Biology,* 43**,** 886-896.

FERREIRO, I., JOAQUIN, M., ISLAM, A., GOMEZ-LOPEZ, G., BARRAGAN, M., LOMBARDÍA, L., DOMÍNGUEZ, O., PISANO, D. G., LOPEZ-BIGAS, N., NEBREDA, A. R. & POSAS, F. 2010. Whole genome analysis of p38 SAPK-mediated gene expression upon stress. *BMC Genomics,* 11**,** 144.

FINDLAY, D. M. 2007. Vascular pathology and osteoarthritis. *Rheumatology (Oxford),* 46**,** 1763-1768.

FINDLAY, D. M. 2013. Long overlooked: the role of subchondral bone in osteoarthritis pathophysiology and pain. *Medicographia,* 35**,** 221-227.

FINDLAY, D. M. & ATKINS, G. J. 2014. Osteoblast-Chondrocyte Interactions in Osteoarthritis. *Current Osteoporosis Reports,* 12**,** 127-134.

FISK, M., GAJENDRAGADKAR, P. R., MÄKI-PETÄJÄ, K. M., WILKINSON, I. B. & CHERIYAN, J. 2014. Therapeutic Potential of p38 MAP Kinase Inhibition in the Management of Cardiovascular Disease. *American Journal of Cardiovascular Drugs,* 14**,** 155-165.

FLETCHER, D. A. & MULLINS, R. D. 2010. Cell mechanics and the cytoskeleton. *Nature,* 463**,** 485-492.

FLORENCIO-SILVA, R., SASSO, G. R., SASSO-CERRI, E., SIMOES, M. J. & CERRI, P. S. 2015. Biology of Bone Tissue: Structure, Function, and Factors That Influence Bone Cells. *BioMed Research International,* 2015**,** 421746.

FORTIER, L. A., BARKER, J. U., STRAUSS, E. J., MCCARREL, T. M. & COLE, B. J. 2011. The Role of Growth Factors in Cartilage Repair. *Clinical Orthopaedics and Related Research,* 469**,** 2706-2715.

FRANZ-ODENDAAL, T. A., HALL, B. K. & WITTEN, P. E. 2006. Buried alive: how osteoblasts become osteocytes. *Developmental dynamics,* 235**,** 176-190.

FUKAZAWA, H., NOGUCHI, K., MURAKAMI, Y. & UEHARA, Y. 2002. Mitogen-activated protein/extracellular signal-regulated kinase kinase (MEK) inhibitors restore anoikis sensitivity in human breast cancer cell lines with a constitutively activated extracellular-regulated kinase (ERK) pathway. *Molecular Cancer Therapeutics,* 1**,** 303-309.

FUNCK-BRENTANO, T. & COHEN-SOLAL, M. 2011. Crosstalk between cartilage and bone: when bone cytokines matter. *Cytokine & Growth Factor Reviews* 22**,** 91-97.

GARUFI, A., PUCCI, D., D'ORAZI, V., CIRONE, M., BOSSI, G., AVANTAGGIATI, M. L. & D'ORAZI, G. 2014. Degradation of mutant p53H175 protein by Zn(II) through autophagy. *Cell Death & Disease,* 5**,** e1271.

GATTINENI, J., BATES, C., TWOMBLEY, K., DWARAKANATH, V., ROBINSON, M. L., GOETZ, R., MOHAMMADI, M. & BAUM, M. 2009. FGF23 decreases renal NaPi-2a and NaPi-2c expression and induces hypophosphatemia in vivo predominantly via FGF receptor 1. *American Journal of Physiology - Renal Physiology,* 297**,** F282-F291.

GAVINE, P. R., MOONEY, L., KILGOUR, E., THOMAS, A. P., AL-KADHIMI, K., BECK, S., ROONEY, C., COLEMAN, T., BAKER, D., MELLOR, M. J., BROOKS, A. N. & KLINOWSKA, T. 2012. AZD4547: an orally bioavailable, potent, and selective inhibitor of the fibroblast growth factor receptor tyrosine kinase family. *Cancer Research,* 72**,** 2045-2056.

GENETOS, D. C., YELLOWLEY, C. E. & LOOTS, G. G. 2011. Prostaglandin E2 signals through PTGER2 to regulate sclerostin expression. *PLoS One,* 6**,** e17772.

GILBERT, S. F. 2006. Developmental Biology. *Sinauer Associates Inc: Massachusetts.,* 8th Edition**,** in: ISBN 0-87893-87250-X.

GIVOL, D. & YAYON, A. 1992. Complexity of FGF receptors: genetic basis for structural diversity and functional specificity. *The FASEB Journal* 6**,** 3362-3369.

GOLDRING, M. B. 2012. Chondrogenesis, chondrocyte differentiation, and articular cartilage metabolism in health and osteoarthritis. *Therapeutic Advances in Musculoskeletal Disease,* 4**,** 269-285.

GOLDRING, M. B. & GOLDRING, S. R. 2010. Articular cartilage and subchondral bone in the pathogenesis of osteoarthritis. *The Annals of the New York Academy of Sciences,* 1192**,** 230–237.

GOSPODAROWICZ, D. 1975. Purification of a fibroblast growth factor from bovine pituitary. *The Journal of Biological Chemistry,* 250**,** 2515-2520.

GOSPODAROWICZ, D., BIALECKI, H. & GREENBURG, G. 1978. Purification of the fibroblast growth factor activity from bovine brain. *Journal of Biological Chemistry,* 253**,** 3736-3743.

GOSPODAROWICZ, D., JONES, K. L. & SATO, G. 1974. Purification of a growth factor for ovarian cells from bovine pituitary glands. *Proceedings of the National Academy of Sciences of the United States of America,* 71**,** 2295-2299.

GOTINK, K. J. & VERHEUL, H. M. W. 2010. Anti-angiogenic tyrosine kinase inhibitors: what is their mechanism of action? *Angiogenesis,* 13**,** 1-14.

GREGORY, M. H., CAPITO, N., KUROKI, K., STOKER, A. M., COOK, J. L. & SHERMAN, S. L. 2012. A review of translational animal models for knee osteoarthritis. *Arthritis,* 2012**,** 764621.

GUO, D., KEIGHTLEY, A., GUTHRIE, J., VENO, P. A., HARRIS, S. E. & BONEWALD, L. F. 2010. Identification of osteocyte-selective proteins. *Proteomics,* 10**,** 3688-3698.

GUO, Y.-C. & YUAN, Q. 2015. Fibroblast growth factor 23 and bone mineralisation. *International Journal of Oral Science,* 7**,** 8-13.

GUPTA, R. R., YOO, D. J., HEBERT, C., NIGER, C. & STAINS, J. P. 2010. Induction of an osteocyte-like phenotype by fibroblast growth factor-2. *Biochemical and Biophysical Research Communications,* 402**,** 258-264.

HADJIARGYROU, M., RIGHTMIRE, E. P., ANDO, T. & LOMBARDO, F. T. 2001. The E11 osteoblastic lineage marker is differentially expressed during fracture healing. *Bone,* 29**,** 149-154.

HAN, Y., COWIN, S. C., SCHAFFLER, M. B. & WEINBAUM, S. 2004. Mechanotransduction and strain amplification in osteocyte cell processes. *Proceedings of the National Academy of Sciences of the United States of America,* 101**,** 16689-16694.

HATTORI, Y., ODAGIRI, H., KATOH, O., SAKAMOTO, H., MORITA, T., SHIMOTOHNO, K., TOBINAI, K., SUGIMURA, T. & TERADA, M. 1992. K-sam-related gene, N-sam, encodes fibroblast growth factor receptor and is expressed in T-lymphocytic tumors. *Cancer Research* 52**,** 3367-3371.

HEBERT, C. & STAINS, J. P. 2013. An Intact Connexin43 is Required to Enhance Signaling and Gene Expression in Osteoblast-like Cells. *Journal of cellular biochemistry,* 114**,** 2542-2550.

HENRIKSON, R. C., KAYE, G. I. & MAZURKIEWICZ, J. E. 1997. OSTEOGENESIS: INTRAMEMBRANOUS OSSIFICATION. *The National Medical Series for Independent study-Histology . Lippincott Williams & Wilkins. London,* 518**,** 132.

HIBI, M., LIN, A., SMEAL, T., MINDEN, A. & KARIN, M. 1993. Identification of an oncoprotein- and UV-responsive protein kinase that binds and potentiates the c-Jun activation domain. *Genes & Development* 7**,** 2135-2148.

HIRAO, M., SATO, N., KONDO, T., YONEMURA, S., MONDEN, M., SASAKI, T., TAKAI, Y., TSUKITA, S. & TSUKITA, S. 1996. Regulation Mechanism of ERM (Ezrin/Radixin/Moesin) Protein/Plasma Membrane Association: Possible Involvement of Phosphatidylinositol Turnover and Rho-dependent Signaling Pathway. *Journal of Cell Biology,* 135**,** 37-51.

HOLMBECK, K., BIANCO, P., PIDOUX, I., INOUE, R., BILLINGHURST, R. C., WU, W., CHRYSOVERGIS, K., YAMADA, S., BIRKEDAL-HANSEN, H. & POOLE, A. R. 2005. The metalloproteinase MT1-MMP is required for normal development and maintenance of osteocyte processes in bone. *Journal of Cell Science,* 118**,** 147-156.

HONG, B., LI, H., ZHANG, M., XU, J., LU, Y., ZHENG, Y., QIAN, J., CHANG, J. T., YANG, J. & YI, Q. 2015. p38 MAPK inhibits breast cancer metastasis through regulation of stromal expansion. *International Journal of Cancer,* 136**,** 34-43.

HORTON, W. A. 1990. The biology of bone growth. *Growth Genetics and Hormones,* 6**,** 1-3.

HOTOKEZAKA, H., SAKAI, E., KANAOKA, K., SAITO, K., MATSUO, K., KITAURA, H., YOSHIDA, N. & NAKAYAMA, K. 2002. U0126 and PD98059, specific inhibitors of MEK, accelerate differentiation of RAW264.7 cells into osteoclast-like cells. *Journal of Biological Chemistry,* 277**,** 47366-47372.

HOUSTON, B., PATON, I. R., BURT, D. W. & FARQUHARSON, C. 2002. Chromosomal localization of the chicken and mammalian orthologues of the orphan phosphatase PHOSPHO1 gene. *Animal Genetics,* 33**,** 451-454.

HOUSTON, D. A., MYERS, K., MACRAE, V. E., STAINES, K. A. & FARQUHARSON, C. 2016. The Expression of PHOSPHO1, nSMase2 and TNAP is Coordinately Regulated by Continuous PTH Exposure in Mineralising Osteoblast Cultures. *Calcified Tissue International,* 99**,** 510-524.

HOYLAND, J. A., THOMAS, J. T., DONN, R., MARRIOTT, A., AYAD, S., BOOT-HANDFORD, R. P., GRANT, M. E. & FREEMONT, A. J. 1991. Distribution of type X collagen mRNA in normal and osteoarthritic human cartilage. *Bone and Mineral.,* 15**,** 151-164.

HU, Y., CHAN, E., WANG, S. X. & LI, B. 2003. Activation of p38 mitogen-activated protein kinase is required for osteoblast differentiation. *Endocrinology,* 144**,** 2068-2074.

HUESA, C., HOUSTON, D., KIFFER-MOREIRA, T., YADAV, M. M., MILLAN, J. L. & FARQUHARSON, C. 2015. The Functional co-operativity of Tissue-Nonspecific Alkaline Phosphatase (TNAP) and PHOSPHO1 during initiation of Skeletal Mineralization. *Biochemistry and Biophysics Reports,* 4**,** 196-201.

HÜGLE, T. & GEURTS, J. 2017. What drives osteoarthritis?—synovial versus subchondral bone pathology. *Rheumatology,* 56**,** 1461-1471.

HURLEY, M. M., MARIE, P. J. & FLORKIEWICZ, R. Z. 2002. Fibroblast growth factor and fibroblast growth factor receptor families. *:in Principles of Bone Biology (Bilezikian J. P., Raisz L. G., Rodan G. A., eds) Academic Press, Inc., San Diego, CA***,** 825-851.

IM, G.-I. & KIM, M.-K. 2014. The relationship between osteoarthritis and osteoporosis. *Journal of Bone and Mineral Metabolism,* 32**,** 101-109.

IMAI, K., ; & TAKAOKA, A. 2006. Comparing antibody and small-molecule therapies for cancer. *Nature Reviews Cancer,* 6**,** 714-724.

INGLIS, J. J., MCNAMEE, K. E., CHIA, S. L., ESSEX, D., FELDMANN, M., WILLIAMS, R. O., HUNT, S. P. & VINCENT, T. 2008. Regulation of pain sensitivity in experimental osteoarthritis by the endogenous peripheral opioid system. *Arthritis & Rheumatism,* 58**,** 3110-3119.

ISEKI, S., WILKIE, A. O. & MORRISS-KAY, G. M. 1999. Fgfr1 and Fgfr2 have distinct differentiation- and proliferation-related roles in the developing mouse skull vault. *Development,* 126**,** 5611.

ISHIDA, S., YAMANE, S., NAKANO, S., YANAGIMOTO, T., HANAMOTO, Y., MAEDA-TANIMURA, M., TOYOSAKI-MAEDA, T., ISHIZAKI, J., MATSUO, Y., FUKUI, N., ITOH, T., OCHI, T. & SUZUKI, R. 2009. The interaction of monocytes with rheumatoid synovial cells is a key step in LIGHT-mediated inflammatory bone destruction. *Immunology,* 128**,** e315-e324.

ITOH, N. & ORNITZ, D. M. 2004. Evolution of the Fgf and Fgfr gene families. *Trends in Genetics,* 20**,** 563-569.

JACKSON, R. A., NURCOMBE, V. & COOL, S. M. 2006. Coordinated fibroblast growth factor and heparan sulfate regulation of osteogenesis. *Gene,* 379**,** 79-91.

JACOB, A. L., SMITH, C., PARTANEN, J. & ORNITZ, D. M. 2006. Fibroblast growth factor receptor 1 signaling in the osteo-chondrogenic cell lineage regulates sequential steps of osteoblast maturation. *Developmental Biology,* 296**,** 315-328.

JAIPRAKASH, A., PRASADAM, I., FENG, J. Q., LIU, Y., CRAWFORD, R. & XIAO, Y. 2012. Phenotypic characterization of osteoarthritic osteocytes from the sclerotic zones: a possible pathological role in subchondral bone sclerosis. *International Journal of Biological Sciences,* 8**,** 406-417.

JARNICKI, A. G., CONROY, H., BRERETON, C., DONNELLY, G., TOOMEY, D., WALSH, K., SWEENEY, C., LEAVY, O., FLETCHER, J., LAVELLE, E. C., DUNNE, P. & MILLS, K. H. G. 2008. Attenuating Regulatory T Cell Induction by TLR Agonists through Inhibition of p38 MAPK Signaling in Dendritic Cells Enhances Their Efficacy as Vaccine Adjuvants and Cancer Immunotherapeutics. *The Journal of Immunology,* 180**,** 3797-3806.

JEON, S., PARK, J.-K., BAE, C.-D. & PARK, J. 2010. NGF-induced moesin phosphorylation is mediated by the PI3K, Rac1 and Akt and required for neurite formation in PC12 cells. *Neurochemistry International,* 56**,** 810-818.

JIA, H., MA, X., WEI, Y., TONG, W., TOWER, R. J., CHANDRA, A., WANG, L., SUN, Z., YANG, Z., BADAR, F., ZHANG, K., TSENG, W. J., KRAMER, I., KNEISSEL, M., XIA, Y., LIU, X. S., WANG, J. H., HAN, L., ENOMOTO-IWAMOTO, M. & QIN, L. 2017. Subchondral bone plate sclerosis during late osteoarthritis is caused by loading-induced reduction in Sclerostin. *Arthritis & Rheumatology***,** doi: 10.1002/art.40351.

JIANG, Z., VON DEN HOFF, J. W., TORENSMA, R., MENG, L. & BIAN, Z. 2014. Wnt16 is involved in intramembranous ossification and suppresses osteoblast differentiation through the Wnt/beta-catenin pathway. *Journal of Cellular Physiology,* 229**,** 384-392.

JIN, H., WANG, B., LI, J., XIE, W., MAO, Q., LI, S., DONG, F., SUN, Y., KE, H. Z., BABIJ, P., TONG, P. & CHEN, D. 2015. Anti-DKK1 antibody promotes bone fracture healing through activation of beta-catenin signaling. *Bone,* 71**,** 63-75.

JOHNSON, C. I., ARGYLE, D. J. & CLEMENTS, D. N. 2016. In vitro models for the study of osteoarthritis. *The Veterinary Journal,* 209**,** 40-49.

KAMEKURA, S., HOSHI, K., SHIMOAKA, T., CHUNG, U., CHIKUDA, H., YAMADA, T., UCHIDA, M., OGATA, N., SEICHI, A., NAKAMURA, K. & KAWAGUCHI, H. 2005. Osteoarthritis development in novel experimental mouse models induced by knee joint instability. *Osteoarthritis Cartilage,* 13**,** 632-641.

KAN, M., WU, X., WANG, F. & MCKEEHAN, W. L. 1999. Specificity for fibroblast growth factors determined by heparan sulfate in a binary complex with the receptor kinase. *Journal of Biological Chemistry,* 274**,** 15947-15952.

KANCZLER, J. M. & OREFFO, R. O. C. 2008. Osteogenesis and angiogenesis: The potential for engineering bone. *European Cells and Materials,* 15**,** 100-114.

KANEKO, M. K., HONMA, R., OGASAWARA, S., FUJII, Y., NAKAMURA, T., SAIDOH, N., TAKAGI, M., KAGAWA, Y., KONNAI, S. & KATO, Y. 2016. PMab-38 Recognizes Canine Podoplanin of Squamous Cell Carcinomas. *Monoclonal Antibodies in Immunodiagnosis and Immunotherapy,* 35**,** 263-266.

KANEKO, M. K., KATO, Y., KITANO, T. & OSAWA, M. 2006. Conservation of a platelet activating domain of Aggrus/podoplanin as a platelet aggregation-inducing factor. *Gene. ,* 378**,** 52-57.

KANNUS, P. & RVINEN, M. J. 1989. Posttraumatic anterior cruciate ligament insufficiency as a cause of osteoarthritis in a knee joint. *Clinical rheumatology,* 8**,** 251-260.

KARSENTY, G. & FERRON, M. 2012. The contribution of bone to whole-organism physiology. *Nature,* 481**,** 314-320.

KATO, Y., KANEKO, M., SATA, M., FUJITA, N., TSURUO, T. & OSAWA, M. 2005. Enhanced Expression of Aggrus (T1alpha/Podoplanin), a Platelet-Aggregation-Inducing Factor in Lung Squamous Cell Carcinoma. *Tumor Biology,* 26**,** 195-200.

KATOH, M. 2016. FGFR inhibitors: Effects on cancer cells, tumor microenvironment and whole-body homeostasis (Review). *International Journal of Molecular Medicine,* 38**,** 3-15.

KAWANO, Y. & KYPTA, R. 2003. Secreted antagonists of the Wnt signalling pathway. *Journal of Cell Science,* 116**,** 2672-2634.

KAWCAK, C. E. 2016. 2 - Biomechanics in Joints. *Joint Disease in the Horse (Second Edition).* Edinburgh: W.B. Saunders.

KAWCAK, C. E., MCILWRAITH, C. W., NORRDIN, R. W., PARK, R. D. & JAMES, S. P. 2001. The role of subchondral bone in joint disease: a review. *Equine Veterinary Journal* 33**,** 120-126.

KERSCHNITZKI, M., KOLLMANNSBERGER, P., BURGHAMMER, M., DUDA, G. N., WEINKAMER, R., WAGERMAIER, W. & FRATZL, P. 2013. Architecture of the osteocyte network correlates with bone material quality. *Journal of Bone and Mineral Research,* 28**,** 1837-1845.

KEVIN, M. P. & STUART, J. D. 1997. Cell cycle arrest mediated by the MEKymitogen-activated protein kinase pathway. *Proceedings of the National Academy of Sciences of the United States of America,* 94**,** 448-452.

KEVORKIAN, L., YOUNG, D. A., DARRAH, C., DONELL, S. T., SHEPSTONE, L., PORTER, S., BROCKBANK, S. M. V., EDWARDS, D. R., PARKER, A. E. & CLARK, I. M. 2004. Expression profiling of metalloproteinases and their inhibitors in cartilage. *Arthritis & Rheumatism,* 50**,** 131-141.

KIM, H. J., KIM, J. H., BAE, S. C., CHOI, J. Y. & RYOO, H. M. 2003. The protein kinase C pathway plays a central role in the fibroblast growth factor-stimulated expression and transactivation activity of Runx2. *The Journal of Biological Chemistry,* 278**,** 319-326.

KNOTHE TATE, M. L., ADAMSON, J. R., TAMI, A. E. & BAUER, T. W. 2004. The osteocyte. *The International Journal of Biochemistry & Cell Biology,* 36**,** 1-8.

KONG, Y. Y., YOSHIDA, H., SAROSI, I., TAN, H. L., TIMMS, E., CAPPARELLI, C., MORONY, S., OLIVEIRA-DOS-SANTOS, A. J., VAN, G., ITIE, A., KHOO, W., WAKEHAM, A., DUNSTAN, C. R., LACEY, D. L., MAK, T. W., BOYLE, W. J. & PENNINGER, J. M. 1999. OPGL is a key regulator of osteoclastogenesis, lymphocyte development and lymph-node organogenesis. *Nature,* 397**,** 315-323.

KWAN TAT, S., LAJEUNESSE, D., PELLETIER, J.-P. & MARTEL-PELLETIER, J. 2010. Targeting subchondral bone for treating osteoarthritis: what is the evidence? *Best Practice & Research Clinical Rheumatology,* 24**,** 51-70.

KWIECINSKI, G. G., KROOK, L. & WIMSATT, W. A. 1987. Annual skeletal changes in the little brown bat, Myotis lucifugus lucifugus, with particular reference to pregnancy and lactation. *American Journal of Anatomy,* 178**,** 410-420.

KYONO, A., AVISHAI, N., OUYANG, Z., LANDRETH, G. E. & MURAKAMI, S. 2012. FGF and ERK signaling coordinately regulate mineralization-related genes and play essential roles in osteocyte differentiation. *Journal of Bone and Mineral Metabolism,* 30**,** 19-30.

KYRIAKIS, J. M. & AVRUCH, J. 2001. Mammalian Mitogen-Activated Protein Kinase Signal Transduction Pathways Activated by Stress and Inflammation. *Physiological Reviews,* 81**,** 807-869.

LAI, C. F., CHAUDHARY, L., FAUSTO, A., HALSTEAD, L. R., ORY, D. S., AVIOLI, L. V. & CHENG, S. L. 2001. Erk is essential for growth, differentiation, integrin expression, and cell function in human osteoblastic cells. *The Journal of Biological Chemistry,* 276**,** 14443-14450.

LAI, W. T., KRISHNAPPA, V. & PHINNEY, D. G. 2011. Fibroblast growth factor 2 (Fgf2) inhibits differentiation of mesenchymal stem cells by inducing Twist2 and Spry4, blocking extracellular regulated kinase activation, and altering Fgf receptor expression levels. *Stem Cells,* 29**,** 1102-1111.

LAJEUNESSE, D. 2002. Altered subchondral osteoblast cellular metabolism in osteoarthritis: cytokines, eicosanoids, and growth factors. *Journal of musculoskeletal & neuronal interactions,* 2**,** 251-260.

LALI, F. V., HUNT, A. E., TURNER, S. J. & FOXWELL, B. M. J. 2000. The Pyridinyl Imidazole Inhibitor SB203580 Blocks Phosphoinositide-dependent Protein Kinase Activity, Protein Kinase B Phosphorylation, and Retinoblastoma Hyperphosphorylation in Interleukin-2-stimulated T Cells Independently of p38 Mitogen-activated Protein Kinase. *Journal of Biological Chemistry,* 275**,** 7395-7402.

LAMOUILLE, S., XU, J. & DERYNCK, R. 2014. Molecular mechanisms of epithelial-mesenchymal transition. *Nature Reviews Molecular Cell Biology,* 15**,** 178-196.

LARSSON, T., MARSELL, R., SCHIPANI, E., OHLSSON, C., LJUNGGREN, O., TENENHOUSE, H. S., JUPPNER, H. & JONSSON, K. B. 2004. Transgenic mice expressing fibroblast growth factor 23 under the control of the alpha1(I) collagen promoter exhibit growth retardation, osteomalacia, and disturbed phosphate homeostasis. *Endocrinology,* 145**,** 3087-3094.

LEE, S. E., WOO, K. M., KIM, S. Y., KIM, H. M., KWACK, K., LEE, Z. H. & KIM, H. H. 2002. The phosphatidylinositol 3-kinase, p38, and extracellular signal-regulated kinase pathways are involved in osteoclast differentiation. *Bone.,* 30**,** 71-77.

LEYDET-QUILICI, H., LE CORROLLER, T., BOUVIER, C., GIORGI, R., ARGENSON, J. N., CHAMPSAUR, P., PHAM, T., DE PAULA, A. M. & LAFFORGUE, P. 2010. Advanced hip osteoarthritis: magnetic resonance imaging aspects and histopathology correlations. *Osteoarthritis Cartilage,* 18**,** 1429-1435.

LI, G., YIN J, GAO, J., CHENG, T. S., PAVLOS, N. J., ZHANG, C. & ZHENG, M. H. 2013. Subchondral bone in osteoarthritis: insight into risk factors and microstructural changes. *Arthritis Research & Therapy,* 15**,** 223.

LI, J., LIU, D., KE, H. Z., DUNCAN, R. L. & TURNER, C. H. 2005a. The P2X7 Nucleotide Receptor Mediates Skeletal Mechanotransduction. *Journal of Biological Chemistry,* 280**,** 42952-42959.

LI, X., AN, H. S., ELLMAN, M., PHILLIPS, F., THONAR, E. J., PARK, D. K., UDAYAKUMAR, R. K. & IM, H. J. 2008a. Action of fibroblast growth factor-2 on the intervertebral disc. *Arthritis Research & Therapy,* 10**,** R48.

LI, X., ELLMAN, M. B., KROIN, J. S., CHEN, D., YAN, D., MIKECZ, K., RANJAN, K. C., XIAO, G., STEIN, G. S., KIM, S.-G., COLE, B., VAN WIJNEN, A. J. & IM, H.-J. 2012. Species-Specific Biological Effects of FGF-2 in Articular Cartilage: Implication for distinct roles within the FGF receptor family. *Journal of Cellular Biochemistry,* 113**,** 2532-2542.

LI, X., OMINSKY, M. S., NIU, Q. T., SUN, N., DAUGHERTY, B., D'AGOSTIN, D., KURAHARA, C., GAO, Y., CAO, J., GONG, J., ASUNCION, F., BARRERO, M., WARMINGTON, K., DWYER, D., STOLINA, M., MORONY, S., SAROSI, I., KOSTENUIK, P. J., LACEY, D. L., SIMONET, W. S., KE, H. Z. & PASZTY, C. 2008b. Targeted Deletion of the Sclerostin Gene in Mice Results in Increased Bone Formation and Bone Strength. *Journal of Bone and Mineral Research,* 23**,** 860-869.

LI, X., OMINSKY, M. S., WARMINGTON, K. S., MORONY, S., GONG, J., CAO, J., GAO, Y., SHALHOUB, V., TIPTON, B., HALDANKAR, R., CHEN, Q., WINTERS, A., BOONE, T., GENG, Z., NIU, Q.-T., KE, H. Z., KOSTENUIK, P. J., SIMONET, W. S., LACEY, D. L. & PASZTY, C. 2009. Sclerostin Antibody Treatment Increases Bone Formation, Bone Mass, and Bone Strength in a Rat Model of Postmenopausal Osteoporosis. *Journal of Bone and Mineral Research,* 24**,** 578-588.

LI, X., ZHANG, Y., KANG, H., LIU, W., LIU, P., ZHANG, J., HARRIS, S. E. & WU, D. 2005b. Sclerostin binds to LRP5/6 and antagonizes canonical Wnt signaling. *Journal of Biological Chemistry,* 280**,** 19883-19887.

LIMA, F., NIGER, C., HEBERT, C. & STAINS, J. P. 2009. Connexin43 potentiates osteoblast responsiveness to fibroblast growth factor 2 via a protein kinase C-delta/Runx2-dependent mechanism. *Molecular Biology of the Cell,* 20**,** 2697-2708.

LIN, H. Y., XU, J., ORNITZ, D., M.;, HALEGOUA, S. & HAYMAN, M. J. 1996. The fibroblast growth factor receptor-1 is necessary for the induction of neurite outgrowth in PC12 cells by aFGF. *Journal of Neuroscience,* 16**,** 4579-4587.

LITTLE, C. B., BARAI, A., BURKHARDT, D., SMITH, S. M., FOSANG, A. J., WERB, Z., SHAH, M. & THOMPSON, E. W. 2009. Matrix metalloproteinase-13 deficient mice are resistant to osteoarthritic cartilage erosion but not chondrocyte hypertrophy or osteophyte development. *Arthritis and Rheumatism,* 60**,** 3723-3733.

LIU, C., MILLER, H., HUI, K. L., GROOMAN, B., BOLLAND, S., UPADHYAYA, A. & SONG, W. 2011. A balance of Bruton's tyrosine kinase and SHIP activation regulates B cell receptor cluster formation by controlling actin remodeling. *Journal of Immunology,* 187**,** 230-239.

LIU, J., MINEMOTO, Y. & LIN, A. 2004. c-Jun N-terminal protein kinase 1 (JNK1), but not JNK2, is essential for tumor necrosis factor alpha-induced c-Jun kinase activation and apoptosis. *Molecular and Cellular Biology,* 24**,** 10844-10856.

LIU, S., TANG, W., ZHOU, J., VIERTHALER, L. & QUARLES, L. D. 2007. Distinct roles for intrinsic osteocyte abnormalities and systemic factors in regulation of FGF23 and bone mineralization in Hyp mice. *American Journal of Physiology - Endocrinology And Metabolism,* 293**,** E1636-E1644.

LIVAK, K. J. & SCHMITTGEN, T. D. 2001. Analysis of relative gene expression data using real-time quantitative PCR and the 2(-Delta Delta C(T)) Method. *Methods,* 25**,** 402-408.

LOESER, R. F., OLEX, A., MCNULTY, M. A., CARLSON, C. S., CALLAHAN, M., FERGUSON, C., CHOU, J., LENG, X. & FETROW, J. S. 2012. Microarray Analysis Reveals Age-related Differences in Gene Expression During the Development of Osteoarthritis in Mice. *Arthritis and Rheumatism,* 64**,** 705-717.

LOESER, R. F., OLEX, A. L., MCNULTY, M. A., CARLSON, C. S., CALLAHAN, M., FERGUSON, C. & FETROW, J. S. 2013. Disease Progression and Phasic Changes in Gene Expression in a Mouse Model of Osteoarthritis. *PLoS ONE,* 8**,** e54633.

LOGAR, D. B., KOMADINA, R., PREZELJ, J., OSTANEK, B., TROST, Z. & MARC, J. 2007. Expression of bone resorption genes in osteoarthritis and in osteoporosis. *Journal of Bone and Mineral Metabolism,* 25**,** 219-225.

LORENZ, H. & RICHTER, W. 2006. Osteoarthritis: cellular and molecular changes in degenerating cartilage. *Progress in Histochemistry and Cytochemistry,* 40**,** 135-163.

LORENZO, P., BAYLISS, M. T. & HEINEGARD, D. 2004. Altered patterns and synthesis of extracellular matrix macromolecules in early osteoarthritis. *Matrix Biology,* 23**,** 381-391.

LOWRY, O. H., ROSEBROUGH, N. J., FARR, A. L. & RANDALL, R. J. 1951. Protein measurement with the folin phenol reagent. *Journal of Biological Chemistry,* 193**,** 265-275.

LU, Y., YUAN, B., QIN, C., CAO, Z., XIE, Y., DALLAS, S. L., MCKEE, M. D., DREZNER, M. K., BONEWALD, L. F. & FENG, J. Q. 2011. The Biological Function of DMP-1 in Osteocyte Maturation Is Mediated by Its 57-kDa C-terminal Fragment. *Journal of Bone and Mineral Research,* 26**,** 331-340.

MACDONALD, B. T., TAMAI, K. & HE, X. 2009. Wnt/beta-catenin signaling: components, mechanisms, and diseases. *Developmental Cell,* 17**,** 9-26.

MACKIE, E. J., TATARCZUCH, L. & MIRAMS, M. 2011. The skeleton: a multi-functional complex organ: the growth plate chondrocyte and endochondral ossification. *Journal of Endocrinology,* 211**,** 109-121.

MACRAE, V. E., AHMED, S. F., MUSHTAQ, T. & FARQUHARSON, C. 2007. IGF-I signalling in bone growth: inhibitory actions of dexamethasone and IL-1beta. *Growth Hormone & IGF Research,* 17**,** 435-439.

MACSAI, C. E., FOSTER, B. K. & XIAN, C. J. 2008. Roles of Wnt signalling in bone growth, remodelling, skeletal disorders and fracture repair. *Journal of Cellular Physiology,* 215**,** 578-587.

MAHMOOD, T. & YANG, P. C. 2012. Western blot: technique, theory, and trouble shooting. *North American Journal of Medical Sciences,* 4**,** 429-434.

MALFAIT, A. M., RITCHIE, J., GIL, A. S., AUSTIN, J. S., HARTKE, J., QIN, W., TORTORELLA, M. D. & MOGIL, J. S. 2010. ADAMTS-5 deficient mice do not develop mechanical allodynia associated with osteoarthritis following medial meniscal destabilization. *Osteoarthritis Cartilage,* 18**,** 572-580.

MALONE, A. M. D., ANDERSON, C. T., TUMMALA, P., KWON, R. Y., JOHNSTON, T. R., STEARNS, T. & JACOBS, C. R. 2007. Primary cilia mediate mechanosensing in bone cells by a calcium-independent mechanism. *Proceedings of the National Academy of Sciences of the United States of America,* 104**,** 13325-13330.

MANCILLA, E. E., DE LUCA, F., UYEDA, J. A., CZERWIEC, F. S. & BARON, J. 1998. Effects of Fibroblast Growth Factor-2 on Longitudinal Bone Growth. *Endocrinology,* 139**,** 2900-2904.

MANEIX, L., BEAUCHEF, G., SERVENT, A., WEGROWSKI, Y., MAQUART, F. X., BOUJRAD, N., FLOURIOT, G., PUJOL, J. P., BOUMEDIENE, K., GALERA, P. & MOSLEMI, S. 2008. 17Beta-oestradiol up-regulates the expression of a functional UDP-glucose dehydrogenase in articular chondrocytes: comparison with effects of cytokines and growth factors. *Rheumatology (Oxford),* 47**,** 281-288.

MANOLAGAS, S. C. 2000. Birth and death of bone cells: basic regulatory mechanisms and implications for the pathogenesis and treatment of osteoporosis. *Endocrine Reviews,* 21**,** 115-137.

MAREK, L., WARE, K. E., FRITZSCHE, A., HERCULE, P., HELTON, W. R., SMITH, J. E., MCDERMOTT, L. A., COLDREN, C. D., NEMENOFF, R. A., MERRICK, D. T., HELFRICH, B. A., BUNN, P. A., JR. & HEASLEY, L. E. 2009. Fibroblast growth factor (FGF) and FGF receptor-mediated autocrine signaling in non-small-cell lung cancer cells. *Molecular Pharmacology,* 75**,** 196-207.

MARIE, P. J. 2003. Fibroblast growth factor signaling controlling osteoblast differentiation. *Gene,* 316**,** 23-32.

MARIE, P. J. 2012. Fibroblast growth factor signaling controlling bone formation: an update. *Gene,* 498**,** 1-4.

MARIE, P. J., DEBIAIS, F. & HAŸ, E. 2002. Regulation of human cranial osteoblast phenotype by FGF-2, FGFR-2 and BMP-2 signaling. *Histology and Histopathology* 17**,** 877-885.

MARIE, P. J., MIRAOUI, H. & SEVERE, N. 2012. FGF/FGFR signaling in bone formation: progress and perspectives. *Growth Factors,* 30**,** 117-123.

MARTEL-PELLETIER, J. 1998. Pathophysiology of osteoarthritis. *Osteoarthritis Cartilage.,* 6**,** 374-376.

MARTÍN-VILLAR, E., DIEGO, M., SUSANNA, C., YURRITA, M. M., VILARÓ, S. & QUINTANILLA, M. 2006. Podoplanin binds ERM proteins to activate RhoA and promote epithelial-mesenchymal transition. *Journal of Cell Science,* 119**,** 4541-4553.

MARTIN-VILLAR, E., SCHOLL, F. G., GAMALLO, C., YURRITA, M. M., MUNOZ-GUERRA, M., CRUCES, J. & QUINTANILLA, M. 2005. Characterization of human PA2.26 antigen (T1alpha-2, podoplanin), a small membrane mucin induced in oral squamous cell carcinomas. *The International Journal of Cancer* 113**,** 899-910.

MARTÍN-VILLAR, E., YURRITA, M. M., FERNÁNDEZ-MUÑOZ, B., QUINTANILLA, M. & RENART, J. 2009. Regulation of podoplanin/PA2.26 antigen expression in tumour cells. Involvement of calpain-mediated proteolysis. *The International Journal of Biochemistry & Cell Biology,* 41**,** 1421-1429.

MARTIN, G. S. 2003. Cell signaling and cancer. *Cancer Cell,* 4**,** 167-174.

MARTIN, R. B. 2007. Targeted bone remodeling involves BMU steering as well as activation. *Bone,* 40**,** 1574-1580.

MATSUGUCHI, T., CHIBA, N., BANDOW, K., KAKIMOTO, K., MASUDA, A. & OHNISHI, T. 2009. JNK activity is essential for Atf4 expression and late-stage osteoblast differentiation. *Journal of Bone and Mineral Research,* 24**,** 398-410.

MATSUSHITA, T., CHAN, Y. Y., KAWANAMI, A., BALMES, G., LANDRETH, G. E. & MURAKAMI, S. 2009a. Extracellular signal-regulated kinase 1 (ERK1) and ERK2 play essential roles in osteoblast differentiation and in supporting osteoclastogenesis. *Molecular and Cellular Biology,* 29**,** 5843-5857.

MATSUSHITA, T., WILCOX, W. R., CHAN, Y. Y., KAWANAMI, A., BUKULMEZ, H., BALMES, G., KREJCI, P., MEKIKIAN, P. B., OTANI, K., YAMAURA, I., WARMAN, M. L., GIVOL, D. &

MURAKAMI, S. 2009b. FGFR3 promotes synchondrosis closure and fusion of ossification centers through the MAPK pathway. *Human Molecular Genetics,* 18**,** 227-240.

MCCLAIN, S. 2017. Bioinformatic screening and detection of allergen cross-reactive IgE-binding epitopes. *Molecular Nutrition & Food Research,* 61**,** 1600676.

MCCORMICK, F. 2000. Small-molecule inhibitors of cell signaling. *Current Opinion in Biotechnology,* 11**,** 593-597.

MCCOY, A. M. 2015. Animal Models of Osteoarthritis: Comparisons and Key Considerations. *Veterinary pathology,* 52**,** 803-803.

MCILWRAITH, C. W., FRISBIE, D. D., KAWCAK, C. E., FULLER, C. J., HURTIG, M. & CRUZ, A. 2010. The OARSI histopathology initiative - recommendations for histological assessments of osteoarthritis in the horse. *Osteoarthritis Cartilage,* 18 S93-S105.

MCNIVEN, M. A. 2013. Breaking away: matrix remodeling from the leading edge. *Trends in Cell Biology,* 23**,** 16-21.

MCWILLIAM, H., LI, W., ULUDAG, M., SQUIZZATO, S., PARK, Y. M., BUSO, N., COWLEY, A. P. & LOPEZ, R. 2013. Analysis Tool Web Services from the EMBL-EBI. *Nucleic Acids Research,* 41**,** W597-W600.

MENKES, C. J. & LANE, N. E. 2004. Are osteophytes good or bad? *Osteoarthritis Cartilage,* 12**,** S53–S54.

MEYER, J. 1984. Can biological calcification occur in the presence of pyrophosphate? *Archives of Biochemistry and Biophysics,* 231**,** 1-8.

MILLER, R. E., TU, Z., TRAN, P. B., QIN, X. C., LUO, J. F., TORTORELLA, M. & MALFAIT, A. M. 2015. Inflammatory protein profiling in the knee joint after DMM surgery in the mouse. *Osteoarthritis and Cartilage,* 23**,** A262.

MILZ, S. & PUTZ, R. 1994. Quantitative morphology of the subchondral plate of the tibial plateau. *The Journal of Anatomy,* 185**,** 103-110.

MIYAGAWA, K., YAMAZAKI, M., KAWAI, M., NISHINO, J., KOSHIMIZU, T., OHATA, Y., TACHIKAWA, K., MIKUNI-TAKAGAKI, Y., KOGO, M., OZONO, K. & MICHIGAMI, T. 2014. Dysregulated gene expression in the primary osteoblasts and osteocytes isolated from hypophosphatemic Hyp mice. *PLoS One,* 9**,** e93840.

MIZUNO, M., FUJISAWA, R. & KUBOKI, Y. 2000. Type I collagen-induced osteoblastic differentiation of bone-marrow cells mediated by collagen-α2β1 integrin interaction. *Journal of Cellular Physiology,* 184**,** 207-213.

MOHAMMAD, K. S., CHIRGWIN, J. M. & GUISE, T. A. 2008. Assessing New Bone Formation in Neonatal Calvarial Organ Cultures. In: Westendorf, J.J. (ed.) Osteoporosis: Methods and Protocols. *Methods in Molecular Biology, © Springer Science+Business Media, LLC 2012,* 455**,** 37-50.

MONTERO, A., OKADA, Y., TOMITA, M., ITO, M., TSURUKAMI, H., NAKAMURA, T., DOETSCHMAN, T., COFFIN, J. D. & HURLEY, M. M. 2000. Disruption of the fibroblast growth factor-2 gene results in decreased bone mass and bone formation. *Journal of Clinical Investigation,* 105**,** 1085-1093.

MORGAN, J. M., NAVABI, H., SCHMID, K. W. & JASANI, B. 1994. Possible role of tissue-bound calcium ions in citrate-mediated high-temperature antigen retrieval. *The Journal of Pathology,* 174**,** 301-307.

MUNDHENKE, C., MEYER, K., DREW, S. & FRIEDL, A. 2002. Heparan Sulfate Proteoglycans as Regulators of Fibroblast Growth Factor-2 Receptor Binding in Breast Carcinomas. *American Journal of Pathology,* 160**,** 185–194.

MURAKAMI, S., BALMES, G., MCKINNEY, S., ZHANG, Z., GIVOL, D. & DE CROMBRUGGHE, B. 2004. Constitutive activation of MEK1 in chondrocytes causes Stat1-independent

achondroplasia-like dwarfism and rescues the Fgfr3-deficient mouse phenotype. *Genes & Development,* 18**,** 290-305.

MURPHY, L. O., MACKEIGAN, J. P. & BLENIS, J. 2003. A Network of Immediate Early Gene Products Propagates Subtle Differences in Mitogen-Activated Protein Kinase Signal Amplitude and Duration. *Molecular and Cellular Biology,* 24**,** 144-153.

MURPHY, L. O., SMITH, S., CHEN, R. H., FINGAR, D. C. & BLENIS, J. 2002. Molecular interpretation of ERK signal duration by immediate early gene products. *Nature Cell Biology,* 4**,** 556-564.

NAKAGAWA, N., KINOSAKI, M., YAMAGUCHI, K., SHIMA, N., YASUDA, H., YANO, K., MORINAGA, T. & HIGASHIO, K. 1998. RANK is the essential signaling receptor for osteoclast differentiation factor in osteoclastogenesis. *Biochemical and Biophysical Research Communications,* 253**,** 395-400.

NAKAMURA, N., OSHIRO, N., FUKATA, Y., AMANO, M., FUKATA, M., KURODA, S., MATSUURA, Y., LEUNG, T., LIM, L. & KAIBUCHI, K. 2000. Phosphorylation of ERM proteins at filopodia induced by Cdc42. *Genes to Cells,* 5**,** 571-581.

NAKAMURA, Y., TENSHO, K., NAKAYA, H., NAWATA, M., OKABE, T. & WAKITANI, S. 2005. Low dose fibroblast growth factor-2 (FGF-2) enhances bone morphogenetic protein-2 (BMP-2)-induced ectopic bone formation in mice. *Bone,* 36**,** 399-407.

NAKANO, Y., TOYOSAWA, S. & TAKANO, Y. 2004. Eccentric Localization of Osteocytes Expressing Enzymatic Activities, Protein, and mRNA Signals for Type 5 Tartrate-resistant Acid Phosphatase (TRAP). *Journal of Histochemistry and Cytochemistry,* 52**,** 1475-1482.

NAKASHIMA, T., HAYASHI, M., FUKUNAGA, T., KURATA, K., OH-HORA, M., FENG, J. Q., BONEWALD, L. F., KODAMA, T., WUTZ, A., WAGNER, E. F., PENNINGER, J. M. & TAKAYANAGI, H. 2011a. Evidence for osteocyte regulation of bone homeostasis through RANKL expression. *Nature Medicine,* 17**,** 1231-1234.

NAKASHIMA, T., HAYASHI, M., FUKUNAGA, T., KURATA, K., OH-HORA, M., FENG, J. Q., BONEWALD, L. F., KODAMA, T., WUTZ, A., WAGNER, E. F., PENNINGER, J. M. & TAKAYANAGI, H. 2011b. Evidence for osteocyte regulation of bone homeostasis through RANKL expression. *Nature Medicine,* 17**,** 1231-1234.

NAKAYAMA, G. R., CATON, M. C., NOVA, M. P. & PARANDOOSH, Z. 1997. Assessment of the Alamar Blue assay for cellular growth and viability in vitro. *Journal of Immunological Methods,* 204**,** 205-208.

NETTER, F. H. 1987. Musculoskeletal system: anatomy, physiology, and metabolic disorders. *Summit, New Jersey: Ciba-Geigy Corporation***,** 129.

NICOLELLA, D. P., FENG, J. Q., MORAVITS, D. E., BONIVITCH, A. R., WANG, Y., DUSECICH, V., YAO, W., LANE, N. & BONEWALD, L. F. 2008. Effects of nanomechanical bone tissue properties on bone tissue strain: Implications for osteocyte mechanotransduction. *Journal of Musculoskeletal & neuronal Interactions,* 8**,** 330-331.

NIGER, C., BUO, A. M., HEBERT, C., DUGGAN, B. T., WILLIAMS, M. S. & STAINS, J. P. 2012. ERK acts in parallel to PKCdelta to mediate the connexin43-dependent potentiation of Runx2 activity by FGF2 in MC3T3 osteoblasts. *American Journal of Physiology-Cell Physiology,* 302**,** C1035-C1044.

NOBLE, B. S., PEET, N., STEVENS, H. Y., BRABBS, A., MOSLEY, J. R., REILLY, G. C., REEVE, J., SKERRY, T. M. & LANYON, L. E. 2003. Mechanical loading: biphasic osteocyte survival and targeting of osteoclasts for bone destruction in rat cortical bone. *American Journal of Physiology -Cell Physiology,* 284**,** C934-C943.

NUDELMAN, F., PIETERSE, K., GEORGE, A., BOMANS, P. H. H., FRIEDRICH, H., BRYLKA, L. J., HILBERS, P. A. J., DE WITH, G. & SOMMERDIJK, N. A. J. M. 2010. The role of collagen

in bone apatite formation in the presence of hydroxyapatite nucleation inhibitors. *Nature Materials,* 9**,** 1004-1009.

NUMMENMAA, E., HAMALAINEN, M., MOILANEN, T., VUOLTEENAHO, K. & MOILANEN, E. 2015. Effects of FGF-2 and FGF receptor antagonists on MMP enzymes, aggrecan, and type II collagen in primary human OA chondrocytes. *Scandinavian Journal of Rheumatology,* 44**,** 321-330.

OLDKNOW, K. J., MACRAE, V. E. & FARQUHARSON, C. 2015. Endocrine role of bone: recent and emerging perspectives beyond osteocalcin. *Journal of Endocrinology,* 225**,** R1-R19.

OLSON, D. C., DENG, C. & HANAHAN, D. 1998. Fibroblast growth factor receptor 4, implicated in progression of islet cell carcinogenesis by its expression profile, does not contribute functionally. *Cell Growth & Differentiation,* 9**,** 557-564.

OMINSKY, M. S., LI, C., LI, X., TAN, H. L., LEE, E., BARRERO, M., ASUNCION, F. J., DWYER, D., HAN, C. Y., VLASSEROS, F., SAMADFAM, R., JOLETTE, J., SMITH, S. Y., STOLINA, M., LACEY, D. L., SIMONET, W. S., PASZTY, C., LI, G. & KE, H. Z. 2011. Inhibition of sclerostin by monoclonal antibody enhances bone healing and improves bone density and strength of nonfractured bones. *Journal of Bone and Mineral Research,* 26**,** 1012-1021.

ORNITZ, D. M. & ITOH, N. 2015. The Fibroblast Growth Factor signaling pathway. *Wiley Interdisciplinary Reviews. Developmental Biology,* 4**,** 215-266.

ORNITZ, D. M. & MARIE, P. J. 2002. FGF signaling pathways in endochondral and intramembranous bone development and human genetic disease. *Genes & Development,* 16**,** 1446-1465.

ORRISS, I. R., HAJJAWI, M. O., HUESA, C., MACRAE, V. E. & ARNETT, T. R. 2014. Optimisation of the differing conditions required for bone formation in vitro by primary osteoblasts from mice and rats. *International Journal of Molecular Medicine,* 34**,** 1201-1208.

ORRISS, I. R., TAYLOR, S. E. B. & ARNETT, T. R. 2012. Rat Osteoblast Cultures. *In: Bone Research Protocols, Methods in Molecular Biology (Helfrich, M.H and Ralston, S.T., eds). Springer Science+Business Media, LLC, London.,* 816**,** 31-41.

ORTEGA, S., ITTMANN, M., TSANG, S. H., EHRLICH, M. & BASILICO, C. 1998. Neuronal defects and delayed wound healing in mice lacking fibroblast growth factor 2. *Proceedings of the National Academy of Sciences of the United States of America,* 95**,** 5672-5677.

PACIFICI, M., KOYAMA, E. & IWAMOTO, M. 2005. Mechanisms of synovial joint and articular cartilage formation: Recent advances, but many lingering mysteries. *Birth Defects Research Part C: Embryo Today: Reviews,* 75**,** 237-248.

PADHI, D., JANG, G., STOUCH, B., FANG, L. & POSVAR, E. 2011. Single-dose, placebo-controlled, randomized study of AMG 785, a sclerostin monoclonal antibody. *Journal of Bone and Mineral Research,* 26**,** 19-26.

PAIC, F., IGWE, J. C., NORI, R., KRONENBERG, M. S., FRANCESCHETTI, T., HARRINGTON, P., KUO, L., SHIN, D. G., ROWE, D. W., HARRIS, S. E. & KALAJZIC, I. 2009. Identification of differentially expressed genes between osteoblasts and osteocytes. *Bone,* 45**,** 682-692.

PALUMBO, C. 1986. A three-dimensional ultrastructural study of osteoid-osteocytes in the tibia of chick embryos. *Cell and Tissue Research,* 246**,** 125-131.

PALUMBO, C., FERRETTI, M. & DE POL, A. 2003. Apoptosis during intramembranous ossification. *Journal of Anatomy,* 203**,** 589-598.

PANG, L., SAWADA, T., DECKER, S. J. & SALTIEL, A. R. 1995. Inhibition of MAP kinase kinase blocks the differentiation of PC-12 cells induced by nerve growth factor. *The Journal of Biological Chemistry,* 270**,** 13585-13588.

PARTANEN, J., MÄKELÄ, T. P., EEROLA, E., KORHONEN, J., HIRVONEN, H., CLAESSON-WELSH, L. & ALITALO, K. 1991. FGFR-4, a novel acidic fibroblast growth factor receptor with a distinct expression pattern. *The EMBO Journal,* 10**,** 1347-1354.

PEARSON, W. R. 1991. Searching protein sequence libraries: Comparison of the sensitivity and selectivity of the Smith-Waterman and FASTA algorithms. *Genomics,* 11**,** 635-650.

PEARSON, W. R. 2013. An Introduction to Sequence Similarity ("Homology") Searching. *Current protocols in bioinformatics* 03**,** 10.1002/0471250953.bi0471250301s0471250942.

PEARSON, W. R. & LIPMAN, D. J. 1988. Improved tools for biological sequence comparison. *Proceedings of the National Academy of Sciences of the United States of America,* 85**,** 2444-2448.

PELLEGRINO, M. J. & STORK, P. J. 2006. Sustained activation of extracellular signal-regulated kinase by nerve growth factor regulates c-fos protein stabilization and transactivation in PC12 cells. *The Journal of Neurochemistry,* 99**,** 1480-1493.

PELLETIER, J. P., MARTEL-PELLETIER, J., GHANDUR-MNAYMNEH, L., HOWELL, D. S. & WOESSNER, J. F. J. 1985. Role of synovial membrane inflammation in cartilage matrix breakdown in the Pond-Nuki dog model of osteoarthritis. *Arthritis and Rheumatism,* 28**,** 554-561.

PERCIVAL, C. J. & RICHTSMEIER, J. T. 2013. Angiogenesis and Intramembranous Osteogenesis. *Developmental dynamics : an official publication of the American Association of Anatomists,* 242**,** 909-922.

PILERI, S. A., RONCADOR, G., CECCARELLI, C., PICCIOLI, M., BRISKOMATIS, A., SABATTINI, E., ASCANI, S., SANTINI, D., PICCALUGA, P. P., LEONE, O., DAMIANI, S., ERCOLESSI, C., SANDRI, F., PIERI, F., LEONCINI, L. & FALINI, B. 1997. Antigen retrieval techniques in immunohistochemistry: comparison of different methods. *The Journal of Pathology,* 183**,** 116-123.

PLOTKIN, L. I. & BELLIDO, T. 2016. Osteocytic signalling pathways as therapeutic targets for bone fragility. *Nature Reviews Endocrinology,* 12**,** 593-605.

POOL, R. R. & MEAGHER, D. M. 1990. Pathologic findings and pathogenesis of racetrack injuries. *Veterinary Clinics of North America: Equine Practice* 6**,** 1-30.

POOLE, K. E., VAN BEZOOIJEN, R. L., LOVERIDGE, N., HAMERSMA, H., PAPAPOULOS, S. E., LÖWIK, C. W. & REEVE, J. 2005. Sclerostin is a delayed secreted product of osteocytes that inhibits bone formation. *The FASEB Journal,* 19**,** 1842-1844.

POPOVICI, C., ADÉLAÏDE, J., OLLENDORFF, V., CHAFFANET, M., GUASCH, G., JACROT, M., LEROUX, D., BIRNBAUM, D. & PÉBUSQUE, M. J. 1998. Fibroblast growth factor receptor 1 is fused to FIM in stem-cell myeloproliferative disorder with t(8;13). *Proceedings of the National Academy of Sciences of the United States of America,* 95**,** 5712-5717.

POULET, B. & STAINES, K. A. 2016. New developments in osteoarthritis and cartilage biology. *Current Opinion in Pharmacology,* 28**,** 8-13.

POWERS, C. J., MCLESKEY, S. W. & WELLSTEIN, A. 2000. Fibroblast growth factors, their receptors and signaling. *Endocrine-Related Cancer,* 7**,** 165-197.

PRIDEAUX, M., LOVERIDGE, N., PITSILLIDES, A. A. & FARQUHARSON, C. 2012. Extracellular Matrix Mineralization Promotes E11/gp38 Glycoprotein Expression and Drives Osteocytic Differentiation. *PLoS ONE,* 7**,** e36786.

QING, H., ARDESHIRPOUR, L., PAJEVIC, P. D., DUSEVICH, V., JÄHN, K., KATO, S., WYSOLMERSKI, J. & BONEWALD, L. F. 2012. Demonstration of Osteocytic Perilacunar/Canalicular Remodeling in Mice during Lactation. *Journal of Bone and Mineral Research* 27**,** 1018-1029.

QUARLES, L. D. 2008. Endocrine functions of bone in mineral metabolism regulation. *The Journal of Clinical Investigation,* 118**,** 3820-3828.

QUASNICHKA, H. L., J.M;, A.-M. & BAILEY, A. J. 2006. Subchondral bone and ligament changes precede cartilage degradation in guinea pig osteoarthritis. *Biorheology,* 43**,** 389–397.

RACHNER, T. D., KHOSLA, S. & HOFBAUER, L. C. 2011. Osteoporosis: now and the future. *The Lancet,* 377**,** 1276-1287.

RADIN, E. L. & ROSE, R. M. 1986. Role of subchondral bone in the initiation and progression of cartilage damage. *Clinical Orthopaedics and Related Research,* 213**,** 34-40.

RADIN, E. L., SCHAFFLER, M., GIBSON, G. & TASHMAN, S. 1995. Osteoarthrosis as the result of repetitive trauma. In: Kuettner KE, Goldberg VM (eds). Osteoarthritic Disorders. *Rosemont: American Academy of Orthopaedic Surgeons.,* II**,** 197-204.

RAMIREZ, M. I., MILLIEN, G., HINDS, A., CAO, Y., SELDIN, D. C. & WILLIAMS, M. C. 2003. T1α, a lung type I cell differentiation gene, is required for normal lung cell proliferation and alveolus formation at birth. *Developmental Biology,* 256**,** 62-73.

RAZZAQUE, M. S. 2009. The FGF23–Klotho axis: endocrine regulation of phosphate homeostasis. *Nature reviews. Endocrinology,* 5**,** 611-619.

REITER, A., SOHAL, J., KULKARNI, S., CHASE, A., MACDONALD, D. H., AGUIAR, R. C., GONÇALVES, C., HERNANDEZ, J. M., JENNINGS, B. A., GOLDMAN, J. M. & CROSS, N. C. 1998. Consistent fusion of ZNF198 to the fibroblast growth factor receptor-1 in the t(8;13)(p11;q12) myeloproliferative syndrome. *Blood.,* 92**,** 1735-1742.

RENO, C., MARCHUK, L., SCIORE, P., FRANK, C. B. & HART, D. A. 1997. Rapid isolation of total RNA from small samples of hypocellular, dense connective tissues. *Biotechniques.,* 22**,** 1082-1086.

REVENU, C., ATHMAN, R., ROBINE, S. & LOUVARD, D. 2004. The co-workers of actin filaments: from cell structures to signals. *Nature Reviews Molecular Cell Biology,* 5**,** 635-646.

REWCASTLE, G. W., PALMER, B. D., THOMPSON, A. M., BRIDGES, A. J., CODY, D. R., ZHOU, H., FRY, D. W., MCMICHAEL, A. & DENNY, W. A. 1996. Tyrosine Kinase Inhibitors. 10. Isomeric 4-[(3-Bromophenyl)amino]pyrido[d]- pyrimidines Are Potent ATP Binding Site Inhibitors of the Tyrosine Kinase Function of the Epidermal Growth Factor Receptor. *Journal of Medicinal Chemistry,* 39**,** 1823-1835.

RICHELDA, R., RONCHETTI, D., BALDINI, L., CRO, L., VIGGIANO, L., MARZELLA, R., ROCCHI, M., OTSUKI, T., LOMBARDI, L., MAIOLO, A. T. & NERI, A. 1997. A novel chromosomal translocation t(4; 14)(p16.3; q32) in multiple myeloma involves the fibroblast growth-factor receptor 3 gene. *Blood,* 90**,** 4062-4070.

RIDLEY, A. J. 2011. Life at the leading edge. *Cell,* 145**,** 1012-1022.

RIECKMANN, T., KOTEVIC, I. & TRUEB, B. 2008. The cell surface receptor FGFRL1 forms constitutive dimers that promote cell adhesion. *Experimental Cell Research,* 314**,** 1071-1081.

RIFKIN, D. B. & MOSCATELLI, D. 1989. Recent developments in the cell biology of basic fibroblast growth factor. *The Journal of Cell Biology,* 109**,** 1-6.

RIOS, H., KOUSHIK, S. V., WANG, H., WANG, J., ZHOU, H.-M., LINDSLEY, A., ROGERS, R., CHEN, Z., MAEDA, M., KRUZYNSKA-FREJTAG, A., FENG, J. Q. & CONWAY, S. J. 2005. periostin Null Mice Exhibit Dwarfism, Incisor Enamel Defects, and an Early-Onset Periodontal Disease-Like Phenotype. *Molecular and Cellular Biology,* 25**,** 11131-11144.

ROBIN, C. A., IRELAND, J., WYLIE, C. E., COLLINS, S. N., VERHEYEN, K. L. P. & NEWTON, J. R. 2013. Prevalence and Risk Factors for Owner- Reported Obesity in Horses and Ponies in Great Britain. *Equine Veterinary Journal,* 45**,** 12-13.

ROBLING, A. G., NIZIOLEK, P. J., BALDRIDGE, L. A., CONDON, K. W., ALLEN, M. R., ALAM, I., MANTILA, S. M., GLUHAK-HEINRICH, J., BELLIDO, T. M., HARRIS, S. E. & TURNER, C. H. 2008. Mechanical stimulation of bone in vivo reduces osteocyte expression of Sost/sclerostin. *The Journal of Biological Chemistry,* 283**,** 5866-5875.

ROMAN-BLAS, J. A., CASTAÑEDA, S., LARGO, R. & HERRERO-BEAUMONT, G. 2009. Osteoarthritis associated with estrogen deficiency. *Arthritis Research & Therapy,* 11**,** 241.

ROSCHGER, A., ROSCHGER, P., KEPLINGTER, P., KLAUSHOFER, K., ABDULLAH, S., KNEISSEL, M. & RAUCH, F. 2014. Effect of sclerostin antibody treatment in a mouse model of severe osteogenesis imperfecta. *Bone,* 66**,** 182-188.

ROSSER, J. & BONEWALD, L. F. 2012. Studying osteocyte function using the cell lines MLO-Y4 and MLO-A5. *In: Bone Research Protocols, Methods in Molecular Biology (Helfrich, M.H and Ralston, S.T., eds). Springer Science+Business Media, LLC, London.,* 816**,** 67-81.

RUAN, J.-L., TULLOCH, N. L., MUSKHELI, V., GENOVA, E. E., MARINER, P. D., ANSETH, K. S. & MURRY, C. E. 2013. An Improved Cryosection Method for Polyethylene Glycol Hydrogels Used in Tissue Engineering. *Tissue Engineering. Part C, Methods,* 19**,** 794-801.

SABAPATHY, K., HOCHEDLINGER, K., NAM, S. Y., BAUER, A., KARIN, M. & WAGNER, E. F. 2004. Distinct Roles for JNK1 and JNK2 in Regulating JNK Activity and c-Jun-Dependent Cell Proliferation. *Molecular Cell,* 15**,** 713-725.

SABBAGH, Y., BOILEAU, G., CAMPOS, M., CARMONA, A. K. & TENENHOUSE, H. S. 2003. Structure and function of disease-causing missense mutations in the PHEX gene. *Journal of Clinical Endocrinology and Metabolism,* 88**,** 2213-2222.

SABBIETI, M. G., MARCHETTI, L., ABREU, C., MONTERO, A., HAND, A. R., RAISZ, L. G. & HURLEY, M. M. 1999. Prostaglandins regulate the expression of fibroblast growth factor-2 in bone. *Endocrinology,* 140**,** 434-444.

SANCHEZ, C., DEBERG, M. A., BELLAHCENE, A., CASTRONOVO, V., MSIKA, P., DELCOUR, J. P., CRIELAARD, J. M. & HENROTIN, Y. E. 2008. Phenotypic characterization of osteoblasts from the sclerotic zones of osteoarthritic subchondral bone. *Arthritis & Rheumatology,* 58**,** 442-455.

SANDER, J. D. & JOUNG, J. K. 2014. CRISPR-Cas systems for editing, regulating and targeting genomes. *Nature Biotechnology,* 32**,** 347-355.

SANKIAN, M., VARASTEH, A., PAZOUKI, N. & MAHMOUDI, M. 2005. Sequence homology: A poor predictive value for profilins cross-reactivity. *Clinical and molecular allergy : CMA,* 3**,** 13-13.

SARABIPOUR, S. & HRISTOVA, K. 2016. Mechanism of FGF receptor dimerization and activation. *Nature Communications,* 7**,** 10262.

SASANO, Y., ZHU, J. X., KAMAKURA, S., KUSUNOKI, S., MIZOGUCHI, I. & KAGAYAMA, M. 2000. Expression of major bone extracellular matrix proteins during embryonic osteogenesis in rat mandibles. *Anatomy and Embryology,* 202**,** 31-37.

SAWA, Y. 2010. New trends in the study of podoplanin as a cell morphological regulator. *Japanese Dental Science Review,* 46**,** 165-172.

SCHAFFLER, M. B., CHEUNG, W.-Y., MAJESKA, R. & KENNEDY, O. 2014. Osteocytes: Master Orchestrators of Bone. *Calcified Tissue International,* 94**,** 5-24.

SCHINDELIN, J., ARGANDA-CARRERAS, I., FRISE, E., KAYNIG, V., LONGAIR, M., PIETZSCH, T., PREIBISCH, S., RUEDEN, C., SAALFELD, S., SCHMID, B., TINEVEZ, J. Y., WHITE, D. J., HARTENSTEIN, V., ELICEIRI, K., TOMANCAK, P. & CARDONA, A. 2012. Fiji: an open-source platform for biological-image analysis. *Nature Methods,* 9**,** 676-682.

SCHLESINGER, P. H., BLAIR, H. C., TEITELBAUM, S. L. & EDWARDS, J. C. 1997. Characterization of the Osteoclast Ruffled Border Chloride Channel and Its Role in Bone Resorption. *Journal of Biological Chemistry,* 272**,** 18636-18643.

SCHMITZ, N., LAVERTY, S., KRAUS, V. B. & AIGNER, T. 2010. Basic methods in histopathology of joint tissues. *Osteoarthritis Cartilage,* 18**,** S113-S116.

SCHOLL, F. G., GAMALLO, C., VILARÓ, S. & QUINTANILLA, M. 1999. Identification of PA2.26 antigen as a novel cell-surface mucin-type glycoprotein that induces plasma membrane extensions and increased motility in keratinocytes. *Journal of Cell Science,* 112**,** 4601-4613.

SEEMAN, E. 2009. Bone modeling and remodeling. *Critical Reviews in Eukaryotic Gene Expression,* 19**,** 219-233.

SEEMAN, E. 2013. Age- and Menopause-Related Bone Loss Compromise Cortical and Trabecular Microstructure. *The Journals of Gerontology: Series A,* 68**,** 1218-1225.

SEMENOV, M., TAMAI, K. & HE, X. 2005. SOST is a ligand for LRP5/LRP6 and a Wnt signaling inhibitor. *Journal of Biological Chemistry,* 280**,** 26770-26775.

SHAPIRO, F. 2008. Bone development and its relation to fracture repair. The role of mesenchymal osteoblasts and surface osteoblasts. *European Cells and Materials,* 15**,** 53-76.

SHARMA, A. R., JAGGA, S., LEE, S.-S. & NAM, J.-S. 2013. Interplay between Cartilage and Subchondral Bone Contributing to Pathogenesis of Osteoarthritis. *International Journal of Molecular Sciences,* 14**,** 19805-19830.

SHIMADA, T., YOSHIDA, T. & YAMAGATA, K. 2016. Neuritin Mediates Activity-Dependent Axonal Branch Formation in Part via FGF Signaling. *The Journal of Neuroscience,* 36**,** 4534-4548.

SIEVERS, F., WILM, A., DINEEN, D., GIBSON, T. J., KARPLUS, K., LI, W., LOPEZ, R., MCWILLIAM, H., REMMERT, M., SÖDING, J., THOMPSON, J. D. & HIGGINS, D. G. 2011. Fast, scalable generation of high-quality protein multiple sequence alignments using Clustal Omega. *Molecular Systems Biology,* 7**,** 539.

SMITH, S. M. & MELROSE, J. 2011. Podoplanin is expressed by a sub-population of human foetal rib and knee joint rudiment chondrocytes. *Tissue and Cell,* 43**,** 39-44.

SMITH, T. F. & WATERMAN, M. S. 1981. Identification of common molecular subsequences. *Journal of Molecular Biology,* 147**,** 195-197.

SOKOLOFF, L. 1993. Microcracks in the calcified layer of articular cartilage. *The Archives of Pathology & Laboratory Medicine,* 117**,** 191-195.

SOLTANOFF, C. S., CHEN, W., YANG, S. & LI, Y. 2009. Signaling Networks that Control the Lineage Commitment and Differentiation of Bone Cells. *Critical Reviews in Eukaryotic Gene Expression,* 19**,** 1-46.

SOMMERFELDT, D. & RUBIN, C. 2001. Biology of bone and how it orchestrates the form and function of the skeleton. *European Spine Journal,* 10**,** S86-S95.

SONG, G., OUYANG, G. & BAO, S. 2005. The activation of Akt/PKB signaling pathway and cell survival. *Journal of Cellular and Molecular Medicine,* 9**,** 59-71.

SPALDING, J. B. & LAMMERS, P. J. 2004. BLAST Filter and GraphAlign: rule-based formation and analysis of sets of related DNA and protein sequences. *Nucleic Acids Research,* 32**,** W26-W32.

STAINES, K. A., JAVAHERI, B., HOHENSTEIN, P., FLEMING, R., IKPEGBU, E., UNGER, E., HOPKINSON, M., BUTTLE, D. J., PITSILLIDES, A. A. & FARQUHARSON, C. 2017. Hypomorphic conditional deletion of E11/Podoplanin reveals a role in osteocyte dendrite elongation. *Journal of Cellular Physiology,* 232**,** 3006-3019.

STAINES, K. A., MACRAE, V. E. & FARQUHARSON, C. 2012. The importance of the SIBLING family of proteins on skeletal mineralisation and bone remodelling. *Journal of Endocrinology,* 214**,** 241-255.

STAINES, K. A., PRIDEAUX, M., ALLEN, S., BUTTLE, D. J., PITSILLIDES, A. A. & FARQUHARSON, C. 2016. E11/Podoplanin Protein Stabilization Through Inhibition of the Proteasome Promotes Osteocyte Differentiation in Murine in Vitro Models. *Journal of Cellular Physiology,* 231**,** 1392-1404.

STERN, A. R., STERN, M. M., VAN DYKE, M. E., JAHN, K., PRIDEAUX, M. & BONEWALD, L. F. 2012. Isolation and culture of primary osteocytes from the long bones of skeletally mature and aged mice. *Biotechniques,* 52**,** 361-373.

STOKER, A. M., COOK, J. L., KUROKI, K. & FOX, D. B. 2006. Site-specific analysis of gene expression in early osteoarthritis using the Pond-Nuki model in dogs. *Journal of Orthopaedic Surgery and Research,* 1**,** 8-8.

SU, N., JIN, M. & CHEN, L. 2014. Role of FGF/FGFR signaling in skeletal development and homeostasis: learning from mouse models. *Bone research,* 2**,** 14003.

SUHARA, T., KIM, H. S., KIRSHENBAUM, L. A. & WALSH, K. 2002. Suppression of Akt Signaling Induces Fas Ligand Expression: Involvement of Caspase and Jun Kinase Activation in Akt-Mediated Fas Ligand Regulation. *Molecular and Cellular Biology,* 22**,** 680-691.

SUZUKI, A., PALMER, G., BONJOUR, J. P. & CAVERZASIO, J. 2000. Stimulation of sodium-dependent phosphate transport and signaling mechanisms induced by basic fibroblast growth factor in MC3T3-E1 osteoblast-like cells. *Journal of Bone and Mineral Research* 15**,** 95-102.

TALJANOVIC, M. S., GRAHAM, A. R., BENJAMIN, J. B., GMITRO, A. F., KRUPINSKI, E. A., SCHWARTZ, S. A., HUNTER, T. B. & RESNICK, D. L. 2008. Bone marrow edema pattern in advanced hip osteoarthritis: quantitative assessment with magnetic resonance imaging and correlation with clinical examination, radiographic findings, and histopathology. *Skeletal Radiology* 37**,** 423-431.

TAN, L., WANG, J., TANIZAKI, J., HUANG, Z., AREF, A. R., RUSAN, M., ZHU, S. J., ZHANG, Y., ERCAN, D., LIAO, R. G., CAPELLETTI, M., ZHOU, W., HUR, W., KIM, N., SIM, T., GAUDET, S., BARBIE, D. A., YEH, J. R., YUN, C. H., HAMMERMAN, P. S., MOHAMMADI, M., JANNE, P. A. & GRAY, N. S. 2014. Development of covalent inhibitors that can overcome resistance to first-generation FGFR kinase inhibitors. *Proceedings of the National Academy of Sciences of the United States of America* 111**,** E4869-E4877.

TATSUMI, S., ISHII, K., AMIZUKA, N., LI, M., KOBAYASHI, T., KOHNO, K., ITO, M., TAKESHITA, S. & IKEDA, K. 2007. Targeted Ablation of Osteocytes Induces Osteoporosis with Defective Mechanotransduction. *Cell Metabolism,* 5**,** 464-475.

TETI, A. & ZALLONE, A. 2009. Do osteocytes contribute to bone mineral homeostasis? Osteocytic osteolysis revisited. *Bone,* 44**,** 11-16.

TEVEN, C. M., FARINA, E. M., RIVAS, J. & REID, R. R. 2014. Fibroblast growth factor (FGF) signaling in development and skeletal diseases. *Genes & Diseases,* 1**,** 199-213.

THIERY, J. P. 2002. Epithelial-mesenchymal transitions in tumour progression. *Nature Reviews Cancer,* 2**,** 442-454.

THISSE, B. & THISSE, C. 2005. Functions and regulations of fibroblast growth factor signaling during embryonic development. *Developmental Biology,* 287**,** 390-402.

THOMPSON, T. J., OWENS, P. D. & WILSON, D. J. 1989. Intramembranous osteogenesis and angiogenesis in the chick embryo. *Journal of Anatomy,* 166**,** 55-65.

TIEDE-LEWIS, L. M., XIE, Y., HULBERT, M. A., CAMPOS, R., DALLAS, M. R., DUSEVICH, V., BONEWALD, L. F. & DALLAS, S. L. 2017. Degeneration of the osteocyte network in the C57BL/6 mouse model of aging. *Aging,* 9**,** 2190-2208.

TOYOSAWA, S., SHINTANI, S., FUJIWARA, T., OOSHIMA, T., SATO, A., IJUHIN, N. & KOMORI, T. 2001. Dentin Matrix Protein 1 Is Predominantly Expressed in Chicken and Rat Osteocytes But Not in Osteoblasts. *Journal of Bone and Mineral Research,* 16**,** 2017-2026.

TURNER, N. & GROSE, R. 2010. Fibroblast growth factor signalling: from development to cancer. *Nature Reviews. Cancer,* 10**,** 116-129.

UCHIHASHI, K., AOKI, S., MATSUNOBU, A. & TODA, S. 2013. Osteoblast migration into type I collagen gel and differentiation to osteocyte-like cells within a self-produced mineralized matrix: A novel system for analyzing differentiation from osteoblast to osteocyte. *Bone,* 52**,** 102-110.

VAANANEN, H. K., ZHAO, H., MULARI, M. & HALLEEN, J. M. 2000. The cell biology of osteoclast function. *Journal of Cell Science,* 113**,** 377.

VAN DER KRAAN, P. M. & VAN DEN BERG, W. B. 2007. Osteophytes: relevance and biology. *Osteoarthritis Cartilage,* 15**,** 237-244.

VAN DIJK, F. S., ZILLIKENS, M. C., MICHA, D., RIESSLAND, M., MARCELIS, C. L. M., DE DIE-SMULDERS, C. E., MILBRADT, J., FRANKEN, A. A., HARSEVOORT, A. J., LICHTENBELT, K. D., PRUIJS, H. E., RUBIO-GOZALBO, M. E., ZWERTBROEK, R., MOUTAOUAKIL, Y., EGTHUIJSEN, J., HAMMERSCHMIDT, M., BIJMAN, R., SEMEINS, C. M., BAKKER, A. D., EVERTS, V., KLEIN-NULEND, J., CAMPOS-OBANDO, N., HOFMAN, A., TE MEERMAN, G. J., VERKERK, A. J. M. H., UITTERLINDEN, A. G., MAUGERI, A., SISTERMANS, E. A., WAISFISZ, Q., MEIJERS-HEIJBOER, H., WIRTH, B., SIMON, M. E. H. & PALS, G. 2013. PLS3 Mutations in X-Linked Osteoporosis with Fractures. *New England Journal of Medicine,* 369**,** 1529-1536.

VAN WEEREN, P. R. 2016a. 1 - General Anatomy and Physiology of Joints. *Joint Disease in the Horse (Second Edition).* Edinburgh: W.B. Saunders.

VAN WEEREN, P. R. 2016b. 7 - Septic Arthritis. *Joint Disease in the Horse (Second Edition).* Edinburgh: W.B. Saunders.

VANDEWEERD, J. M., HONTOIR, F., KIRSCHVINK, N., CLEGG, P., NISOLLE, J. F., ANTOINE, N. & GUSTIN, P. 2013. Prevalence of naturally occurring cartilage defects in the ovine knee. *Osteoarthritis Cartilage,* 21**,** 1125-1131.

VARGHESE, S., RAMSBY, M. L., JEFFREY, J. J. & CANALIS, E. 1995. Basic fibroblast growth factor stimulates expression of interstitial collagenase and inhibitors of metalloproteinases in rat bone cells. *Endocrinology,* 136**,** 2156-2162.

VILLUNGER, A., HUANG, D. C. S., HOLLER, N., TSCHOPP, J. & STRASSER, A. 2000. Fas Ligand-Induced c-Jun Kinase Activation in Lymphoid Cells Requires Extensive Receptor Aggregation But Is Independent of DAXX, and Fas-Mediated Cell Death Does Not Involve DAXX, RIP, or RAIDD. *The Journal of Immunology,* 165**,** 1337-1343.

WAKELING, A. E., BARKER, A. J., DAVIES, D. H., BROWN, D. S., GREEN, L. R., CARTLIDGE, S. A. & WOODBURN, J. R. 1996. Specific inhibition of epidermal growth factor receptor tyrosine kinase by 4-anilinoquinazolines. *Breast Cancer Research and Treatment,* 38**,** 67-73.

WALLACE, I. J., WORTHINGTON, S., FELSON, D. T., JURMAIN, R. D., WREN, K. T., MAIJANEN, H., WOODS, R. J. & LIEBERMAN, D. E. 2017. Knee osteoarthritis has doubled in

prevalence since the mid-20th century. *Proceedings of the National Academy of Sciences of the United States of America,* 114**,** 9332-9336.

WALSH, D. A., BONNET, C. S., TURNER, E. L., WILSON, D., SITU, M. & MCWILLIAMS, D. F. 2007. Angiogenesis in the synovium and at the osteochondral junction in osteoarthritis. *Osteoarthritis cartilage,* 15**,** 743-751.

WALSH, D. A., MCWILLIAMS, D. F., TURLEY, M. J., DIXON, M. R., FRANSES, R. E., MAPP, P. I. & WILSON, D. 2010. Angiogenesis and nerve growth factor at the osteochondral junction in rheumatoid arthritis and osteoarthritis. *Rheumatology (Oxford),* 49**,** 1852-1861.

WAN, P. T. C., GARNETT, M. J., ROE, S. M., LEE, S., NICULESCU-DUVAZ, D., GOOD, V. M., PROJECT, C. G., JONES, C. M., MARSHALL, C. J., SPRINGER, C. J., BARFORD, D. & MARAIS, R. 2004. Mechanism of Activation of the RAF-ERK Signaling Pathway by Oncogenic Mutations of B-RAF. *Cell,* 116**,** 855-867.

WANG, N., RUMNEY, R. M. H., YANG, L., ROBAYE, B., BOEYNAEMS, J. M., SKERRY, T. M. & GARTLAND, A. 2013. The P2Y13 receptor regulates extracellular ATP metabolism and the osteogenic response to mechanical loading. *Journal of Bone and Mineral Research,* 28**,** 1446-1456.

WANG, Q., GREEN, R. P., ZHAO, G. & ORNITZ, D. M. 2001. Differential regulation of endochondral bone growth and joint development by FGFR1 and FGFR3 tyrosine kinase domains. *Development 128, 3867-3876 (2001),* 128**,** 3867-3876.

WATANUKI, M., SAKAI, A., SAKATA, T., TSURUKAMI, H., MIWA, M., UCHIDA, Y., WATANABE, K., IKEDA, K. & NAKAMURA, T. 2002. Role of Inducible Nitric Oxide Synthase in Skeletal Adaptation to Acute Increases in Mechanical Loading. *Journal of Bone and Mineral Research,* 17**,** 1015-1025.

WAUSON, E. M., GUERRA, M. L., BARYLKO, B., ALBANESI, J. P. & COBB, M. H. 2013. Off-target effects of MEK inhibitors. *Biochemistry,* 52**,** 5164-5166.

WEI, J. & KARSENTY, G. 2015. An overview of the metabolic functions of osteocalcin. *Reviews in Endocrine & Metabolic Disorders,* 16**,** 93-98.

WEINER, S., TRAUB, W. & WAGNER, H. D. 1999. Lamellar bone: structure-function relations. *Journal of Structural Biology,* 126**,** 241-255.

WEKSLER, N. B., LUNSTRUM, G. P., REID, E. S. & HORTON, W. A. 1999. Differential effects of fibroblast growth factor (FGF) 9 and FGF2 on proliferation, differentiation and terminal differentiation of chondrocytic cells in vitro. *The Biochemical Journal,* 342**,** 667-682.

WENG, T., YI, L., HUANG, J., LUO, F., WEN, X., DU, X., CHEN, Q., DENG, C., CHEN, D. & CHEN, L. 2012. Genetic inhibition of fibroblast growth factor receptor 1 in knee cartilage attenuates the degeneration of articular cartilage in adult mice. *Arthritis and rheumatism,* 64**,** 3982-3992.

WENHAM, C. Y. J. & CONAGHAN, P. G. 2010. The Role of Synovitis in Osteoarthritis. *Therapeutic Advances in Musculoskeletal Disease,* 2**,** 349-359.

WENZ, W., BREUSCH, S. J., GRAF, J. & STRATMANN, T. U. 2000. Ultrastructural Findings after Intraarticular Application of Hyaluronan in a Canine Model of Arthropathy. *The Journal of Orthopaedic Research,* 18**,** 604-612.

WERGEDAL, J. E. & BAYLINK, D. J. 1969. DISTRIBUTION OF ACID AND ALKALINE PHOSPHATASE ACTIVITY IN UNDEMINERALIZED SECTIONS OF THE RAT TIBIAL DIAPHYSIS. *Journal of Histochemistry & Cytochemistry,* 17**,** 799-806.

WETTERWALD, A., HOFFSTETTER, W., CECCHINI, M. G., LANSKE, B., WAGNER, C., FLEISCH, H. & ATKINSON, M. 1996. Characterization and cloning of the E11 antigen, a marker expressed by rat osteoblasts and osteocytes. *Bone.,* 18**,** 125-132.

WHITE, M. J., DICAPRIO, M. J. & GREENBERG, D. A. 1996. Assessment of neuronal viability with Alamar blue in cortical and granule cell cultures. *Journal of Neuroscience Methods,* 70**,** 195-200.

WICKI, A. & CHRISTOFORI, C. 2007. The potential role of podoplanin in tumour invasion. *The British Journal of Cancer,* 96**,** 1-5.

WILLING, M. C., DESCHENES, S. P., SCOTT, D. A., BYERS, P. H., SLAYTON, R. L., PITTS, S. H., ARIKAT, H. & ROBERTS, E. J. 1994. Osteogenesis imperfecta type I: molecular heterogeneity for COL1A1 null alleles of type I collagen. *American Journal of Human Genetics,* 55**,** 638-647.

WILSON, A. J., MURPHY, W. A., HARDY, D. C. & TOTTY, W. G. 1988. Transient osteoporosis: transient bone marrow edema? *Radiology,* 167**,** 757-760.

WINKLER, D. G., SUTHERLAND, M. K., GEOGHEGAN, J. C., YU, C., HAYES, T., SKONIER, J. E., SHPEKTOR, D., JONAS, M., KOVACEVICH, B. R., STAEHLING-HAMPTON, K., APPLEBY, M., BRUNKOW, M. E. & LATHAM, J. A. 2003. Osteocyte control of bone formation via sclerostin, a novel BMP antagonist. *The EMBO Journal,* 22**,** 6267-6276.

WONG, B., JOSIEN, R., LEE, S., VOLOGODSKAIA, M., STEINMAN, R. M. & CHOI, Y. 1998. The TRAF Family of Signal Transducers Mediates NF-κB Activation by the TRANCE Receptor. *The Journal of Biological Chemistry,* 273**,** 28355–28359.

WRIGHT, H. L., MOOTS, R. J. & EDWARDS, S. W. 2014. The multifactorial role of neutrophils in rheumatoid arthritis. *Nature Reviews Rheumatology,* 10**,** 593-601.

WU, L., GUO, H., SUN, K., ZHAO, X., MA, T. & JIN, Q. 2016. Sclerostin expression in the subchondral bone of patients with knee osteoarthritis. *International Journal of Molecular Medicine,* 38**,** 1395-1402.

WULF, E., DEBOBEN, A., BAUTZ, F. A., FAULSTICH, H. & WIELAND, T. H. 1979. Fluorescent phallotoxin, a tool for the visualization of cellular actin. *Proceedings of the National Academy of Sciences of the United States of America,* 76**,** 4498-4502.

XIAO, L., LIU, P., LI, X., DOETSCHMAN, T., COFFIN, J. D., DRISSI, H. & HURLEY, M. M. 2009. Exported 18-kDa isoform of fibroblast growth factor-2 is a critical determinant of bone mass in mice. *The Journal of Biological Chemistry,* 284**,** 3170-3182.

XIAO, L., NAGANAWA, T., LORENZO, J., CARPENTER, T. O., COFFIN, J. D. & HURLEY, M. M. 2010a. Nuclear isoforms of fibroblast growth factor 2 are novel inducers of hypophosphatemia via modulation of FGF23 and KLOTHO. *The Journal of Biological Chemistry,* 285**,** 2834-2846.

XIAO, L., SOBUE, T., ESLIGER, A., KRONENBERG, M. S., COFFIN, J. D., DOETSCHMAN, T. & HURLEY, M. M. 2010b. Disruption of the Fgf2 gene activates the adipogenic and suppresses the osteogenic program in mesenchymal marrow stromal stem cells. *Bone,* 47**,** 360-370.

XIAO, Z., ZHANG, S., MAHLIOS, J., ZHOU, G., MAGENHEIMER, B. S., GUO, D., DALLAS, S. L., MASER, R., CALVET, J. P., BONEWALD, L. & QUARLES, L. D. 2006. Cilia-like structures and polycystin-1 in osteoblasts/osteocytes and associated abnormalities in skeletogenesis and runx2 expression. *The Journal of Biological Chemistry,* 281**,** 30884-30895.

XIE, L., SU, X., ZHANG, L., YIN, X., TANG, L., ZHANG, X., XU, Y., GAO, Z., LIU, K., ZHOU, M., GAO, B., SHEN, D., ZHANG, L., JI, J., GAVINE, P. R., ZHANG, J., KILGOUR, E., ZHANG, X. & JI, Q. 2013. FGFR2 gene amplification in gastric cancer predicts sensitivity to the selective FGFR inhibitor AZD4547. *Clinical cancer research,* 19**,** 2572-2583.

XIONG, J., ONAL, M., JILKA, R. L., WEINSTEIN, R. S., MANOLAGAS, S. C. & O'BRIEN, C. A. 2011. Matrix-embedded cells control osteoclast formation. *Nature Medicine,* 17**,** 1235-1241.

YADAV, M. C., SIMÃO, A. M. S., NARISAWA, S., HUESA, C., MCKEE, M. D., FARQUHARSON, C. & MILLÁN, J. L. 2011. Loss of Skeletal Mineralization by the Simultaneous Ablation of PHOSPHO1 and Alkaline Phosphatase Function: A Unified Model of the Mechanisms of Initiation of Skeletal Calcification. *Journal of Bone and Mineral Research,* 26**,** 286-297.

YAMAGUCHI, A., KOMORI, T. & SUDA, T. 2000. Regulation of osteoblast differentiation mediated by bone morphogenetic proteins, hedgehogs, and Cbfa1. *Endocrine Reviews,* 21**,** 393-411.

YAN, D., CHEN, D., COOL, S. M., VAN WIJNEN, A. J., MIKECZ, K., MURPHY, G. & IM, H.-J. 2011. Fibroblast growth factor receptor 1 is principally responsible for fibroblast growth factor 2-induced catabolic activities in human articular chondrocytes. *Arthritis Research & Therapy,* 13**,** R130-R130.

YAN, D., CHEN, D. & IM, H.-J. 2012. Fibroblast Growth Factor–2 Promotes Catabolism Via FGFR1–Ras–Raf–MEK1/2–ERK1/2 Axis That Coordinates With the PKCδ Pathway in Human Articular Chondrocytes. *Journal of cellular biochemistry,* 113**,** 2856-2865.

YANG, J., ZHANG, D., YU, Y., ZHANG, R. J., HU, X. L., HUANG, H. F. & LU, Y. C. 2015. Binding of FGF2 to FGFR2 in an autocrine mode in trophectoderm cells is indispensable for mouse blastocyst formation through PKC-p38 pathway. *Cell Cycle,* 14**,** 3318-3330.

YANG, Y. 2009. Skeletal Morphogenesis during Embryonic Development. *Critical Reviews in Eukaryotic Gene Expression,* 19**,** 197-218.

YANG, Y. 2013. Skeletal Morphogenesis and Embryonic Development. *Primer on the Metabolic Bone Diseases and Disorders of Mineral Metabolism.* John Wiley & Sons, Inc.

YANG, Y. Q., TAN, Y. Y., WONG, R., WENDEN, A., ZHANG, L. K. & RABIE, A. B. 2012. The role of vascular endothelial growth factor in ossification. *International journal of oral science,* 4**,** 64-68.

YAO, T. J., ZHU, J. H., PENG, D. F., CUI, Z., ZHANG, C. & LU, P. H. 2015. AZD-4547 exerts potent cytostatic and cytotoxic activities against fibroblast growth factor receptor (FGFR)-expressing colorectal cancer cells. *Tumour biology,* 36**,** 5641-5648.

YOSHIMURA, N., SANO, H., HASHIRAMOTO, A., YAMADA, R., NAKAJIMA, H., KONDO, M. & OKA, T. 1998. The expression and localization of fibroblast growth factor-1 (FGF-1) and FGF receptor-1 (FGFR-1) in human breast cancer. *Clinical Immunology and Immunopathology,* 89**,** 28-34.

YUN, Y.-R., WON, J. E., JEON, E., LEE, S., KANG, W., JO, H., JANG, J.-H., SHIN, U. S. & KIM, H.-W. 2010. Fibroblast Growth Factors: Biology, Function, and Application for Tissue Regeneration. *Journal of Tissue Engineering,* 2010**,** 218142.

ZANATTA, L. C. B., BOGUSZEWSKI, C. L., BORBA, V. Z. C. & KULAK, C. A. M. 2014. Osteocalcin, energy and glucose metabolism. *Arquivos Brasileiros de Endocrinologia & Metabologia,* 58**,** 444-451.

ZAREI, A., HULLEY, P. A., SABOKBAR, A. & JAVAID, M. K. 2017. Co-expression of DKK-1 and Sclerostin in Subchondral Bone of the Proximal Femoral Heads from Osteoarthritic Hips. *Calcified Tissue International,* 100**,** 609-618.

ZHANG, J., ZHANG, L., SU, X., LI, M., XIE, L., MALCHERS, F., FAN, S., YIN, X., XU, Y., LIU, K., DONG, Z., ZHU, G., QIAN, Z., TANG, L., SCHOTTLE, J., ZHAN, P., JI, Q., KILGOUR, E., SMITH, P. D., BROOKS, A. N., THOMAS, R. K. & GAVINE, P. R. 2012. Translating the therapeutic potential of AZD4547 in FGFR1-amplified non-small cell lung cancer through the use of patient-derived tumor xenograft models. *Clinical Cancer Research,* 18**,** 6658-6667.

ZHANG, K., BARRAGAN-ADJEMIAN, C., YE, L., KOTHA, S., DALLAS, M., LU, Y., ZHAO, S., HARRIS, M., HARRIS, S. E., FENG, J. Q. & BONEWALD, L. F. 2006. E11/gp38 selective expression in osteocytes: regulation by mechanical strain and role in dendrite elongation. *Molecular and Cellular Biology,* 26**,** 4539-4552.

ZHANG, Q., LIN, S., LIU, Y., YUAN, B., HARRIS, S. E. & FENG, J. Q. 2016. Dmp1 Null Mice Develop a Unique Osteoarthritis-like Phenotype. *International Journal of Biological Sciences,* 12**,** 1203-1212.

ZHANG, R., LU, Y., YE, L., YUAN, B., YU, S., QIN, C., XIE, Y., GAO, T., DREZNER, M. K., BONEWALD, L. F. & FENG, J. Q. 2011. Unique Roles of Phosphorus in Endochondral Bone Formation and Osteocyte Maturation. *Journal of Bone and Mineral Research,* 26**,** 1047-1056.

ZHANG, W., PEI, Y., ZHONG, L., WEN, B., CAO, S. & HAN, J. 2015. Pluripotent and Metabolic Features of Two Types of Porcine iPSCs Derived from Defined Mouse and Human ES Cell Culture Conditions. *PLoS One,* 10**,** e0124562.

ZHANG, Y., SU, N., LUO, F., WEN, X., TANG, Y., YANG, J., CHEN, S., JIANG, W., DU, X. & CHEN, L. 2014. Deletion of Fgfr1 in osteoblasts enhances mobilization of EPCs into peripheral blood in a mouse endotoxemia model. *International Journal of Biological Sciences,* 10**,** 1064-1071.

ZHOU, M., SUTLIFF, R. L., PAUL, R. J., LORENZ, J. N., HOYING, J. B., HAUDENSCHILD, C. C., YIN, M., COFFIN, J. D., KONG, L., KRANIAS, E. G., LUO, W., BOIVIN, G. P., DUFFY, J. J., PAWLOWSKI, S. A. & DOETSCHMAN, T. 1998. Fibroblast growth factor 2 control of vascular tone. *Nature medicine,* 4**,** 201-207.

Appendix 1

Reagents for this work were obtained from Sigma-Aldrich (Dorset, U.K.) and cell/organ culture media and additives were sourced from Thermo Fisher Scientific (Paisley, U.K.) unless otherwise stated.

Cell culture

Culture media

(αMEM supplemented with 10% v/ FBS, and 0.05 mg/ml gentamycin)

Calvariae Culture media

(αMEM containing 0.2% w/v BSA and 0.05 mg/ml gentamycin)

Treatment media

(αMEM supplemented with 1% v/v FBS), and 0.05 mg/ml gentamycin)

Histology

10 mM Citric acid buffer pH 6.0

1.92 g citric acid /1000 ml dH_2O

Tris/EDTA (TE) Buffer (pH 9.0)

10 mM Tris-HCl and 1 mM EDTA in dH2O.

1 mM EDTA (pH 8.0)

0.292g EDTA /1000 ml dH_2O

Sodium acetate buffer (Store at 4^oC)

Disolve 13.6 g in 1 L dH_2O. Stir well

Titrate solution to pH 4 using glacial acetic acid

Immunofluorescence recipe

Blocking buffer

1X PBS / 5% v/v normal serum / 0.3% v/v Triton X-100

Antibody Dilution Buffer

1X PBS / 1% w/v BSA / 0.3% v/v Triton X-100

Appendix 1

Western Blotting

LDS Sample reducing agent

40% glycerol, 4% LDS, 4% Ficoll*-400, 0.8 M triethanolamine-Cl pH 7.6, 0.025% phenol red, 0.025% coomassie G250, 2 mM EDTA disodium

10X Transfer buffer

29.3 mg/ml glycine, 58mg/ml Tris Base (trismethylamine), 18.8ul/ml 20% v/vSDS in dH2O

1X Transfer buffer

100 ml 10X transfer buffer, 200 ml 98% Ethanol, 700 ml dH2O.

TBS/T

Tris-buffered saline/Tween-20 consisting of 50 mM Tris-HCl, 300 mM NaCl, 0.1% v/v Tween-20

1X TBS/T

100 ml TBS/T, 900 ml water, 1 ml Tween 20

MOPS running buffer

50 mM MOPS pH 7.7, 50 mM Tris, 0.1% v/v SDS, 1 mM EDTA

5% Marvel

5 g of skimmed milk powder (Oxoid ltd, UK), in 100 ml of 1X TBS/T,

Stripping buffer

25 mM glycine, 1% v/v SDS and pH2

Bio-Rad DC protein assay Reagent A

1 ml Bio-Rad DC protein assay Reagent A (Bio-Rad, Hertfordshire, UK)

20 uM of Bio-Rad DC protein assay Reagent S (Bio-Rad, Hertfordshire, UK)

Appendix 1

Table 1. Primers used for RT-qPCR analysis.

Gene of Interest	Source	S	Sequence (5′-3′)
E11	Primer Design	F	AACAAGTCACCCCAATAGAGATAAT
		R	CTAACAAGACGCCAACTATGATTC
Dmp1	Primer Design	F	ATACCACAATACTGAATCTGAAAGC
		R	CACTATTTGCCTGTCCCTCTG
ATP5b (Housekeeping)	Primer Design	F	Not disclosed
		R	Not disclosed
Phex	Primer Design	F	CTAACCACCCACTCCCACTT
		R	CCAATAGACTCCAAACCTGAAGA
Sost	Primer Design	F	TGAGAACAACCAGACCATGAAC
		R	TCAGGAAGCGGGTGTAGTG
Col1a1	Primer Design	F	GCTCCTCTTAGGGGCCACT
		R	CCACGTCTCACCATTGGGG
Postn	Primer Design	F	TTCCTCTCCTGCCCTTATATGC
		R	CCTGATCCCGACCCCTGAT
Bglap	Eurofins MWG	F	TGCACGAAAGCAAGATGCTG
		R	GGAGCGTCTGAATAGTCGCC
Alpl	Sigma	F	GGGACGAATCTCAGGGTACA
		R	AGTAACTGGGGTCTCTCTC
Fgfr1	Qiagen	F	Not disclosed
		R	Not disclosed
Fgfr2	Sigma	F	CCTGCGGAGACAGGTAACAG
		R	CGCGTTGTTATCCTCACCA
Fgfr3	Qiagen	F	Not disclosed
		R	Not disclosed
Gapdh	Primer Design	F	Not disclosed
		R	Not disclosed

Appendix Table 2. Primary antibodies

Antibody	Species	Source	Use	Dilution
E11	Goat	R&D Systems	Western Blotting	1:1000
Sost	Goat	R&D Systems	Western Blotting	1:500
p-ERK1/2	Rabbit	Cell Signalling Tech.	Western Blotting	1:1000
Total ERK1/2	Rabbit	Cell Signalling Tech.	Western Blotting	1:1000
pAKT	Rabbit	Cell Signalling Tech.	Western Blotting	1:1000
Total AKT	Rabbit	Cell Signalling Tech.	Western Blotting	1:1000
p-p38	Rabbit	Cell Signalling Tech.	Western Blotting	1:1000
P38	Rabbit	Cell Signalling Tech.	Western Blotting	1:1000
pJNK	Rabbit	Cell Signalling Tech.	Western Blotting	1:1000

Total JNK	Rabbit	Cell Signalling Tech.	Western Blotting	1:1000
β-actin (HP-linked)	Mouse	Sigma	Western Blotting	1:70000
E11	Goat	R&D Systems	Immunohistochemistry	1:500
Sclerostin	Goat	R&D Systems	Immunohistochemistry	1:500
p-ERK1/2	Rabbit	Cell Signalling Tech.	Immunohistochemistry	1:100
E11	Goat	R&D Systems	Immunofluorescence	1:900
p-ERK1/2	Rabbit	Cell Signalling Tech.	Immunofluorescence	1:100

Table 3. Secondary antibodies

Antibody	Source	Use	Dilution
Rabbit anti-goat	Dako	Western Blotting	1:3000
Goat anti-rabbit	Dako	Western Blotting	1:3000
Donkey anti-goat	Abcam	Immunofluorescence	1:250
Donkey anti-rabbit	Abcam	Immunofluorescence	1:250
Rabbit anti-goat	Vector Lab	Immunohistochemistry	1:200
Goat anti-rabbit	Vector Lab	Immunohistochemistry	1:200

Algorithm 1.

[IMARIS 8.4 Algorithm]
Enable Region of Interest = false
Enable Region Growing = false
Enable Tracking = false
[Source Channel]
Source Channel Index = 1
Enable Smooth = true
Surface Grain Size = 0.300 um
Enable Eliminate Background = false
Diameter of Largest Sphere = 0.713 um
[Threshold]
Enable Automatic Threshold = false
Manual Threshold Value = 685.082
Active Threshold = true
Enable Automatic Threshold B = true
Manual Threshold Value B = 4073.13
Active Threshold B = false
[Classify Surfaces]
"Number of Voxels" between 5495 and 2.94e5

Received: 23 June 2017 | Accepted: 29 November 2017
DOI: 10.1002/jcp.26345

ORIGINAL RESEARCH ARTICLE

WILEY Journal of Cellular Physiology

FGF-2 promotes osteocyte differentiation through increased E11/podoplanin expression

Ekele Ikpegbu[1,2] | Lena Basta[1] | Dylan N. Clements[1] | Robert Fleming[1] | Tonia L. Vincent[3] | David J. Buttle[4] | Andrew A. Pitsillides[5] | Katherine A. Staines[6] | Colin Farquharson[1]

[1] Roslin Institute and R(D)SVS, The University of Edinburgh, Edinburgh, UK

[2] Michael Okpara University of Agriculture, Abia, Nigeria

[3] Arthritis Research UK Centre for Osteoarthritis Pathogenesis, Kennedy Institute of Rheumatology, University of Oxford, Oxford, UK

[4] Department of Infection, Immunity & Cardiovascular Disease, The University of Sheffield Medical School, Sheffield, UK

[5] Comparative Biomedical Sciences, The Royal Veterinary College, London, UK

[6] School of Applied Sciences, Edinburgh Napier University, Edinburgh, UK

Correspondence
Katherine Staines, School of Applied Sciences, Edinburgh Napier University, Edinburgh, UK.
Email: k.staines@napier.ac.uk

Funding information
Arthritis Research UK, Grant number: 20413; Biotechnology and Biological Sciences Research Council, Grant numbers: BB/J004316/1, BBS/E/D/20221657; Tertiary Education Trust Fund Nigeria (TETFund)

E11/podoplanin is critical in the early stages of osteoblast-to-osteocyte transitions (osteocytogenesis), however, the upstream events which regulate E11 expression are unknown. The aim of this study was to examine the effects of FGF-2 on E11-mediated osteocytogenesis and to reveal the nature of the underlying signaling pathways regulating this process. Exposure of MC3T3 osteoblast-like cells and murine primary osteoblasts to FGF-2 (10 ng/ml) increased *E11* mRNA and protein expression ($p < 0.05$) after 4, 6, and 24 hr. FGF-2 induced changes in E11 expression were also accompanied by significant ($p < 0.01$) increases in *Phex* and *Dmp1* (osteocyte markers) expression and decreases in *Col1a1*, *Postn*, *Bglap*, and *Alpl* (osteoblast markers) expression. Immunofluorescent microscopy revealed that FGF-2 stimulated E11 expression, facilitated the translocation of E11 toward the cell membrane, and subsequently promoted the formation of osteocyte-like dendrites in MC3T3 and primary osteoblasts. siRNA knock down of E11 expression achieved >70% reduction of basal *E11* mRNA expression ($p < 0.05$) and effectively abrogated FGF-2-related changes in E11 expression and dendrite formation. FGF-2 strongly activated the ERK signaling pathway in osteoblast-like cells but inhibition of this pathway did not block the ability of FGF-2 to enhance E11 expression or to promote acquisition of the osteocyte phenotype. The results of this study highlight a novel mechanism by which FGF-2 can regulate osteoblast differentiation and osteocyte formation. Specifically, the data suggests that FGF-2 promotes osteocytogenesis through increased E11 expression and further studies will identify if this regulatory pathway is essential for bone development and maintenance in health and disease.

KEYWORDS
E11/podoplanin, FGF-2, osteoblasts, osteocytes, osteocytogenesis

Katherine A. Staines and Colin Farquharson are the joint senior authors.

1 | INTRODUCTION

Osteocytes are derived from osteoblasts and are the most abundant cells, residing in mineralized bone of the adult skeleton. It has long been accepted that osteocytes are formed by the passive entrapment of redundant osteoblasts by osteoid synthesized by their close neighbors (Palumbo, Ferretti, & Marotti, 2004; Skerry, Bitensky, Chayen, & Lanyon, 1989). The transition from the cuboidal-like osteoblastic morphology to a dendritic shape characteristic of an osteocyte is, however, a more active and tightly regulated process than originally recognized (for reviews see Dallas & Bonewald, 2010; Franz-Odendaal, Hall, & Witten, 2006).

The mechanisms which govern this osteoblast to osteocyte transition (osteocytogenesis) are generally unknown but fundamental studies by Bonewald and coworkers identified E11/podoplanin, a mucin-type transmembrane glycoprotein, as the earliest osteocyte marker protein expressed during osteocytogenesis (Zhang et al., 2006). Furthermore, E11 triggers actin cytoskeletal dynamics (Staines et al., 2016), which are required for dendrite formation and transient *E11* knockdown blocks dendrite elongation (Zhang et al., 2006). E11 glycoprotein is not unique to bone and is ubiquitously expressed by many tissues in which it has a range of regulatory functions including cell development, differentiation and invasiveness, epithelial–mesenchymal transition, and oncogenesis (Astarita, Acton, & Turley, 2012; Martín-Villar, Yurrita, Fernández-Muñoz, Quintanilla, & Renart, 2009; Thiery, 2002; Wicki & Christofori, 2007). Owing to its wide tissue expression, it is now recognized by several names which include podoplanin in kidney podocytes, T1α in alveolar type 1 epithelial cells, PA2.26 in skin keratinocytes, gp38 in lymphoid organs, and E11 in lymphatic endothelial cells, osteoblasts, and osteocytes (Breiteneder-Geleff et al., 1997; Farr, Nelson, & Hosier, 1992; Ramirez et al., 2003; Scholl, Gamallo, Vilaró, & Quintanilla, 1999; Wetterwald et al., 1996).

The intracellular signaling mechanisms by which E11 influences dendrite formation involve the activation of the small GTPase, RhoA, and its downstream effector kinase, ROCK (Martín-Villar et al., 2006). ROCK phosphorylates ezrin/moesin/radixin (ERM) and influences the actin cytoskeleton and subsequently cell shape (Martín-Villar et al., 2006, 2014; Sprague, Wetterwald, Heinzman, & Atkinson, 1996). Much less, however, is known about the upstream regulatory events, specifically those that influence levels of E11 expression during osteocytogenesis. Nonetheless, clues from other model systems have indicated that fibroblast growth factor 2 (FGF-2) is able to change chondrocyte gene expression in vitro, including that of *E11* (Chong et al., 2013). FGF-2, one of the earliest members identified in the FGF polypeptide family, signals through FGF receptors that have intrinsic tyrosine kinase activity (Powers, Mcleskey, & Wellstein, 2000). In addition to chondrocytes, FGF-2 is expressed by osteoblasts and is stored in the extracellular matrix where it regulates bone formation via influence on progenitor cell lineage commitment and/or osteoblast differentiation (Hurley, Marie, & Florkiewicz, 2002; Montero et al., 2000; Sabbieti et al., 1999; Xiao et al., 2010). Indeed, mice deficient in *Fgf2* have decreased bone mass and altered trabecular architecture whereas *Fgf2* transgenic mice present with increased bone mineral density and cortical and trabecular thickness, as well as a variety of skeletal malformations including shortening and flattening of long bones (Coffin et al., 1995; Montero et al., 2000; Xiao et al., 2009).

Cognizant of FGF-2 stimulation of E11 expression in cartilage explants and osteoblast-like cells, we, therefore, hypothesized that FGF-2 may influence bone remodeling via increased osteoblast E11 expression and concomitant osteocyte dendrite formation (Chong et al., 2013; Gupta, Yoo, Hebert, Niger, & Stains, 2010). Hence, the aims of this current study were to examine the effects of FGF-2 on E11 expression in osteoblasts during osteocytogenesis and to explore putative signaling pathways controlling this process.

2 | MATERIALS AND METHODS

2.1 | Animals

FGF-2-deficient mice (KO) were originally created by Tom Doetschman and obtained from the Jackson Laboratory, and were backcrossed onto a C57BL/6J wild-type (WT) background (Chong et al., 2013). Animal experiments were performed after obtaining ethical and statutory approval in accordance with local policy. Mice were maintained in accordance with UK Home Office guidelines for the care and use of laboratory animals.

2.2 | MC3T3 cell culture

Murine MC3T3-E1 (subclone 14), pre-osteoblast-like cells (American Type Culture Collection [ATCC], Manassas, VA) were plated at 1×10^4 cells/cm^2 in six-well plates and cultured in α-MEM medium supplemented with 10% (v/v) FBS (Invitrogen, Paisley UK) and 50 μg/ml gentamicin (Invitrogen) at 37°C in a humidified atmosphere with 5% CO_2 and the medium was changed every 2–3 days. Cell viability was assessed using a commercially available Alamar Blue kit (Invitrogen) and cell cytotoxicity using an LDH assay according to the manufacturer's instructions (Promega, Southampton, UK).

2.3 | Primary osteoblast isolation

Primary calvarial osteoblasts were obtained from 3-day-old WT mice by serial enzyme digestion of dissected calvarial bones according to published procedure (Orriss, Hajjawi, Huesa, Macrae, & Arnett, 2014; Staines, Zhu, Farquharson, & Macrae, 2014). In brief, calvaria were digested in 1 mg/ml collagenase type II (Thermo Fisher Scientific, Loughborough, UK) in Hanks' balanced salt solution (HBSS) for 10 min and the supernatant discarded; then repeat digestion in 1 mg/ml collagenase type II in HBSS for 30 min; 4 mM EDTA for 10 min and finally 1 mg/ml collagenase type II in HBSS for 30 min. After discarding the first digest, the cells were re-suspended in growth medium consisting of α-MEM supplemented with 10% (v/v) FBS and gentamycin at 50 μg/ml. Osteoblasts were seeded at a density of 1×10^4 cells/cm^2, and incubated at 37°C/5%CO_2 with media changes every 2–3 days.

2.4 | FGF-2 treatments

When MC3T3 cells and primary osteoblasts were confluent (day 0), the culture media were replaced with α-MEM supplemented with 1% (v/v) FBS, 50 μg/ml gentamicin and 0-50 ng/ml FGF-2 (PeproTech, London, UK) in 0.1% bovine serum albumin (BSA). Each test condition was completed in triplicate.

2.5 | Signaling inhibitors

MC3T3 cells were incubated with appropriate concentrations (specific details in results) of the MEK1/2 inhibitor, U0126, the PI3K inhibitor, LY294002 (InvivoGen, Toulouse, France), and the p38 inhibitor, SB203580 (Cell Guidance Systems, Cambridge, UK). These inhibitors have been reported to be selective for these molecules (Choi et al., 2008; Hotokezaka et al., 2002; Macrae, Ahmed, Mushtaq, & Farquharson, 2007). Control cultures contained vehicle (0.1% dimethylsulfoxide, DMSO) only.

2.6 | RNA extraction and quantitative real-time PCR (RT-qPCR)

Total RNA was extracted from MC3T3 cells and primary osteoblasts using a Qiagen RNeasy Mini kit (Qiagen, Manchester, UK) according to the manufacturer's recommendations. The RNA samples were reverse-transcribed into cDNA using Superscript II reverse transcriptase (Invitrogen) according to the manufacturer's instructions. RT-qPCR was carried out in a Stratagene Mx3000P cycler with each reaction containing 50 ng template cDNA, 250 nM forward and reverse primers (Supplementary Table S1), and PrecisionPlus Mastermix (Primer Design, Chandler's Ford, UK). The cycle threshold (Ct) values for the samples were normalized to that of *Atp5b* or *Gapdh* (Supplementary Table S1) and the relative expression was calculated using the 2ΔCt method (Livak & Schmittgen, 2001).

2.7 | Western blotting

Cells were scraped in RIPA lysis buffer containing protease inhibitors (Roche, Germany), and protein concentrations were determined using the Bio-Rad protein DC assay (Bio-Rad, Hemel Hempstead, UK). Protein (8–15 μg) was separated using a 10% Bis-Tris gel and then transferred to a nitrocellulose membrane and probed with appropriate primary antibody (Supplementary Table S2), and appropriate HRP-linked secondary antibody (Supplementary Table S3). Immune complexes were visualized by chemiluminescence using an ECL detection kit and ECL film (GE Healthcare, Amersham, UK). HRP-conjugated anti β-actin antibody (1:70,000, Sigma, Dorset UK) was used as a loading control. Densitometry analysis of protein was performed using Image J (https://imagej.nih.gov/ij/) (Baldari, Ubertini, Garufi, D'orazi, & Bossi, 2015).

2.8 | E11 immunofluorescence

MC3T3 cells were plated on cover slips at a density of 6.3×10^3 cells/cm^2 and following treatment with FGF-2, were fixed with 4% paraformaldehyde (PFA) for 15 min, washed in PBS and incubated in blocking buffer (1× PBS, 5% normal donkey serum and 0.3% Triton X-100) for 1 hr at room temperature (RT). E11 antibody (Supplementary Table S2) was added to each well (1:900 in 1× PBS, 0.3% Triton X-100 and 1% BSA) overnight at 4°C. Control cells were incubated with an equivalent concentration of goat IgG (Supplementary Figure S1). Wells were subsequently incubated with AlexaFluor-conjugated donkey anti-goat secondary antibodies (Supplementary Table S3) in the dark for 2 hr at RT. Glass coverslips were then mounted onto slides using ProLong Gold antifade reagent with DAPI (Thermo Fisher Scientific) for nuclei staining (Dobie, Macrae, Huesa, Van't Hof, & Ahmed, 2014). The slides were finally visualized using a Leica DMRB fluorescence microscope and images were taken with a Leica DFC300 digital color camera (Leica, Milton Keynes, UK).

2.9 | Transfection of MC3T3 cells with E11 siRNA

E11 siRNA and scrambled siRNA stocks (Qiagen) were diluted to 10nM. MC3T3 cells were plated at 8×10^3 cells/cm^2 and maintained in reduced serum medium. Cells were transfected as per manufacturer's instructions with complexes of E11siRNA with HiPerFect (Qiagen), while control cells were transfected with either complexes of scrambled siRNA, with HiPerFect; or HiPerFect alone. After 24 hr incubation at 37°C/5%CO_2, FGF-2 (10 ng/ml) was added for a further 24 hr to the cells containing the siRNA/HiPerFect complexes or the HiPerFect alone.

2.10 | Immunohistochemistry

The knee joints of 6-week-old male FGF-2 KO and WT mice (Chong et al., 2013), were fixed in 4% PFA for 24 hr before decalcification in 10% ethylenediaminetetraacetic acid (EDTA) pH 7.4 for approximately 3 weeks at 4°C with regular changes. Tissues were dehydrated and embedded in paraffin wax, using standard procedures, after which they were sectioned at 6 μm. Sections were dewaxed in xylene, rehydrated, and incubated at 37°C for 30 min in 1 mg/ml trypsin for antigen demasking. Endogenous peroxidases were blocked by treatment with 3% H_2O_2 in methanol. E11 and sclerostin antibodies (Supplementary Table S2) were used with appropriate IgG controls and secondary antibodies (Supplementary Table S3). The Vectastain ABC universal kit (Vector Laboratories, Peterborough, UK) was used according to the manufacturer's instructions. The sections were dehydrated, counterstained with haematoxylin and mounted in DePeX. Images were captured with Nikon Eclipse Ni microscope (Nikon, UK), fitted with Zeiss Axiocam 105 color camera (Carl Zeiss). The number of positively stained E11 osteocytes within diaphyseal cortical bone were calculated as a percentage of total osteocytes present.

2.11 | Phalloidin staining for cell culture

MC3T3 cells were seeded at 1×10^4 cells/cm^2 and when subconfluent they were treated with 10 ng/ml FGF-2 or 0.1% BSA for

control cultures. After 24 hr, the cells were fixed in 4% PFA, rinsed in PBS and permeabilized in 0.1% (w/v) triton X-100 (Sigma) in PBS for 10 mins, and then rinsed in PBS. The cells were incubated in 200 µl of Alexa Fluor 488-conjugated phalloidin (Thermo Fisher Scientific) (5 µM in PBS with 2% BSA) in the dark at RT for 3 hr. The cells were imaged on a Zeiss Axiovert 25s inverted microscope and digital imaging system (Carl Zeiss Microscopy, LLC, Oberkochen, Germany).

2.12 | Phalloidin staining for histological sections

Femurs were decalcified as described above and then cryoprotected in 30% sucrose (w/v) at 4°C for 48 hr. The femora were cut in the mediolateral plane in serial longitudinal 20 µm thick-sections using a cryostat and thaw-mounted on gelatin-coated slides for processing. Slides were dried at room temperature for 45 min, washed in PBS twice for 5 min each, and incubated with 0.1% Triton-X 100 (Sigma-Aldrich) for 30 min and then rinsed with PBS. Slides were then incubated with Alexa Fluor 488-conjugated phalloidin (1:20; Thermo Fisher Scientific) for 1 hr. Bone sections were washed in PBS and mounted in VectaShield (Vector Laboratories). Preparations were allowed to dry at room temperature for 12 hr. Sections were imaged on a Zeiss LSM 710 Laser Scanning Confocal Microscope with 488 nm laser excitation and detection settings from 493 to 634 nm. Z-stacks were produced with optimal Nyquist overlap settings using a 63×/1.4na oil immersion lens. Voxel sizes were 0.1 × 0.1 × 1.00 µm in *x*,*y*,*z* planes, respectively. A comparable region of interest was analyzed for osteocyte parameters in all samples located in the diaphyseal cortical bone. Image stacks were imported into Bitplane Imaris 8.2.0 software and algorithms were created with Imaris FilamentTracer to render and measure dendritic processes. Surface rendering was used for osteocyte cell body measurements.

2.13 | Statistical analysis

Data are expressed as the mean ± standard error of the mean (S.E.M) of at least three replicates per experiment. Statistical analysis was performed by Student's *t*-test, one-way analysis of variance (ANOVA) or a suitable non-parametric test. $p < 0.05$ was considered to be significant and noted as $^{*}p$ values of <0.01 and <0.001 were noted as ** and ***, respectively.

3 | RESULTS

3.1 | FGF-2 promotes osteoblast E11 gene and protein expression

Treatment of MC3T3 cells with 10 ng/ml FGF-2 for 4, 6, and 24 hr stimulated *E11* mRNA expression in comparison to control cultures, at all time-points examined ($p < 0.05$, Figure 1a). We observed a concomitant increase in E11 protein expression in these cells (Figure 1b). Stimulation of *E11* mRNA ($p < 0.05$, Figure 1c) and E11 protein (Figure 1d) expression by FGF-2 was similarly noted in primary osteoblast cultures. The levels of FGF-2 induced E11mRNA and protein were more prominent in the MC3T3 cells at the early time points (4 and 6 hr), whereas in primary cells these increases peaked at the later time points (24 hr) (Figure 1).

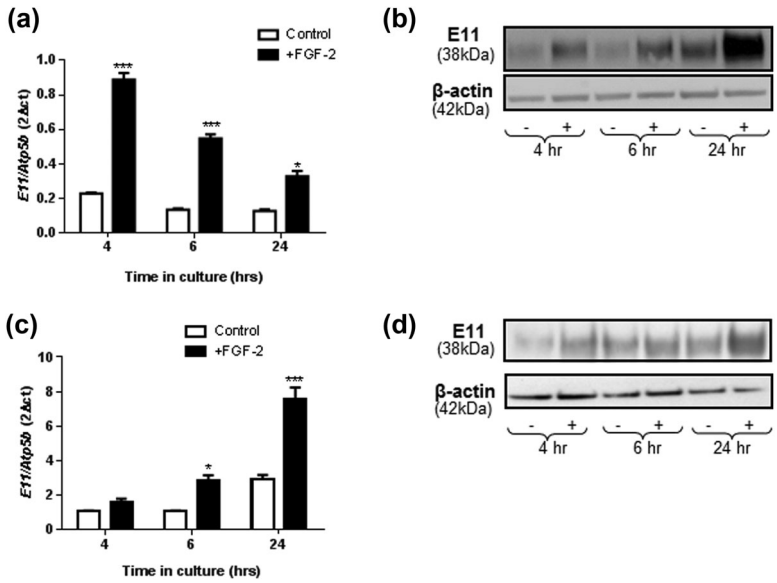

FIGURE 1 The effect of FGF-2 (10 ng/ml) on (a) *E11* mRNA expression and (b) E11 protein expression in MC3T3 cells after 4, 6, and 24 hr challenge, where (+) is FGF-2 treated cell, and (−) is untreated control. The effect of FGF-2 (10 ng/ml) on (c) *E11* mRNA expression and (d) E11 protein expression in primary osteoblast cells after 4, 6, and 24 hr challenge, where (+) is FGF-2 treated cell, and (−) is untreated control. Results were normalized to the *Atp5b* housekeeping gene and β-actin for Western loading control. Data are presented as mean ± S.E.M for $n = 3$; $^{*}p < 0.05$; $^{***}p < 0.001$ compared to untreated cells

3.2 | FGF-2 promotes osteoblast–osteocyte differentiation

In light of the increased E11 expression by FGF-2, we next examined the expression of known osteocyte and osteoblast marker genes to determine whether exposure of osteoblast-like cells to FGF-2 promoted osteocytic differentiation. In MC3T3 cells, FGF-2 increased the mRNA expression of the osteocyte marker *Phex* (phosphate regulating endopeptidase homolog, X-linked) at 4 ($p < 0.01$), 6 (not significant), and 24 ($p < 0.001$) hours (Figure 2a). Similarly, *Dmp1* (dentin matrix protein 1) expression was significantly increased at both 6 and 24 hr in MC3T3 cells ($p < 0.001$; Figure 2b). In primary osteoblasts, both *Phex* and *Dmp1* mRNA expressions were also increased by FGF-2 treatment, although the temporal changes were slightly different to those observed in the MC3T3 cells. Specifically, the stimulation of *Phex* expression by FGF-2 was greater at late time points whereas the up-regulation of *Dmp1* was noted at earlier time points when compared with MC3T3 cells (Figures 2c and 2d).

In contrast to the increased expression of osteocyte markers by FGF-2, there was a consistent downward trend in the mRNA expression of the osteoblast markers *Col1a1* (collagen type 1), *Bglap* (osteocalcin), *Alpl* (tissue non-specific alkaline phosphatase), and *Postn* (periostin) in MC3T3 cells treated with exogenous FGF-2 (Figure 3a–d). This down-regulation of osteoblastic marker expression was most consistently observed 24 hr after exposure to FGF-2, although *Alpl* expression was also reduced at 4 ($p < 0.001$) and 6 ($p < 0.01$), as well as 24 ($p < 0.001$) hour time points (Figure 3c). A similar down-regulation of *Col1a1*, *Bglap*, *Alpl*, and *Postn* expression was also observed in FGF-2 treated primary osteoblast cells, which was also most pronounced at longer (24 hr) times following FGF-2 challenge (Figure 3e–h). Together these data indicate that exposure of MC3T3 as well as primary osteoblasts to exogenous FGF-2 promotes early expression of both E11 and osteocyte markers, with a diminution in the expression levels of markers of the osteoblast phenotype following only at later time points.

Assessment of cell viability in the FGF-2 treated MC3T3 cells by the alamar blue assay revealed that after 24 hr of FGF-2 treatment there was no significant differences between the control and FGF-2 treated cells (Figure 3i). We also observed a significant reduction in LDH release in our FGF-2 treated cells ($p < 0.05$, Figure 3j) suggesting that there is less cell death. Taken together, these data are consistent with FGF-2 promoting E11 expression and osteoblast–osteocyte differentiation in vitro.

3.3 | FGF-2 promotes E11 dependent osteocyte dendrite formation

The differential regulation of osteoblast and osteocyte marker genes, including *E11*, by FGF-2 strongly supports the tenet that FGF-2 can induce osteocytogenesis. To examine this further, we next investigated whether FGF-2 promotes the differentiation of MC3T3 osteoblast-like cells into osteocytes with the adoption of their characteristic dendritic appearance through alterations to the intracellular cytoskeleton. We found that Phalloidin stained control cells displayed a typical rounded morphology with little evidence of dendrite formation (Figure 4a). In contrast, cells treated with FGF-2 for 24 hr displayed numerous delicate dendrites radiating from individual cells and intertwining and connecting with dendrites from neighbouring cells, in a manner characteristic of an osteocyte-like phenotype (Figure 4b). To clarify E11 involvement in this FGF-2

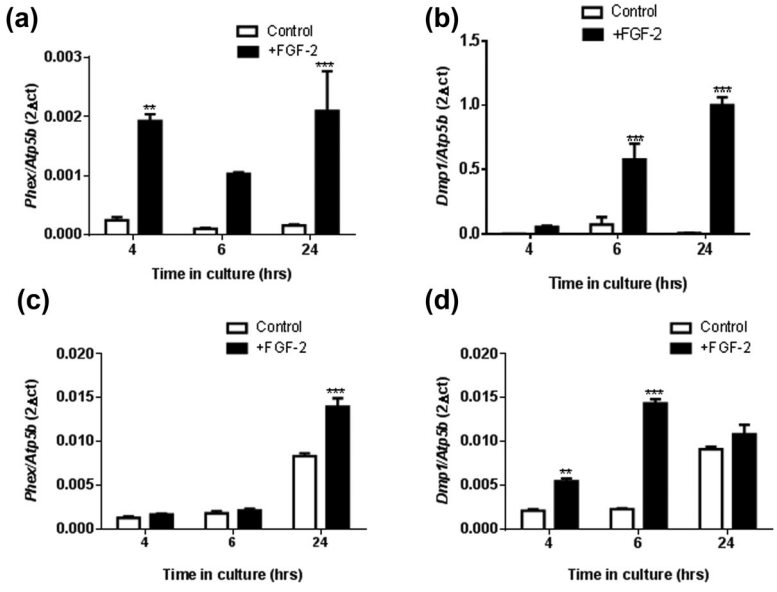

FIGURE 2 The effect of FGF-2 (10 ng/ml) on the mRNA expression of (a) *Phex* and (b) *Dmp1* in MC3T3 cells after 4, 6, and 24 hr challenge. The effect of FGF-2 (10 ng/ml) on the mRNA expression of (c) *Phex* and (d) *Dmp1* in primary osteoblast cells after 4, 6, and 24 hr challenge. Results were normalized to the *Atp5b* housekeeping gene. Data are presented as mean ± S.E.M for $n = 3$; $^{**}p < 0.01$; $^{***}p < 0.001$ compared to untreated cells

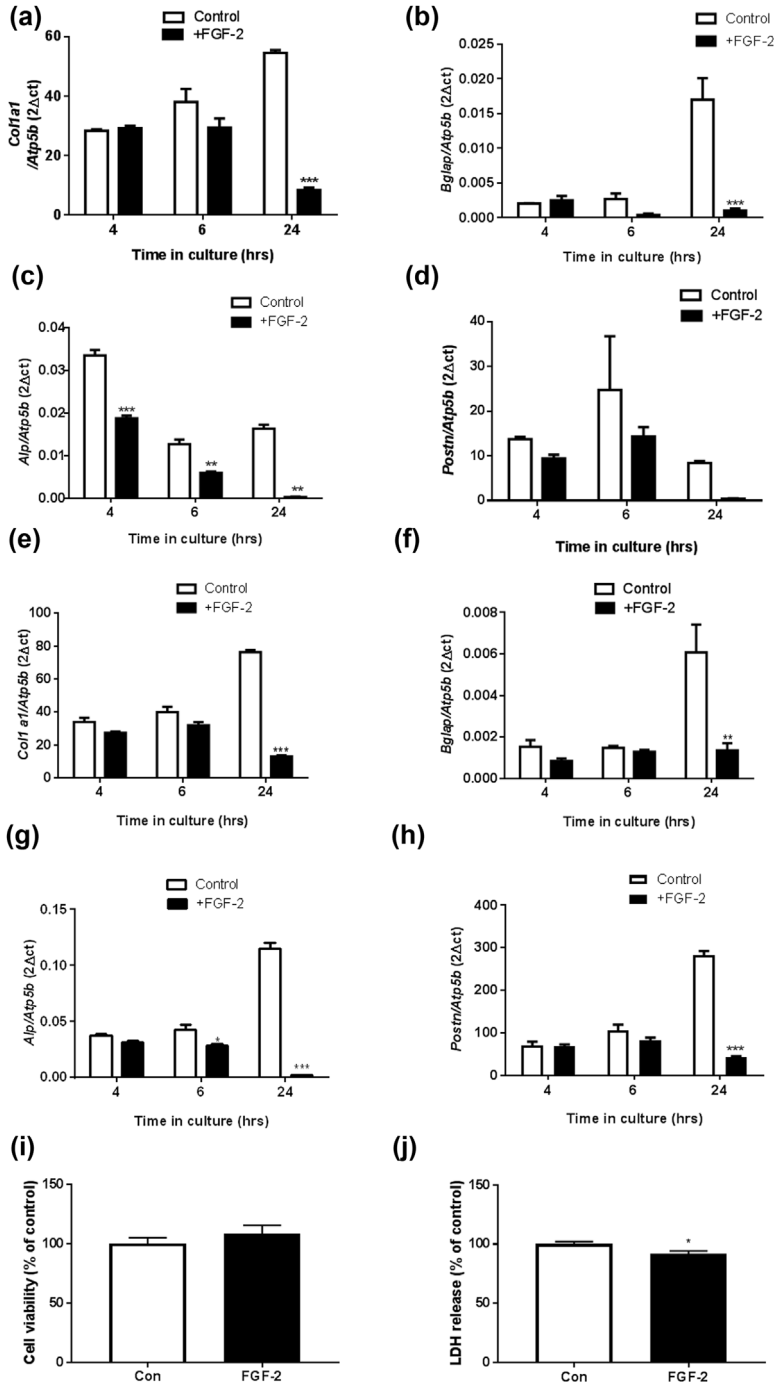

FIGURE 3 The effect of FGF-2 (10 ng/ml) on the mRNA expression of (a) *Col1a1*, (b) *Bglap*, (c) *Alpl*, and (d) *Postn* in MC3T3 cells after 4, 6, and 24 hr challenge. The effect of FGF-2 (10 ng/ml) on the mRNA expression of (e) *Col1a1*, (f) *Bglap*, (g) *Alpl*, and (h) *Postn* in primary osteoblast cells after 4, 6, and 24 hr challenge. Results were normalized to the *Atp5b* housekeeping gene. (i) Alamar blue assay for cell viability and (j) LDH release assay in FGF-2 treated MC3T3 cells after 24 hr treatment. Data are presented as mean ± S.E.M for $n = 3$; $^{*}p < 0.05$; $^{**}p < 0.01$; $^{***}p < 0.001$ compared to untreated cells

induced change to dendritic phenotype, MC3T3 cells were challenged with FGF-2 for 24–72 hr and immunostained for E11 (Figure 4c). All FGF-2 treated MC3T3 cells exhibited modified morphology with numerous E11 positive dendritic processes radiating from the cell membrane (Figure 4c); these were only rarely observed in control cells. Furthermore, the distribution of intra-cellular E11 expression changed with both time in culture and FGF-2 treatment. In control cells, it was mostly uniformly distributed within the cytoplasm but after 72 hr in culture, cytoplasmic staining appeared less strong and the predominant staining was associated with focal accumulations at the cell membrane (Figure 4c). This redistribution of E11 to the cell membrane was more obvious and

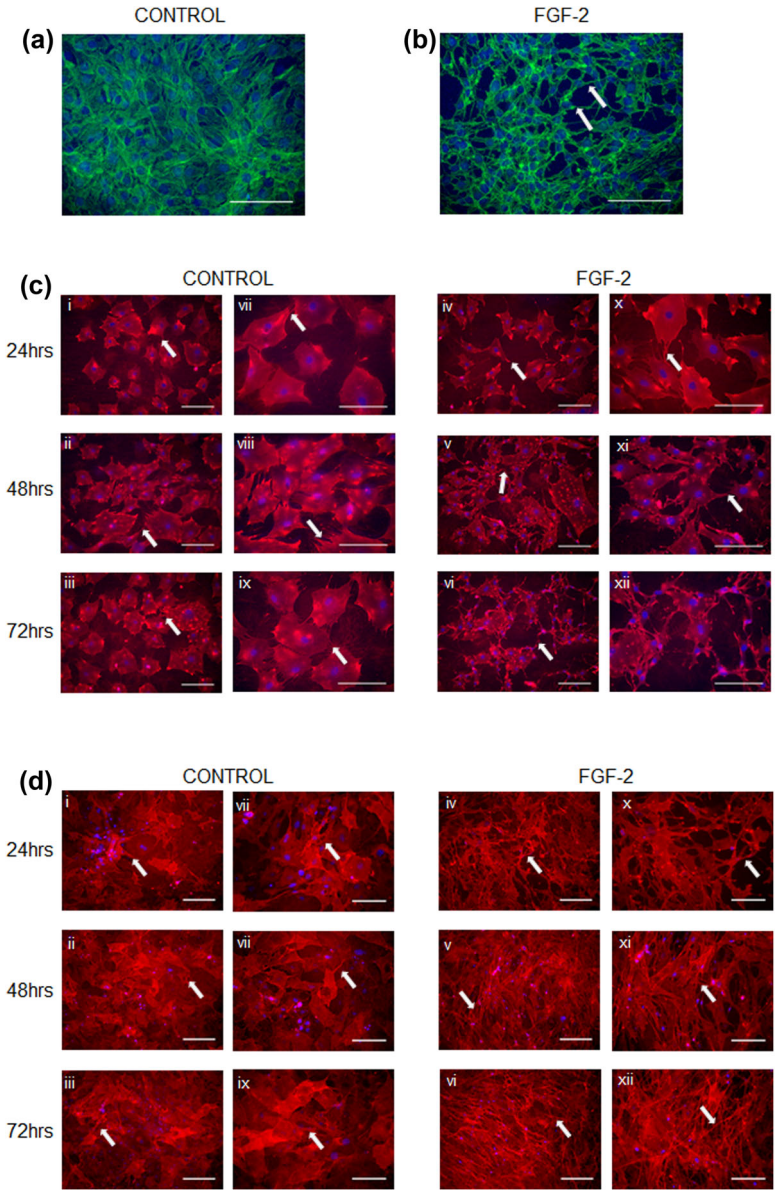

FIGURE 4 The effect of FGF-2 (10 ng/ml) on MC3T3 osteoblast-like cell morphology. (a) Phalloidin staining for F-actin of control cultures, and (b) FGF-2 treated cultures. Scale bar A & B = 150 µm). Immunofluorescence microscopy showing E11 expression and distribution in cells treated with FGF-2 (10 ng/ml) for 24–72 hr in (c) MC3T3, and (d) primary osteoblasts. Note the arrows pointing at the dendrites. Images are representative of three separate experiments. Scale bar c & d (i–vi) = 200 µm; c & d (vii–xii) = 150 µm)

more rapid in the FGF-2 treated cells, where it was achieved within only 24 hr of treatment (Figure 4c). Similarly, FGF-2 promoted dendrite formation and the re-distribution of E11 expression in primary osteoblast cultures (Figure 4d). To determine if the promotion of the osteocyte phenotype by FGF-2 was E11 mediated we studied cells in which MC3T3 cells were transfected with E11 siRNA before being challenged with FGF-2 for 24 hr. E11 gene (77% vs. mock control, 70% vs. scrambled control; $p < 0.05$; Figure 5a) and protein (Figure 5b) expression were silenced successfully by E11 siRNA transfection. Immunofluorescence labeling for E11 and phalloidin staining indicated that compared with mock or scrambled control cell cultures, cells treated with FGF-2 developed less dendrites after silencing of E11 expression (Figures 5c and 5d).

3.4 | FGF-2 cell signaling in MC3T3 cells is mediated principally by phosphorylated ERK

FGF receptors (*Fgfr*) 1, 2, and 3, but not *Fgfr4*, were found to be expressed by MC3T3 cells (data not shown). FGF-2 treatment had no effect on *Fgfr1* expression at all-time points studied (Figure 6a), however, it reduced *Fgfr2* ($p < 0.01$; Figure 6b) and *Fgfr3* ($p < 0.05$; Figure 6c) expression after 4 and 24 hr. Treatment of MC3T3 cells with FGF-2 for 15 min revealed that of the pathways examined, there was particularly marked ERK (p44/p42) activation ($p < 0.001$; Figures 6d and 6e), while in comparison there was only slight activation of both Akt ($p < 0.01$; Figures 6d and 6f) and p38 ($p < 0.05$; Figures 6d and 6g), and no effect on JNK phosphorylation (Figures

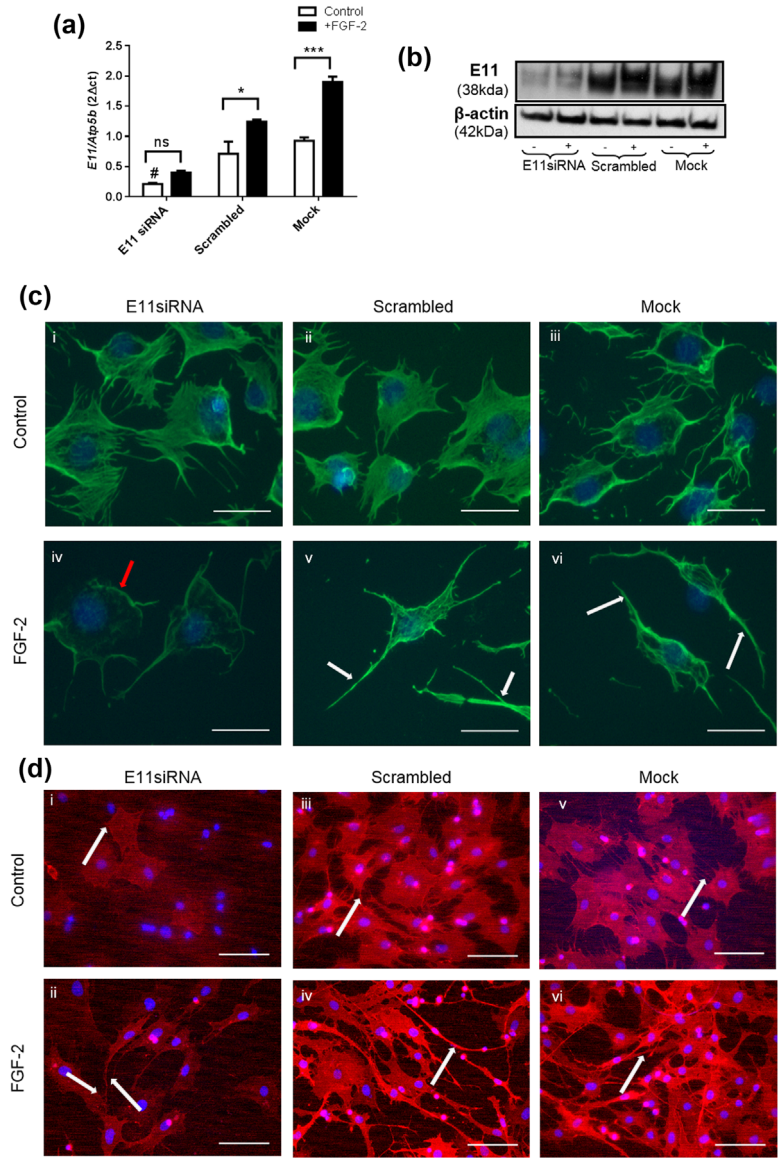

FIGURE 5 The effect of E11siRNA transfection on FGF-2 (10 ng/ml) stimulation of *E11* (a) mRNA. Results were normalized to the *Atp5b* housekeeping gene. Data are presented as mean ± S.E.M for $n = 3$; $^{*}p < 0.05$; $^{***}p < 0.001$ compared to untreated control cells; $\#p < 0.05$ refers to significant decrease of E11siRNA control when compared to the controls of scrambled and Mock treated cells (b) The effect of FGF-2 (10 ng/ml) on E11 protein expression after E11 siRNA transfection, where (+) is FGF-2 treated cells, and (−) is untreated cells. Results are normalized to β-actin for loading control. (c) Phalloidin staining for F-actin in E11 siRNA, mock and scrambled cultures. Images are representative of three separate experiments. Scale bar = 100 μm. (d) Immunofluorescence staining for E11 localization in E11 siRNA, mock and scrambled cultures. Images are representative of three separate experiments. Scale bar = 150 μm

6d and 6h). Furthermore, the temporal expression of ERK activation upon FGF-2 treatment revealed a sustained activation over a 48 hr period (Figure 6i), which has been shown previously to be associated with pathways leading to cell differentiation (Pellegrino & Stork, 2006). These data suggest that ERK activation, rather than phosphorylation of alternative Akt, p38, or JNK mediated signaling pathways is likely most influential in regulating E11 downstream of FGF-2.

To further explore the likely role of MEK-ERK signaling in FGF-2 induced differentiation of osteoblast-like cells into osteocytes, we next treated MC3T3 cells with the ERK inhibitor U0126 (25 μM) in the presence or absence of FGF-2 (15 min). While ERK activation by FGF-2 was blunted by U0126 (15 min) treatment (Figure 7a), the prolonged treatment of cells with U0126 (24 hr) did not affect the ability of FGF-2 to enhance E11 gene expression (Figures 7b and 7c). Similarly, treatment of MC3T3 cells with p38 (SB203580) or PI3K (LY294002) inhibitors did not affect the ability of FGF-2 to enhance E11 expression (Figure 7d–g). Further investigations indicated that Akt activation was increased in the presence of MEK inhibition by U0126 and FGF-2 treatment (Figure 7h) and it is possible that this

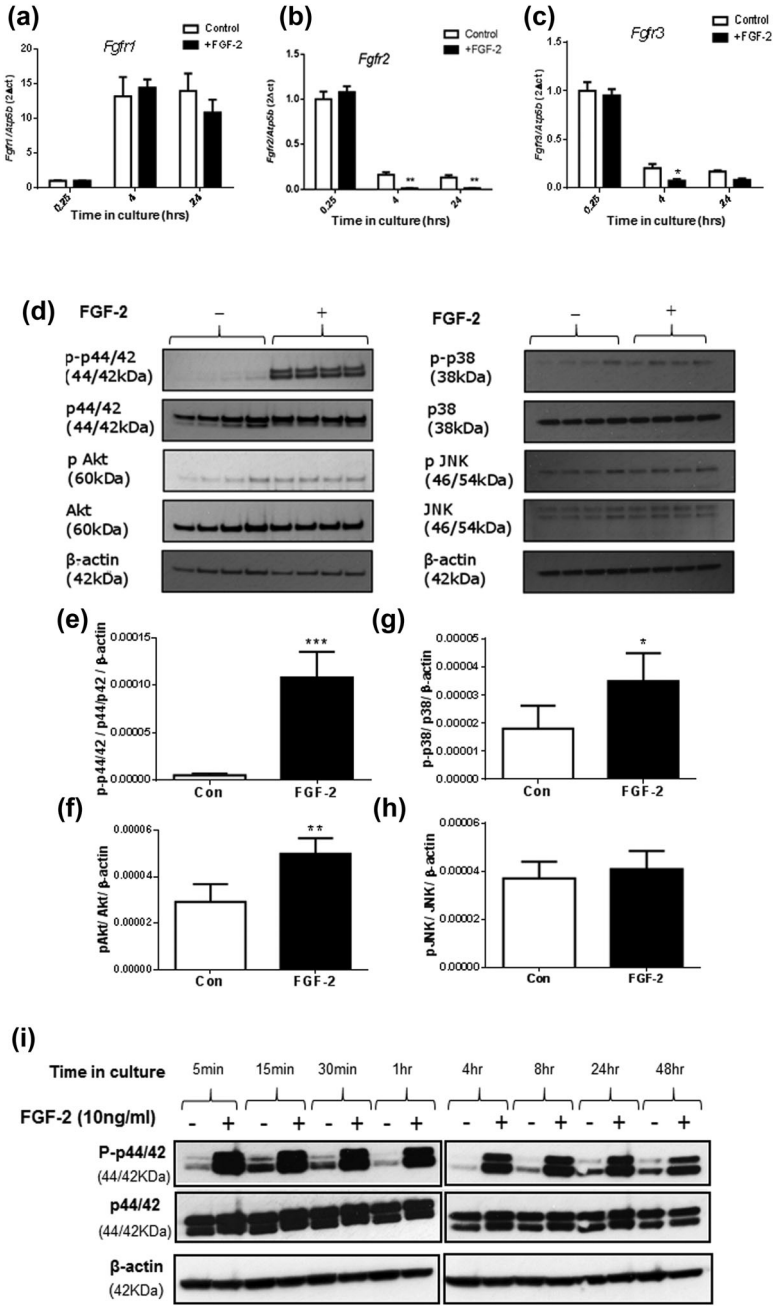

FIGURE 6 The effect of FGF-2 (10 ng/ml) on the mRNA expression of (a) *Fgfr1*, (b) *Fgfr2*, and (c) *Fgfr3* in MC3T3 cells after 4, 6, and 24 hr challenge. Investigating the downstream signaling pathways involved in FGF-2 stimulation of E11 expression. (d) Western blotting analysis of MC3T3 cells for phosphorylated and total p44/42 (ERK), Akt, p38, and JNK. Densitometry analysis of Western blotting revealed significant upregulation of activated (e) p44/42, (f) Akt, and (g) p38 in treated MC3T3 cells with FGF-2 when compared to control cells. There was no significant increase in (h) JNK expression in both cultures. (i) Western blotting analysis of MC3T3 cells for phosphorylated and total p44/42, in MC3T3 cells treated with FGF-2 when compared to control cells showed an increase in phosphorylated p44/42 in the treated cells at all time points. Results were normalized to the *Atp5b* housekeeping gene and β-actin for Western blotting loading control. Data are presented as mean ± S.E.M for $n = 4$ and analyzed with student *t*-test. $^{*}p < 0.05$; $^{**}p < 0.01$; $^{***}p < 0.001$

increased Akt signaling may be a compensatory change to allow FGF-2 to promote E11 expression in the absence of full ERK activation (Figures 7b and 7c). However, the combined inhibition of MEK and PI3K signaling by the inhibitors U0126 and LY294002, respectively, did not affect the ability of FGF-2 to enhance E11 protein expression (Figure 7i).

3.5 | Deletion of FGF-2 in vivo results in dysfunctional osteocytogenesis

Finally, we used immunohistochemistry to examine whether FGF-2 KO mice exhibited altered skeletal E11 expression and distribution. Unexpectedly, E11 staining in osteocytes situated within trabecular

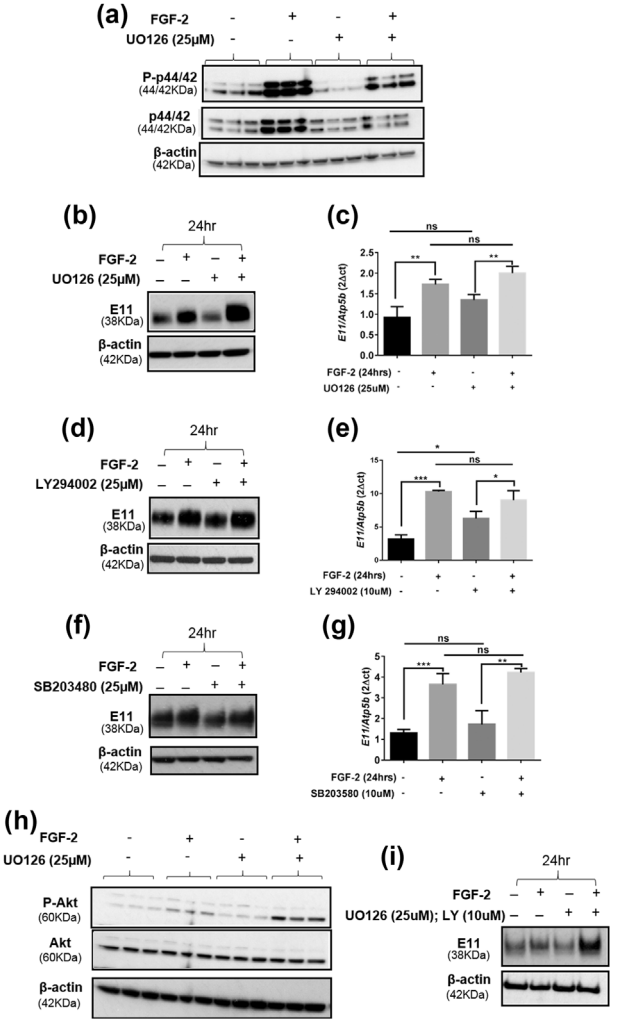

FIGURE 7 (a) Western blot analysis of ERK signaling in the presence (+) and absence (−) of U0126 (25 μm) incubation and subsequent FGF-2 treatment. (b) Western blotting and (c) RT-qPCR analysis of cells stimulated with FGF-2 for 24 hr, in the presence or absence of U0126 (ERK inhibition). (d) Western blotting and (e) RT-qPCR analysis of cells stimulated with FGF-2 for 24 hr, in the presence or absence of LY294002 (Akt inhibition). (f) Western blotting and (g) RT-qPCR analysis of cells stimulated with FGF-2 for 24 hr, in the presence or absence of SB203480 (p38 inhibition). Effect of UO126 (25 μM) on Akt protein expression by (h) Western blotting. (i) Effect of U0126 (25 μM) and LY294002 (10 μM), P-ERK, and P-Akt inhibitors, respectively, on E11 protein expression. Results were normalized to the *Atp5b* housekeeping gene and β-actin for Western blotting loading control. Data are represented as mean ± S.E.M for $n = 3$. Data are analyzed via one-way ANOVA; $p < 0.05$ was considered to be significant. $^*p < 0.05$

and cortical bone of FGF-2 KO mice appeared stronger than in osteocytes from WT bones (Figure 8a–d). Quantification of the number of E11 positive cells was, however, similar to those noted in bones from WT mice (Figure 8e). No differences in sclerostin expression or distribution in bones of FGF-2 KO mice in comparison to those from WT mice were observed (data not shown). Histological analysis of osteocyte morphology in FGF-2 KO mice revealed apparent increases in cell body volume (Figure 8a–d). To confirm and extend these results, we performed phalloidin staining of osteocytes in the cortical bone of FGF-2 KO and WT mice (Figures 9a and 9b). We observed a significant increase in cell body volume ($p < 0.05$, Figure 9c) in concordance with our histological observations. Despite this, no differences in cell sphericity were observed (Figure 9d). Similarly, the total number of dendrites (Figure 9e) and the dendrite volume (Figure 9f) were unchanged between FGF-2 KO and WT mice. We did, however, observe a significant decrease in average dendrite volume in FGF-2 KO in comparison to WT mice ($p < 0.01$; Figure 9g), suggestive of dysfunctional osteocytogenesis in FGF-2 KO mice.

4 | DISCUSSION

The transmembrane glycoprotein E11, has recently been recognized to be an early driver of the osteoblast to osteocyte transition and the acquisition of the dendritic phenotype (Gupta et al., 2010; Zhang et al., 2006). Consistent with previous data, here we reveal that FGF-2 is able to increase E11 expression and promotes osteocyte dendrite formation, likely independent of intracellular signaling pathways that may involve concomitant FGF-2 induced ERK activation.

Previous brief reports have shown that FGF-2 treatment of osteoblast-like cells induces an increase in E11 expression and the appearance of the osteocyte phenotype (Gupta et al., 2010; Miyagawa et al., 2014). In this present study, we confirm and extend these observations in both MC3T3 osteoblast-like cells and primary osteoblasts. The significant upregulation of *E11*, *Phex*, and *Dmp1* and down-regulation of *Col1a1*, *Bglap*, *Alpl*, and *Postn* in the FGF-2 treated cultures suggests that FGF-2 promotes the differentiation of the osteoblast to the osteocyte stage. Concomitant with this, fluorescence microscopy of cultured cells also disclosed altered E11 expression and localization within the differentiating osteoblast in response to FGF-2. The presence of increased E11 in the cytoplasm and perinuclear area suggests that FGF-2 not only stimulates E11 expression, but also facilitates the translocation of E11 toward the cell membrane. Indeed, the ability of FGF-2 to alter subcellular protein distribution is supported by a previous finding on the expression of Twist and Spry4 proteins in mesenchymal stem cells (Lai, Krishnappa, & Phinney, 2011). Here we observed E11 localization concentrated at the base of the dendritic spikes of the osteocytes after 24–72 hr of FGF-2 treatment. E11 immunofluorescence localization at osteocyte dendritic projections has been reported in MLO-Y4 osteocyte-like cells and primary osteocytes isolated from long bones (Stern et al., 2012). It is, therefore, likely that this redistribution of E11 within the cell is necessary for the transformation of the osteoblast from a cuboidal shape to the osteocytic phenotype characterized by stellate-like morphology with long dendritic processes (Zhang et al., 2006). We also reveal that these morphological changes do not occur because of altered cell proliferation, nor do they precede cell death, therefore, highlighting the role for FGF-2 in regulating E11 expression and osteocyte differentiation in vitro.

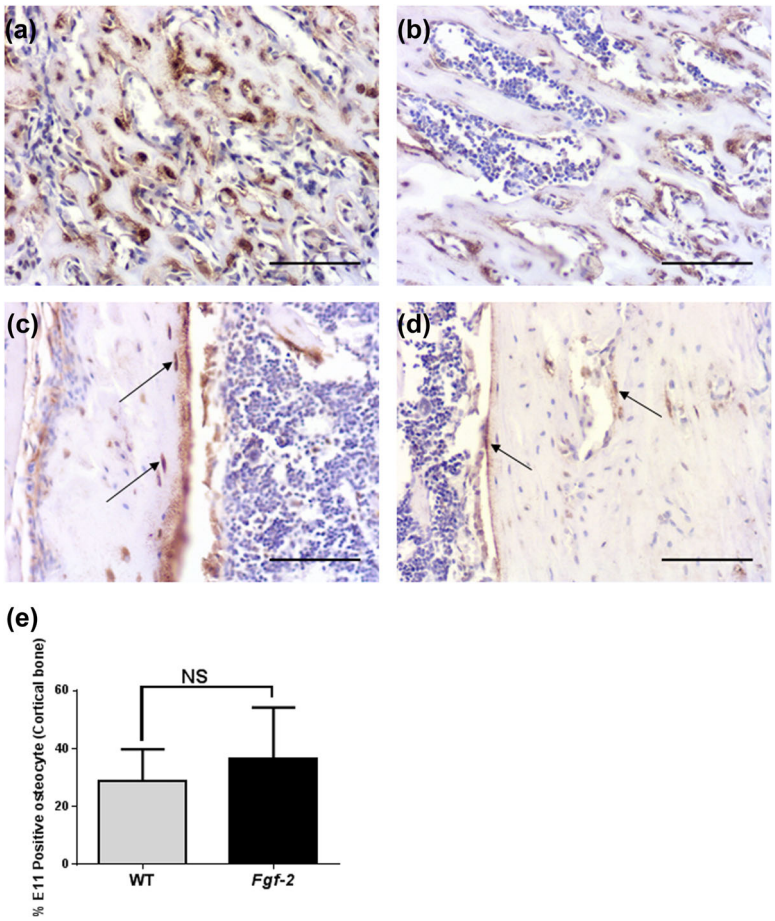

FIGURE 8 Sections of (a and b) trabecular bone and (c and d) cortical bone osteocytes from *Fgf-2* KO and WT mice immunostained for E11. (a and b) Scale bar = 150 μm. (e) The number of E11 stained osteocytes was similar in cortical bone from *Fgf-2* KO and WT mice. Images are representative of three mice

The intracellular effects of FGF-2 are activated via binding to its cell surface receptors, for example, FGFRs which have intrinsic receptor tyrosine kinase activity. Signaling pathways downstream of FGF-2-receptor binding are known to include ERK, p38, Akt, and PKC (Turner & Grose, 2010). Of those examined in the present study, ERK showed the most robust activation in response to FGF-2 in MC3T3 osteoblast-like cells; although p38 and Akt phosphorylation was also significant. Phosphorylation of ERK has been shown to mediate cell proliferation, differentiation, and matrix mineralization in human osteoblasts (Lai et al., 2001; Marie, Miraoui, & Severe, 2012). The sustained activation of the MEK-ERK pathway and phosphorylation of ERK over long time periods suggests a central role for FGF-2 stimulation of cell differentiation (Murphy, Mackeigan, & Blenis, 2003; Pellegrino & Stork, 2006). This is supported by studies that report the importance of ERK signaling in osteoblast initiation and commitment to the differentiation process (Lai et al., 2001), and in osteocyte dendrite formation (Kyono, Avishai, Ouyang, Landreth, & Murakami, 2012). Indeed, the conditional deletion of ERK ablates the formation of osteocytes with characteristic dendritic processes in vivo (Kyono et al., 2012).

Somewhat surprisingly, however, the MEK inhibitor, UO126 was unable to block FGF-2's ability to promote E11 protein expression despite a significant reduction in ERK activation. Similar results were observed upon inhibition of PI3K/Akt and p38 signaling. These results suggest that alternative pathways may exist by which FGF-2 is able to enhance E11 expression and osteocyte formation. Such pathways may include the activation of p38 and Akt. Previous reports have indicated that activation of p38 is involved in osteoblast differentiation (Hu, Chan, Wang, & Li, 2003) whereas Akt phosphorylation is associated with cell survival (Debiais et al., 2004). The down regulation of Akt by FGF-2 has, however, also been reported in human and mouse cells (Chaudhary & Hruska, 2001). In our hands, however, the dual inhibition of Akt and ERK activation by LY294002 and U0126, respectively, did not result in a block in E11 expression by FGF-2 and further work is required to unravel the signaling pathways that mediate FGF-2 effect on the up-regulation of E11 expression. The lack of JNK activation by FGF-2 in this study is consistent with JNK phosphorylation (P-JNK) mediating late osteoblast maturation (Matsuguchi et al., 2009).

Having shown that FGF-2 promotes E11 expression in MC3T3 osteoblast like-cells and murine primary osteoblasts, it was surprising to note that E11 protein expression by early osteocytes appeared to be increased in sections of bone from *Fgf-2*-deficient mice albeit no

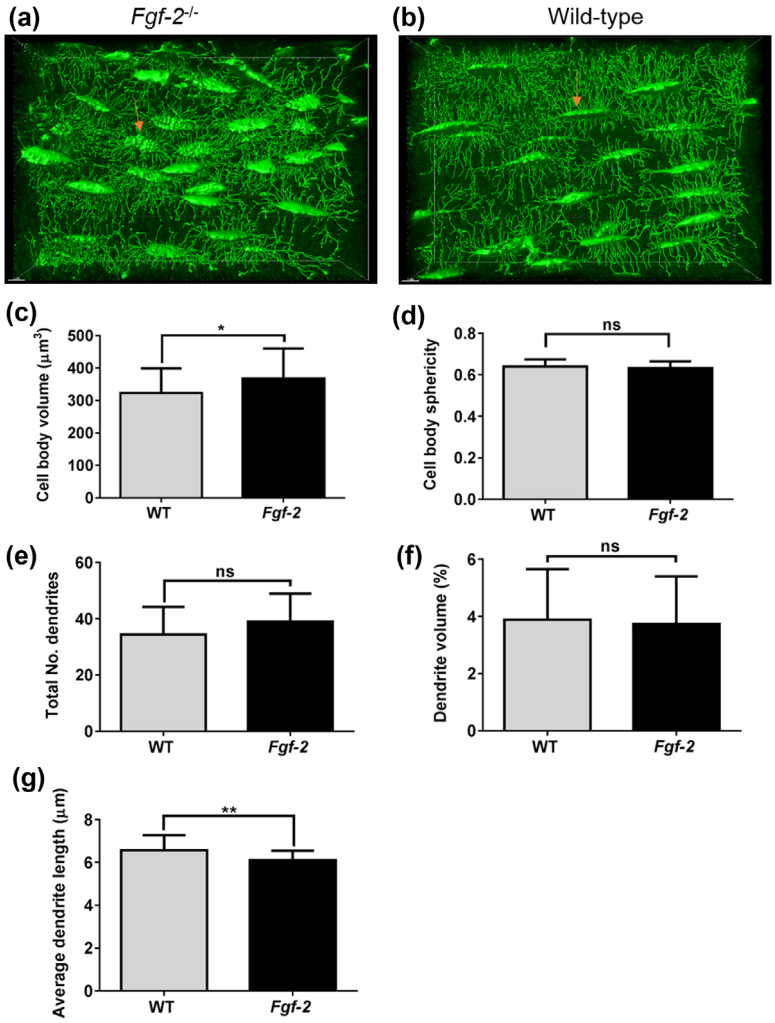

FIGURE 9 Phalloidin stained *Fgf-2* KO and WT mice tibial cortical bone osteocytes and dendritic processes (arrow). Representative image of cortical bone osteocytes in both *Fgf-2* KO (a) with larger cell body volume than the WT (b) as was confirmed by quantification (c), but no difference in cell spherical shape (d). While the total dendrite number (e) and volume (f), were not significantly different, the average length of the WT was longer than the *Fgf-2* KO (g). Data are presented as mean ± S.E.M for $n = 3$ mice; $^{*}p < 0.05$, $^{**}p < 0.01$. Scale bar = 7 µm

differences were noted in the number of E11 stained osteocytes. It is recognized that heparin-like glycosaminoglycans can regulate the signaling behavior of FGF-2 and, therefore, it is a possibility that in our cell culture experiments FGF-2 is more available to the cells due to a less mature extracellular matrix being formed (Padera, Venkataraman, Berry, Godavarti, & Sasisekharan, 1999). Alternatively, the increased E11 staining intensity in the osteocytes from *Fgf-2*-deficient mice is maybe a compensatory response in an attempt to overcome the deficit in FGF-2 related promotion of the osteoblast to osteocyte transition, potentially through the upregulation of other members of the FGF family. Similarly, it may simply be a consequence of the significantly increased cell body volume observed in FGF-2 KO osteocytes. Indeed FGF-2 has been reported to decrease chondrocyte hypertrophy in a murine metatarsal organ culture model and as such, may play a similar role in the formation of the osteocyte (Mancilla, De Luca, Uyeda, Czerwiec, & Baron, 1998). Our phalloidin staining also revealed a significant decrease in average dendrite length in FGF-2 KO mice compared to WT mice; a similar phenotype to that observed in our bone specific E11 conditional knockout mice (Staines et al., 2017). This, therefore, suggests that the absence of FGF-2 in vivo results in dysfunctional osteocytogenesis.

In conclusion, these data taken together show that FGF-2 promotes the osteocyte phenotype and that this is mediated by increased E11 expression which is redistributed within the differentiating osteoblast. If further studies confirm this regulatory role for FGF-2 in osteocyte formation, we will be in a better position to understand the full repertoire of FGF-2 on bone cell function which may provide insights into the etiology of skeletal disorders such as osteoporosis and osteoarthritis.

ACKNOWLEDGMENTS

We are grateful to the Tertiary Education Trust Fund Nigeria (TETFund) for funding this research (EI). We are also grateful to Arthritis Research UK (20413, (KAS) and to the Biotechnology and Biological Sciences Research Council (BBSRC) in the form of an

Institute Strategic Programme Grant (BB/J004316/1; BBS/E/D/20221657) (CF).

ORCID

Katherine A. Staines http://orcid.org/0000-0002-8492-9778

REFERENCES

Astarita, J. L., Acton, S. E., & Turley, S. J. (2012). Podoplanin: Emerging functions in development, the immune system, and cancer. *Frontiers in immunology*, *3*, 283.

Baldari, S., Ubertini, V., Garufi, A., D'orazi, G., & Bossi, G. (2015). Targeting MKK3 as a novel anticancer strategy: Molecular mechanisms and therapeutical implications. *Cell Death & Disease*, *6*, e1621.

Breiteneder-Geleff, S., Matsui, K., Soleiman, A., Meraner, P., Poczewski, H., Kalt, R., ... Kerjaschki, G. (1997). Podoplanin, novel 43-kd membrane protein of glomerular epithelial cells, is down-regulated in puromycin nephrosis. *American Journal of Pathology*, *151*, 1141–1151.

Chaudhary, L. R., & Hruska, K. A. (2001). The cell survival signal Akt is differentially activated by PDGF-BB, EGF, and FGF-2 in osteoblastic cells. *Journal of Cellular Biochemistry*, *81*, 304–311.

Choi, S. C., Kim, S. J., Choi, J. H., Park, C. Y., Shim, W. J., & Lim, D. S. (2008). Fibroblast growth factor-2 and -4 promote the proliferation of bone marrow mesenchymal stem cells by the activation of the PI3K-Akt and ERK1/2 signaling pathways. *Stem Cells and Development*, *17*, 725–736.

Chong, K. W., Chanalaris, A., Burleigh, A., Jin, H., Watt, F. E., Saklatvala, J., & Vincent, T. L. (2013). Fibroblast growth factor 2 drives changes in gene expression following injury to murine cartilage in vitro and in vivo. *Arthritis & Rheumatism*, *65*, 2346–2355.

Coffin, J. D., Florkiewicz, R. Z., Neumann, J., Mort-hopkins, T., Dorn, G. W., Lightfoot, P., ... O'toole, B. A. (1995). Abnormal bone growth and selective translational regulation in basic fibroblast growth factor (FGF-2) transgenic mice. *Molecular Biology of the Cell*, *6*, 1861–1873.

Dallas, S. L., & Bonewald, L. F. (2010). Dynamics of the transition from osteoblast to osteocyte. *Annals of the New York Academy of Sciences*, *1192*, 437–443.

Debiais, F., Lefevre, G., Lemonnier, J., Le Mee, S., Lasmoles, F., Mascarelli, F., & Marie, P. J. (2004). Fibroblast growth factor-2 induces osteoblast survival through a phosphatidylinositol 3-kinase-dependent, -beta-catenin-independent signaling pathway. *Experimental Cell Research*, *297*, 235–246.

Dobie, R., Macrae, V. E., Huesa, C., Van't Hof, R., & Ahmed, S. F. (2014). Direct stimulation of bone mass by increased GH signalling in the osteoblasts of Socs2-/- mice. *Journal of Endocrinology*, *223*, 93–106.

Farr, A., Nelson, A., & Hosier, S. (1992). Characterization of an antigenic determinant preferentially expressed by type I epithelial cells in the murine thymus. *Journal of Histochemistry and Cytochemistry*, *40*, 651–664.

Franz-Odendaal, T. A., Hall, B. K., & Witten, P. E. (2006). Buried alive: How osteoblasts become osteocytes. *Developmental Dynamics*, *235*, 176–190.

Gupta, R. R., Yoo, D. J., Hebert, C., Niger, C., & Stains, J. P. (2010). Induction of an osteocyte-like phenotype by fibroblast growth factor-2. *Biochemical and Biophysical Research Communications*, *402*, 258–264.

Hotokezaka, H., Sakai, E., Kanaoka, K., Saito, K., Matsuo, K., Kitaura, H., ... Nakayama, K. (2002). U0126 and PD98059, specific inhibitors of MEK, accelerate differentiation of RAW264.7 cells into osteoclast-like cells. *Journal of Biological Chemistry*, *277*, 47366–47372.

Hu, Y., Chan, E., Wang, S. X., & Li, B. (2003). Activation of p38 mitogen-activated protein kinase is required for osteoblast differentiation. *Endocrinology*, *144*, 2068–2074.

Hurley, M. M., Marie, P. J., & Florkiewicz, R. Z. (2002). Fibroblast growth factor and fibroblast growth factor receptor families. In J. P. Bilezikian, L. G. Raisz, & G. A. Rodan (Eds.), *Principles of bone biology* (pp. 825–851). San Diego, CA: Academic Press, Inc.

Kyono, A., Avishai, N., Ouyang, Z., Landreth, G. E., & Murakami, S. (2012). FGF and ERK signaling coordinately regulate mineralization-related genes and play essential roles in osteocyte differentiation. *Journal of Bone and Mineral Metabolism*, *30*, 19–30.

Lai, C. F., Chaudhary, L., Fausto, A., Halstead, L. R., Ory, D. S., Avioli, L. V., & Cheng, S. L. (2001). Erk is essential for growth, differentiation, integrin expression, and cell function in human osteoblastic cells. *Journal of Biological Chemistry*, *276*(17), 14443–14450.

Lai, W. T., Krishnappa, V., & Phinney, D. G. (2011). Fibroblast growth factor 2 (Fgf2) inhibits differentiation of mesenchymal stem cells by inducing Twist2 and Spry4, blocking extracellular regulated kinase activation, and altering Fgf receptor expression levels. *Stem Cells*, *29*, 1102–1111.

Livak, K. J., & Schmittgen, T. D. (2001). Analysis of relative gene expression data using real-time quantitative PCR and the 2(-Delta Delta C(T)) Method. *Methods*, *25*, 402–408.

Macrae, V. E., Ahmed, S. F., Mushtaq, T., & Farquharson, C. (2007). IGF-I signalling in bone growth: Inhibitory actions of dexamethasone and IL-1beta. *Growth Hormone and IGF Research*, *17*, 435–439.

Mancilla, E. E., De Luca, F., Uyeda, J. A., Czerwiec, F. S., & Baron, J. (1998). Effects of fibroblastic growth factor-2 on longitudinal bone growth. *Endocrinology*, *139*, 2900–2904.

Marie, P. J., Miraoui, H., & Severe, N. (2012). FGF/FGFR signaling in bone formation: Progress and perspectives. *Growth Factors*, *30*, 117–123.

Martín-Villar, E., Borda-D'agua, B., Carrasco-Ramirez, P., Renart, J., Parsons, M., Quintanilla, M., & Jones, G. E. (2014). Podoplanin mediates ECM degradation by squamous carcinoma cells through control of invadopodia stability. *Oncogene*, *34*, 4531–4544.

Martín-Villar, E., Diego, M., Susanna, C., Yurrita, M. M., Vilaró, S., & Quintanilla, M. (2006). Podoplanin binds ERM proteins to activate RhoA and promote epithelial-mesenchymal transition. *Journal of Cell Science*, *119*, 4541–4553.

Martín-Villar, E., Yurrita, M. M., Fernández-Muñoz, B., Quintanilla, M., & Renart, J. (2009). Regulation of podoplanin/PA2. 26 antigen expression in tumour cells. Involvement of calpain-mediated proteolysis. *International Journal of Biochemistry & Cell Biology*, *41*, 1421–1429.

Matsuguchi, T., Chiba, N., Bandow, K., Kakimoto, K., Masuda, A., & Ohnishi, T. (2009). JNK activity is essential for Atf4 expression and late-stage osteoblast differentiation. *Journal of Bone and Mineral Research*, *24*, 398–410.

Miyagawa, K., Yamazaki, M., Kawai, M., Nishino, J., Koshimizu, T., Ohata, Y., ... Michigami, T. (2014). Dysregulated gene expression in the primary osteoblasts and osteocytes isolated from hypophosphatemic Hyp mice. *PLoS ONE*, *9*, e93840.

Montero, A., Okada, Y., Tomita, M., Ito, M., Tsurukami, H., Nakamura, T., ... Hurley, M. M. (2000). Disruption of the fibroblast growth factor-2 gene results in decreased bone mass and bone formation. *Journal of Clinical Investigation*, *105*, 1085–1093.

Murphy, L. O., Mackeigan, J. P., & Blenis, J. (2003). A network of immediate early gene products propagates subtle differences in mitogen-activated protein kinase signal amplitude and duration. *Molecular and Cellular Biology*, *24*, 144–153.

Orriss, I. R., Hajjawi, M. O., Huesa, C., Macrae, V. E., & Arnett, T. R. (2014). Optimisation of the differing conditions required for bone formation in vitro by primary osteoblasts from mice and rats. *International Journal of Molecular Medicine*, *34*, 1201–1208.

Padera, R., Venkataraman, G., Berry, D., Godavarti, R., & Sasisekharan, R. (1999). FGF-2/fibroblast growth factor receptor/heparin-like glycosaminoglycan interactions: A compensation model for FGF-2 signaling. *FASEB Journal*, *13*(13), 1677–1687.

Palumbo, C., Ferretti, M., & Marotti, G. (2004). Osteocyte dendrogenesis in static and dynamic bone formation: An ultrastructural study. *Anatomical Record Part A Discoveries in Molecular Cellular and Evolutionary Biology*, *278*, 474–480.

Pellegrino, M. J., & Stork, P. J. (2006). Sustained activation of extracellular signal-regulated kinase by nerve growth factor regulates c-fos protein stabilization and transactivation in PC12 cells. *Journal of Neurochemistry*, *99*, 1480–1493.

Powers, C. J., Mcleskey, S. W., & Wellstein, A. (2000). Fibroblast growth factors, their receptors and signaling. *Endocrine-Related Cancer*, *7*, 165–197.

Ramirez, M. I., Millien, G., Hinds, A., Cao, Y., Seldin, D. C., & Williams, M. C. (2003). T1α, a lung type I cell differentiation gene, is required for normal lung cell proliferation and alveolus formation at birth. *Developmental Biology*, *256*, 62–73.

Sabbieti, M. G., Marchetti, L., Abreu, C., Montero, A., Hand, A. R., Raisz, L. G., & Hurley, M. M. (1999). Prostaglandins regulate the expression of fibroblast growth factor-2 in bone. *Endocrinology*, *140*, 434–444.

Scholl, F. G., Gamallo, C., Vilaró, S., & Quintanilla, M. (1999). Identification of PA2. 26 antigen as a novel cell-surface mucin-type glycoprotein that induces plasma membrane extensions and increased motility in keratinocytes. *Journal of Cell Science*, *112*, 4601–4613.

Skerry, T. M., Bitensky, L., Chayen, J., & Lanyon, L. E. (1989). Early strain-related changes in enzyme activity in osteocytes following bone loading in vivo. *Journal of Bone and Mineral Research*, *4*, 783–788.

Sprague, L., Wetterwald, A., Heinzman, U., & Atkinson, M. J. (1996). Phenotypic changes following over-expression of sense or antisense E11 cDNA in ROS 17/2.8 cells. *Journal of Bone and Mineral Research*, *11*, S132.

Staines, K. A., Javaheri, B., Hohenstein, P., Fleming, R., Ikpegbu, E., Unger, E., … Farquharson, C. (2017). Hypomorphic conditional deletion of E11/Podoplanin reveals a role in osteocyte dendrite elongation. *Journal of Cellular Physiology*, *232*, 3006–3019.

Staines, K. A., Prideaux, M., Allen, S., Buttle, D. J., Pitsillides, A. A., & Farquharson, C. (2016). E11/podoplanin protein stabilization through inhibition of the proteasome promotes osteocyte differentiation in murine in vitro models. *Journal of Cellular Physiology*, *231*, 1392–1404.

Staines, K. A., Zhu, D., Farquharson, C., & Macrae, V. E. (2014). Identification of novel regulators of osteoblast matrix mineralization by time series transcriptional profiling. *Journal of Bone and Mineral Metabolism*, *32*, 240–251.

Stern, A. R., Stern, M. M., Van Dyke, M. E., Jahn, K., Prideaux, M., & Bonewald, L. F. (2012). Isolation and culture of primary osteocytes from the long bones of skeletally mature and aged mice. *Biotechniques*, *52*, 361–373.

Thiery, J. P. (2002). Epithelial-mesenchymal transitions in tumour progression. *Nature Reviews Cancer*, *2*, 442–454.

Turner, N., & Grose, R. (2010). Fibroblast growth factor signalling: From development to cancer. *Nature Reviews Cancer*, *10*, 116–129.

Wetterwald, A., Hoffstetter, W., Cecchini, M. G., Lanske, B., Wagner, C., Fleisch, H., & Atkinson, M. (1996). Characterization and cloning of the E11 antigen, a marker expressed by rat osteoblasts and osteocytes. *Bone*, *18*, 125–132.

Wicki, A., & Christofori, C. (2007). The potential role of podoplanin in tumour invasion. *British Journal of Cancer*, *96*, 1–5.

Xiao, L., Liu, P., Li, X., Doetschman, T., Coffin, J. D., Drissi, H., & Hurley, M. M. (2009). Exported 18-kDa isoform of fibroblast growth factor-2 is a critical determinant of bone mass in mice. *Journal of Biological Chemistry*, *284*, 3170–3182.

Xiao, L., Naganawa, T., Lorenzo, J., Carpenter, T. O., Coffin, J. D., & Hurley, M. M. (2010). Nuclear isoforms of fibroblast growth factor 2 are novel inducers of hypophosphatemia via modulation of FGF23 and KLOTHO. *Journal of Biological Chemistry*, *285*, 2834–2846.

Zhang, K., Barragan-Adjemian, C., Ye, L., Kotha, S., Dallas, M., Lu, Y., … Bonewald, L. F. (2006). E11/gp38 selective expression in osteocytes: Regulation by mechanical strain and role in dendrite elongation. *Molecular and Cellular Biology*, *26*, 4539–4552.

SUPPORTING INFORMATION

Additional Supporting Information may be found online in the supporting information tab for this article.

How to cite this article: Ikpegbu E, Basta L, Clements DN, et al. FGF-2 promotes osteocyte differentiation through increased E11/podoplanin expression. *J Cell Physiol*. 2017;1–14. https://doi.org/10.1002/jcp.26345